UNIVERSITÀ POLITECNICA DELLE MARCHE
Dipartimento di Scienze Agrarie, Alimentari, Ambientali – D3A

PhD in Food Science and Technology - XXXI - 17° cycle

New Approach to Investigate the Quality of Parmigiano Reggiano Cheese: Coupling of Structure Virtualization to Thermal, Rheological and Fracture Properties

Academic Tutor
Dott. Pasquale Massimiliano Falcone

PhD Thesis
Elisa Sabatinelli

Academic Co-tutor
Prof.ssa Deborah Pacetti

Academic year 2015-2018

ABSTRACT

The Parmigiano Reggiano cheese is regulated by a **Protected Designation of Origin** (PDO) Disciplinary, which imposes achievement of requirements about product characteristics and production process, as well as its commercial quality and designation of origin. One of the Disciplinary features concerns the **structure**. According to the disciplinary, the typical structure of the cheese is defined as *finely-granulose structure* ("pasta finemente granulosa") and it *brittle fracture* ("frattura a scaglie"); therefore, when cheese is fractured, it breaks into scale-like fragments. Nevertheless, the two related-structure requirements are specified in the disciplinary without a clear definition nor an objective method to evaluate them.

The aim of this PhD project was to **investigate the cheese structure, fundamental rheological and fracture properties** with non-destructive methodology and identification of the functional relationships between composition, microstructure and thermo-rheological properties in a multi-scale level: from sub-micron to macroscopic level.

A second aim was to find a definition to flake fracture and being able to quantitatively determine it, and therefore develop an objective method for assessing fracture behaviour as a quality requirement for Parmigiano Reggiano. With these aims, more than 1700 cheese samples were obtained from cheese wheels from different raw milk composition and with a ripening age ranging from 12-months to 72-months, with the assumption of having the most different structures as possible. Cheese samples were provided by Parmigiano-Reggiano Consortium and selected among different cheese factories: 12 ripening times with 12, 14, 16, 18, 24, 28, 30, 36, 46, 54, 60 and 72 months of ripening. Then, each cheese wheel was divided in two parts along the sagittal plane to obtaining two specular half cheese wheels: A and B. Each half was divided in 10 cloves. Then, each clove was cut to obtain samples of parallelepiped-shaped to be analyzed under three-point bending test. In the three-point bending test, since there are discontinuities in the material, a standardized incision was created in the sample, in order to concentrate the stresses applied on the tip of the notch and not on the internal discontinuities, and reduce their variability.

Then, from the half obtained from the bending test, cubic-shaped samples (2cm size) were cut, in order to be analyzed under uniaxial compression and isothermal creep tests. Finally, round disk-shaped samples were obtained from the second half of the bending test (with 20mm of diameter and 2.5mm of height), in order to be subjected to thermo-rheological tests. Results suggested that the fracture mode is strictly related to the heterogeneity of cheese structure over a large range of scale. The applied stresses concentrate around the tips of sub-micron discontinuities, this latter arise from

partially fused curd junctions originated during milk clotting and cutting; consequently new surfaces originate and propagate along with the interfaces between fat and protein matrices due to their different relaxation times.

The extent of crack propagation within the cheese bulk is limited by the presence of micro-voids, as well as by plastic and viscous dissipative forces both decreasing during ripening of the cheese. Bending tests quantitatively described the extent of mode-I fracture. Creep and stress relaxation data were analysed to compare cheese samples by relaxation times. Finally, temperature and frequency sweep oscillatory tests provided quantitative data of both elastic recovery and viscous or plastic deformations.

Differential scanning calorimetry (DSC) has been used to evaluate the thermal behaviour, at a temperature between -80 and 350°C, with a heating rate of 10°C/min.

Cheese structure has been characterized with imaging techniques, by means of Electron Scanning Environmental Microscopy (ESEM) and X-ray computed tomography. The specimens were first fractured to analyze the fracture surfaces, in order to investigate the 2D and 3D-microstructure on a microscopic and sub-microscopic scale. The ESEM with different types of detectors (SSD-BSD, LFD and EDAX) gave us different types of information about the structure: phases making up the composition, morphology and chemical elements. ESEM has allowed us to evaluate the distribution of water, proteins, fats and air, and scale in which they extend (sub-microscopic, as well as macroscopic scale). The casein structure looks branched, moisturizes and incorporated a certain amount of still unmelted fat globules. The fat phase, no longer globular, which was formed during the cooking of the curd, appears smooth.

In addition, we assessed the macroscopic structure through the analysis of the fracture surface images with the use of a video camera and Image J software. The investigation of the macroscopic, microscopic and sub-microscopic structure, gave us details on the surface characteristics. The structure of the fracture surfaces is characterized by the partial overlap and **complementarity** of the fracture surfaces and by a structural irregularity.

We therefore hypothesized that the mechanism of origin and propagation of the fracture depends on the structural characteristics of the surface. The structure of the PR originates from the caseous granules that partially melt together during the cooking of the curd. The fracture of the PR originates near the discontinuities that correspond to the intergranule junctions, i.e. interface between two or more granules. The junctions represent a preferential point for the concentration of the stresses applied from the outside both for the presence of microcracks and for the distribution of

salt crystals. Both represent points where the two surfaces will detach. The propagation of the fracture therefore occurs in two ways: with an **inter-granular** mechanism if the fracture occurs following the intergranular junctions; and with a **trans-granular** type mechanism. In the latter case, the mechanically applied effort is distributed at the interface of different phases: the protein and lipid phase. Proteins and lipids in fact have different relaxation times and for this reason, at the interface of the two phases, a tension is created that facilitates the detachment of the two surfaces.

An industrial tomograph was used to virtualize the inner structure and reconstruct three-dimensional volumes. With industrial tomography, a porous structure was highlighted, which was originated due to the effect of microbial fermentation. Tomographic analysis has allowed us to virtually reconstruct the three-dimensional distribution of the pores, and calculate their volume. In the more mature PR there are smaller and more numerous pores, while in the younger PR there are larger pores. From the evaluation of the distribution of the pores within the volume, it was deduced that the PR has an elasto-plastic behaviour and that the different distribution of the pores affects the deformation mechanisms. This means that the older PR will be elastic and the younger more plastic, because the coalescence mechanisms are more dissipative.

This research sets the basis for the optimisation of the making process of Parmigiano Reggiano, considering fracture requirements as a key quality driver in a reversed engineering approach.

INDEX

PREMISE

The research focus and the experimental plan of this PhD thesys belong to a wider research project entitled to as "*Industrial research and experimental development on instrumental characterization of rheological and mechanical properties of the Parmigiano Reggiano cheese*", committed to the Department of Agricultural, food and Environmental Sciences of the Polytechnical University of Marche (Italy) and funded by the Parmigiano Reggiano cheese's Consortium, the Italian authority which is engaged to assure both the quality and authenticity of this worldwide famous Italian-style cheese, for which the European Unipon has deserved the Protected Designation of Origin (PDO) status. The scientific and technological focus of this dissertation deals with the development of a new paradigm to investigate and characterize the quality of the Parmigiano Reggiano Cheese in terms of the structure-related law requirements, both under descriptive and predictive perspectives. The proposed approach is science-based, accurate, and rapid but requires coupling of multi-scale virtualization of the structure to thermal, rheological and fracture properties

The **Parmigiano Reggiano** (PR) **cheese** is a hard cooked and lont-time ripened cheese, produced with raw and partially skimmed milk. The commercial quality od PR cheese is regulated by an official PDO disciplinary, which imposes requirements about product cow diet, milk treatments, cheesemaking process and typical product characteristics. One of the product characteristics concerns the **cheese texture** as perceived sensorially. At visual inspection, the inner structure of PR cheese appears inhomogeneous and grainy. Using a hammer by hand, PR cheese fractures breaking into tyical irregular scale-like slivers. According to the disciplinary, the typical structure of the cheese dough is defined as *finely grainy* ("minutamente granulosa") and it *is breaking in slivers* ("frattura a scaglie"). The structure of the cheese originates along the process: from the destabilization of the casein, through the coagulation and "*spinatura*" phase, which is the curd breaking, and it continues throughout the long ripening period (at least 12 months). The "*spinatura*" phase is decisive in the formation of the structure, which is strictly carried out by hand by an expert cheesemaker. The production of this PDO cheese combines, in fact, production technology with the close link with tradition and artisan techniques that have been going on for decades because they are linked to the cultural patrimony and protected by a Consortium of protection.

Studying the structure and understanding its properties is important, as it will enable to control and improve the process phases in order to reach the expected quality, but also to designing and optimizing the whole productive process. Unfortunately, the two related-structure requirements are

specified in the disciplinary without a clear definition nor an analytical method for a quantitative measurement of these key quality attributes related to the cheese structure.

Therefore, the aim of this PhD thesis was to investigate the cheese structure in a multi-scale level, to individuate the fundamental material properties underpinning its quality requirements and to identify new physical markers structure-related, able to describe the fracture propagation according to main theoretical models under linear elastic, elasto-plastic and viscoelastic regimes for mechanical solicitations. It would set the basis towards the standardization and optimization of the making process and the quality product.

PART I

1. INTRODUCTION

Structure, rheological and fracture properties of a cheese (in gaergal terms it is referred as to “texture” or “consistency”) are of great importance to the scientists and manufacturer, the trade and consumer. Theese properties affect the eating quality, i.e. the texture as perceived in the mouth; the usage (for example the ease of cutting, grating or spreading, and melting characteristics); handling and packaging (for ensuring shape retention); hole formation (for example whether eyes or slits are formed). Fracture properties are law requirements closely-related to the cheese authenticity of both the Parmigiano Reggiano and Grana Padano cheeses, two Italian-style cheese famous worldwide for which the European Union deserved the Protection of the Designation of Origin. Rheological and fracture properties depend on cheese composition (notably water, protein, fat, salts, pH, calcium), structure (porosity, microcracks, slits, protein-fat interfaces) and environmental factors (temperature); they change markedly during ripening. Consequently, they are all considered important quality markers.

Because of the interrelations between the factors affecting cheese structure, rheological and fracture properties, it is difficult to arrive at clear-cut conclusions on their effects. Cheese is a viscoelastic or visco-plastic material, which implies that the ratio of elastic to viscous (or plastic) properties depends on the time scale of the deformation. At short time scales its behavior is mainly elastic, i.e. cheese specimen regains its original shape after the stress applied to it is removed. At long time scales the behavior is mainly viscous or plastic: most of deformation remains after the stress is removed. Most of cheeses show no significant yield stress, which implies that even a small applied stress causes some permanent deformation, albeit very slow. However, the rheological behavior is also non-linear. The deformation or the deformation rate is no longer proportional to the applied stress if the relative deformation is greater than, say, 2%. Under large stress the cheese may either show a kind of yielding, i.e. it suddenly starts to deform more rapidly after a certain stress is reached, or it fractures. This depends both on the deformation rate and on the type of cheese. Also, the way in which a cheese sample fractures is, as such, an important property. In general, two fracture modes may be distinguished, viz fracture in tension or in shear.

A further complication is the marked and inherent inhomogeneity and sizes of most cheese. That include casein sub-micelles (6-10μm), paracasein micelles (7-10μm), protein network strands (4-10μm), fat globules (6-10μm), unevenness of network (5-10μm), bacterial colonies (4-10μm), curd grains (2-10μm), acid spots (2-10μm), holes (2-10μm), crystalline salts or amino acids (3-10μm), difference rind-centre (1-10μm). For this reason, cheese exhibits anisotropic behavior. The stress

distribution in a deformed specimen of cheese may thus be quite uneven. It may also be difficult to obtain representative samples. At the best, the results of rheological tests show considerable spread, say, a relative standard deviation of 5-25% and for some cheese even more.

The results obtained on cheese structure, rheological and fracture properties also greatly depend on measuring conditions. Two kinds of errors can affect rheological and fracture measurements. One originates from a fautly logical basis of the test concept, and the other reflects the structural features and mechanical characteristics of the material. The first kind refers to all tests that are based on arbitrary geometry and conditions, and where the results are reported in terms of such absolute force, deformation, etc.. notable examples are results from Texture Profile Analysis in all its instrumental varietis, all evaluations based on the Lee-Kramer “shear press”, and mesaurements with “viscosimeters” of the Brabender Farinograph kind. In all these methods, dependency on test conditions is inherent to the test and therefore must lead to inconsistent results. A few illustrations will suffice. Since attributes from Texture Profile Analysis such as “fracturability” and “hardness” are expressed in force units, samples with different diameters must have different textural properties if expressed in such terms. Furthermore, if the “first bite” is terminated at, say, 80% deformation, the material automatically becomes “harder” than if it were deformed to 75% only (in its original setup the “first bite” in texture profile analysis is terminated at a constant relative deformation). The magnitude of every parameter that is derived from “shear press” instrument largely depends on the thickness and the distance between the blades. Thus, the “texture” on the tested cheese must depend on these two (and other) factors that in themselves bear no relation to texture at all. Because of their faulty logical basis, the attempts to standardize such tests or the efforts to find “optimal” conditions for their use are doomed to failure. The only recommendation regarding their application is that their use should be discouraged. Such methods can, of course, detect the existence of texture differences between samples, particularly when these differences are large. This, however, does not mean that the magnitude of the observed differences is of any significance, or that identical or similar readings are indication that the corresponding samples have the same or similar texture. A second type of error dependence is that related to the test geometry where it is well defined (for example, uniaxial deformation and torsion) and where the data are presented in normalized terms, namely stresses, strain, moduli, work per unit volume, etc. In such cases, the dependency is truly a reflection of food’s structural and mechanical features and manner in which it responds to an imposed deformation. Important variables are temperature, sample, size and shape, deformation mode, extent of deformation and deformation rate. Consequently, selection of test method should be

done with great care. It must be realized that no single test can provide a complete account of all relevant rheological properties. Therefore, the test or tests to be selected should depend on the question to be answered. Some examples of such questions are the following:

- What are the stand-up properties of a cheese? Determine the effective viscosity at a very small stress
- What are the eating characteristics? Determine, for istance, the extent of deformation at fracture and the fracture energy, all at a high deformation rate. It should, however, be realized that unequivocal relations between the rheological and fracture properties of cheese and the texture as perceived by the consumer have not yet been established
- Can slits be formed instead of eyes? Determine the fracture stress and the biaxial elongational viscosity on a long-time scale slow rate).

In principle, if one measures a well-defined rheologicasl property, such as the shear modulus, by different methods, the result is independent of the method used as long as the time scale of thee experiment (or the deformation rate) is the same. Parenthetically, a measured Young modulus E (from a tension or bending experiment) should differ from a measured shear modulus G (from, for example, as experiment in shear or torsion). The relation between them is the following:

$$E = 2 \cdot G \cdot (1 + \nu) \quad (1)$$

Where v is the Poisson ratio, i.e. σx/σy, which for cheese is probably about 0.45 if the cheese contains no holes. But even such simple relations usually hold for small deformations only. The higher the stress and/or the strain, the more the result may depend on type and time scale of measurement, measuring geometry and sample history. This mainly because the stress and/or strain applied may irreversibly affect the structure of the sample. Such complications are more important if the strain and/or stress are less evenly distributed throughout the sample.

A further complication is the inherent difficulty of relating variation in cheese composition (in the widest sense, thus including changes during ripening) to variation in cheese structure, rheological and fracture properties, whether determined by mechanical testing or organoleptic by a panel of trained judges. Since variations in compositions are often correlated, it is often not possible, except to some extent in laboratory experiments, to vary one compositional parameter without varying others.

There is a plethora of factors affecting the inherent uncertainty (lack of reproducibility) to be linked to the experimental measurement of the structure, rheological and fracture properties. This means

that multiple regression analysis between compositional and consistency parameters can be risky endeavor. Be aware that chance correlations may be found that do not really exist. In some cases, a "principal components" or "polyfactor" analysis may be more useful.

1.1. Statement of the problem

The authenticity and quality of the Parmigiano Reggiano (PR) cheese is regulated by the official disciplinary for the *Protected Designation of Origin* (P.D.O.), which imposes requirements about both final product and making process. Among the product requirements, two key **structure properties** of the cheese, i.e. *brittle fracture and finely-granulose structure* ("frattura a scaglie" and "pasta finemente granulosa"), must be accomplished to obtain the authenticity certification mark. Brittle fracture is intended as the ability of the cheese to propagate spontaneously a crack; the extent of spontaneous crack propagation is a quantitative measure of the "frattura a scaglie".

As known among dairy food manufacturers and widely documented in last decade literature, there is an increasing interest about the characterization of the PR structure mainly because it is strictly related to three key quality aspects. Firstly, the **sensory quality** of the PR cheese is closely related to its structure. Secondly, the inner structure is strictly related to making process **artisanality** and product **authenticity**.

The structure of the cheese is the result of the constituent's interaction over a very large-scale length, i.e. from sub-micron to macroscopic sale. The PR's structure takes origin during hand cutting of the cheese curd, and it evolves throughout making and ripening processes. Casein's micelles undergo physical and biochemical destabilization during milk clotting until to the cheese curd forms into the whole vat volume. The cheese curd then is accurately broken by hand (such phase is known as "spinatura") until to reach granules having rice-like size. All cheese granules undergo thermal-induced aggregation followed by serum syneresis, while a cheese wheel takes place within surrounding solid geometry. As a result of the mass transfer of the serum between the inner and outer part of the cheese wheel during the salting step, a semi-solid grainy structure forms. Finally, such a semi-solid product evolves throughout the long-term ripening steps (at least 12 months) into a hard product showing brittle fracture behaviour. The guarantee about both authenticity and quality of such precious cheese is seriously compromised by more than one criticism. The official disciplinary does not provide a clear definition of the two key quality requirements related to the cheese structure. Moreover, it does not indicate any objective analytical method to quantitatively determine and standardize such material properties. These are two very

weak points because the cheese structure is actually characterized by very heterogeneous physical and sensory properties. The routine verification of the cheese authenticity by Authorities is actually based on empirical and not scientific knowledge. Traditionally, a panel of trained judges has evaluated sensorially these structure-related properties, but the judges have gained only empirical skills inherited from family parents over the years. The panel evaluates the fracture behaviour following two different empirical tests. Firstly, it evaluates the way cheese wheels propagate sound under mechanical solicitation (using a hammer by hand). Secondly, a piece of cheese undergoes cutting using a knife with typical drop shape: the spontaneous fracture propagation is visually evaluated. In such a way, the cheese property known as "frattura a scaglie" is assessed under non-standardized empirical conditions, providing judgments neither not objective nor comparable. Accounting for the weakness of the sensory classification of food structure proposed by Szczesniak (1963), which cannot be applied directly to hard cheeses as proven by Rohm (1990), as well as for the weakness of the international technical standard FIL 99A (1987) that so descriptive and superficial, a new guideline for the sensory evaluation of the structure of hard and semi-hard cheeses was recently published as the result of an international project (FLAIR-COST 902), participated by different partners including the PR Consortium (Lavanchy et al., 1994). Different authors evaluated through a trained judge panel the so-called texture-related attribute known as "brittleness" as the resistance of cheese samples to resist fragmentation during the first step of oral processing; while other authors evaluated instrumentally the texture-related property known as "fracturability" as the maximum force during the first step of a texture profile analysis of hard cheeses. Unfortunately, none of these experimental works don't provide any descriptor of the cheese ability to propagate a crack spontaneously, i.e. the "fracture toughness": such fundamental property is directly linked to the two above mentioned key law requirements of PR cheese. All authors studied only the apparent fracture behaviour of unnotched specimens, i.e. without taking into account for the natural discontinuities of the investigated cheeses. Luyten (1988) performed a study focused on the "fracture toughness" of Gouda cheese. This author performed notch-sensivity tests providing results on the crack initiation, without consider the dissipation of mechanical energy required for plastic deformation, i.e. the tearing properties. Consequently, PR cheese classification into the commercial categories is neither easy nor affordable; rational management of the critical steps of the making process is yet a challenge.

1.2. Purpose

The fracture analysis of a cheese is a complex matter: several factors such as sample geometry, strain rate, viscoelastic and plastic behaviour as well as temperature dependence of the relaxation time of the cheese structure will affect the uncertainty of results from both sensory and instrumental tests. For this reason, the PhD project aimed to investigate the microstructure, fundamental rheological and fracture properties aiming to esthablish a scientific definition to flake fracture and provide instrumental methods able to quantify fracture properties under different test geometry and strain conditions. Material properties were provided able to quantify individually the "fracture toughness", i.e. the resistance to crack initiation, and the "fracture tearing modulus", i.e. the resistance to fracture propagation. An innovative approach is proposed that is based on digital virtualization of the microstructure over a wide scale range coupled to high-performance techniques to investigate thermal, rheological and fracture properties of the cheese over a wide range of controlled loading and temperature conditions. With this aim, more than 1700 cheese samples with different microstructure were obtained from cheese wheels from different raw milk composition and with a ripening extent ranging from 12-months and 72-months. To reduce the inherent uncertainty some original devices were in-lab designed and developed allowing to prepare standardized specimens. This PhD project is the first step for a large-scale characterization aiming to perform the metrological analysis of the factors affecting the structure-related properties of the PR cheese, which includes the milk composition, curd cutting management, syneresis and ripening extent.

1.3. Assumption

This study is based on the assumption that the differences in structure do not depend only on ripening time, but also on other factors.

The objective of finding a definition of flake fracture and of being able to quantitatively determine it, and therefore develop an objective method for assessing fracture behaviour as a quality requirement for Parmigiano Reggiano, is based on the assumption of having the most different structures as possible. The structure of the finished product is influenced by many factors (eg. the technological quality of the incoming milk, the craftsmanship of the production process and the different extension of the ripening period).

For this purpose, in this study it was decided to use samples according to a representative sampling plan of the Parmigiano Reggiano cheese production, coming from different producers, and with different ages.

1.4. Definitions of terms

PR = Parmigiano Reggiano

ESEM = environmental scanning electron microscopy

SSD = secondary electron detector

BSD = back-scattered electron detector

LFD = large field detector

EDAX = energy dispersive x-ray spettrometer

SENB = single edge notched bending test

DENT = double edge notched tensile test

SAOS = small amplitude oscillatory shear

LEFM = linear elastic fracture mechanics

M = months of ripening (eg. 12M: 12 months ripened cheese; 30M: 30 months ripened cheese)

L = length [mm]

W = width [mm]

B = height [mm]

a = notch [mm]

K_I = stress intensification factor [MPa*$m^{0.5}$]

K_{Ic} = fracture toughness [MPa*$m^{0.5}$]

E_B = elastic modulus [MPa]

σ = stress [MPa]

ν = Poisson ratio [dimensionless]

Y = a dimensionless constant depending on material geometry

CEX(K)media = crack extension medium [mm/s^2]

CEX(K) max =crack extension max [mm/s^2]

Δa(UCi)max = maximum fracture extension [mm]

Σ(Δa(UCi) = complete crack propagation [mm]

Jic (Jq) = J initial crack [KJ/m^2]

J_{UC1} = J unstable crack [KJ/m^2]

(JEL/ EPL) Uci max = maximum elasto-plastic energy ratio in the last point of the fracture [dimensionless]

Σ(JEL)/ Σ(EPL) = mechanical resistance related to the entire fracture process [dimensionless]

Jtot Δa (mm1) = resistance when the fracture is 1 mm [KJ/m^2]

Jtot Δa (mm5) = resistance when the fracture is 5 mm [KJ/m^2]

Jtot Δa (mm10) = resistance when the fracture is 10 mm [KJ/m^2]

Wf Pmax = work of fracture, area under the curve [KJ/m^2]

εUTS/εE_Bmax = deformation max/deformation elastic max [dimensionless]

1.5. Limitation

The limit of this study consists in the fact that, despite having taken into account that there is a wide variability of structure, it was not possible to have a representativeness of the production of Parmigiano Reggiano cheese. This is because random samples of different producers and ripening ages have been taken. It was guaranteed structures different from each other, but with the limitation of not being able to extend in quantitative terms the results obtained to the production of the various maturations of the entire sector.

In the perspective of a technology transfer, a study with a representative sampling plan will be needed. This operation in turn requires a preliminary analysis of all the factors that influence variability (metrological analysis). This requires a broader and larger-scale study.

1.6. Methodology

The followed strategy has provided a theoretical analysis of what can be important in the mechanical behaviour of cheeses fracture, from a structural point of view.

The methodology involved a series of sequential phases:

1. study and analysis of the state of the art related to hard cheeses
2. theoretical study on the mechanics of fracture laws for elasto-plastic behaviour
3. study of the cheese structure on a large dimensional scale
4. cause-effect relationships between microstructure and fracture behaviour
5. characterization of the thermal, rheological and mechanical behaviour
6. development of a methodology of interpretation of the results (on an excel spreadsheet).

2. PROTECTED DESIGNATION OF ORIGIN

According to the UE Regulation n. 1151/2012, only the long-standing tradition food products, that is at least 40 years old, can carry the PDO brand (Protected Designation of Origin); they must be originating from a specific geographical region or place and their characteristics must depend essentially or exclusively on the geographical environment including natural and human factors. Therefore, the production and processing of these products must take place within the determined geographical area. To benefit from a protected designation of origin the product must therefore be compliant with a disciplinary that describes its main physical, chemical, microbiological or organoleptic characteristics, defines its geographical area and describes its production process.
The very close link with the territory makes the Parmigiano Reggiano cheese a Protected Designation of Origin.

2.1. The origin of Parmigiano Reggiano

The production area of Parmigiano-Reggiano cheese is limited only to some regions of northern Italy: in the provinces of Reggio Emilia, Parma, Modena, Mantova (on the right of the Po river) and Bologna (on the left of the Reno river). In 1934, it was decided that the cheese wheels produced in the territories of Parma, Reggio Emilia, Modena and Mantova to the right of the river Po would be marked with the mark "C.G.T. Parmigiano Reggiano". In 1937, the area of origin was then extended to the territories of the province of Bologna to the left of the Reno river.
Throughout the territory, there are about 4000 farms producing milk only for Parmigiano Reggiano cheese production, and almost 350 dairies that process it and ripen it for a minimum of 12 months.
Most of the milk is produced on small- or medium-sized dairy farms. The milk is then processed into Parmigiano-Reggiano cheese in hundreds of small-scale dairies that receive milk daily from farmers.
Parmigiano-Reggiano cheese production is a good example of a type of production system that is heavily dependent on the local ecology and climate and, in general, makes intensive use of artisan labour to produce final product. Parmigiano-Reggiano cheese manufacture has a long history and variations in quality and production processes are heavily determined by local socio-economic conditions of the territory.
More than 70 percent of Parmigiano-Reggiano production takes place on the fertile, highly productive plains. The remaining part is produced in the hills and mountain areas.

2.2. Link between artisanship and product

The most significant difference between industrial and artisan system is the difference in the ratio of capital to labour. Although in both systems the final valorisation at the stage of the milk marketing chain may be the same, an industrial system will remunerate primarily invested capital and an artisan system will remunerate high labour input in particular. Infact, large-scale processing units, supported by a universal technology and heavy inputs of capital, characterize global industrial systems. While, the local, artisan Parmigiano-Reggiano system is characterised by a low capital to labour ratio and by production techniques that cannot easily be reproduced. Over the years, the organisation of production has been modified, but most of its distinctive features remain intact.

The artisan nature of the production techniques involved in making Parmigiano-Reggiano cheese is one of the main reasons why it provides an interesting case study of a very specific economic system.

Another reason why Parmigiano-Reggiano cheese makes an interesting case study is that, unlike many other regionally specific products, it does not occupy a niche market. Almost 15% of Italian milk is processed into Parmigiano-Reggiano cheese. Emilia-Romagna, where Parmigiano-Reggiano is produced, is the second most important milk-producing region in Italy. In production terms, Parmigiano-Reggiano is the most valuable cheese in the country. It is sold all over Italy and 5% of total production is exported.

A third reason why Parmigiano-Reggiano cheese makes an interesting case study is that it retails at a high price and this contributes to the added value of the product. Consumers are very willing to pay for this quality cheese and it is an important ingredient in many Italian dishes.

Parmigiano-Reggiano is regarded as having the best qualities among the hard, ripened cheeses that are grated before use, and this fact is reflected in its retail price.

Fourthly, because artisan techniques feature prominently in production, the high added value of the product favours the employment of labour in the system. Most of the dairies are small- to medium-sized farms, and all of them use artisan techniques and are guided by a quality concept that is linked to the cultural patrimony of the local production area.

2.3. Law requirements for production

The milk processing techniques used to produce Parmigiano-Reggiano are rooted in an ancient tradition that is closely linked to Emilian customs and practices. It is only recently that a formal set of rules has been developed to prescribe correct practice. The principle of recognising designations of origin for cheeses in Italy has been introduced by the National Act No. 125, 1954 following the Convention of Stresa of 1951. Standards for Parmigiano-Reggiano production were then defined legally for the first time in Presidential Decree No. 1269 of October 30th, 1955. These rules have been supplemented by the cow-feeding production and quality branding regulations issued by the Consortium of Parmigiano-Reggiano cheese. These are constantly being updated as new technological developments take place. According to the Presidential Decree No. 1269, 1955 the rules that define the characteristics of the cheese production techniques concentrate mainly on product description. The procedures for processing and ripening Parmigiano-Reggiano cheese are as follows:

1. Parmigiano-Reggiano is defined as being a half-fat, hard, fully cooked cheese that is ripened in natural conditions. The ripening phase must continue from the year of production to the end of the summer in the following year. In practice the ripening phase usually lasts from 18-36 months.
2. Milk is processed once a day beginning in early morning. The milk used comes from the previous evening's milking. This is left in special settling tanks over-night and the fat that rises naturally to the surface is creamed off. Whole milk that arrives from the morning's milking is added to it.
3. Anti-fermentation substances are forbidden.
4. Coagulation is initiated by using rennet derived from the stomachs of unwearied calves.
5. Two to three days after the cheese-making process has been completed, the cheese is immersed in saturated brine for a period that varies from 20 days to a month.

According to the Presidential Decree No. 1269, 1955 the production standard used to define the cheese is as follows:

I. The cheese is cylindrical in form. It is 35 to 45 centimetres in diameter and between 18 and 24 centimetres in height. The upper surfaces of the cheese are flat while the base is slightly convex. The weight of a cheese can vary between 24 and 40 kilograms.

II. Traditionally in the past the external appearance of the cheese was dark in colour because linseed oil was applied during the ripening phase. With the passage of time this oiling

technique has been abandoned in favour of an automated cheese cleaning process. Today the outer rind is yellow-gold in colour, corresponding to the natural colouring of the ripened cheese. The rind is about six millimetres thick.

III. The regulations permit variations of a slightly straw-like colouring for the interior of the cheese. Again, with the passage of time and change in consumer preference, the inside colour of Parmigiano-Reggiano cheese has become increasingly white.

IV. The texture of the cheese is made up of tiny structured granules and when fractured the cheese breaks into scale-like fragments. When cut, the cheese reveals tiny holes that are just visible to the eye.

V. Parmigiano-Reggiano has a characteristic and fragrant taste. It is delicate but does not 'burn'.

VI. The fat content should not be less than 32 percent on a dry matter basis.

These requirements laid down in the Presidential Decree No. 1269, 1955 leave relatively wide margins of tolerance as far as the dimensions and weight of Parmigiano-Reggiano cheeses are concerned. In reality, there is considerable similarity in the production techniques of the various dairies. The most produced ripened Parmigiano-Reggiano cheese varies from 35 to 37 kilo, its height can be between 20 and 22 centimetres and its diameter is usually between 40 and 45 centimetres. A small cheese of 24 kilograms could be expected to ripen faster and although it would cost less, its taste would not be greatly appreciated by the consumer Presidential Decree 1269 recognises production techniques for the first time in defending the product and its name against unfair competition. This is the main objective of the decree. Actors comply with the rules laid down in the decree because the regulations are based on local, fair and constant uses and the customs of the production area.

After the European recognizing of its Designation of Origin, law requirements for the PR production is ruling out by the Official Disciplinary of Production indicated by the Italian Gazette n.185 published at August 10, 2006. Few important improvements have been introduced with respect to the Presidential Decree No. 1269, 1955. According to the Disciplinary of Production in force, the PR cheese has a cylindrical shape, with slightly convex or almost straight sides and it must respect the following characteristics:

- Dimensions: diameter of the flat faces from 35 to 45 cm, height of the heel from 20 to 26 cm;
- Minimum weight of a cheese wheel: 30 kg;

- External appearance: natural straw-coloured crust;
- Colour of the dough: slightly straw-yellow to straw;
- Characteristic aroma and flavour of the dough: fragrant, delicate, tasty but not spicy;
- Dough structure: minutely grainy, flake fracture;
- Thickness of the crust: about 6 mm;
- Fat on dry matter: minimum 32%.

The Disciplinary of Production in force allows only three raw materials to produce the Parmigiano Reggiano cheese that are cow's milk (from cows bred in the defined geographical area), salt and calf rennet. The use of additives is not allowed. The feeding of cows is based on the use of fodder from the defined geographical area, and the use of any type of silage is prohibited. Dairy cow farms whose production is destined for processing in Parmigiano-Reggiano are located in the defined geographical area, as well as the production of milk and its transformation must take place in the defined geographical area. The minimum ageing for cheese ripening must be at least 12 months. At the end of the minimum ageing, the Consortium carries out the inspection operations, with the purpose to verify the conformity of cheese properties to the production disciplinary requirements.
For further details, see *Annex I*, Disciplinary of production.

2.4. Consortium

The Parmigiano-Reggiano Consortium is the Italian Authority engaging duty and responsibility of assuring authenticity and quality of the cheese. It is an association joining more than 380 dairies producers operating within the area of origin (*Table 1*); it was officially born on July 27th, 1934 and it has its central headquarters in Reggio Emilia.
In previous years, the producers had set themselves the goal of distinguishing, by marking, the production of the cheese known as "Parmigiano" and "Reggiano". After several years of debate and after some attempts undertaken at the provincial level, in 1934 the producers succeeded in establishing a unitary body, which represents the oldest institution for the protection and promotion of a typical cheese, and expresses the history and culture of a precise territory. On 12 November 1954, the first aggregation of 1934 took the name of "Parmigiano-Reggiano Cheese Consortium", to which all the producers joined.

Table 1 Cheese factories belonging to the Consortium divided into the different provinces of the protected geographical area

Province of	Bologna	Mantova	Modena	Parma	Reggio Emilia	**Tot.**
N. Dairies	9	21	62	158	93	**343**

The Consortium carries out several important tasks:

- Verifing that the production of PR cheese follows the strict rules imposed by the PDO Disciplinary;
- Protecting Parmigiano Reggiano from imitations;
- Encouraging and promoting knowledge and consumption;
- Applying brands and marks;
- Improving the quality of Parmigiano-Reggiano to safeguard its peculiar characteristics and typicality.

The Consortium assigns traceability's code to each Parmigiano-Reggiano cheese factory. The Consortium's experts evaluate cheese authenticity and quality one at year. Firstly, they inspect visually the possible presence of external defects; then, they use a hammer to tap cheese surfaces to assess the compactness of the dough and absence of inner cracks or internal holes. Finally, they use a screw needle to evaluate cheese consistency and flavour (*Figure 1*).

After individual cheeses have been positively tested, the Consortium signs the wheel with the official fire marks. The Consortium is the holder of the Parmigiano-Reggiano PDO marks; furthermore it establishes the procedures for using Parmigiano-Reggiano's marks in compliance with the Production Regulations and supervises their correct use in dairies. In case of incorrect use of the marks of origin or other non-compliance with the specification, the Consortium arranges for the withdrawal of the marking matrices and eventually the application of sanctioning measure according to the regulations in force.

The factors considered for each individual Parmigiano Reggiano cheese during the classification process can be summarised as follows:

• *Age.* The month and year of production are established from the dates stencilled on the sides of the cheese.

• *Degree of maturation.* This is in relation to its age, but it can also be deduced from the flavour, smell and the consistency of the cheese body.

• *Aroma.* Produced by tasting and smelling the body of the cheese.

• *Structure.* The structure of the cheese body must be radial and converge towards the centre of the cheese. When cut with a knife the cheese should open up along a straight line and show slight cavities.

• *Colour.* The colour of the cheese (hay-coloured) must be uniform.

• *Consistency.* The cheese body must be soft, showing white grains derived from the transformation of the substances used. Consistency is primarily related to the degree of maturation and the fat level.

• *Rind.* It should be soft and waxy and an old gold yellow in colour. It should have a width of about five millimetres.

• *Cheese size.* The weight of each individual cheese should be between 30 to 35 kilogrammes. Its vertical sides should be between 20 and 26 centimetres high and 35 and 45 centimetres in diameter.

Figure 1 Sensory Evaluation of inner Defects, Grainy Texture and Fracture Behavior of the PR cheese (PDO requirements)

2.5. Commercial classification and marks

Parmigiano Reggiano cheese (PR), among the protected designation of origin products, represents one of the most important economic value in the Italian agri-food sector. According to Istat data, in 2017 production of Parmigiano Reggiano is attested to almost 1 million and 300 thousand wheels, and it has recorded an increase of 6.5% over the previous year. Its quality is certified according to the Protected Designation of Origin rules under European law. Only cheeses with this distinctive designation mark can be considered authentic. The quality of Parmigiano Reggiano is strictly related to the mode of fracture and to HOW GRAINY are the FRACTURED SURFACES. The fracture mode of the excellent cheese must be "brittle-like". The PDO disciplinary imposes requirements on the manufacturing process, specifically time of ripening and some texture properties, among which the most important are the shape, the weight and two texture-related features, officially known as "*struttura finemente granulosa*" and "*frattura a scaglie*". The simplest way to prove both the artisan process and cheese authenticity is by evaluating to what extent fine granules split into brittle slivers. Traditionally, the commercial grading of the Parmigiano Reggiano cheese has been performed following two empirical approaches, i.e. (1) cutting by-hand a piece of cheese using a drop-shaped knife, and (2) beating by-hand with a hammer. Inner macroscopic defects that includes slits and cavities as well as the grainy texture and fracture behavior are usually evaluated empirically by the Consortium's experts during the so-called "expertization activities" aimed to evaluate the cheese authenticity according to the PDO disciplinary and to assign the PDO mark only to these cheese wheels that show no inner structural defects, grainy texture of the fracture surfaces as well as a brittle fracture.

The quality assessment **OF TEXTURE** results in a standard three-category classification. From the commercial point of view, there are three market categories of PR cheese based on the structure quality of each cheese wheel:

1) 1° category:
    a. **Scelto sperlato**: the wheel is immune from any defect both outside and inside, both to the sight and to the examination with the needle and the hammer;
    b. **Zero**: the wheel may have on the crust superficial cracks, small erosions and slightly ruined edges without being deformed;
    c. **Uno**: the wheel with slight structural anomalies, in particular one or two "vescicotti" (cavities of circular or oblong form in the paste) or cracks of a diameter not exceeding

3-4 cm, or “vespai” (spongy zone) of a few centimeters, or holes rare, without presenting olfactory defects;

2) 2° category:
    a. **Mezzano**: the wheel with “vescicotti” of a diameter greater than 3-4 cm or “vespai”, immune to olfactory defects, diffuse holes, or cracks and slits arranged horizontally;
3) 3° category:
    a. **Scarto**: the wheel with very pronounced bulge of the plates of the wheel, or spongy paste with diffused holes and multiple horizontal fissures or large splits on a large part of the wheel, or evident olfactory defects;
    b. **Scartone**: to this class belong all the wheels in which is noted the presence of numerous and serious defects and all those that cannot be included in the previous categories.

The “FIRST GRADE” is the quality level only given to those cheese wheels that have no defects. The marks are distinguished in **origin marks** and **selection marks**. The **origin marks** are placed by the individual dairies through:

1. application of a casein plate on the surface (*Figure 2*), showing alphanumeric code/CFPR that identifies each individual form;
2. use of special matrices (marking bands) imprints on the surface of the rind of each wheel the Parmigiano-Reggiano dot markings, the matriculation number of the dairy, the month and year of production.

The **selection marks** are affixed indelibly after an evaluation carried out by experts of the Consortium ("expertization") who examine all the wheels produced when the minimum maturing period is reached (12 months).

On the cheese wheels belonging to the 1st and 2nd commercial category, the Consortium of Parmigiano Reggiano cheese affixes an oval fire mark with the words "Parmigiano Reggiano Consorzio Tutela" (*Figure 3*) and laterally the year of production.

The cheeses of the 3rd category, together with those with serious structural defects that have not allowed maturing, are "bleached" by eliminating from the hell all the identification signs and any marks.

There is also the possibility to carry out a further qualitative selection on the wheels already marked with at least 18 months of maturation, belonging at the first category "scelto sperlato", in order to qualify Parmigiano-Reggiano as “Extra" or "Export" and be destined for foreign trade (*Figure 4*).

As required by D.P.C.M. 4.11.1991, the denomination of origin of the Parmigiano Reggiano cheese is extended to the grated type obtained exclusively from whole cheese entitled to the designation of origin in question.

The grating operations must be carried out within the area of origin in order to guarantee quality, traceability and control, and the packaging must be carried out immediately without any treatment and without adding any substance capable of modifying the preservability and original organoleptic characteristics. Parmigiano-Reggiano PDO in the typologies of portioned or grated cannot be subjected to any treatment, including heat treatment, drying, freezing and freeze-drying.

In addition, grated Parmigiano must comply with the following technical and technological parameters specified below:

- absence of additives;
- humidity: not less than 25% but not more than 35%;
- appearance: not pulverulent and homogeneous, particles with diameter lesser than 0,5 mm up to 25%;
- amount of crust: not more than 18%;
- amino acid composition typical of Parmigiano-Reggiano (it is registered at the Protection Consortium, at the Control Body and the Ministry of Agricultural, Food and Forestry Policies and determined using spectrometric methods).

However, it is also allowed to cut and pack the cheese outside the area of origin, following these conditions:

- parts of certified cheese wheel not inferior to eighths of wheel;
- each part must bear the word in dots "Parmigiano-Reggiano", clearly visible;
- each part must have the oval mark "Parmigiano-Reggiano Consorzio Tutela" or the mark “Extra” or "Export";
- they are not intended to be presented as such to the final consumer;
- in addition, these products must be accompanied by documentation with the indication "Parmigiano-Reggiano cut in accordance with the specification".

The Disciplinary requires that each package must bear a mark with the graphic representation showed in *Figure 5*, in order to guarantee authenticity and allow a correct identification of the grated, portioned and prepacked PR cheese placed on the market. On the label must appear the minimum age of the cheese, in order to guarantee maximum transparency to the consumer.

Finally, all the operators (milk producers, dairies, seasoners, portioners and grating-makers) are included in a control system and registered in special lists managed by the Control Body. Operators shall ensure the origin with regard to feed, raw materials and products coming from the origin area, using registers and documentations from HACCP, which are subject to verification by the Control Body.

Figure 2 Casein plate

Figure 3 Oval fire-mark on the 1st and 2nd category PR cheese

Figure 4 Mark Extra and Export

Figure 5 Parmigiano Reggiano packaging mark

3. TECHNOLOGICAL ORIGIN OF CHEESE STRUCTURE

As for other food products, cheese structure expresses the chemical and physical interactions among its constituents through weak and covalent bonds that may extent at different scales size, from atomic to macroscopic. Chemical and microbiological compositions of milk together with the manufacture technology affect the cheese structure. Coupling both mass and energy transfer to the microbiological and enzymatic bioconversion of the milk constituents dictate the way microstructure evolves throughout the production process. Cheese structure is closely linked to the texture as perceived sensorially as well as to its mechanical and rheological properties.

Microbiological and compositional characteristics of the milk intended for processing into Parmigiano Reggiano cheese (PR), the whey-starter quality and the processing technology determine the structural and sensory characteristics (Tosi et al., 2008).

Studying the structure and understanding structure-related properties of Parmigiano Reggiano, is of fundamental importance, since this knowledge allows controlling and improving the process aiming to match the expected quality characteristics of the product, avoiding texture defects.

3.1. Flow-chart of cheese making process

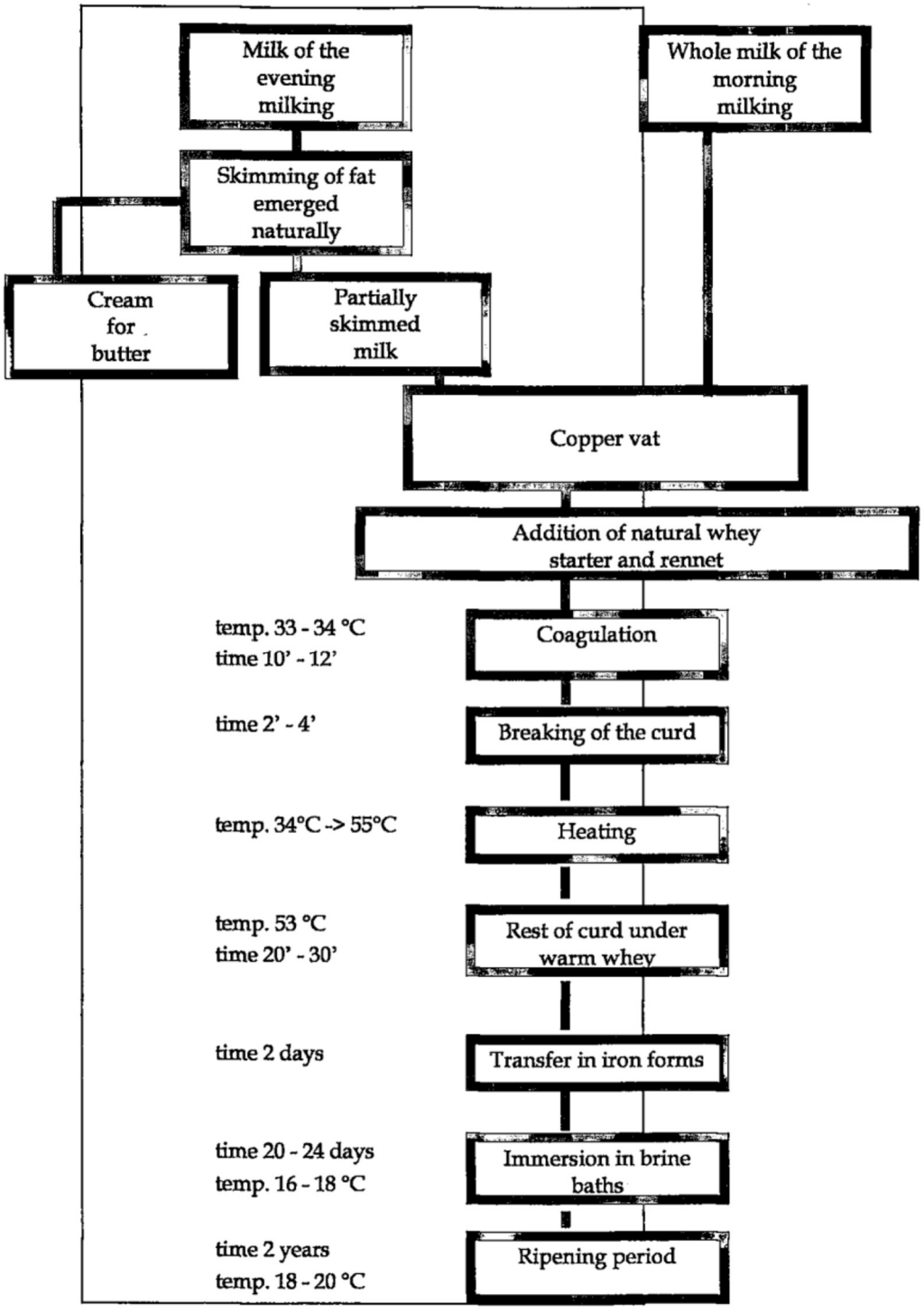

Figure 6 Flow-chart to process milk for the production of Parmigiano-Reggiano cheese

In processing milk for Parmigiano-Reggiano cheese, the human element is critical and exerts a heavy influence on the product quality. The production process is predominantly artisan. The cheese-maker's professional skills ensure that the various phases in the cheese making process are carried out correctly. Parmigiano-Reggiano cheese belongs to that group of cheeses that, unlike most industrial cheeses, uses raw milk in their manufacture. Furthermore, Parmigiano-Reggiano differs from other cheeses that are based on raw milk including Italian cheese Grana Padano, in that no additives or substances from outside the production environment are used.

The cheese production starts with the breeding of dairy cows which must have, according to the production regulations, a feed consisting mainly of fodder from the area of origin because silage or fermented fodder are forbidden, as well as by-products of the food industry and animal origin products. About 550-600 litres of milk are needed to produce a wheel of Parmigiano Reggiano cheese. The dairy farmers who produce Parmigiano-Reggiano milk make two deliveries a day. The milk is usually transported in milk churns. The large lorry-mounted containers are only used for milk from large herds. To inhibit over-rapid microbe growth, the milk is chilled briefly to about 18°C. The milk is delivered within two hours of milking from the farm to the cheese factory, and the dairy farm uses two types of milk: one derives from evening milking and one from early morning milking. Fresh milk is extremely complex in its composition. It is therefore extremely fragile and subject to rapid changes. The temperature and humidity of its surroundings exert an enormous influence on the biological processes taking place within the milk. Once milk from the evening's milking has arrived at the dairy, it is first filtered to remove any solid contaminants, then it is poured into shallow tanks to allow the fats to rise to the surface overnight. The fat rises spontaneously to the milk surface bringing up even the impurities and microbes. Cold water is sprayed onto the under-sides of the tanks to keep the milk temperature between 15 and 20°C. If the milk is too deep, only a limited amount of cream will rise to the surface. The shallow tanks ensure that a high proportion of the cream rises to the surface. The large globules of fat agglomerate more quickly, while the smaller globules accumulate later. The cheese-maker is thus able to regulate the amount of cream rising to the surface by adjusting the depth of the milk kept in the tanks. In the morning, the cream floated on the top of the milk is removed and used for the butter production. The cheese-maker decides how much cream must be removed and this depends on the bacterial quality of the milk. If the milk is too 'dirty' it needs to be creamed off more thoroughly than would be necessary in the case of cleaner milk. Once the cream has been removed, the skimmed milk from the previous evening is poured into the typical truncated-cone shaped **copper vats** (*Figure 7*). The

milk from the morning's milking arrives between seven and eight a.m. then, it can rest in tanks for about one hour at a temperature close to 18°C. At this moment, the two milks, conveniently filtered, are mixed.

Immediately after milking, the milk has a natural acidity of between 3.4 and 3.8 SH degree. Following the gradual fermentation process the natural acidity of the evening milk's rises by a few points and after it has been mixed with the morning milk it will have an acidity of between 3.5 and 3.9 SH degree. The correct timing for initiating the manufacturing process depends on the degree of acidity of the milk in the vat. The cheese-maker uses visual and tactile clues to decide whether acidity has reached an optimum level. The chemical and microbiological quality of milk received from different producers is extremely variable. A large herd with cows producing high quantities and stalled in a cow-shed with cubicle houses produces milk of a completely different quality than that produced by a small herd of cows tethered in the traditional way. The cheese-maker decides on the combination of different milks from the different suppliers that should go into each vat, although his choice is limited to some extent by the order in which milk consignments arrive. He knows from past experience how the milk from the different producers reacts in the vats during the cheese-making process. The cheese-maker also marks the different cheeses with the symbol of the different producers. In this way he is able to identify the producer in the event of anomalies or defects that may arise during the ripening phase.

Once the milk is in the vat, the production of PR cheese begins. A vat usually has a capacity of 10-11 quintals and it is equipped with an interspace allowing steam flowing to transfer the heat to the milk mass, through a pressure valve controlled by hand. From each vat, two wheels will be obtained.

The first move is to add the triggering whey. The "**whey-starter**" (or "**whey-ferment**") is added to the milk. It comes from a natural starter culture obtained from the spontaneous acidification of the residual whey from the processing of the previous day: at the end of each cheese making process, the cheese-maker removes a limited quantity of whey. The sample of the whey-ferment is left to acidify in special churns, a process that depends on the presence of milk enzymes that act on the remaining lactose in the whey to produce lactic acid. If the acidity of the whey-ferment is about three SH when a sample is taken, it will have increased to about 25-30 SH after some 18-20 hours. If the whey is left for a longer period of time, the quantity of milk enzymes would begin to decline. Adding acid whey-ferment as a natural whey-started at the beginning of the treatment of the milk in the vat enriches the milk with milk enzymes beneficial to the cheese-making process. These act to

prevent the spread of microbes that are deleterious to the cheese-making. The triggering whey increases the acidity of the milk in the vat and also introduces a series of enzymes. These enzymes will go on being effective throughout the lengthy ripening stage. The whey also helps to create a good structure in terms of cheese texture and water and fat retention capacity (Zannoni, 1979). The addition of whey was an innovation introduced at the beginning of the century and represents an extremely important factor in the successful production of the cheese. To determine the amount of whey-starter to be added, the cheesemaker has to measure the acidity of the whey and the acidity of the milk in the vat. On the bases on these two values, he then calculates how much whey is needed. The whey-starter raises the level of milk acidity: pH decreases and guides the cheese towards an appropriate fermentation. It is a very important phase helping the coagulation and prevents the producing of unwanted microorganism in the curd. The whey introduces also a series of enzymes that will go on being effective throughout the lengthy ripening stage. The whey also helps to create a good structure in terms of cheese texture and water and fat retention capacity.

At this point the milk is heated to a temperature of about 33°C stirring slowly. When the heating is suspended, rennet is added. The **rennet** must be exclusively calf rennet: natural enzyme extract, containing rennin, obtained from the fourth stomach of the calf; it digests the milk proteins facilitating the coagulation of milk, which takes about 12-15 minutes. Rennet to be added is provided from a number of specialist firms. Before he adds rennet to the milk, the cheese-maker checks its strength. So-called normal strength rennet is such that one centilitre coagulates one litre of milk at 35°C in four minutes. The cheese-maker is able to test the coagulating force of the rennet by a quick acting test and from the results of the test is able to decide the amount that must be added. These can vary from vat to vat and from day to day dependant on the characteristics of the milk in the vats and on the quantity of triggering whey added. The coagulation process begins within about ten minutes after rennet addition.

The coagulation process occurs (*Figure 8*) thanks to the presence of the casein in the milk, organized in sub-micelles, each of which is composed by the sub-micelles alpha-S1, alpha-S2, beta and negatively charged K-casein. In PR production the casein coagulation is due both to the acid lactic and enzymatic hydrolysis of casein. The added rennet contains a mixture of proteolytic enzymes, mainly chymosin, that is able to hydrolyse K-casein by breaking the peptide bond, which in turn determines the removal of the negatively charged part of K-casein, i.e. the macro peptide colloidal-protector. This detachment induces the aggregation and precipitation of alpha-caseins, which form a gel-like network. The small casein particles begin to come together under the

influence of increased acidity, first as a result of the triggering whey and later as a result of the rennet. Milk which has not been sufficiently fermented, or which has been disturbed during its journey coagulates less than normal quality milk. The product obtained from coagulation is called "**curd"** that is going to be broken manually, even today as tradition dictates, by the master cheesemaker using a curd knife, an instrument characteristic of cheese-making called "*spino*" (*Figure 9*) and this stage is called "*spinatura*". In order to produce a uniform break and a regular purge, the master cheese maker can continue the curd break with a mechanical spinning until when the granules are rough to the touch of his hand, but consistent and with similar dimensions to grains of rice, about 2-4 mm *(Figure 10*). The small granules will cause the typical grainy texture and granular behaviour during sliver fracture. It is by observing the coagulation process that the cheesemaker reaches a decision on how he should proceed with the breaking up of the curd. Deciding on the right moment to break up the curd is particularly important: if it is done too late, the curd is too hard and the whey does not get rid of the granules; if it is done too early, the soft granules are squashed and are not uniform in size. It is necessary to produce a compact and homogeneous mass where the curd granules formed during the breaking up process come together and fuse spontaneously.

The cheese-maker decides whether the curd granule size is right for the cheese he is making by feeling the milk with his hands. He then decides when the cooking phase can begin. The temperature is increased from 33°C to 55°C. During cooking, the curd must be continuously stirred to avoid any danger of compacting and solidifying at the base of the vat, i.e. the burning of the granules along the walls of the boiler, with the possible inconvenience formation of a film outside the granules that would hinder the purge of whey. This process used to be carried out by hand, but nowadays motor-driven machines fixed to the edge of the vat are used to continually mix and agitate the mass of milk granules. The cooking stage lasts about 10-15 minutes and is carried out in two stages. First, proceeding slowly and dosing the heat gradually up to about 43-45°C, or when the granules compressed slightly in the palm of the hand tend to bind together. Second, proceeding with a faster temperature increase up to 55°C. At the end of this phase the fire is suspended and the caseous granules sediment at the bottom of the vat, where they will form a single compact mass. During cooking the whey drays off from the granules. The cheese-maker notes the speed at which the whey is removed and he decides when the cooking phase should end. He does this by closing off the steam inlet in the cavity between the double walls of the vat. Once the right amount of whey has been removed from the curd granules, they collect and solidify at the bottom of the vat and form

a cheese mass. The coagulated mass is left to settle under the whey for almost an hour. Every now and then, the mass is pressed down with a spade-like instrument to expel the last of the whey. Subsequently, the curd is cooked slowly and it reaches a temperature of about 55°C. After sedimentation, the caseous mass is wrapped in a linen cloth (*Figure 11*). The curd is cut in two halves and one-half passes into another linen cloth. The two halves are then extracted from the vat (*Figure 12*). Each boiler gives life to two wheels of Parmigiano-Reggiano cheese, called "**twins**". The mass of cooked coagulum, still wrapped in the cloth, is then transferred (*Figure 13*) into a special mould template, called "*fascera*" (*Figure 14*), where a special marking point-matrix (*Figure 15*) is applied between lateral surface of the wheel and an aluminium mould. During this stage a wooden disk that exerts a constant stress (creep) on the top of the plastic coagulum allowing gradual squeezing of the remains whey. Once the curd has been through the above described basic manufacturing steps, it is referred to as "**cheese**". In the evening the trademark of origin 'Parmigiano Reggiano' is pressed onto the base of the cheese.

The name as well as needful data for the purpose of traceability of the supply chain are inscribes:

- the **registration number** of the cheese factory;
- the **month** of production;
- the **year** of production.

The craftsmanship involved in the cheese-maker's work and the work of his assistants becomes clear when we consider the various operations they must carry out. The raw milk varies greatly in composition from one zone to another, from one producer to another and from one day to the next. It is a living product, containing millions of microbes interacting with the different fat particles, casein and lactose present in the milk. Their fermenting action changes the composition of the milk from hour to hour. The cheese-maker's skill lies in his ability to control the fermentation process. The cheese-maker decides the timing of various crucial operations, the quantities of triggering whey and rennet to be added, and the extent of the creaming-off process. He relies on his years of experience and training when making these decisions.

For traceability purposes, to each wheel is applied a **plate of casein** with a unique and progressive code. The plate of casein is the identity card of the cheese that will accompany it throughout his entire life and it will make it possible the traceability (possibility of tracing in every place and at any time all stages of its production and marketing, starting from its origin, up to the finished product). The cheese is left inside of the aluminium mould for about four days and it is frequently turned on one or the other flat face in order to make it take definitively its characteristic appearance.

After four days the cheeses are ready to **salting** by immersion (*Figure 16*), which it consists of immersing the wheels in full immersion salting rooms with recirculation of a saturated saline solution (22% NaCl), for an immersion time proportional to the weight of the wheels (generally 24h/kg). The brine temperature is kept at about 17°C, so that the salt can diffuse at the correct speed throughout the cheese. The cheeses are turned once a day and remain in the brine for a period of 15 to 23 days. During this period, cheeses absorb salt, salt promotes syneresis, the release of whey, resulting in an average weight loss of about 4%, other than have the right taste and a better conservation. Salt is the only preservative that can be added to Parmigiano-Reggiano, according to the regulation.

At this point the cheeses are deposited in storehouses for ripening, a phase which lasts for a minimum of 12 months, but normally continues for up to 24 months. During this time, the cheese undergoes a series of chemical, physical and microbiological changes that are influenced by the temperature, humidity and ventilation of the ripening environment. The cheese loses about five percent of its weight during the ripening phase. The wheels of Parmigiano are arranged in long rows on wooden tables supported by a metal structure called "*scalera*" and they are left to rest in well-ventilated ripening rooms (*Figure 17*), with a temperature of 16-18°C and a relative humidity of 82-85%. The cheeses are then constantly checked and brushed, turned on the other side every 4-5 days in the first ripening months and later every 10-12 days. The younger cheeses are arranged on the lower axes of the shelving, where the air is more humid and the temperature lower, and then they gradually pass to the higher floors. In this way a superficial crust is formed naturally as a result of drying, without treatments.

Before being put on the market, every wheel of PR must have the stamp in fire of authenticity mark, which impresses the mark of the PDO; therefore, a selection of the wheels is made by to be assessed for matching to the quality requirements. Consortium's expert performs tasting of the wheel firstly through a visual evaluation of the external appearance with the aim of ensure the conformity of the crust and of the marks. Then, he continues with the beating using hammer test: beating the hammer on the cheese wheel and listening to the sound emitted (auscultation) he gives a judgment of the internal structure of the cheese (*Figure 18*). Finally, using a screw needle ("pricking" or "*spillatura*" operation), the expert gives two types of judgments. The first judgment is related to the cheese consistency, based on the sensory perception of resistance to needle penetration. The second judgment concerns olfaction by tasting the flavour composition and intensity as expected as a function of the claimed cheese ripeness. In order to deepen the objectivity of tasting and texture

perception, the experts' commissions proceed to cut one cheese wheel per lot at least, or not less than one cheese wheel in every thousand wheels.

When the expert's judgment is negative, it means that the cheese does not meet with the law requirements and it cannot receive the final PDO mark; in this case, the dot writing and the temporary marks on the bottom surface must be removed and the cheese can be sold only as generic hard cheese. If the expert's judgment is positive, the cheese meets with the requirements and it can be sold as PDO cheese.

Figure 7 Milk mixed in the copper cauldrons

Figure 8 Milk clotting

Figure 9 Breaking the curd with the

Figure 10 Curd granules size (2-4 mm)

Figure 11 Caseous mass

Figure 12 Mass divided in two parts and wrapped in linen cloths

Figure 13 Movimentation of the cooked mass into the "fascera"

Figure 14 Forms wrapped in the template "fascera"

Figure 15 Matrix marking the surface of the heel

Figure 16 Parmesan forms immersed in brine

Figure 17 Storerooms for ripening and aging cheeses

Figure 18 Expert evaluates the quality of Parmesan

3.2. Technological factors affecting the final structure

According to the law requirement, the final **structure** of the PDO Parmigiano Reggiano cheese is characterized on macroscopic scale by a "grainy texture" and without macroscopic discontinuities both on surfaces and into the bulk. Grainy texture is strictly related to the characteristic flake fracture of this traditional cheese. Moreover, according to its long history, the presence of two different "white domains" are widely recognized as traditional markers. One of the two white domains is known as "crunchy **speck**" and contains mainly tyrosine crystals and is perceived sensorially brighter and more localized macro aggregate. The last one of the white domains is known as powdery smear and diffuse "**spot**" rich in leucine crystals. As for other handcrafted artisanal cheeses, crystals observed in such as Parmigiano-Reggiano are viewed as important contributors to cheese character and commercial quality (Noël et al., 1996; Zannoni et al., 1984). Growing consumer appreciation of traditional and artisanal cheeses is also fuelling interest in understanding the nature and origins of both the fracture properties and their contributions to cheese quality and character.

The structure evolves from liquid state of the milk to a semi-solid state of the casein curd and, finally, to the solid state of the ripened cheese. A huge number of factors affect the structure of cheese firstly including the milk production, i.e. cow breed, lactation state, feeding and other environmental conditions all affecting milk composition and technological quality. Under physical standpoint, the milk consists of water, lipids, lactose, caseins, serum proteins, mineral salts and a long list of miscellaneous constituents. The fat in milk is almost entirely in the form of globules in the emulsion phase: the fat globules are held together by proteins and surrounded by hydrophilic

membrane of carbohydrates and charged groups, attached to cholesterol molecules, while the inner part of the globule is instead hydrophobic. Casein micelles are dispersed in the colloidal state and calcium and phosphate as soluble ions. In the PR production, the maturation of milk represents one of the key technological steps. The dairy "maturation" of milk is defined as the period between milk collection in the farm and the beginning of the cheese making process. This phase can be further divided in two steps: the first one that last about 6 hours, occurs from the milking in the parlour to the delivery in the cheese factory; in the second step, full cream milk rests in large flat vats, for about 10-12 hours, to obtain partially skimmed milk by the gravity separation of fat (natural creaming process). During this time, physico-chemical, microbiological and technological modifications occur in milk affecting the number and size of fat globules that will be processed in the next technological steps.

The structure at microscopic scale finds theoretical and experimental fundamentals on its artisanal making process history. During PR cheese production, fat and protein (casein) of milk are concentrated between 6- and 12-fold and while the pH is reduced from 6.6 in milk to between 4.6 and 5.4 in freshly made curd due to the lactic acid bacteria acidification. The basic unit operations in cheesemaking are milk acidification, gelation (casein coagulation), dehydration (e.g., by cutting the gel, syneresis/whey expulsion of resultant curd pieces by stirring and cooking in the expressed whey, drainage of whey, pressing of curd mass, continued acidification), moulding/shaping (by placing pieces of curd mass in forms and pressing) and salting. Once the curd has been through the five basic manufacturing steps, it is referred to as cheese. The first three steps are managed into the same plant, i.e. the vat.

3.3. Critical unit operations of cheese making process

3.3.1. Casein coagulation

Technological Objectives

The technological objective of this unit operation is to transform milk from a liquid to a gel-like state (curd), that is the right physical state to undergo successive unit operation. Casein micelle coagulation is the basis for the transformation of milk into cheese. During PR cheese production, the colloidal casein micelles from milk undergo destabilization by combined effect of lactic acid bacteria and calf rennet to form a hydrated casein network entrapping fat globules and aqueous serum phase Lactic acid-producing bacteria, in form of whey-ferment, are added to milk and the

mixture is stirred at a constant temperature: pH is lowered because of lactose to acid lactic bioconversion. When sufficient acidity has developed, calf rennet can be added to the milk. Calf rennet is a natural enzyme extract containing rennin, obtained from the fourth stomach of the calf. Enzymatic hydrolysis leads to colloidal destabilization of the casein micelles through hydrolysis of the kappa-casein in the milk, i.e. the negatively charged moiety, causing the loss of electrostatic repulsion among the casein micelles. Lowering of pH causes the soluble calcium to become insoluble and colloidal favouring aggregation of the destabilized casein micelles so that they coagulate forming a gel structure (the curd) that extent into the entire volume.

Technological Variables

The main technological variables are temperature and time. The coagulation takes place in about 12-15 minutes, while the cheese maker as a function of the gel evolution and its texture properties as evaluated sensorially increase temperature according a variable program from 32°C to 35°C. Such temperature interval is the optimum for lactic acid bacteria for milk acidification.

In *Figure 19*, in PR cheese production a scheduled time-temperature program is followed during casein micelles coagulation and subsequent cooking.

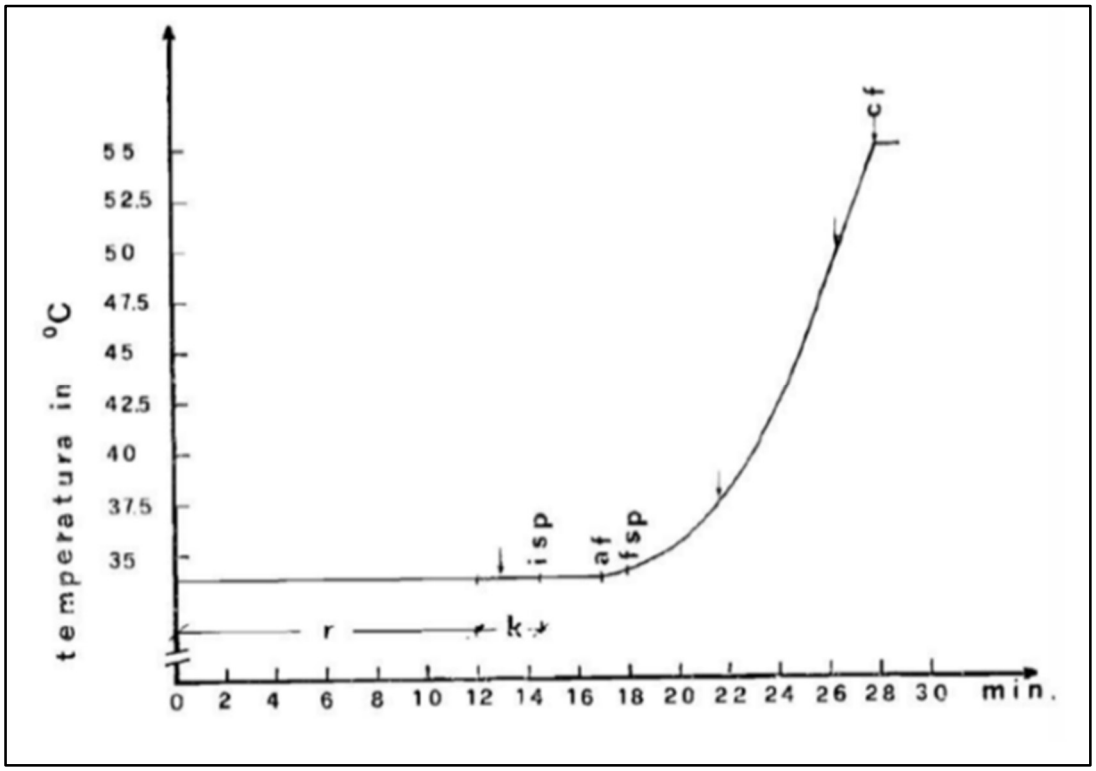

Figure 19 Management of temperature-time conditions during Parmigiano Reggiano cheese production, where r = coagulation time of casein micelles; k = firming time; isp = beginning of "spinatura", af = opening of fire; fsp = end of "spinatura"; cf = steam closure. (adapted from Nanni and Annibaldi, 1982)

3.3.2. Breaking of curd (kowns as to "*Spinatura*")

Technological Objectives

The technological objective of this unit operation the reduction of the entire clot volume into free curd granules having a size like a rice granule (2-4mm), that is the that is the right physical state to undergo successive unit operation. Curd granules consist mostly of insoluble calcium-caseinate entrapping fat droplets and serum. The entire curd is broken manually by the master cheesemaker. Currently the mechanical breaking of curd is only partially used in the early step of cutting operation, because it is a very critical step affecting the cheese structure and final quality. In *Figure 20* and in *Figure 21*, we can see the distribution frequency of cheese granules of different sizes, in hard cheeses samples taken horizontally and in samples taken vertically (Ruegg and Moor, 1987). The diameters of the cross sections of the curd granules ranges from about 0.5 to 5.0 mm.

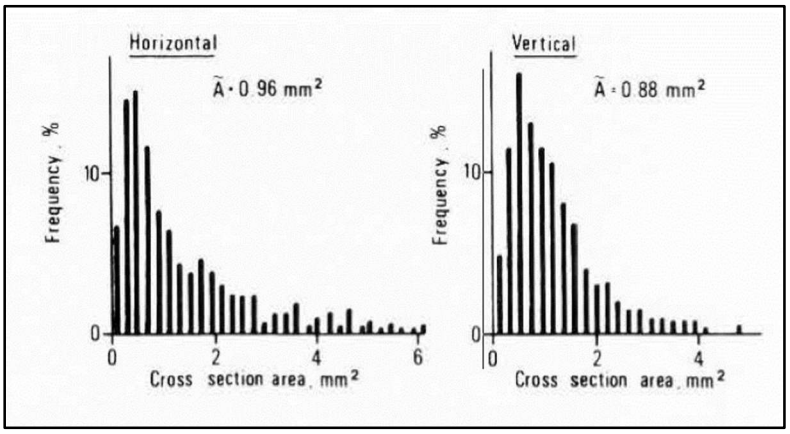

Figure 20 Size distribution of curd granules in a hard cheese in a horizontal or vertical cross section area, according to the scheme in fig.15

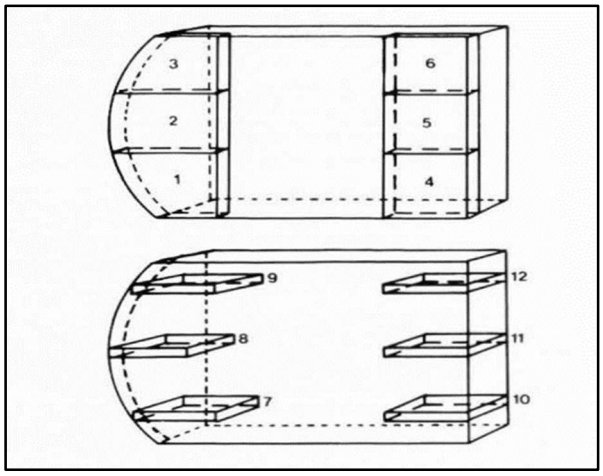

Figure 21 Schematic drawing of cheese samples in vertical (1 to 6) or horizontal section (7 to 12)

Technological Variables

The main technological variables are the starting time, amplitude and frequency sweep as well as the stress intensity applied by the cheesemaker with the cutter (spino). The starting time for cutting, i.e. the moment when the cheesemaker decides to break the curd, affect the curd granule strength and size. In fact, if it is cut too early the granules are too soft and not in uniform size; on the other hand, if it is cut too late the curd is too hard and the granules will release the whey more difficultly.

3.3.3. Curd Cooking and Drayinig

Technological Objectives

The curd cooking has two specific goals. Cooking first aims to regulate the moisture content, the degree of mineralization and the lactose content of the curd granules, which in turn will influence the progress of fermentation processes and physical mechanisms underlying structure changes from gel to semi-solid and visco-plastic caseous mass. Secondly, cooking allow the formation of partially fused intergranular junctions, that will further evolve during ripening allowing the grainy texture to develop.

When the curd is broken into small-dispersed individual granules and a caseous mass (coagulum) of about 140kg precipitates at the bottom of the vat. The sites, where the granules close with each other, form the so-called inter-granule curd junctions. **Whey purge** (serum syneresis) takes place plenty during cooking under mass and energy transfer. The patterns formed between inter-granule curd junctions inside the newly formed caseous mass became more complex because additional type of junctions develops when it is kept under serum and medium-high temperature (from 35°C to

55°C in 10-14 minutes). Under these circumstances, the heat is transferred from surrounding serum towards the curd bulk allowing destabilization of the fat globules entrapped inside the casein network to form a viscous phase, mainly due to the partial melting of the triglycerides. At the meantime, the bulk stress induced by the curd mass under gravity causes the syneresis of the lipid phase flowing from the bulk towards the skin of the curd granules as well as of the aqueous serum from curd granules towards the surrounding medium. Melted fat exerts a plasticizing role mainly on the external layers of the curd granules generating a partially fuse "skin" in a complex pattern of inter-granule junctions. Inter-granule spaces are depleted of fat and rich in serum concentrated in both organic and inorganic insoluble constituents.

Technological Variables

The main variable that the cheesemaker has to keep under control is the time to start fire as well as both time and temperature of cooking. Temperature is raised gradually to reach the final level of 55°C. The cooking rate of temperature increase as well as the overall cooking time is decided by the cheesemaker. The fire is stopped when the granules compressed slightly in the palm of the hand tend to bind together. This rheological behaviour indicates that the fat globules are melt and the individual curd granule can partially fusing through the skin.

3.3.4. Pressing, moulding and salting

Technological Objectives

Pressing and moulding operations occur under creep conditions (constant stress generated under gravity by the topping) using a moulding aluminum template. This unit operation causes further extent of the serum syneresis, while the caseous mass takes the typical shape of a cylindrical wheel with the convex lateral surface. Moulding allows the curd granules to get closer one to each other and cheese structure to become firmer. At this point, the moulding step takes about 72 hours.

The next unit operation is the salting aiming to further concentrate the serum residual inside the inter-granule spaces. It occurs inside brine concentrating sodium chloride and represent a critical step in the structure development. Salt has a positive impact on the cheese taste, then it selects dairy microflora, such as lactic bacteria, inhibiting negative microorganisms belonging to Clostridia and Coliforms; finally, it creates a solute gradient able to govern slow serum syneresis through osmosis mechanism. The penetration of salt, which begins with immersion in brine, proceeds during

maturation with a centripetal trend, from the outside to the inside of the wheel (Resmini et al., 1974; Fossa et al., 2002).

PR cheeses are salted by immersion of moulded curd in brine solution towards the end of manufacture when the recovered curd is formed and moulded. The practice of adding salt to the curd at the end of curd manufacture, rather than to the milk, was undoubtedly deliberate in early cheese manufacture as rennet coagulability and gelation of bovine milk of typical composition (3.3%, w/w, protein) are markedly impaired by the addition of 2% (w/w) salt to milk, and completely inhibited at salt levels of 4% (w/w) (Grufferty and Fox, 1985; El-Nour, 1998; Fox, 2004). Moreover, the addition of salt to milk prior to renneting severely impairs curd syneresis and whey expulsion during curd manufacture (Pearse and Mackinlay, 1989), and leads to excessively high moisture levels in the final cheese. The adverse effects of salt addition are due to the solubilization of colloidal calcium phosphate (sodium/calcium ion exchange), and the resultant increase in casein hydration, which impairs casein aggregation.

For several months the area near the rind has a higher salt content than the central area, and this will influence a radial and axial oriented trend of ripening transformations inside the cheese wheel. It will take several months, normally 10-15 months, so that the salt distribution will become uniform (Resmini et al., 1974; Tosi et al., 2008). The salt content can vary from 1.5g/100g of dry matter in the first 3 ripening months to 1.84g/100g of dry matter in 12 months of ripening (*Figure 22*), up to 2.10g/100g of dry matter in 30 months.

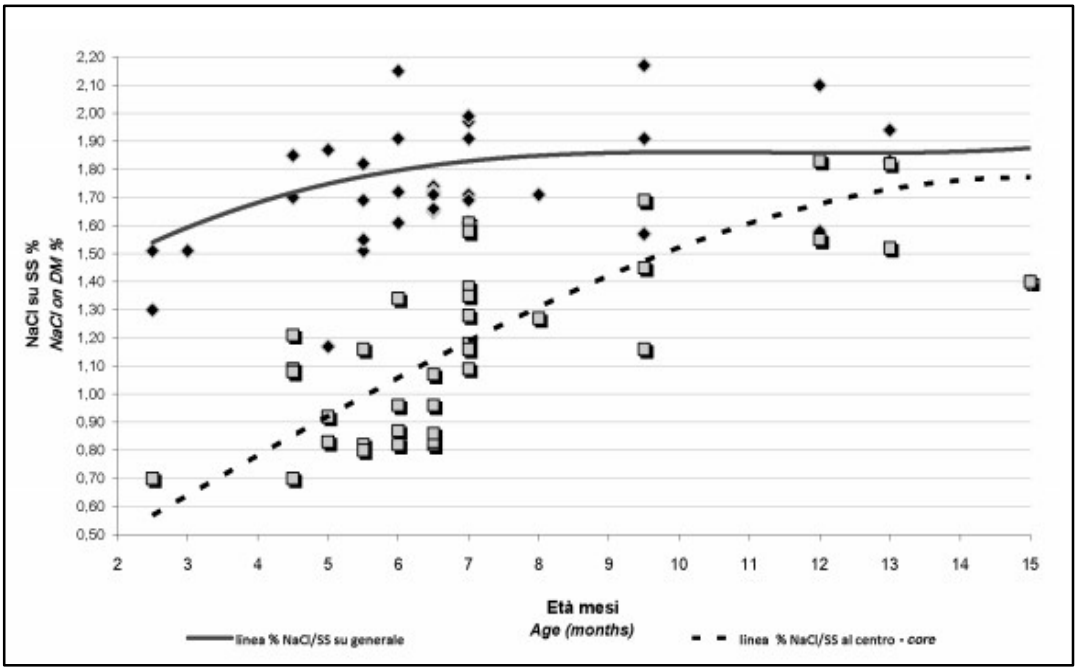

Figure 22 Variation of NaCl/dm % content throughout ripening: comparison between whole wheel and core centre. (Tosi et al.2008)

Technological Variables

Immersion time, temperature and brine concentration are the main technological variables affecting salt diffusion from the rind to the core. Brine solutions contain about 22% of NaCl, and salt concentrates in the first 2-3 cm from the crust and continues to spread even during the ripening phase with a lower concentration gradient. The immersion time of the wheels of PR cheese varies from 2 weeks to more than 20 days.

3.3.5. Ripening

Technological Objectives

The ripening or aging in this hard cheeses represents one of the most important and complex phases of the entire production cycle, connecting together a series of chemical-physical, biochemical and biological events. The main transformations essentially consist of:

- Loss of moisture;
- Lactose fermentation;
- Partial metabolism of lactic acid and citric acid;
- pH variation;

- Proteolysis: solubilization of casein and degradation to low molecular weight peptides and free aminoacids;
- Lipolysis: hydrolysis of lipids increasing the free fatty acid pools;
- Rind formation.

The responsible for these transformations are: natural milk enzymes, starter bacteria and their enzymes, rennet enzymes, pollutant microflora enzymes.

Under structural standpoint, proteolysis and lipolysis cause structure erosion and weakness of both casein network and plastic inter-granule junctions. In the meantime, the water loss during the early months of ripening allows establishing chemical-physical conditions promoting the formation of salt crystals. Literature reported that certain conditions promote the formation of several types of crystals (*Figure 23*) in ripened cheese and that calcium is a key factor controlling the rheological and fracture properties of ripened cheeses. Firstly, the components of a crystalline entity must exceed the solubility of that entity (Rajbhandari and Kindstedt, 2005); nucleation sites must provide a place for crystal growth to begin (Swearingen et al., 2004); and physical space, in the form of an open structure inside a cheese piece or exposed surface of a cheese slab, must provide room for the crystal deposit to grow (Johnson et al., 2006). Secondly, the amount and the physical state of the retained calcium influences the physical characteristics of cheese during ripening, including fracture stress, fracture strain, and cheese firmness (Guinee et al., 2009). Acid development during cheese making dictates the loss of insoluble calcium (Johnson et al., 2006). Changes in the physical properties of cheese during ripening occur in two stages: one is governed by pH and changes to the insoluble calcium content and this may take hours, days or weeks to be fully realized; the other stage is governed by the extent of proteolysis of intact casein that occurs throughout cheese ripening. From that the importance of controlling the factors affecting insoluble calcium throughout cheese making chain including the ripening stage. In traditional cheeses such as Parmigiano-Reggiano and other hand-crafted artisanal cheeses, crystals are viewed as important contributors to cheese character and quality (Noël et al., 1996; Zannoni et al., 1984). Growing consumer appreciation of traditional and artisanal cheeses is also fueling interest in understanding the nature and origins of crystals and their contributions to cheese quality and character.

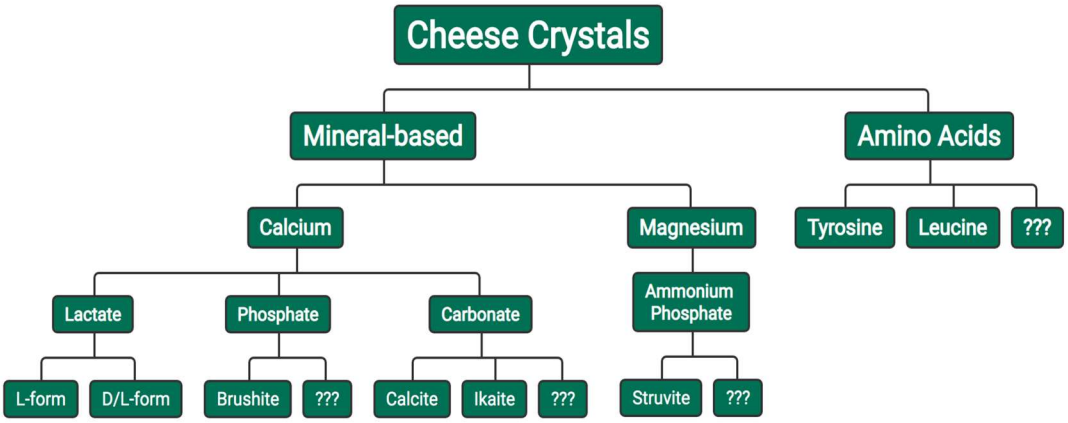

Figure 23 Cheese Crystal Types by the Kindstedt Lab (available online at https://www.cheesescience.org/crystal_types/)

3.3.5.1. Water loss

During the whole process of ripening a progressive loss of moisture due to evaporation takes place, which leads to a reduction in the weight of the cheese wheel. The weight loss of the cheese starts from the immersion in brine, with a reduction of about 4-5% in weight; the subsequent dehydration takes place during the whole ripening phase, which contributes to reduce the initial weight of the cheese by 10-12%, during the first 24 months of maturing (Resmini et al., 1974). Time and temperature-humidity conditions of the ageing warehouse affect the loss of moisture. Temperature and humidity conditions are in fact fundamental factors for ripening phase: the temperature of the aging rooms must be between 16 and 18°C, and the relative humidity between 82 and 85%. *Figure 24* shows the average humidity profile of PR cheese, depending on the ripening time. The graph confirms that the humidity decreases with the months, as attested by the literature (Zapparoli et al., 1997; Panari et al., 1988; Panati et al., 2003).

The humidity decreases rapidly, especially during the initial stages of ripening. The initial humidity is about 39% in weight as measured at the output of the caseous mass from the vat. Then it goes to 33% after 6 months of ripening. The cheese humidity drops very quickly with a reduction of 6 percentage points in the first six-twelve months, where the cheese reaches the typical texture and firmness. Then it continues to decrease more slowly to 31% at 24 months, where the cheese becomes more hard and brittle. Going forward with ripening, there is a moderate drop in humidity up to about 27% of moisture at 55 months of ageing. The latter moisture value represents the proportion of water in the wheel associated with caseins (Malacarne et al., 2006). However, the centre of the wheel is always more humid than the periphery, as confirmed by Tosi et al. (2008); in

fact the centre of the cheese compared to the external portion has a higher humidity of about 2 percentage units (Panari et al., 2003). This difference was previously established during brine immersion and it is held during the whole ripening time (Tosi et al., 2007).

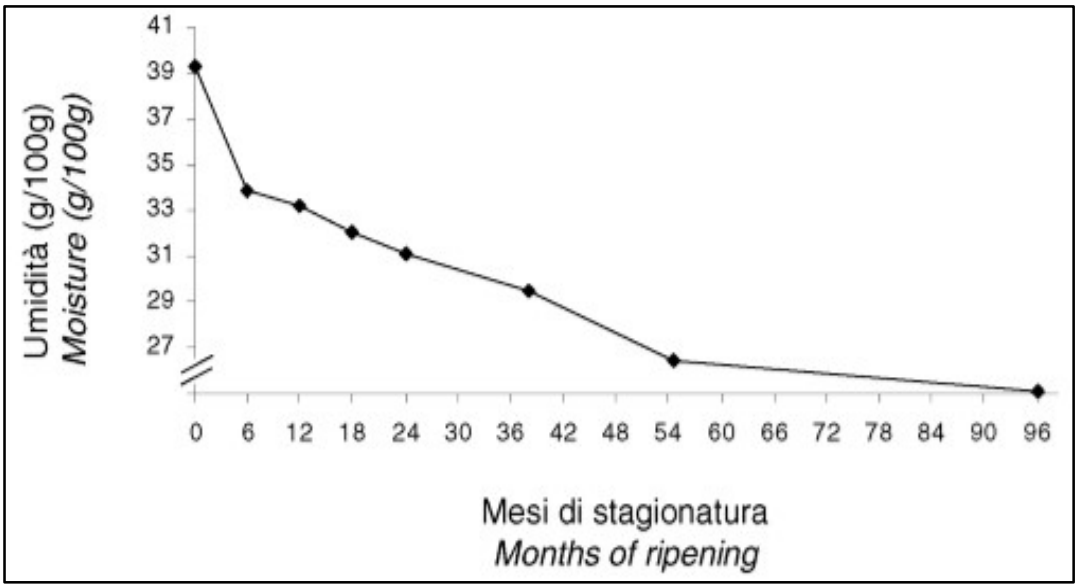

Figure 24 Moisture of PR cheese during ripening months (Malacarne et al. 2006)

3.3.5.2. pH variation

The pH value of the cheese, measured directly in paste, progressively decreases during the first hours of cheese-life in a non-homogeneous way between the different areas of the pasta and after about 48-72 hours it reaches almost similar values between the peripheral and the central part of the cheese (Mucchetti et al., 1995; Zapparoli et al., 2005). The cheese wheel size affects the gradient extent of ripening transformations along with axis and radial direction. It is widely accepted that the lactic acid bacteria develop with a different trend between the centre and the periphery of the wheel, resulting in an uneven distribution of enzymatic activities, proteolysis and lipolysis. After the first hours of cheese moulding, a different temperature gradient is established between the centre and the periphery, which induces selective pressure on mesophilic microorganisms close to the cheese rind and thermophilic bacteria at the cheese centre, resulting in a centripetal trend of the acidification process and consequently a corresponding maturation gradient (Mucchetti et al., 1995; Pecorari et al., 1995; Pellegrino et al., 1997).

As we can see in *Figure 25*, during the first months of ageing, the pH remains almost constant, then it increases rapidly until the sixth month. This increase was related to the alkalinization of the paste

consequently to the increase in ammonia due to the proteolysis, since ammonia nitrogen is the terminal ring of nitrogen catabolism, this tends to increase progressively. After the sixth month and up to 18 months the pH continues to increase but less markedly and reaches the maximum value around the values of 5.37-5.38. This is the result of two opposing effects: **proteolysis** from which ammonia is produced, and, on the other hand, **lipolysis** instead leading to the release of fatty acids which contribute to lowering the pH. After 24 months, however, the pH tends to fall, according to studies saying that after 24 months of maturation the proteolysis has a stop while continuing the release of fatty acids (Malacarne et al., 2006). The pH values measured at the centre of the wheel are generally higher than those of the peripheral areas, both at the exit from the brine and during ageing (Tosi et al., 2008). In fact, the acidification is faster at the periphery and the number of thermophilic lactic bacteria, introduced with the whey-starter, reaches higher values in the external part rather than at the centre (Mora et al., 1984).

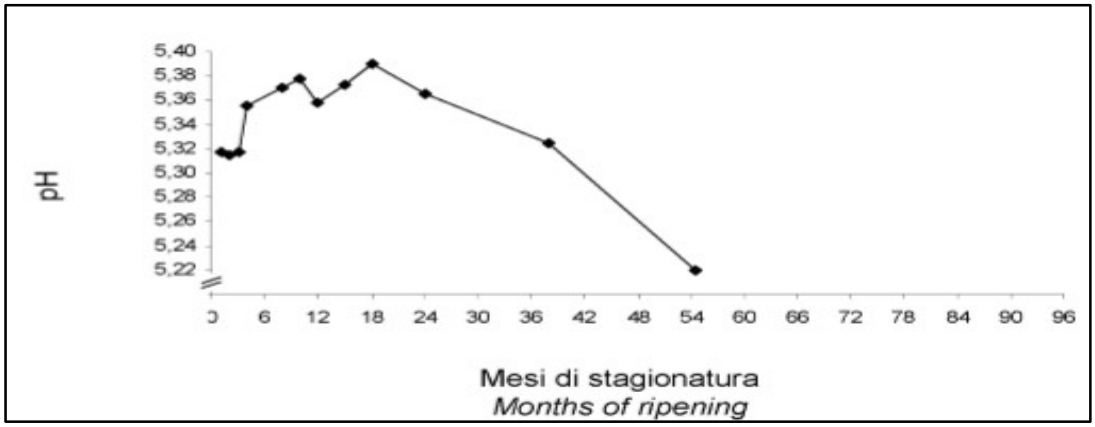

Figure 25 pH of the PR cheese during months of ripening (Malacarne et al. 2006)

3.3.5.3. Proteolysis

Proteolysis is one of the most important chemical transformations affecting the cheese structure development. The protein fraction, in particular the milk casein, is the quantitatively most important component of Parmigiano-Reggiano, equal to about 47% of the dry substance (Pecorari et al., 1995). Proteolysis is therefore the main phenomenon at the base of the cheese ripening process. Casein degradation occurs by the residual rennet coagulating enzymes as well as by native milk enzymes during the earlier months of ripening; later, it occurs by the action of the enzymes released from lactic acid bacteria and other endogenous microorganisms. The proteolysis involves the degradation of the caseins molecules in peptides with high molecular weight by means of *endopeptidase* enzymes. The peptides are then hydrolysed to peptones and peptides at medium-low

molecular weight by the *exopeptidases*. Finally the terminal amino acids of the proteins chains are released increasing the pool of free aminoacid inside the inter-granular space. The proteolysis' products contribute to both the production of flavourings and microstructure erosion, aiming to get the peculiar texture characteristics of this traditional cheese.

The development of proteolysis during the maturation of PR cheese is generally monitored analyticallyby determining the so-called **ripening index**. The ripening index is calculated as percentage ratio between soluble nitrogen at pH 4.6 and total nitrogen. This parameter represents the quantity of casein, which is progressively completely hydrolysed by proteolytic enzymes. In *Figure 26,* it can be observed that the casein is solubilized by 5% (ripening index %) when extracted from the vat (up to 48 hours), then it starts to increase and after 2-3 month of age it is solubilized by almost 10%. The degree of solubilisation of casein increases progressively with the age of cheese, especially during the first 6 months (up to 23-24%), then it continues and reach values of around 30% at 18 months of aging and around 33% at 24 months, as confirmed by the study by Pecorari et al. (1997). The soluble nitrogen increases rapidly during the first year of maturing, while in the second year the speed of growth is significantly lower and in subsequent years almost constant. In fact, after the 24 months of maturing, the ripening index remains almost unchanged, thus confirming that the proteolysis process takes place mainly in the first two years of maturation, as evidenced by literature (Panari et al., 2003; Malacarne et al., 2006).

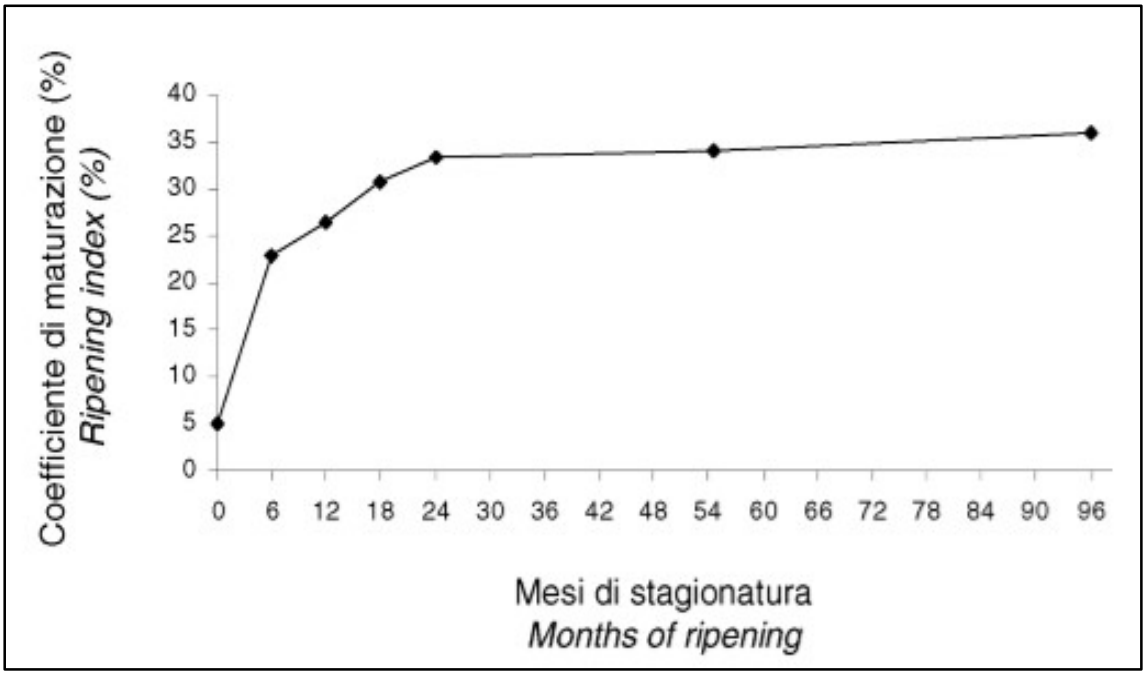

*Figure 26 Ripening index (N soluble at pH 4.6*100/N Tot) of PR cheese during ripening months (Malacarne et al. 2006)*

3.3.5.4. Lipolysis

In general, lipolysis (tryglicerides hydrolysis) in hard cheeses is very limited. Lipolysis determines important changes in both texture and rheological properties as well as in the formation of the aroma. The amount of fat contained in the PR cheese is principally conditioned by the fat/casein ratio of the starting milk in the vat, which is influenced by the initial fat content in milk, by its capacity for natural outcrop during nighttime rest, and finally by partial skimming of the milk. During maturation, the lipase enzymes of bacterial origin release fatty acids, whose consequent oxidative degradation leads to the formation of low molecular weight carbonyl compounds that have an impact on the aroma. The trend of lipolysis has been studied, as can be seen in *Figure 27,* by examining the trend of the percentage ratio between total content of free fatty acids (FFAs) and fat content in cheese, over ripening months. During the first 24 months, free fatty acids increase from 1% to 4.2%.

Unlike what is observed for proteolysis, the lipolysis process does not stop after 24 months of maturing but it continues with the same trend up to 55 months, reaching a percentage of free fatty acids of 7.7% compared to total fat. After 55 months there is a clear slowdown of the lipolysis process.

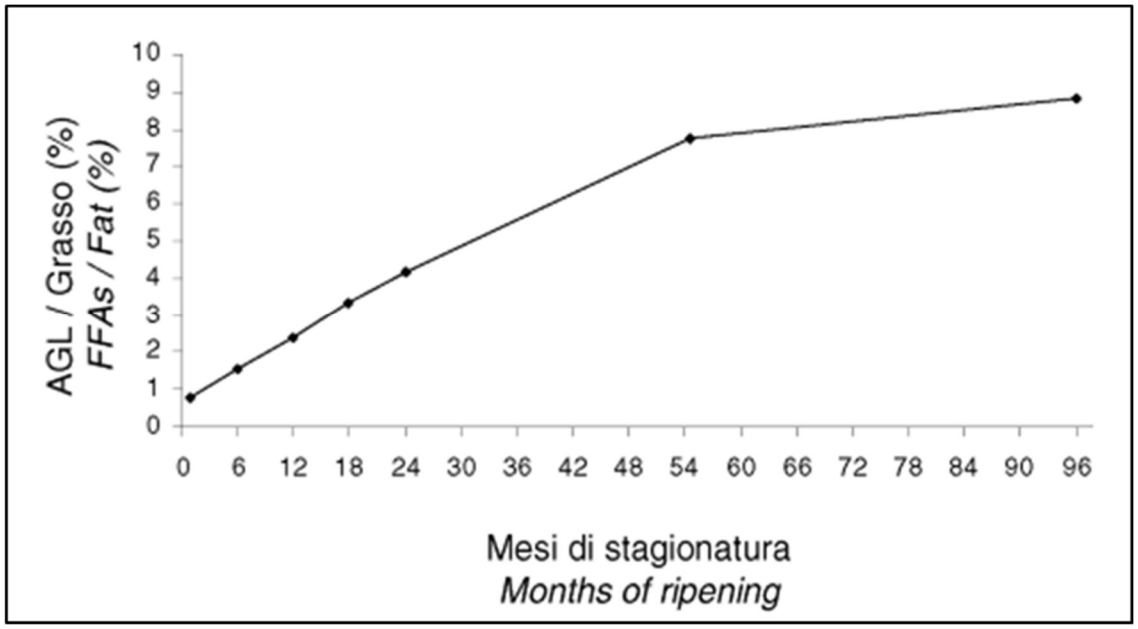

Figure 27 Lipolysis index of PR cheese during aging: value expressed as a proportion of the total content of free fatty acids (FFAs) and the fat content in cheese, compared to the months of ripening (Malacarne et al. 2006)

3.3.5.5. Crust formation

The structre development in PR chees follows diffusion limited mechanisms. The cheese crust arises from the strong gradients eshablished in both water and salts along with axial and radial directions. The crust rpresents about 18% of the entire cheese weight and has. The crust has a packaging-like function to protect the inner dough (cheese paste) from environmental contaminants as well as to modulate oxigen and water vapor exchanges with the environment.

Technological Variables

The ripening is influenced by all factors that can influence the development of microorganisms, their ability to produce enzymes and enzymatic activities such as pH, water activity, oxidation-reduction potential, salt concentration, temperature etc. (Malacarne et al., 2006). However, time of ripening, environmental temperature and relative humidity and cheese size are the main technological variable affecting the extent of proteolysis, lipolysis, and water loss along with axial and radial direction inside the cheese wheel.

4. RELATIONSHIP BETWEEN STRUCTURE AND CHEESE QUALITY

The texture of Parmigiano Reggiano cheese is made up of tiny structured granules and when fractured the cheese breaks into scale-like fragments. As already said, studying the internal structure of the PR cheese is important, because one of the characteristics imposed by the production disciplinary is related to the structure of the pasta: "*minutely grainy and flake fracture*", particularity certainly connected with the structure acquired during the production phases. To this we can add that almost all the defects, affecting this product especially during the ripening period, are structural defects (holes, vescicles, spongy areas, detachments, bulges).

The internal structure can be studied through different techniques, such as image analysis techniques, but also with mechanical and rheological tests, or finally with the aid of sensory analysis.

In instrumental analysis, the material interacts with the instrument that receives a physical stimulus and records it; through the recorded data, a statistical elaboration can be performed. While in the sensorial analysis the material interacts with the senses of man, more precisely with the sensorial perceptors that are special cells capable of perceiving stimuli and sending them to the brain, they send specific signals for each stimulus. The stimulus is then processed, translated and it generate a sensory perception, but the latter is influenced by various factors such as, for example, psychological, physical, cultural factors but also distractions in test environments etc.

4.1. Analysis of the State-of-the-Art

Searching of scientific documents focused on cheese structure and structure-related properties was carried out by using three major search engines, i.e. *Google scholar*, *Web of knowledge* and *Scopus*. With this aim, several keywords were used for selecting documents that include «traditional cheese», «parmigiano reggiano», «cheese texture», «rheological properties», «large-deformation rheology», «small-deformation rheology», «structure», «microstructure», «sensory analysis», «dairy products», «fracture mechanics», «fracture properties», «fracture stress», «fracture strain», «fracture mechanisms», «fragile fracture», «plastic fracture», «crack initiation and propagation». In order to manage the bibliography, the documents were exported in Bibtex language and managed with two widely known software, i.e. *Jabref* and *Mendeley*. More than 120 documents were analysed and categorized primarily by type of document (*Figure 28*):

- article (88%),

- book (6%),
- thesis (3%),
- conference (2%),
- in proceedings (1%).

Furthermore, the bibliography were catalogued according to the year of publication (*Figure 29*): most of the scientific works found on cheese structure are concentrated in the last 20 years, from about the end of the 90s, a period that also coincides with the birth of Internet, with peaks in 2002 (18 documents), followed by 2010 (14 documents) and 2012 (11 documents). Then, the documents were categorized by country of the corresponding author (*Figure 30*). The first country that has been involved in studying cheese and dairy products structure is USA with 46 documents, followed by France and in third place Italy with respectively 15 and 14 scientific papers, which correspond at 29% for USA, 10% for France and 9% for Italy.

The scientific papers were also divided per journal (*Figure 31*), noting that the scientific journals that have published more works on the themes are: *International dairy journal* (21 papers), *Journal of texture studies* (17) and *Journal of dairy science* (13).

Finally, the documents were divided on the basis of the instrumental approaches investigated, as can be seen in descending order, they are classified in this way (*Figure 32*):

I. Destructive mechanical techniques (37% of the total scientific documents),
II. Sensory analysis (29%),
III. Non destructive rheological techniques (15%),
IV. Imaging techniques (14%),
V. Calorimetry (5%).

Many of the scientific papers analysed coupled different independent techniques.

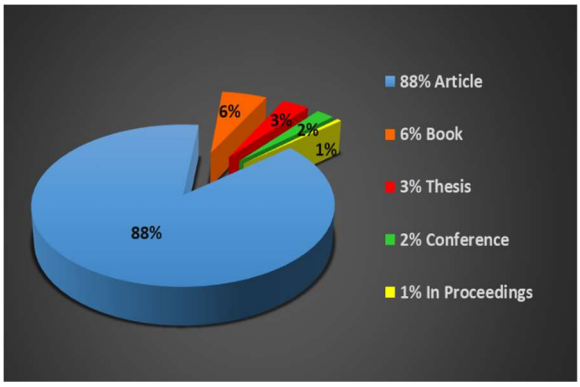

Figure 28 Type of documents focused on cheese structure

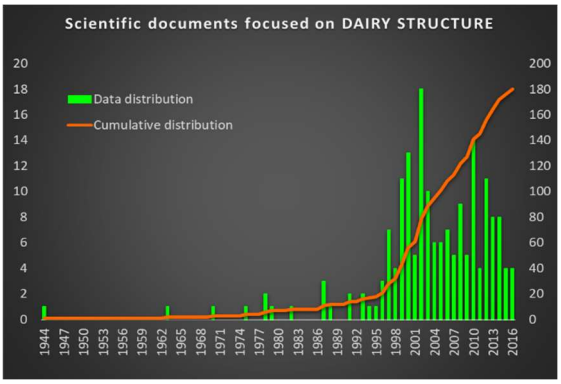

Figure 29 Year of publication of docs focused on cheese structure

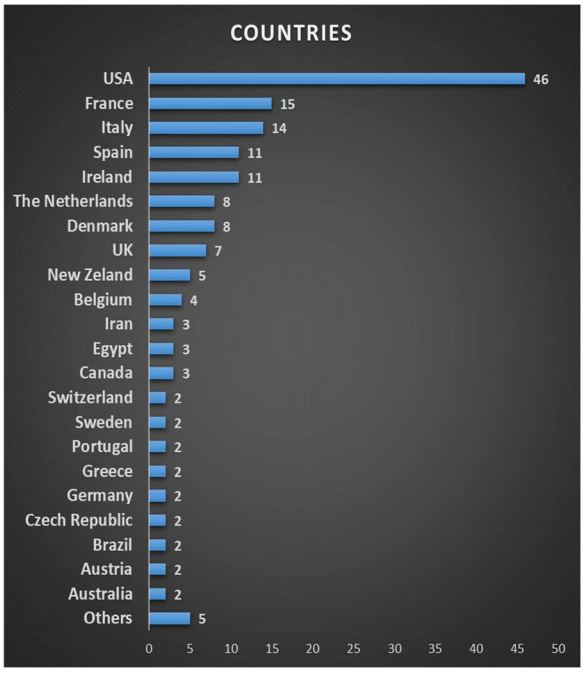

Figure 30 Country involved in cheese structure studies

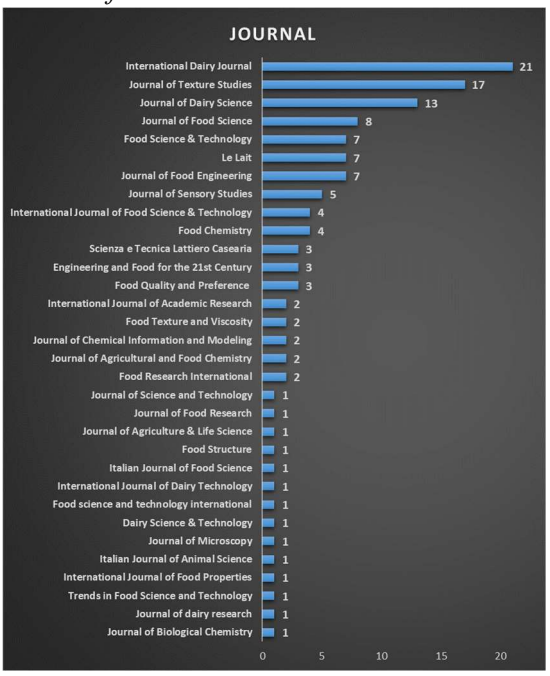

Figure 31 Scientific journal focused on cheese structure

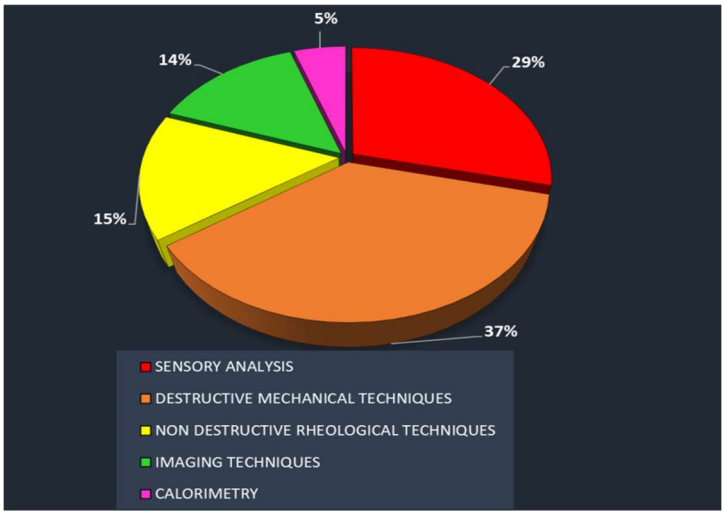

Figure 32 Approaches followed to investigate cheese structure

4.2. Sensory analysis

Under a sensorial perspective, a technical definition of cheese appearance is commonly used as to "grainy texture"; while an empirical definition of its fracture behaviour is "granulation", “breaking into splits” or "showing flake fracture". Unfortunately, tasting and sensory analysis are not the same thing, the tasting can be done by tasters, even non-expert ones, including consumers, to understand if the product is liked or not. The sensory analysis has a scientific foundation requiring training of tasters to distinguish sensation (chemical and physical stimuli) from their perception (psycho-rheology). The ability to register chemical and physical stimuli is linked to the sensitivity of the sense organs and is constantly masked by the effects of perception. The latter implies a complex brain-mediated processing of the stimuli received from the sense organs as influenced by numerous individual factors that include sex, age, health, habits, culture, emotions, personal experience and knowledge of the product to be tasted.

The capacity of the judges registered for the stimuli is assessed on the basis of the following criteria:

- discrimination, a capacity that a judge has to use the entire scale of available values to describe a certain characteristic;
- repeatability, the ability of a judge to assign the same value to a specific characteristic, of the same sample evaluated at different times;
- collimation, the ability to have consistent assessments among several judges.

Sensory analysis is performed according to standardized procedures and the results are statistically processed (Lavanchy, 1994). The tools used are the 5 senses:

1) **Sight**: even before the consumption of the food, the view creates stimuli for the consumer, which allow us to become aware of the size, appearance, shape and colour of the product, the external appearance is one of the most considered features.
2) **Smell**: it is the most subtle of our senses, smells and aromas are due to volatile substances which have the ability to interact with the mucus film located at the top of the nasal cavities that covers nerve receptors. Breathing in the air enters the nose and reaches the nerve receptors, the mucus envelops the volatile substances allowing it to come into contact with the hair cells that will recognize the molecule. The air, however, can come into contact with the hair cells even not directly, during the chewing process through the movements of the throat and the palate small movements of air are created which is sent to the nasal cavity

through the posterior passage constituted by the portion nasal pharynx, in this case we speak of retro-smell.

3) **Taste**: in this case, the receptors are the taste buds, which are found on the tongue but also in the palate and pharynx. The molecules are dissolved with saliva and reach the taste buds in liquid form. The tongue is a very important organ that perceives both tactile stimuli such as heat or food structure and chemical stimuli, flavours. Unlike the olfactory sensations the flavours remain identifiable manifesting at different times from one another. The basic tastes are five: the sweet, perceived mainly on the tip of the tongue; the salty perceived at the sides, anteriorly; the bitter on the bottom of the tongue and the sour on the sides, posteriorly; finally the umami taste is the fifth element at the center of the tongue. The salty and sweet, are perceived after about 1 second from the contact of the substance with the taste buds, the acid in a time space a little higher than 1 second and the bitterness takes 2 to 3 seconds. In the mouth, we also perceive the spicy, astringent, burning, stimuli called trigeminal sensations, because they are carried by the free ends of the trigeminal nerve.
4) **Hearing**: collects sound stimuli, in the case of Parmigiano-Reggiano it is not widely used, more used to appreciate the crunchy taste of an apple or the friability of a biscuit.
5) **Touch**: which involves two distinct sensory systems, in fact, we have tactile receptors in the buccal cavity and pharynx, and the tactile receptors of the skin; but also, in the muscles we find receptors that act in chewing and sucking. These stimuli give us answers on the structure of the food, on the resistance to hardness, on tenderness based on muscular effort to chewing or even and above all by touching and deforming the food.

The Judges carry out the sensory analysis using the sensory card. Each card is set according to the chemical or physical stimuli whose signal intensity is to be known, identifying the descriptive parameters and the intensity scales.

To date, the sensory analysis of Parmigiano-Reggiano is being perfected. In accordance with that stated by the guide for the sensory evaluation of the structure of hard or semi-hard cheeses. Within the FLAIR program (COST 902), a group was formed for the sensory analysis of cheeses. On the one hand, this group set out to harmonize the training of tasting juries and, on the other, to identify a common method of characterization for hard or semi-hard cheeses. A survey was carried out on five cheeses with "Controlled Denomination of Origin" (DOC): Comtè (France), Parmigiano Reggiano and Fontina (Italy), Mhaòn (Spain) and Appemzeller (Switzerland). After determining the importance of the structure of the cheese, which is located between appearance and flavour, and

after finding that no method mentioned in the literature was directly applicable, the group agreed on a common method. Surface, mechanical, geometric characteristics, as well as other kinesthetic and intraboccal sensations have been studied. To better clarify these sensations and their intensities, reference food products other than cheeses have been identified. It is, for example, apples, biscuits or the inside of a banana peel. Moreover, to allow the study of the relations between the instrumental and the sensorial analysis - the main objective of the FLAIR - the mechanical characteristics have been specified by physical and sensorial definitions, as well as by an original evaluation technique. The breadth of perception is given by a seven-point scale, in which three have been fixed to reference products standardized and known in all European countries. Semantic and socio-cultural difficulties have been taken into consideration. This guide was originally prepared in French and subsequently, according to the indications of FLAIR, translated into Italian, Spanish, German and English. The responsibilities of these translations fall on the various authors of this method.

The evaluation of the structure of a given food is based on the one hand on the choice of sensory characteristics to be perceived and on the other, on the training and training of the tasting group. If the classification of structure characteristics, proposed in 1963 by Szczesniak, is suitable for the study of different foods, however it cannot be applied directly in the sensory analysis of the structure of hard and semi-hard cheeses as it is too general. The recent work of Rohm (1990) on the rheological properties of dairy products confirms it. The international FIL 99A: 1987 standard for cheeses is descriptive and too superficial. In most cases the structure plays an important role in the evaluation of a cheese. Given the nature of the perceptions produced, it occupies a specific position between appearance and taste.

To evaluate the structure of the cheeses, these characteristics must be taken into consideration: surface area, mechanical, geometric and others. The descriptors taken into consideration were therefore classified in these four great classes of characteristics. The perceived intensity is expressed on an 7-point scale, which seems sufficient to express the differences between cheeses of different nature.

Several authors have tried to relate the sensory properties to the rheological properties of hard cheeses using the rating scale from 1 to 7 (proposed by EC FLAIR) for elasticity, firmness, deformability, brittleness, adhesivity, humidity, solubility, while granularity is sub-divided into four characteristics (fine, floury, grainy and coarse) each one with a three-level scale (low, medium, high). (Noel, 1996 and 1998; Drake, 1999a).

Noel et al. (1996) according to the Lavanchy's guideline requirements, as well as Romani et al. (2002), based on similar texture definitions as provided in G.A.s.Pa.Re. by the PR Consortium, determined the "**brittleness**" as the resistance of cheese samples to resist fragmentation during the first step of oral processing.

Different author evaluated instrumentally a texture-related property known as "fracturability" as the maximum force during the first step of a texture profile analysis of hard cheeses, i.e. Mahon (Benedito, 2000), mozzarella cheese (Tunick et al., 2000), Monte-rey Jack cheese (Brown, 2002).

4.3. Electron microscopy

A pioneering study by Annibaldi and Nanni (1979) monitored the evolution of the microstructure of the Parmigiano Reggiano at 24 hours after its production and after 5, 9 and 24 months of ripening. The internal architecture is a peculiar element of this traditional cheese. These authors discussed also on the origin of some defects affecting this traditional cheese during the ripening, since almost all the structural defects must be recognized for classification purposes. After 24 hours from production, the cheese shows curd granules not yet welded together and very deformed due to the bulk stress within caseous mass, under gravity. Between the granules, there are some interspaces that divide them; these cavities therefore contain aqueous serum. Furthermore, the external surface of the granules appears smooth and compact. The internal structure of the curd granule is porous with short, cylindrical caseous filaments, like a spongy structure. After 5 months of maturation, the internal structure of the curd granules is becoming more compact; the authors attributed this change to a probable a welding process of the fibres. From 9 up to 24 months of maturation, the dough continues to weld and appears almost a uniform and dense mass, rich in very small alveolations, probably due to the metabolic activity of lactic bacteria. The same authors in 1982 studied the structure of the curd starting from the moment of its formation under milk clotting condition, in order to evaluate the changes that occur in the structure of the curd granules after the action of the "spino" and after the increase in temperature during cooking. The authors used the SEM technique with a resolution up to 1µm. After the rupture of the caseous mass with the "spino" in the vat, the curd granules appear with a smooth outer surface and have intergranular spaces between them (*Figure 33*), confirming that the formation of the curd granules is caused by the breaking action of the spino and not by the thermal increase. Inside curd granules, the casein particles appear well bonded together to form casein agglomerates, in an evident protein network (*Figure 34*).

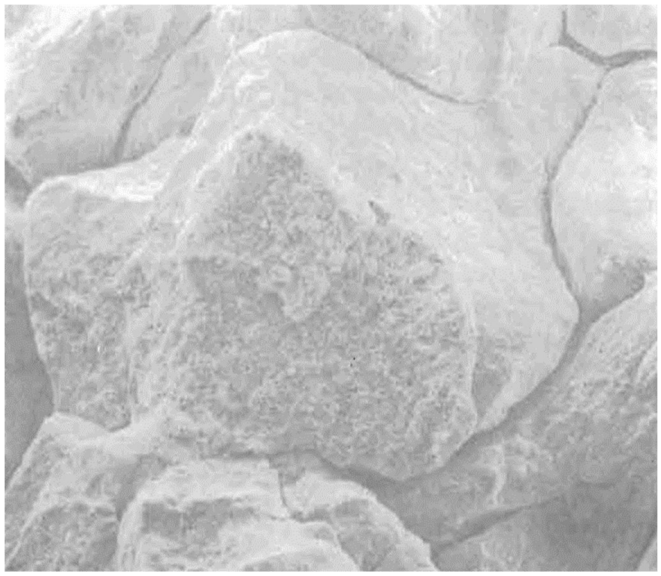

Figure 33 Intergranlar Giunctions of caseous curds in a 24hours Parmigiano Reggiano cheese specimen as pictured by SEM at magnification of 80x (ADAPTED FROM Annibaldi, 1982)

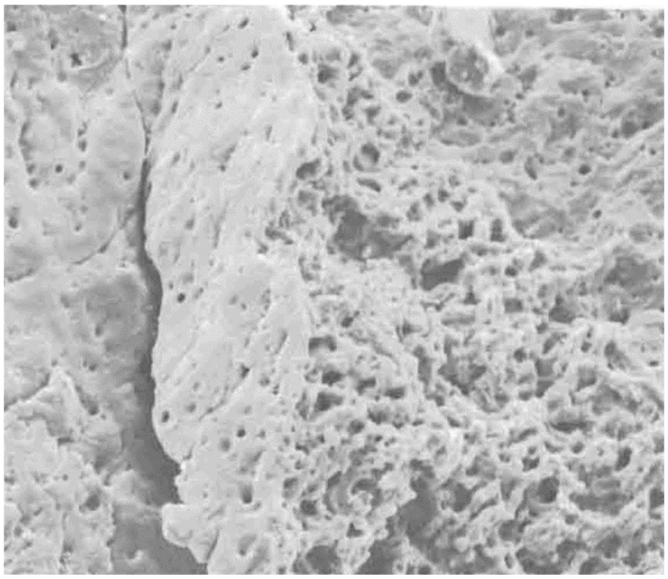

Figure 34 Inner Microstructure of caseous curds as pictured by SEM at magnification of 640x in a 24hours Parmigiano Reggiano cheese specimen (adapted from Annibaldi, 1982)

Brooker (1987) investigated calcium phosphate crystallization at the surface of mould-ripened cheeses using transmission electron microscopy (TEM).

Using TEM and light microscopy (LM), D'Incecco (2016) investigated composition and structure of different crystals usually present on cheese surface, widely known as crunchy "specks" and powdery smear, diffuse "spots" aiming to assess their chemical nature and technological origin in Parmigiano-Reggiano and Grana-Padano cheeses. The author showed that the spots appear to

consist of different coagulum particles having irregular shapes, which derive from manual cutting with the “spino”. The spots are rich in proteins and have cavities that include the joints between the curd granules. Compared to granule particles, the junctions appear at a resolution up to 50μm as thick protein strings, free of fat and rich in microcrystals. Therefore, the authors concluded that the intergranule spaces are rich in substances that then become crystalline, but also the interface between proteins and fats is rich in microcrystals, as it appears to be very irregular to TEM, due to the presence of needle structures (crystals). These aspects of microstructure are connected to the whole cheese production process. The crystals are formed by over-saturation of the hydrated areas; in turn the hydrated areas are conditioned by the way the cheese is produced, not only by the size and shape of the granules and inter-granular spaces, but also by the syneresis processes and by the cheese ripening itself. Water loss, salt spread are all factors that contribute to the increase in solute concentration during the whole process. All biochemical microbiological chemical transformations influence flavour and texture as perceived sensorially.

Other authors analysed cheese structure using confocal laser scanning microscopy (CLSM). CLSM offers an alternative way to observe food structure and it offers several advantages over conventional optical light microscopy, such as improved resolution (~0.2 μm) without disturbing the internal structure avoiding sample-cutting artefacts at the surface, and the ability to penetrate the surface of a sample and to visualize thin optical sections. Huc et al. (2013) used CLSM to study the organisation of fat and protein network in Swiss-type cheese matrix, around eyes and (2014) in semi-hard cheese examining fat and protein distribution during maturation. Fat globules were analyses using CLSM in Cheddar cheese (Gunasekaran, 1999) and in Emmental cheese (Michalski, 2004), the latter highlighting the distribution of small fat globules (~3 μm) and large fat globules (~6 μm).

The conventional SEM has some disadvantages regarding the sample preparation, as the cheese sample need to be frozen and fractured in liquid nitrogen to prevent any damage to the fat globules. Environmental scanning electron microscopy (ESEM) compared to the SEM has some advantages: in ESEM technique there is no need of any prior sample preparation, while in SEM the sample must undergo a complex preparation that limits the application of the technique and often can causes the introduction of artefacts. In fact, in ESEM samples do not need to be desiccated and coated with gold–palladium, and thus their original characteristics can be preserved for further testing or manipulation. ESEM differs from conventional SEM in that ESEM uses a gaseous environment in the chamber in which the sample is being microscopically examined. Compared to the examination

under vacuum in the case of the conventional SEM, ESEM allows the specimen to be examined at a relatively higher pressure, so it is not required to have the samples completely dry. This means that if water vapour is the gas used in the sample chamber of ESEM, hydrated samples can be imaged in their native state, with no alterations due to sample preparations (El-Bakry, 2014). ESEM performed at low intensity is not destructive. In addition, there is another major advantage of using ESEM rather than conventional SEM, in that the samples are not subjected to very low temperatures, e.g. -210°C when liquid nitrogen is used, during their preparation prior to the microscopical examination. However, both techniques have the limitation of having the possibility of exploring small samples: from a resolution of around 5 microns with a maximum field of view of 0.5 mm, to a resolution of the order of millimeters having a visual field of 2 cm and the structure image obtained is only related to the upper surface. Another limitation to ESEM imaging is the slight degradation of image quality and resolutions of about 5 nm are normally the resolution limit. Therefore, ESEM allows for the microscopical examination by a high resolution microscopy technique of food matrices with nearly no significant negative effects (artefacts created), particularly artefacts related to freezing and using very low temperature during the microscopical examination. Very few authors have studied the structure of cheese using the ESEM technique. Ayyash et al. (2011) analysed the structure of Halloumi cheese (a typical Cyprus cheese) with the aim of evaluating the effect of the NaCl and KCl salt on the quality of the cheese. Noronha et al. (2008) compared the effectiveness of a number of imaging techniques (cryo-SEM, ESEM, LM) for microstructural analysis of fat-reduced imitation cheeses containing different starch types. The author found that there was a considerable difference between cryo-SEM and ESEM micrographs in processed cheese, and they explained this difference as a result of the sample preparation required for the cryo-SEM. The ESEM micrographs showed a porous protein matrix rather than a smoothed surfaced matrix in the cryo-SEM micrographs. However, ESEM was not useful for distinguishing starch and fat globules. This might be a result of a lower resolution of the micrographs obtained, compared to cryo-SEM, which is considered a disadvantage of using ESEM technique for the microstructural analyses of cheese.

4.4. X-ray computed tomography

The use of X-rays to evaluate food microstructure has developed considerably in recent years. Several scientific articles in literature employed X-ray in order to study cheese structure.

Lee (2012) employed X-ray computed tomography (CT) to compare the eye formation at different stages of the Gouda-type cheese ripening. Guggisberg (2013) used CT to evaluate and quantify cheese eye volume in several type of cheese, and Schuetz (2013) evaluated eye number and total eye volume in Emmental cheese, and developed a procedure for an automatic recognition of opening defects such as cracks and coalesced eyes.

X-ray tomography has been applied also in other studies of food microstructure: (a) visualizing the 3-D structure of selected moist and dry food products by advanced X-ray imaging at micro- and nanometer resolution (Herremans et al., 2011); (b) visualizing and analysing the 3D microstructure of several aerated food products (De Man et al., 2015); (c) analysing of fat microstructure and quantification of the fat present in cream cheese-type products (Laverse et al., 2011a); (d) probing the porous structure of bread (Falcone et al., 2005); (e) visualizing skim milk powder deposits on a pilot-scale spray drier (Kota & Langrish, 2006); (f) visualizing and quantitatively characterizing intercellular air spaces in apple tissue (Mendoza et al., 2007); and (g) probing the microstructure of cream cheese and yoghurt (Laverse et al., 2011b).

Notable attributes of the CT technique are its non-destructive nature and an ability to view the internal structure and create a three-dimensional (3D) view of interior details of a sample. X-rays pass through the sample and projecting an image, then the sample rotates (along a vertical axis) of an angle and projects another image, then it rotates of another angles projects another image and so on. Thus, a large number of images are obtained and are processed with an algorithm to get a 3D view of the internal sample structure.

4.5. Differential Scanning Calorimetry

Differential scanning calorimetry (DSC) is useful to investigate the thermal properties (thermal conductivity, thermal diffusivity and heat capacity) of the cheese and is a useful tool to determine the melting and crystallization temperatures of fat.

Marschoun et al. (2001) evaluated the thermal properties (thermal conductivity, thermal diffusivity, and heat capacity) of Cheddar cheese with DSC, as a function of composition (fat, protein and moisture content) and age. The author explored a range of temperature between -10°C and 110°C with a programmed heating rate of 5°C/min.

Gliguem et al. (2009) in his work had the objective to investigate the structural and thermal behaviours of the fat fraction and to relate them to the small deformation rheological properties of

processed cheese and to the polymorphism of TGs. A temperature range between 3° and 60°C was explored with different rates (cooling rate of 0.5, 1, 2, 5, 10°C/min and heating rate of 2°C/min).

4.6. Rheological Analysis

In rheology one measures the relation between the stresses applied on a material and the corresponding deformations as a function of the time scale of the experiment (Steffe, 1996). Each force applied from the outside corresponds to an internal reaction force (mechanical resistance) that opposes deformation. The deformation can be reversible (elastic) or irreversible (plastic or viscose) and may imply a change in shape or volume. Rheological methods are analytical procedures that use instruments capable of subjecting a sample to controlled conditions of stress or deformation, to record mechanical spectra and to estimate resistance characteristics. Food can exhibit both solid and liquid characteristics, and rheology can identify the properties of such foods (Giese, 1995). The rheological behaviour of cheese is viscoelastic. A viscoelastic material exhibits both elastic solid and viscous liquid behaviour simultaneously under a wide range of conditions (Gunasekaran, 2002). The study of rheological properties can be realized with non-destructive tests or destructive tests. If it is true that the rheological properties are properties related to the physical structure of the material and, when evaluated in particular operating conditions that include manipulation, chewing or visual exposure, they are able to generate physical stimuli that are only virtually recognizable and distinguishable; it is also true that, due to adaptation and perceptive phenomena, the sensory evaluation of the rheological properties can become little reproducible and therefore of little relevance in the evaluation and classification of the quality of food products. Knowledge of the rheological properties measured instrumentally is also useful for designing the quality of a food product. The mechanical response that the cheese will have to the application of an **stress** or to a **strain** reflects its structure properties. The stress can be for example those that are applied during processing (for example, portioning, shearing, crushing or grating) and consumption (slicing and mastication) or those generated by universal machines used for the instrumental measurement of rheological properties. These properties include intrinsic characteristics of the material such as: elastic modulus, viscosity, plasticity, viscoelasticity, and other properties that are related to the structure at different levels of scale and therefore to the strength of the chemical bonds between the constituents of the cheese. The elastic properties are essentially linked to the number of covalent, conservative bonds within the limits of resistance; while the viscous, plastic properties are linked to weak bonds. The rheology of cheese is therefore the function of its composition and structure, that

is of the type and intensity of chemical-physical interactions between the components within the continuous volume of the material, at different levels of scale reflecting the presence of structural heterogeneities such as the junctions of curd granules, cracks and fissures and micro-pores generated during fermentation. The rheological methods therefore measure the mechanical properties of the material subjected to various defined stress and strain conditions (Brown, 2002).
Two classes of rheological tests have been identified: **small strain tests** and **large strain tests**. Small strain rheological methods are implemented within the linear viscoelastic region of the material and therefore, are designed to be non-destructive for the material. On the contrary, large strain rheological methods occur outside of the linear viscoelastic region and characterize the fracture properties of the material (Walstra, 1983).

4.6.1. Creep and Recovery test

Compression performed at constant load is known as "creep": in this case a constant load is applied, and the deformation is recorded over time. After the maximum deformation the imposed load is eliminated to evaluate the ability of a material to return to its original shape (elastic recovery). Each of these parameters provides useful information on the physical characteristics of the material in question.
Compression tests are used to determine how a product or material reacts when compressed, crushed or flattened by measuring the basic parameters that determine the behavior of the sample under a compression load (*Figure 35*). These include the elastic modulus, and the compressive force, the compression work. Compression tests can be performed as part of the design process, in the production environment or in the quality control laboratory. Many important parameters are obtained for the study of the material as the Young's Modulus a value that represents how much the material deforms during the compression load applied before the plastic deformation. After deformation the ability of a material to return to its original form is described as the elasticity of the material. Once a certain stress threshold is reached, a plastic or permanent deformation will occur and this is displayed on the graphs as a point where the linear behaviour is interrupted. A material can show one of two types of behavior: it will continue to deform until it breaks, or it will deform until it is flat. In both cases, a maximum stress or strength will be evident, providing its maximum value of compressive strength.
During a creep test a load is applied to a specimen maintaining constant temperature conditions. Analysing a creep curve (*Figure 36*) it is highlight three characteristic regions:

- The **first region** represented by the section **A-B**, where the instantaneous and completely reversible application of the stress takes place; (Elastic deformation)
- The **second region** represented by the **B-C** section, in this phase the deformation increases very quickly; (Visco-elastic deformation)
- The **third region** represented by the stroke **after point C**, in this phase the deformation increases in a linear way.

After the removal of the stress at point D (*Figure 37*), recovery follows a sequence similar to the creep, with three evident regions: an **instant elastic recovery** (D-E), a **delayed elastic recovery** (E-F) and a **flattening**.

The vertical distance from the flat part of the curve to the time axis is the non-recoverable deformation for unit stress, which is correlated to the amount of structural damage of the sample during the test. In the elastic region, the cheese matrix absorbs and retains the applied stress energy, this energy is released immediately after the stress is removed, allowing the cheese to resume its original size.

It is also important to remember that viscoelastic behaviour is significantly influenced by temperature. The viscoelastic properties are therefore functions not only of time but also of **temperature**. Dependence on time and temperature can be considered two phenomena linked to each other. In many cases, viscoelastic mechanisms can be attributed to processes of structure adjustment or to molecular diffusion processes under the action of applied stress. The speed with which these processes occur determines the viscoelastic response of the material. This speed, however, in turn depends on the speed of the molecules' motion, which is measured precisely with temperature.

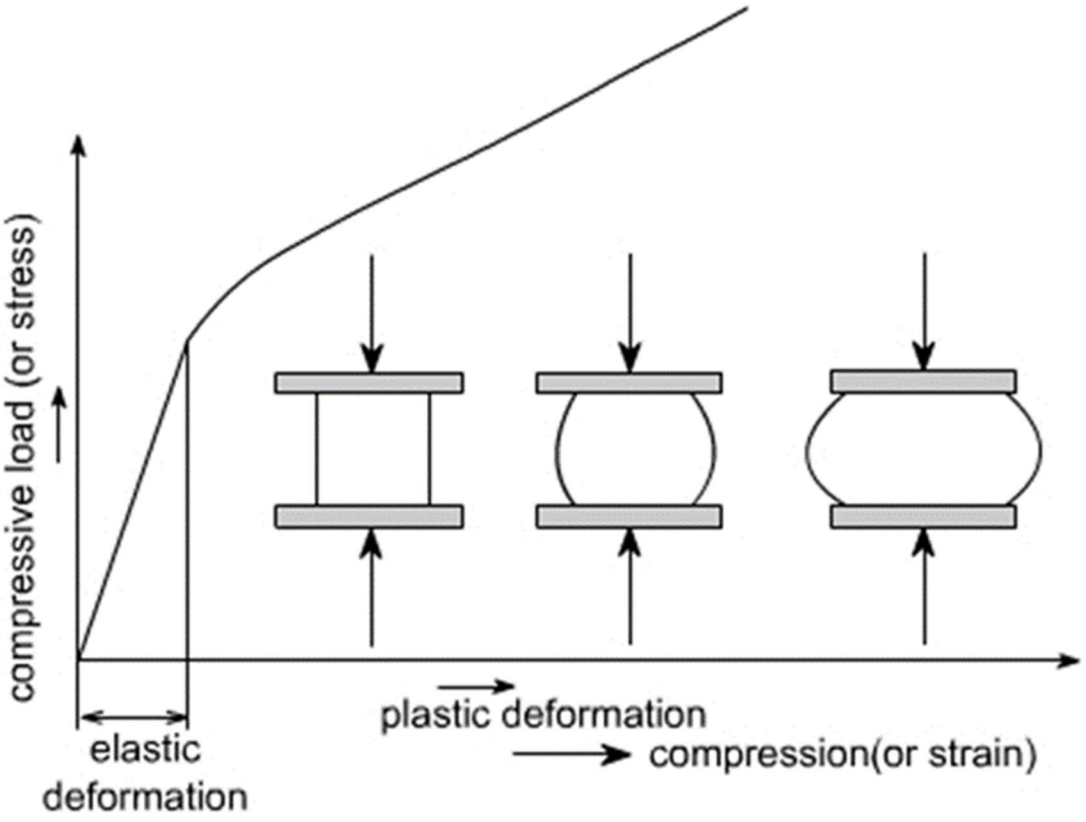

Figure 35 Example of compression and deformation of a material

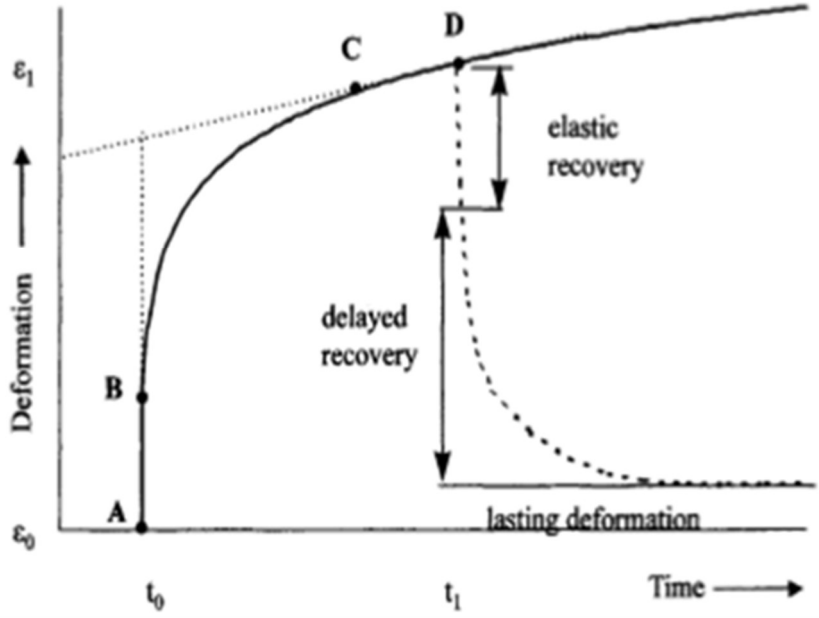

Figure 36 Three phases in the CREEP curve: A-B elastic deformation; B-C viscoelastic deformation; C-D plastic deformation

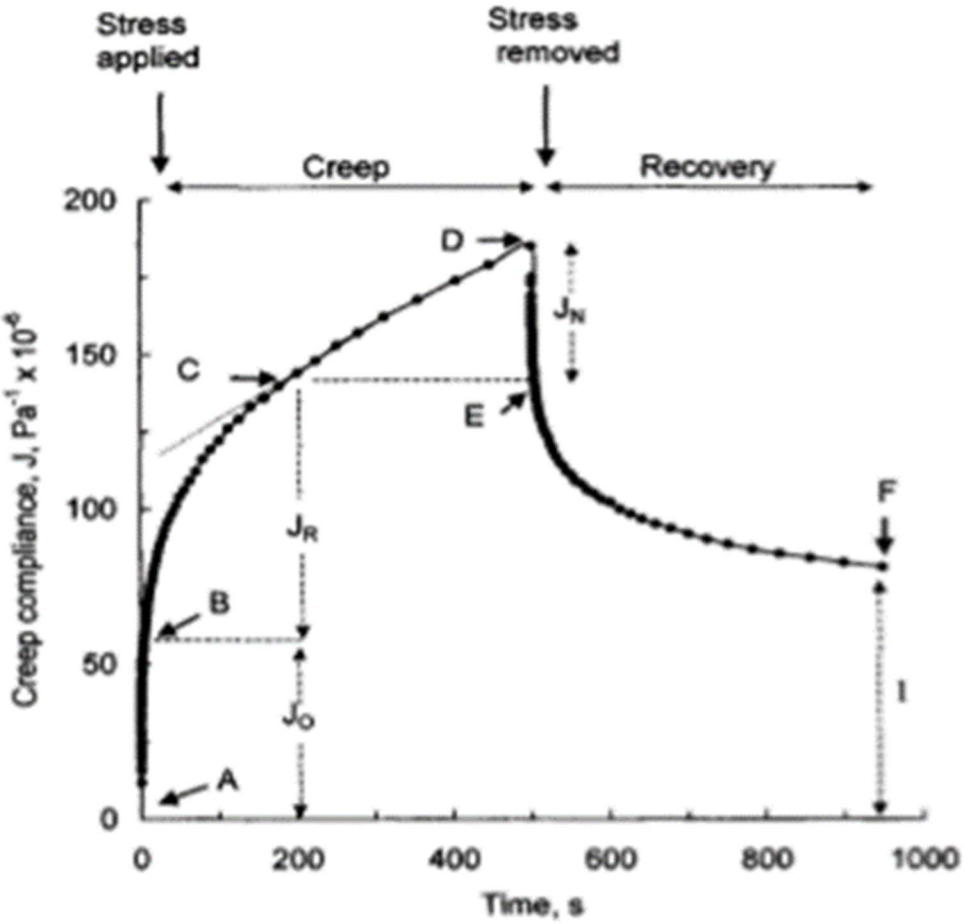

Figure 37 Creep-recovery curve

4.6.2. Small amplitude oscillation shear

The oscillatory tests when they are carried out in reversible conditions (small stresses or small deformations) allow to determine the fundamental elastic and viscous (plastic) properties, i.e. that depend exclusively on the composition and structure of the material and not on the experimental conditions adopted for their determination. The possibility of setting the temperature allows us to estimate the dependence of the rheological properties on temperature.

The small amplitude oscillatory shear (SAOS) measurements are commonly used to study the linear viscoelasticity of cheese and other foods. In SAOS analysis, stress and strain are varied harmonically with time within the linear viscoelastic region. The main feature of SAOS tests is that, due to small strain and stress used, they can be considered as objective and non-destructive tests suitable for probing material structure and structure development during different processes.

SAOS is a technique that provides information on the energy stored and released in the sample being tested. The data obtained during a test include the complex modulus G, which is a measure of the total energy required to deform the specimen and is defined as:

$$G^2 = (G')^2 + (G'')^2 \quad (2)$$

Where G' is the **elastic modulus** (or storage modulus), a measure of the energy stored in the material during an oscillation, and G'' is the **viscous modulus** (or loss modulus), a measure of energy dissipated as heat.

$$tan\delta = \frac{G''}{G'} \quad (3)$$

When, G′ = G″, tanδ = 1 and the modulus value at this point is called the "crossover modulus." At tan δ = 1, the material is equally liquid and solid. When tan δ<1, the material is more solid-like, and when tan δ>1, the material is more liquid-like.

There are four major experimental variables in any dynamic test: strain (or stress), frequency, temperature, and time. Thus, changing one or more of these experimental variables, the commonly performed tests are: strain (or stress) sweep, frequency sweep, temperature sweep, and time sweep.

Many authors used SAOS on cheese. Tunick (2010) evaluated the usefulness of activation energy data in cheese analysis by examining a range of cheeses (cheddar cheese, mozzarella, Parmesan-type cheese) with a variety of characteristics. Gliguem (2009) studied thermal and rheological properties in spreadable processed cheese. Del Nobile (2007) evaluated the changes in the elastic modulus, storage modulus and loss modulus of Canestrello Pugliese cheese during ripening. Bowland (2001) conducted small strain analysis to investigate properties of a model processed cheese exhibiting different large strain mechanical properties. Drake (1999b) evaluated the relationship between sensory and instrumental texture measurements of cheddar cheese, Brie, Feta, Parmesan-type cheese and others.

4.7. Mechanical Analysis

Universal testing machines allow to apply stresses or deformations in a much wider range than rheometers. Universal testing machines are used classically for destructive tests, offering the possibility to choose between a large number of experimental conditions that include the stress mode (compression, traction, bending), the speed of application of force or deformation.

4.7.1. Uniaxial Compression test

Compression tests are used to determine how a product or material reacts when it is compressed, crushed or flattened by measuring the fundamental parameters that determine the behaviour of the sample under a constant or variable load. These include the elastic modulus, and the compressive force, the compression work. Since the elastic modulus should preferably be measured in traction conditions, the measurement of the elastic modulus in compression is constrained by the need to operate at relatively contained loads or deformations to avoid the effects due to the interpenetration of the material and the response of the constraint (support).

Uniaxial testing is also the most popular method for instrumental evaluation of cheese texture (Meullenet, 1997).

4.7.2. Three-point bending test

There are different types of bending tests that differ from each other by the type of support for the specimen and the number of load points. The most used and common ones are those with 2 to 3 and 4 points. Three-point bending tests are usually standardized (international standards of the ISO and ASTM series). They are performed to determine the bending properties of the materials and for the visual analysis of the behaviour during flexion. In this type of test, the sample is placed on two supports and is centrally positioned with respect to the upper anvil support. The distance between the lower supports can be adapted according to the size of the specimen. This test is particularly suitable for fragile products for which the application of traction conditions may become difficult. During the three-point bending tests, the compression of the upper layer of the sample and the traction of the lower layer of the same occur simultaneously. The resistance to bending and breaking of a sample allows better understanding the structure of a material.

In general, a three-point bending test must be performed by applying the load to the central part of the specimen, in this way a torque is generated along with the applied load direction. Under these conditions, a null stress is generated along with the central plane that divides the specimen width (W). The applied stress is distributed in a compressive way in the upper half and in a tensile way in the lower half of the specimen with a gradient of equal intensity but opposite with the respect to its direction (*Figure 38*).

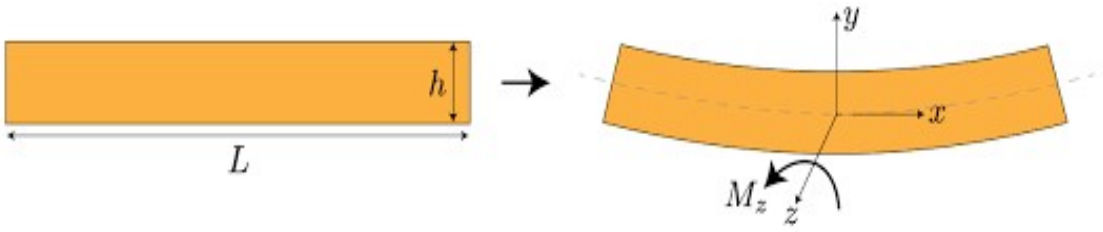

Figure 38 Bending moment under three-point bending test

Very few authors investigated the cheese mechanical properties using three point bending test. Imbeni (2001) studied the mechanical properties of mature cheddar cheese at different rates and different temperatures using both uniaxial compression test and three point bending test. Confirming that, in viscoelastic materials, mechanical properties will depend on testing conditions, therefore the resistance to cracking and yielding of cheddar cheese is both rate and temperature dependent. Vanevenhoven (2012) characterize the mechanical properties of Gouda cheese, through single-edge notched bend test. The author evaluated the fracture toughness, noting that, increasing with ripening time this decreases up to a constant value for the remainder of the aging period.

Theoretical analysis of the torque enhables to define key mechanical properties as a function of geometrical features of the specimen as well as of inertia and applied stress as follow (Kim et al., 2011):

Mechanical properties of SENB specimen	*Formula*	*Description*
Linear Elastic Stress	$\sigma_{EL}(i) = \frac{3P_{EL}(i) \cdot S}{2B \cdot \left(\frac{W}{2}\right)^2}$	*$P_{EL}(i)$ is the maximum elastic load as determined at the end of linear part of the load-displacement curve (it represent the maximum rate of change in load-displacement relation)*
Non linear Elastic Stress	$\sigma_0 = \frac{3P_0 \cdot S}{2BW^2}$	*P_0 is the maximum elastic load at the non linear part of the load-displacement curve (it represents the upper limit of reversible but non linear relation between load and displacement)*
Maximum Stress (Stress required before crack propagation)	$\sigma_{FR} = \frac{3P_{UTS} \cdot S}{2B \cdot W^2}$	*P_{UTS} is the maximum load registered on load-displacement curve (it represents the upper load the specimen will be able to bear before a crack to propagate)*
Yielding Stress (Material Strength)	$\sigma_{YS} = \frac{3P_{YS} \cdot S}{2BW^2}$	*P_{YS} is the load at which the specimen undergoes yielding before crack initiation (it ranges from P_0 and P_{UTS})*

Effective Stress (Stress required to start a crack)	$\sigma_y = \frac{\sigma_{YS} + \sigma_{UTS}}{2}$	*It represents the stress status where a plastic strain occurs effectively to start a crack*
Linear Elastic Strain	$\varepsilon_{EL}(i) = \frac{6 \cdot W \cdot P_{EL}(i)}{S^2 m}$	*It represents the maximum strain linearly related to the applied stress*
Non Linear Elastic Strain	$\varepsilon_0 = \frac{6 \cdot W \cdot P_0}{S^2 \cdot m}$	*m is the maximum rate of change of the load-displacement relation (it is calculated on the non linear part of the experimental curve before the yielding)*
Flexture Modulus	$E_f = \frac{S^3 \cdot m}{4 \cdot B \cdot W^3}$	*It represents the maximum resistance to the elastic deformation (Young Modulus)*

4.8. Fracture Mechanics Theory

The stress status of a material in a generic point is generally a function of both the boundary conditions (body geometry, geometry and size of structural discontinuity, applied stress mode) as well as the constitutive law of the material that rule out its behavior in response to the applied stress.

If we analyze the fracture at the atomic level, we can show that the bond strength between the atoms for a generic material is approximately equal to E / π (where E is the elastic modulus). This does not agree with the experimental evidence because the experimentally detected fracture stress is from 2 to 3 orders of magnitude lower than the elastic modulus. From an engineering point of view this phenomenon is actually associated with the concentration of the stress around the apex of the structural discontinuity. Microcracks, pores, slits, may originate from debonding of atoms, nucleation, growth and coalescence of microcracks and microcavities. Also interfaces between different chemical phases can concentrate the applied stress. The extent of stress concentration depends on both the stress magnitude and the way in which the external load is applied to the material. The following simple load modes can be defined for a hard cheese (Gunasekaran, 2003):

1. Brittle or quasi-brittle failure — fracture, i.e. the cracking resulting in two or more separate pieces, occurs without appreciable strain

2. Ductile failure — rupture at large plastic strain at low temperature (~1/4 of the melting temperature)
3. Creep failure — rupture at large plastic strain at high temperature (>1/3 of the melting temperature)
4. Fatigue failure — rupture due to repetitious loading either above or below the Yield Stress; may be further classified into low-cycle, high-cycle, and gigacycle fatigue damage.

Any fracture, rupture or crack mechanism are closely related to the material's microstructure.

The way in which a cheese sample fractures may be different. In general, two fracture modes may be distinguished, viz. fracture in tension and in shear mode. However, tfracture mode is not always unequivocally related to the way in which the test piece is stressed. Both in atension and in a uniaxial compression test the test piece may fracture either in tension or in shear. In the frequently applied iuniaxial compression test, fractue always starts at the outside if it occurs in tension, while it normally starts in the interior of the test piece if it occurs in shear. In compression, the tensile stress is caused by the increase in circumference of the test piece. The science of fracture mechanics approaches analytically the relations between stress and strain during fracture under standardadized fracture conditions, in which one mode of fracture can be considered dominant. According to fracture mechanics, there are three ways of simple loading *Figure 39*, that is the way in which the external load is applied to the material:

I. **Mode I**: it refers to the material **opening** under tension, in which the load is applied orthogonally to the crack plane, causing the so-called "plane strain condition", i.e. the stress is negligible along with the direction orthogonal to the crack plane;
II. **Mode II**: it refers to the **sliding** or cutting, in which the stress is of parallel along with the crack plane, causing the so-called "plane stress condition", i.e. the strain is negligible along with the direction orthogonal to the crack plane;
III. **Mode III**: it refers to the **tearing**, in which the stress is of cutting along the plane of the crack in a direction orthogonal to it, causing the material to tear and slide along itself and causing the so-called "plane stress condition", i.e. the strain is negligible along with the direction orthogonal to the crack plane

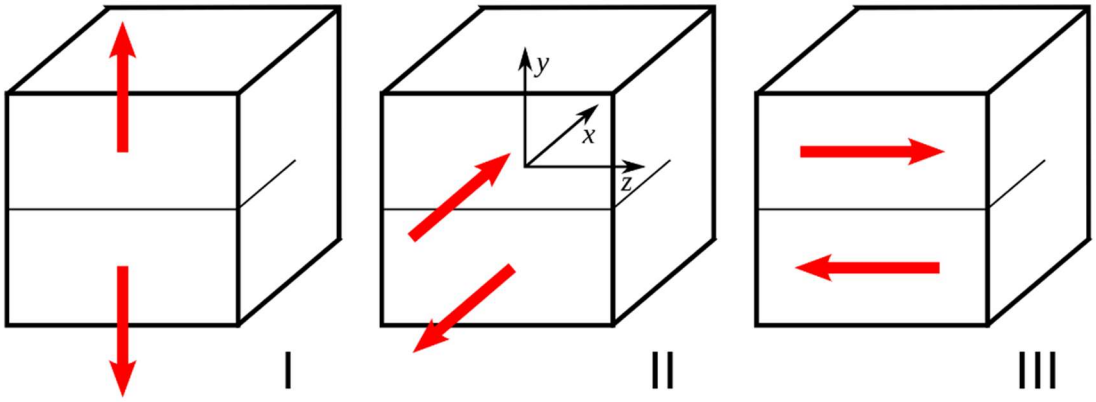

Figure 39 Typical failure modes in engineering materials

The application **Mode I** is the typical stress\status that can be achieved under three-point bending test using a specimen in which a notch was previously created centrally on the surface opposite the load application point.

The **mode of fracture** is required for standardization of measuring the law requirement for PR cheese, i.e. the "frattura a scaglie".

Energy Balance in Fracture Mechanics

Considering a material containing a structural discontinuity subject to an external load P, the work carried out under equilibrium conditions by the external force P causes an increase of potential energy that is equal to the elastic strain energy, i.e the mechanical energy stored inside the elastic atomic bond (it can be released completely when the stress is removed) (Gunasekaran, 2002):

$$U_{ext} = U_{el} \tag{4}$$

The elastic strain energy U_{ext} is calculated by integrating the energy density on the volume of the test material as follows:

$$U_{ext} = \int \sigma \cdot d\varepsilon \tag{5}$$

where (σ) is the stress tensor (Pa / mm ^ 2) and (ε) the strain (dimensionless)

If the external force P increases to the level required for a crack to propagate, the energy balance due to the infinitesimal increase of the crack area (dA) can be rewritten:

$$\frac{dU_{ext}}{dA} = \frac{dU_{el}}{dA} + \frac{dU_{sup}}{dA} + \frac{dU_{cin}}{dA} \tag{6}$$

where, U_{sup} is the inner energy required to break the interatomic bonds of the material along with the fracture surface and it represents the energy of formation of the new fracture surfaces); U_{cin} è represents the inner energy expended to strain small portions of material around the new apex of the

crack (Process Zone) during crack propagation (it represents the kinetic energy to propagate the crack).

Defining as the releasing rate of potential energy (G) as the difference between the mechanical energy provided by the external load and the reversible energy stored in elastic deformations:

$$G = \frac{dU_{ext}}{dA} - \frac{dU_{el}}{dA} \tag{7}$$

the balance equation is rewritten as follows:

$$G = \frac{dU_{sup}}{dA} + \frac{dU_{cin}}{dA} \tag{8}$$

This expression indicates that a fracture can propagate when the work done by the external load compensates the elastic deformations of the material. Thiis means that the elastic strain energy due to elastic deformations (reversible) is enough to compensate for the energy required (i) to form new fracture surfaces through covalent bond breakage and (ii) to propagate the Process Zone ahead inside the material bulk.

The kinetic energy involved during propagation of a crack of size (2a) inside a plate of thickness (B) is calculated as follows:

$$U_{cin} = \int_0^A (G - R)dA = \int_{a_0}^W (G - R)Bda \tag{9}$$

where the maximum elastic energy (R) is the material resistance to initiate a fracture, that is the fractional strain energy enough to break the covalent bonds:

$$R = \frac{dU_{sup}}{dA} \tag{10}$$

thus, the balance equation can be rewritten in a definitive way

$$G = R - \frac{dU_{cin}}{dA} \tag{11}$$

This analytical expression indicates that the crack can propagate inside a material when the potential energy released under external work is enough to win both the elastic and plastic strains.

Energy criterion for crack propagation from a material discontinuity

In general, the fracture criterion from a cracked material include both the geometrical and/or energetic conditions for a discontinuity to advance within its structure. Regardless of the methods of application of the external load (I, II or III), the energy balance equation represents the most accepted criterion provided by the fracture mechanics theory:

$$G = R - \frac{dU_{cin}}{dA} \tag{12}$$

The energy balance suggests that a discontinuity start to propagate when the releasing of potential energy (G) equals (or exceeds) the energy consumption to break the covalent bonds (R):

$$G > R$$

Any excess of potential energy that is released will be transformed into kinetic energy required for the crack to propagate inside the material bulk. The first member is called **Strain Energy Release Rate** at the apex of the crack or **Driving Force** of the fracture mechanics (it has units of a force per crack surface increase). The second member, indicated by, represents the energy required to break the covalent bonds where the fracture initiates, it is called **Crack Resistance** or **Fracture Toughness**. The rate of strain energy release (G) is a function of the geometry of the test specimen, of discontinuity size and stress intensity. G can be obtained either experimentally or analytically for a given configuration of cracked test specimens and stress intensity. The resistance of the material (R) required to initiate the fracture is measured experimentally using standardized test specimens and test conditions. For perfectly fragile materials (linear elastic behavior), R can be considered a material property that does not depend on the initial crack size. However, for materials that present plastic deformations (the most of real materials), R must be considered a material property strictly dependent on initial crack size. The materials that present phenomena known as "work hardening" of the structure under strain, that is when the strain work requires increasing stress, it will undergo an increasing of fracture toughness before crack initiation. Thus, the energy-based fracture criterion indicates also the conditions for a crack to propagate. Indeed, when a crack advances by an infinitesimal (da), both parameters G and R vary; therefore, in order a crack to propagate further, the criterion must be verified again. The instability criterion, that is the conditions under which the fracture occurs spontaneously and rapidly (it is known as **Unstable Fracture**) is:

$$\begin{cases} G \geq R \\ \dfrac{dG}{da} \geq \dfrac{dR}{da} \end{cases}$$

A graphical representation of the energy criterion for fracture mechanics is obtained by placing the magnitudes G and R on the y-axis and dividing the x-axis into two parts, i.e. on the left part of the axis origin the length of the initial crack (a_i), while, on the right the length increments of the crack Δa (fracture propagation).

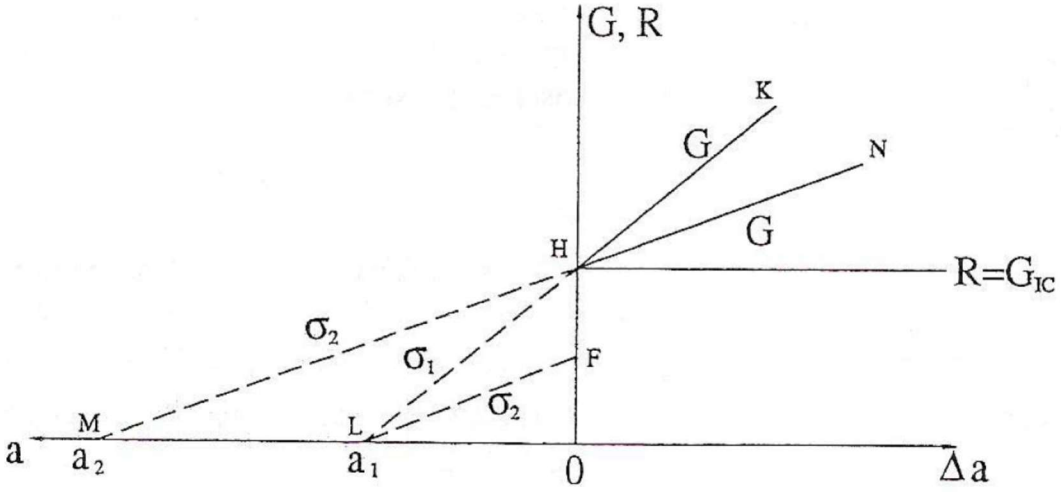

For an initial crack of size a_1 and an external stress σ_2, the **Strain Energy Release Rate** (G) is represented by the point F. For the crack a1, when the stress varies between 0 and σ_2, G varies from O to F. Increasing the stress to σ_1, G reaches the point H where the **Fracture Toughness** is equal to R, i.e. the material fracture resistance. The propagation of the crack under the stress σ_1 occurs along the HK line where the strain energy release rate G is always greater than the fracture toughness R. A crack $a_2 > a_1$, under a stress variable from 0 to σ_2, the strain energy release rate G vary from 0 to H (the parallel lines LF and MH correspond to the same level of the applied stress). The crack propagation occurs at H point where the strain energy release rate G is always greater than the fracture toughness R alongwith the HN line.

Stress Intensity Factor rules for the stress state at the apex of a material discontinuity

From the physical point of view, the material fracture occurs due to the concentration of the tensional state around the apex of a structural discontinuity. For various configurations of the discontinuity and different ways of applying the external load it is possible to obtain simple and compact expressions able to describe the state of stress at different distances from the apex. In the case of load application Mode I the following general expression is:

$$\sigma = \frac{K_I}{\sqrt{2\pi r}} \tag{13}$$

K_I is widely known as the Stress Intensity Factor at distance r from the apex of the discontinuity as it is subjected to tension stresses (fracture mode I). The entire state of stress at the apex of a discontinuity is univocally determined by the dimensional K_I. K_I can be used directly as a criterion for estimating the initiation for the fracture of a solid material showing linear elastic fracture

mechanics (LEFM). In general, for ideal elastic bodies or for real bodies for which only the elastic deformation and microscopic plasticization around the discontinuity apex take place, K_I can be calculated using the following formula:

$$K_I = \mathrm{Y}\left(a_{eff}\right) \cdot \sigma \cdot \sqrt{2\pi a_{eff}} \tag{14}$$

where the term a_{eff} represents the effective distance from the apex of a crack able to account for the so-called Process Zone, i.e. the small volume around the discontinuity where the strain phenomena were bounded during crack propagation; $Y(a_{eff})$ is known as a geometric factor and it is related analytically to the radius r_y of the Process Zone:

$$a_{eff} = a + r_y \tag{15}$$

$$r_y = \left[\frac{1}{2\pi} \cdot \left(\frac{K_I}{\sigma}\right)^2\right] \tag{16}$$

Literature focused on the theoretical analysis of the stress field around the discontinuity apex have been carried out based on Finite Element Modelling (FEM) provided usefull analytical solutions for the geometrical factor to be considered for a test specimen. When the applied stress reaches the critical value (σ_Y) of the material, i.e. it is sufficient to overcome the mechanical resistance and propagate a crack, K_I reaches a critical value, in this case it is indicated with K_{IC}, and it can be calculated taking into account the width (ry) of the plasticization area at the apex of the crack and using an analytical Finite Element Modelling (FEM) solution for the geometrical factor from literature.

Crack propagation resistance according to ASTM recommendations

The resistance to stable fracture and unstable fracture is based on the calculation of different values of the elastic and plastic contributes to the whole J-Integral as calculated around the crack apex. The J-Integral is a mathematical expression representing a line or surface integral that encloses the crack front from one crack surface to the other, used to characterize the local stress-strain field around the crack front:

$$\mathrm{J} = \int_{\Gamma}^{n} W dy - \vec{T} \cdot \frac{\delta_{\vec{u}}}{\delta x} ds \tag{17}$$

Where

W is the loading work per unit volume or, for elastic bodies, strain energy density;

Γ is the path of the integral, that encloses (that is, contains) the crack tip;

Ds is the increment pf the contour path;

$\vec{T}$ is the outward traction vector on ds

$\vec{u}$ is the displacement vector at ds

x, y, z are the rectangular coordinates

Is the rate of work input from the stress field into the area enclosed by Γ.

The J-Integral obtained from this equation is taken to be path-independent in standardized test specimens, but caution is needed to adequately consider loading interior to Γ such as from fast crack propagation or from residual or thermal stresses. In the elastic (linear or non linear) solids, the J-Integral equals the crack-extension force G (releasing rate of strain energy), i.e. the elastic energy per unit of new separation area that is made available at the front of an ideal crack in an elastic solid during a virtual increment of forward crack extension In the elastic (linear or non linear) solids for which the mathematical expression is path independent, the J-Integral is equal to the value obtained from two identical bodies with infinitesimally differing crack areas each subject to stress. The parameter J is the difference in work per unit difference in crack area at a fixed value of displacement or, where appropriate, at a fixed value of load.

Under Mode I of fracture, when both the conditions of plane deformation and of the small scale of deformation on the apex of the crack (SSY) are guarantee, the following mathematical expressions can be used to couple the elastic to plastic contributes:

$$\begin{cases} J_{tot} = J_{EL} + J_{PL} \\ J = \frac{K_I^2 \cdot (1-\nu^2)}{E} + J_{PL} \end{cases} \tag{18}$$

PART II

5. MATERIALS AND METHODS

5.1. Sampling criteria

The availability of whole cheese wheels of PR with a large variability of structure was the starting requirement for the design of experiments as well as for preparation of cheese specimen to be investigated for their structure and structure-related properties. With this aim, a multilevel sampling was performed.

The **first-level** of **sampling** aimed at acquiring cheese wheels with inner structure varying in the widest range possible. With this aim, 12 ripening times were selected among different cheese factories operating within the PDO territory: in this way ripening, milk composition, technological management of cheese making process were all considered the main factors affecting the final structure of the cheese. Cheese wheels with 12 months, 14 months, 16 months, 18 months, 24 months, 28 months, 30 months, 36 months, 46 months, 54 months, 60 months, 72 months of ripening were selected for this study. Three replicates were selected for the most commercially known ripening times, i.e. 12, 24, 30 months of ripening.

The **second-level** of **sampling** was aimed at drawing specimens that were representative of the inner structure of the whole cheese wheel. For this purpose, each cheese wheel was divided in two parts along the sagittal plane to obtaining two specular half cheese wheels. Ten cheese cloves of about 2 kg were obtained from one-half wheel to be representative of radial composition/structure gradients as established during the cheese making process. Ten cheese cloves of about 2 kg were obtained from one-half wheel to be representative of the axial composition/structure gradients. The cloves were numbered from 1 to 10 and the ones coming from the upper half-wheel were named with the letter A (“alta”) and the ones from the lower wheel were named with the letter B (“bassa”) (*Figure 40-Figure 41-Figure 42*).

In the **third-level** of **sampling**, each clove was cut to obtain samples of parallelepiped-shaped to be analysed under three-point bending test.

In the **four-level** of **sampling** cubic-shaped samples were cut from one half obtained with the bending test, in order to be analysed under uniaxial compression and isothermal creep tests.

In the **fifth-level** of **sampling** disk-shaped samples were cut from the second half obtained with the bending test, in order to be analysed under temperature-sweep shearing tests.

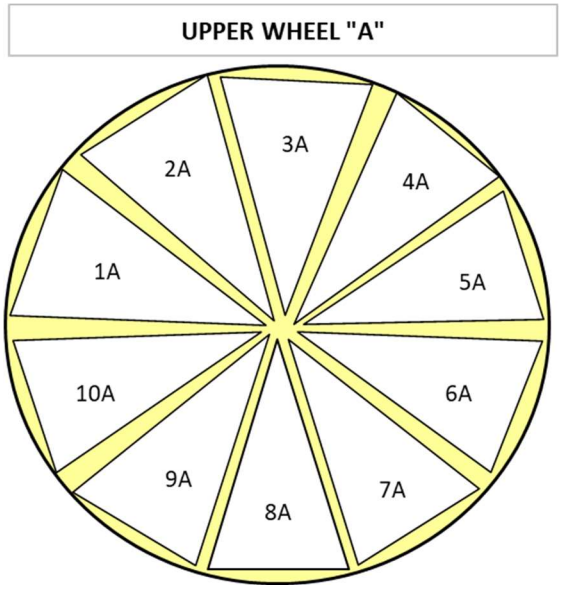

Figure 40 Scheme for clove portioning from upper half-wheel [A]

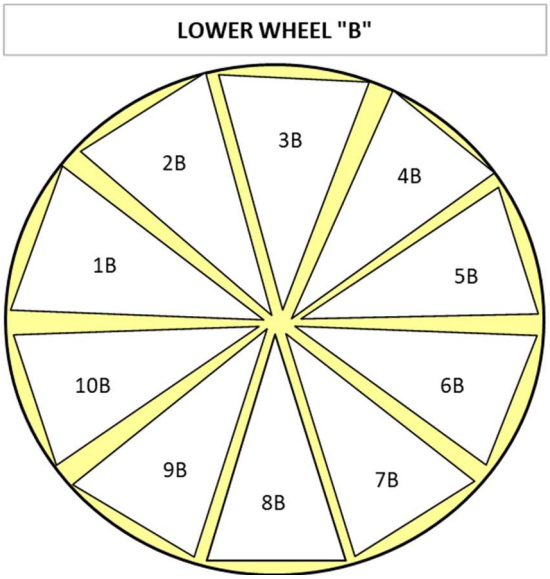

Figure 41 Scheme for clove portioning from bottom half-wheel [B]

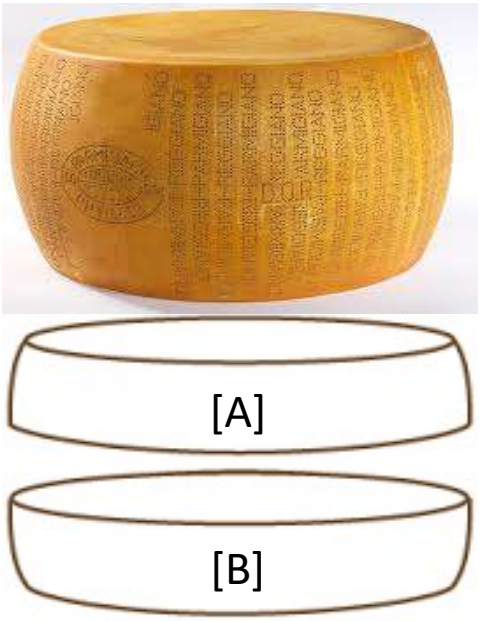

Figure 42 PR cheese portioning cloves from upper and bottom half-wheels

5.2. Preparation of test geometries for rheological and mechanical tests

To prepare test specimens with rectangular section and very accurate geometry, viz. having parallel sides and accuracte sizes, each cheese clove was cut coupling a micrometric positioning stage to an original wire-cutting device, see (*Figure 43-Figure 44*), the latter designed to operate under sress-controlled conditions when gripped to the universal testing machine such as the Zwick Roell (1kN). Wire diameter was selected bearing ten times the maximum stress encountered (< 900N) during preliminary cheese cutting tests under a constant strain rate of 50mm/min. Wires with a diameter of 1.17mm thick were used to cut the cheese near the crust and cables with diameters equal to 0.30 and 0.33mm thick (depending on the seasoning) to cut the remaining parts. Precise position for the clove and then for the smaller pieces was guaranted by fixing the wall distances by fixing a moveable wall on the positioning stage, aiming to create a cheese cage with rectangular cross-section able to avoid time-dependente relaxation phenomena during cheese cutting. The use of such micrometric positioning stage allowed to drastically reduce the experimental error in the test specimen geometry. All the samples were cut two hours at least before the fracture tests, thus allowing to complete residual stresses to completely relax inside the test specimens.

Test geometries were prepared as bars having rectangular section and different scale sizes (*Figure 45-Figure 46-Figure 47-Figure 48*):

a) geometry A - 10.0 x 2.2 x 2.2cm
b) geometry B - 5.0 x 1.1 x 1.1cm
c) geometry C - 5.0 x 2.2 x 1.1cm
d) geometry D - 10.0 x 4.4 x 4.4cm

Test specimens from the one half-wheel “A” were withdrawn with axial orientation with respect to the acheese wheel axis. Test specimens from one-half wheel “B” were withdrawn with radial orientation (*Figure 49* and *Figure 50*).

To assess the influence of the position of each specimen within the entire cheese wheel on the characteristics of mechanical properties, each specimen was labelled with an alphanumeric code to be always traceable. The code identifies:

1) ripening time (es. 12M)
2) clove of origin (es. 6)
3) wheel of the upper (A) or lower (B) half
4) position of the specimen (eg. 1, 2, 3..)
5) geometry (A, B, C, or D)

6) horizontal (O) or vertical (V) cut

For the sake of the example, the specimen code “12M 6B1DO” indicates a specimen of parallelepiped shape withdrawn from the cheese clove n.6, which in turn was obtained from the lower half-wheel of the cheese having 12 months of ripening.

The test geometry D (*Figure 51*) were used for flexural tests. The test geometry A (*Figure 52*) were used for creep tensile fracture tests (*Figure 53*). After mechanical fracture, two cheese blocks were obtained from which eight cubic specimens were finally obtained (2 x 2 x 2cm size) to be subjected to both compression and creep tests using the universal testing machine. Finally, round disk-shaped samples with 20mm of diameter and 2.5mm of height) were obtained from cubic specimens and subjected to thermo-rheological tests using the stress-controlled Rheometer.

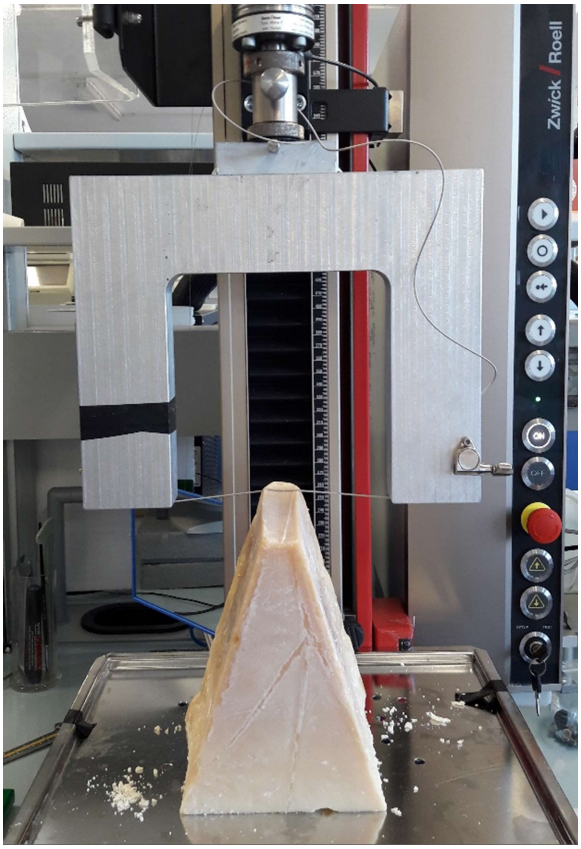

Figure 43 In-house developed Stress-Controlled Cutting Device

Figure 44 In-house developed Micrometric Positioning Stage for Test Specimen preparation

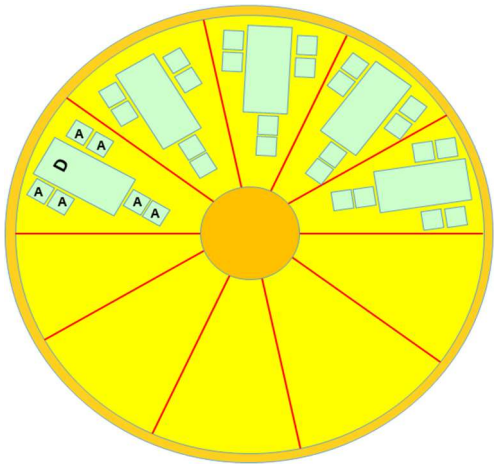

Figure 45 Top view scheme for the portioning test geometries A and D from wheel "B" cloves)

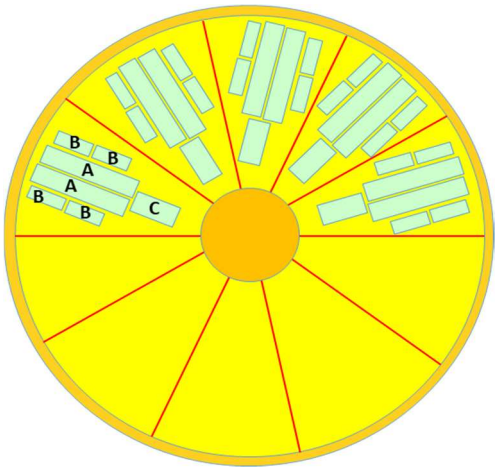

Figure 46 Frontal view scheme for the portioning test geometries A, B and C from wheel "B" cloves)

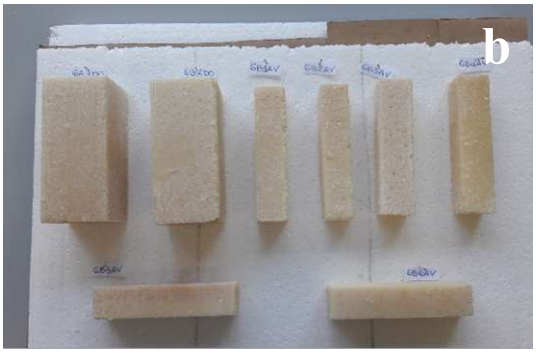

Figure 47a-b Test specimens D and A for SENB fracture tests (different levels for a/W)

Figure 48 Test geometry A for DENT creep fracture tests

This is the scheme for clove portioning into the radially- and axially-oriented test geometry D:

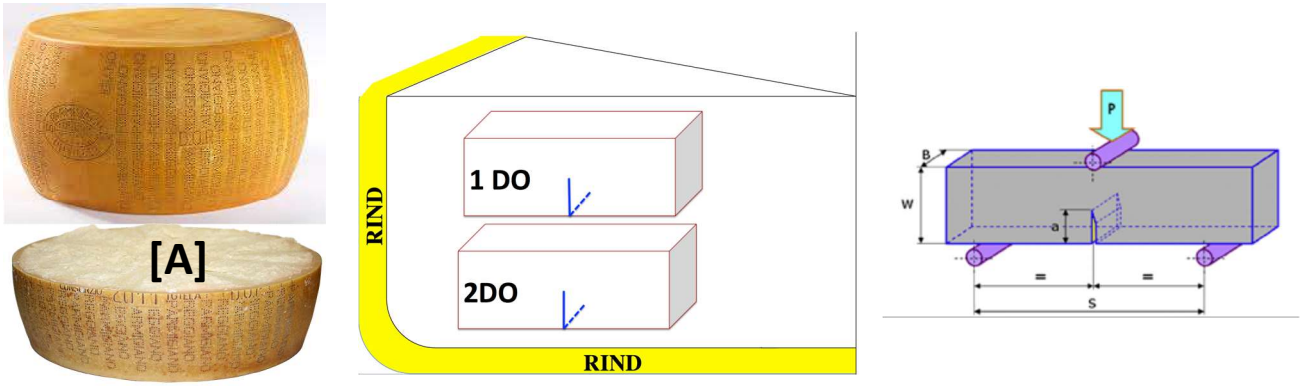

Figure 49 Radial-oriented test geometry D for SENB

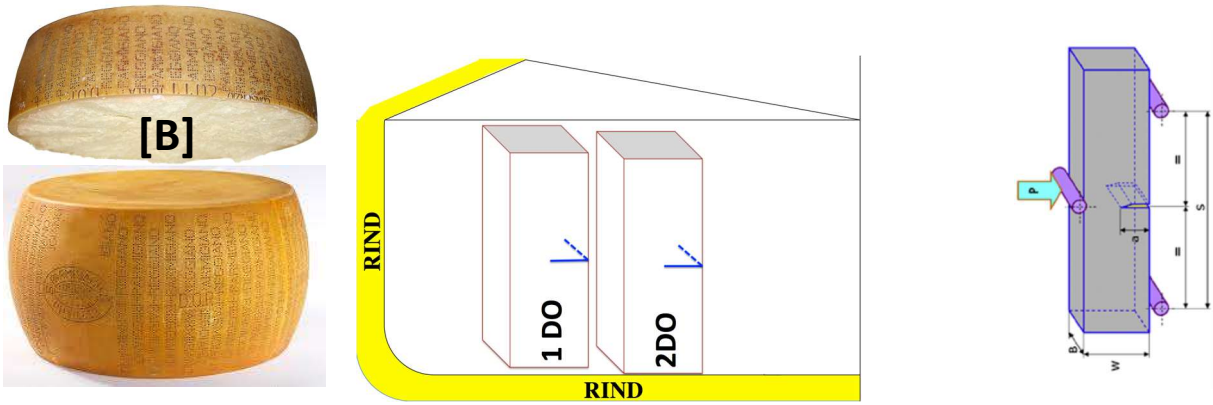

Figure 50 Axial-oriented test geometry D for SENB

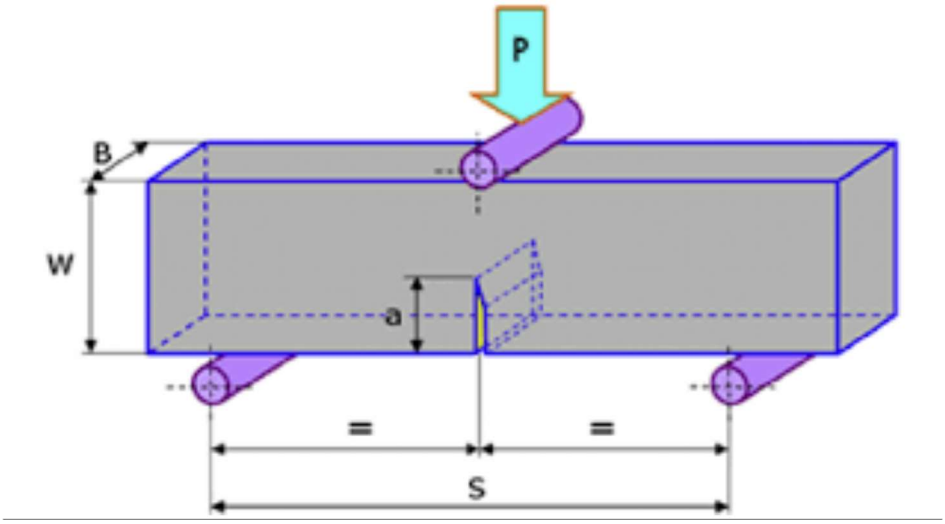

Figure 51 Test geometry D sizes for Single-Edge notched Bending (SENB) fracture test (L=100mm; S=90mm; B=44mm; W=44mm; a_0=19mm)

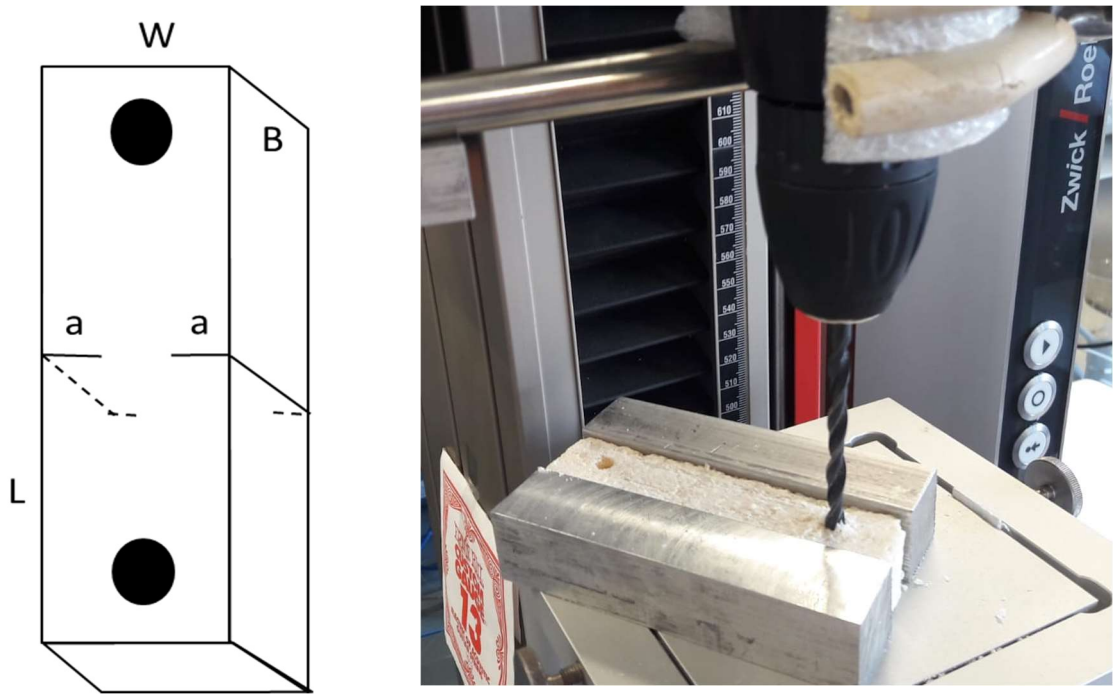

Figure 52 Test geometry A drilled for Double-Edge Notched Tension (DENT) creep fracture test (L=100mm, B=22mm W=22mm a=6mm, ligament (W-a) =10mm)

Figure 53 Instrumental alignment to the test geometry A for DENT creep fracture test

5.3. Assessment of uncertainty of geometry size

Each cheese specimen was imaged before mechanical/rheological tests using a digital camera (Panasonic DMC-FZ1000) operating with high-resolution (pixel size of 5.7micron). Imaging was performed under uniform light, using a metal specimen having standardized sizes for calibration purposes (*Figure 54*). Geometry's sizes, notches and fracture surface imaged with very-high accurately. The digital image of the four sides of each specimen was analysed using the open-source IMAGE J software (version n. 1.52); while, some descriptive statistics, i.e. mean, standard deviation and variability coefficient, were calculated aiming to estimate the experimental uncertainty to be associated to the material properties measurements.

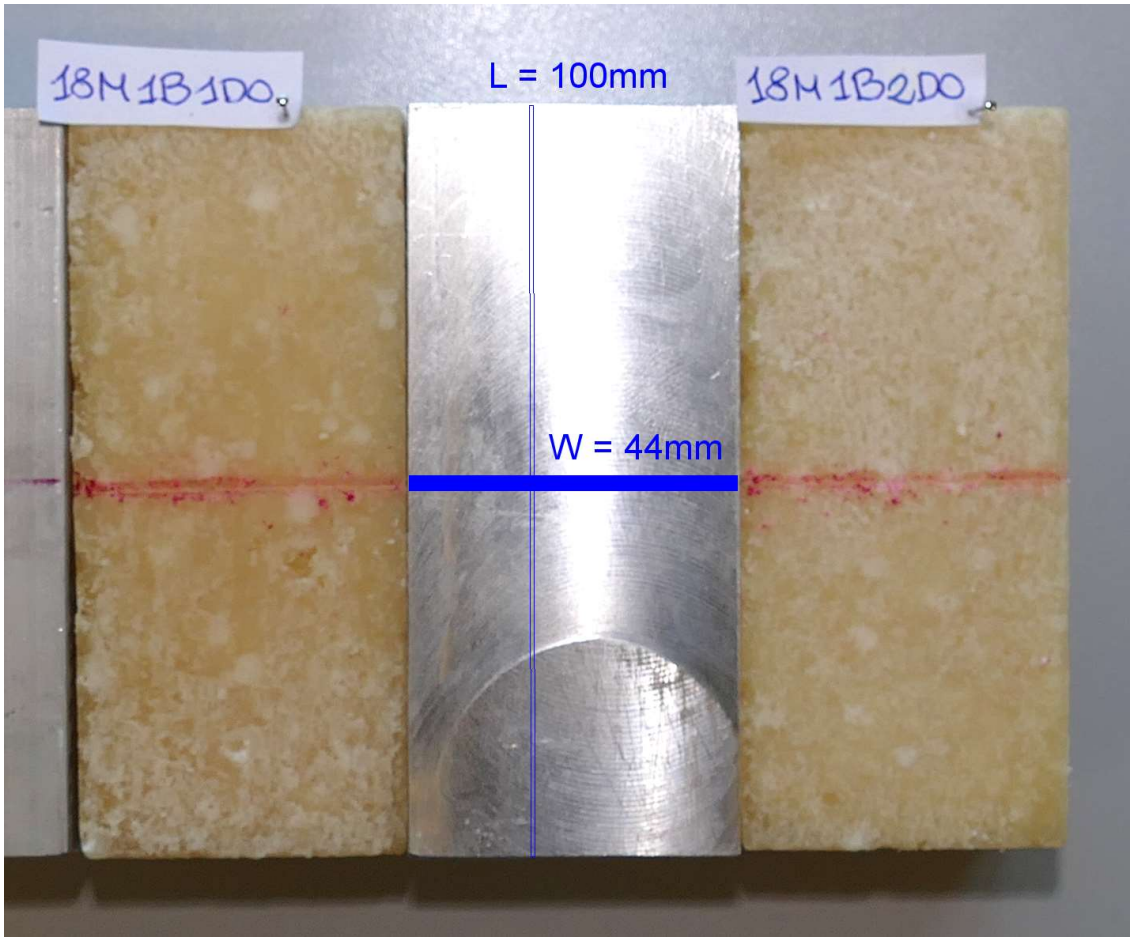

Figure 54 Standardized metal test geometry for internal calibration through ImageJ

5.4. Design of Experiments

At least n. 200 PR samples were initially analyzed for their internal microstructure and for the structure of the fracture surfaces using high-resolution microscopy techniques.

Subsequently, at least n. 1050 samples were analyzed for viscoelastic and elasto-plastic properties through compression and flow control tests in non-destructive conditions.

Finally, at least n. 450 samples were analyzed under controlled fracture conditions by performing compression, tensile and flexural tests.

The investigative strategy has allowed us to establish the limits of applicability of the principles of the theory of fracture mechanics and the corresponding numerical solutions of the laws governing the triggering and propagation of a mechanical fracture.

5.5. Gross compositional analysis

Gross composition of the PR cheese was performed through NIR technique (Near InfraRed) aiming to estimate the overall content of proteins, fats, moisture and salt content. Three replicates of cheese cloves for each cheese ripening time were analysed.

5.6. 2D Imaging and analysis of the Fracture Surfaces

5.6.1. Microscopic features by ESEM

To obtain wide-scale information about the structure of the fracture surfaces, cheese specimens having 12, 30 and 72-months and previously fractured under SENB test conditions were analysed by the ESEM technique using a FEI Quanta 200 FEG Environmental Scanning Electron Microscope (FEI, Hillsboro, Oregon, USA) (*Figure 55*). The microscope was equipped with an energy dispersive X-ray spectrometer (EDAX inc., Mahwah, NJ, USA) to have more detailed information on the elemental composition of the samples in relation to their morphology. Images were acquired. Just before the analysis, samples of cheese were broken by hand with a spontaneous fracture, to create new breaking surfaces. About 1-2cm^2 of surface were deposited onto aluminium specimen stubs previously covered with a conductive carbon adhesive disk (TAAB Ltd, Berks, England). The analysis was performed by using a strong accelerated and focalised electron beam in a vacuum (5.0 e-6mbar). The ESEM was utilized in low vacuum mode, with a chamber pressure set from 0.80 to 0.91mbar, an accelerating voltage from 5.1 to 15.8kV, and a magnification from 47x to 36924x. The images were acquired by means of a secondary electron detector (SSD), or with a back-scattered electron detector (BSD) or with large field detector (LFD). The spectrometer unit was equipped with Edax Carbon Oxigen Nitrogen (ECON) x-ray detector and a Genesis Analysis software. Each sample was measured with a time count of 100sec. and an Amp Time of 51, while the probe current was 290μA.

Figure 55 ESEM microscope facility

5.6.2. Macroscopic features by high-resolution Camera

Cheese specimens were imaged using a high-resolution digital camera (Panasonic DMC-FZ1000) before and after SENB tests (*Figure 56*). Fracture surfaces were analysed using IMAGE J (version n. 1.52) using plugins able to characterize both the fractal dimension, as an index of structure irregularity, and surface profile as an index of structure complementarity.

Figure 56 Digital camera Panasonic DMC-FZ1000

5.7. 3D Imaging and-analysis of Bulk Microstructure

A X-View M5000 tomograph (North Star Imaging, Inc) at the Tec-EuroLab facility (Campogalliano, Modena, Italy) was used to virtualize and quantify the three-dimensional inner structure (*Figure 57*). Cheese samples were scanned on the rotation stage after the optimization of the X-ray energy exposition time and intensity, contrast and phase contrast. All two-dimensional images from x-ray projection were mathematically convoluted using a Filtered Back Projection Feldkamp algorithm aiming to reconstruct three-dimensional volumes of the investigated sample and then digitalized in Tiff arrays for further image processing (*Figure 58*).

Cheese sizes of 10-20cm^2 with 12, 30 and 72 months of ripening, were analysed with the following grid sizes: PR 30 months (voxel of 20 micron: x 1680, y 1794, z 1542); PR 30 months (voxel of 50micron: x 1216, y 931, z 1959); PR 72 months (voxel of 50micron: x 1606, y 1068, z 1833).

Figure 57 X-ray Tomography facility (with courtesy of TEC-EUROLAB, Campogalliano – MO, Italy)

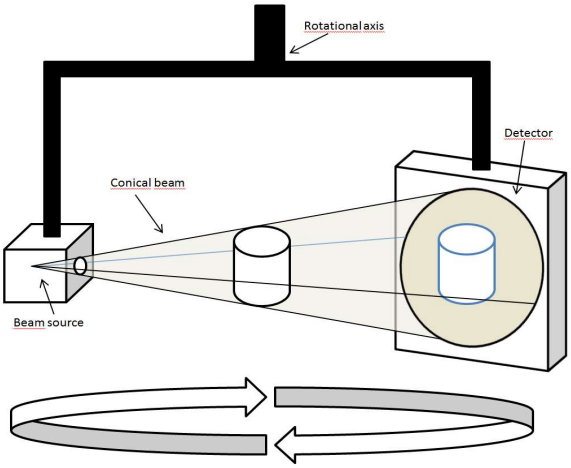

Figure 58 Three-dimensional imaging by tomograph

5.8. Thermal and thermo-rheological analysis

5.8.1. Differential scanning calorimetry

Cheese samples with a ripening time of 12, 24, 30, 36 and 72-months were analysed by differential scanning calorimetry, using a DSC Q20 (TA Instruments) (*Figure 59*), aiming to characterize both thermodynamic and kinetic transitions. The instrument was calibrated using indium standard. Cheese samples were weighted in aluminium pans and scanned at a programmed cooling/heating rate of 10°C/min or 2°C/min in the range of temperature between -80°C and 350°C as in the following:

With the purpose to evaluate local differences in thermal behaviour, cheese samples were withdrawn accounting for the two structure domains usually evolvoing during ripening known as "**SPECKS**" domain, represented by the smallest-size and bright crystal aggregates (they are easily perceived sensorially into the mouth as crispy and cruncy); "**SPOTS**" domain, represented by the smeared and diffused crystal aggregates (their size extent in the range of few millimetres). Paste, specks and spots were analysed at the same cooling/heating program in the range of temperature between -80°C and 300°C. Finally, thermal cycles were performed to the cheeses samples between 0° and 100°C with a cooling/heating rate of 10°C/min.

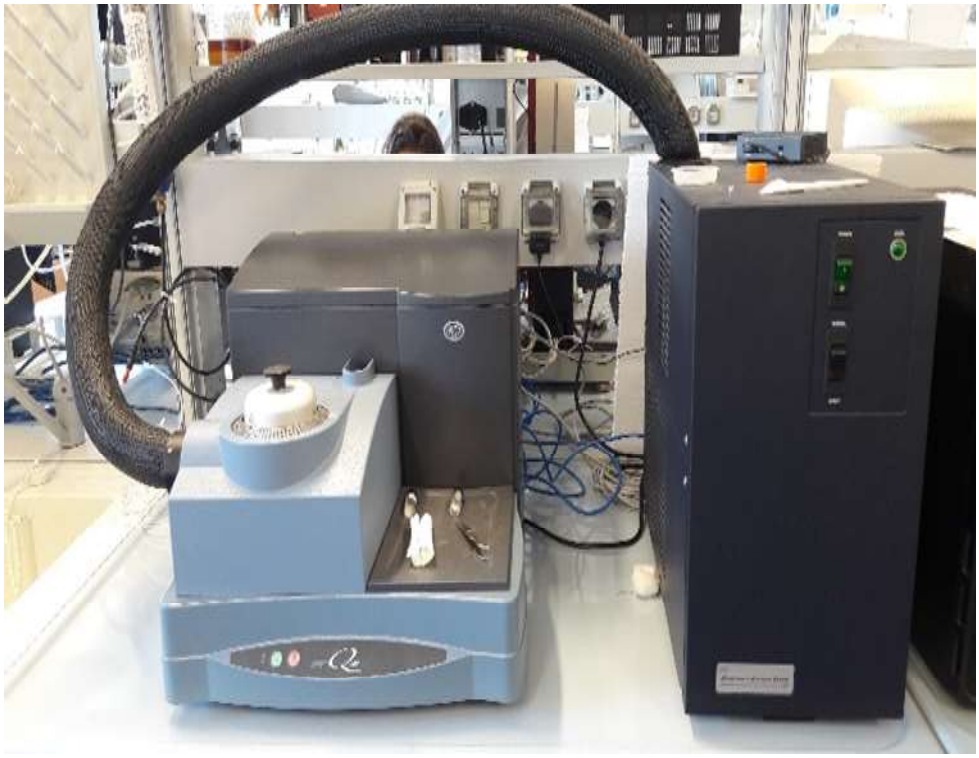

Figure 59 Differential Scanning Calorimeter with temperature modulation

5.8.2. Temperature sweep in Shearing Creep-Recovery tests

Rheological behaviour under temperature sweeping conditions was evaluated performing shearing tests on a strain-controlled DHR-2 Discovery Rheometer (TA Instruments, Wathers SpA, USA) equipped with a Peltier system for temperature control with an accuracy of +/- 0.2°C and parallel knurled plates geometry of 20 mm diameter (*Figure 60*). Aiming to evaluate both conservative and dissipative strain, the test was carried out by applying a tangential stress under complete reversibility. The linear viscoelastic regime (LVR) was individuated by preliminary stress and frequency-sweep tests in the interval 0.01Pa - 1000Pa and 0,01Hz – 10Hz, respectively.

Creep tests involve two consecutive steps. Firstly, a constant stress of 3Pa was kept constant for 120 seconds (**creep**) while the deformation is recorded. Secondly, the stress is removed, and the residual deformation was recorded for 120 seconds (**recovery**). The time scale chosen for recovery was not enough to completely relax the cheese structure but it allowed full evaluating of the instantaneous recovery step. The residual strain at 120 seconds was used for comparative purposes. To evaluate the dependence of shear deformation mechanism on temperature, isothermal tests were consecutively run at 0°C, 10°C, 20°C, 30°C, 40°C, 50°C, 60°C, 70°C, 80°C, 90°C, 100°C, and

110°C. The instrumental control was focused both on the axial and tangential stress, aiming: the axial load was dynamically tunedaiming to assure the grip of the test specimen during plate shear.

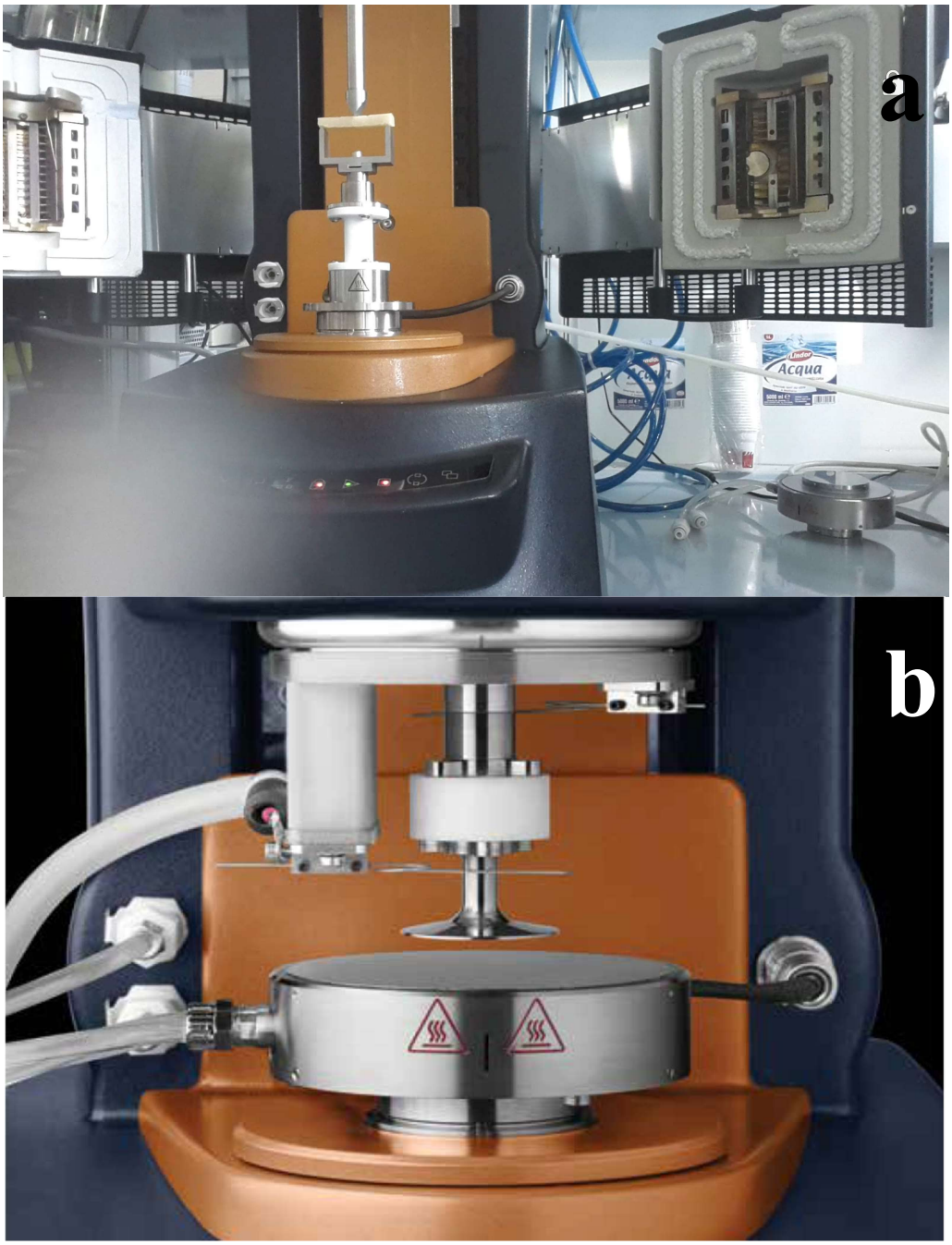

Figure 60 a-b. DHR-2 Rheometer equipped with Environmental Testing Chamber (a) and Peltier (b) systems for tighty temperature control

5.8.3. Isothermal Creep-Recovery in compression mode

Rheological behaviour under compressive conditions was evaluated performing uniaxial compression tests with a Zwick Universal Testing machine (Zwick Roell, TA Instruments, model 1KN Zwicki) equipped with parallel plates (*Figure 61*). The lower plate is fixed and it is the plate where the specimen will be placed. It measures 0.9mm of height, length 90mm and width 100mm. The upper compression plate is 15mm thick, 100mm long and 100mm wide, and it is fixed to the mobile crosspiece, in connection with the load cell.

The specimens were obtained from the sub-specimens generated after the rupture in the bending test. The samples are in cube dimensions of 22 x 22 x 22mm. The specimen is positioned at the centre of the lower plate. The test begins when a preload of 1N has been reached, at preload speed 5mm/min. The creep test of a specimen consists in the repetition of **7 cycles** composed of 2 steps. In the **first step** is applied a constant load for a given time (120s) and record both the deformation and force; in the **second step** the stress is removed and the corresponding strain is measured as well during further 120 seconds, while the sample is recovering. The first cycle starts with a load of 10N and it increases by 10N at each cycle, up to 70 N: 10, 20, 30, 40, 50, 60, 70N. The test takes place at room temperature. The upper plate was covered with paper to prevent the Parmigiano-Reggiano specimens adhered to it, remaining attached during decompression, as was noted in the preliminary tests.

5.8.4. Temperature sweep in SAOS tests

The instrument used is the DHR-2 Discovery Rheometer (TA Instruments, Wathers SpA, USA) equipped with a peltier system for temperature control with an accuracy of +/- 0.2°C, in order to minimize the variability of results, and using a geometry of two flat plates knurled (not smooth). The sample is loaded into the lower plate and the upper tool is approached by hand, taking care not to touch it. The test was performed at a constant frequency (0.25, 0.5, 1, 5, 10 and 20Hz) with a constant strain of 0.02%. The temperature starts at 10°C and ends at 120°C with a ramp rate of 1.5°C/min. The storage modulus (G') and loss modulus (G'') are measured.

5.8.5. Strain sweep in SAOS tests

A stress-controlled rheometer was used the DHR-2 Discovery Rheometer (TA Instruments, Wathers SpA, USA) equipped with a peltier system for temperature control with an accuracy of +/- 0.2°C,

and a geometry of two flat plates knurled (not smooth). The sample is loaded into the lower plate and the upper tool is approached by hand, taking care not to touch it. The frequency of the oscillation is held constant (1Hz) while the strain varied (a range between 0.001% to 500%). The test was performed at constant temperature of 30°C, 50°C, 60°C, 80°C, 90°C and 100°C, to see the differences of the linear region, depending with the temperature.

5.8.6. Frequency sweep in SAOS tests

Once evaluated the linear viscoelastic region (LVR) in strain sweep test, it has been evaluated how cheese structure change by changing the frequency. Frequency sweep test is carried out in order to characterize differences in viscous and elastic behaviour in cheese, by changing the rate of strain application (frequency).

A DHR-2 Discovery Rheometer (TA Instruments) was used, equipped with 20mm parallel knurled plates. All the parameters are still within the linear viscoelastic region: starting at 0.01Hz up to 16Hz of frequency with a strain of 0.1%, at room temperature (25°C). The storage modulus (G') and loss modulus (G'') are measured.

5.9. Analysis of Fracture and Yielding Behavior

In our study the fracture and yielding behavior of standardized test specimens of cheese was analyzed in different stress and/or strain conditions. Firstly, the uniaxial compressione test was carried out under constant strain rate. Secondly, uniaxial creep in tension was performed under constant load using double-edge notched test specimens (DENT). Thirdly, bending tests were carried out under constant strain rate using single-edge notched test specimens (SENB).

5.9.1. Uniaxial Compression Test

Uniaxial compression test was carried out with a Zwick Universal Testing machine (Zwick Roell, TA Instruments, model 1KN Zwicki) equipped with compression tools (*Figure 61*). The compression tools were two parallel plates, both with a surface area larger than the sample surface. The lower plate is fixed and it is the plate where the specimen will be placed. It measures 0.9mm of height, length 90mm and width 100mm. The upper compression plate is 15mm thick, 100mm long and 100mm wide, and it is fixed to the mobile crosspiece, in connection with the load cell. The

specimen is positioned at the centre of the lower plate. The test begins when a preload of 1N has been reached, at preload speed of 2mm/min. Then the specimen undergoes a compression at a test speed of 10mm/min, controlled in position, up to 30% of the sample height.

Figure 61 Zwick – Parallel plate for Uniaxial Compression Tests

5.9.2. Fracture properties under DENT Creep conditions

Uniaxial tensile tests were carried out under creep conditions until to completely break the test specimens. In this case, the test geometry was like SENB but with some differences. Firstly, the scale size was 100 x 22 x 22mm. Secondly, 2 notches of 6mm were provided at the centre of each W side. Moreover, the test specimens were made suitable for both upper and bottom grip by drilling them accurately according to the test specimen preparation paragraph. The test was performed with a universal testing machine: Zwick Universal Testing Machine (Zwick Roell, TA Instruments, model 1KN Zwicki) equipped with two original tensile tools (*Figure 62*). The latter toosl were designed and realized in D3A department for the scope. A preload of 1N was imposed to be reached with a preload speed of 5mm/min. Then a constant force of 15N was applied as a constant tension load. A creep was realized for a time of 120 seconds, using a control in force of 50N/s. The test was stopped when the test specimen completely broken.

Figure 62 Zwick - Universal testing machine equipped with two original tensile devices

5.9.3. Fracture Properties under SENB conditions

In this work, an original fracture analysis procedure was developed according to the reccomendations from the international ASTM-E1820 standard based on the material properties K, J, CMOD and CTOD well-established by the fracture mechanics theory aiming to codify and interpret experimental results from SENB test under opening mode (Mode I) of loading. ASTM-E1820 covers procedures and guidelines explicitally focused on the determination of fracture toughness for metallic materialsTo make the standard's reccomendations applicable to the investigated cheese, thus aiming to assure reliability of results, some important modifications for both the size and notch requirements were proposed for the SENB cheese geometry as well as for

the limits on experimental data qualification. The new fracture procedure developed in this study encloses the instrumental setup specifications, geometrical factors for cheese test specimens,

The fracture analysis procedure developed in tis work, provides theoretical and technical specifications on how to couple and use (i) some original devices able to shape the cheese samples to obtain standardized test specimens with rectangular section and with required geometrical accuracy; (ii) some metal specimens for size calibration; (iii) a high performance universal machine for applying of compression and tension loads, aiming to measure the Poisson ratio and Young modulus, respectively; as well as for application of bending loads able to assure during the entire fracture process both the **small-scale yielding (SSY) condition** close to the crack-tip and the **plane-strain condition**, i.e. the stress is negligible along with the direction orthogonal to the crack plane; (iv) a high-performance video camera for the acquisition and recording of images in 4K, (v) the ImageJ as software for image analysis; (vi) a numerical procedure coded in visual-basic language and running on an easy-to-use Excel spreadsheet appropriately designed for the execution of algorithms able to estimate both the thermodynamic and kinematic properties of the cheese fracture process together with their uncertainty. Among the material properties, the Fracture Toughness of the cheese, i.e. the material resistance to the fracture initiation, as well as the Tearing Modulus, i.e. the material resistance to the fracture propagation. All the material properties were accurately estimated from the whole resistance curve, allowing to analyze one test specimen only.

More in detail, the objective of SENB fracture test is to submit a standardized test geometry of the cheese to fracture experiments under strain-controlled conditions, i.e. at a constant strain rate of 5mm/min, to induce one or both two possible mechanical responses:

1. *Steady-state extent of the crack (stable fracture),*
2. *Unstable crack propagation (instability of the fracture)*

The “load - displacement" curve was constructed and processed according to the recomendations codified by the ASTM standard, aiming to construct the so-called Material Resistance Curve (or J-R Curve) which quantitatively describes the increase of fracture toughness during the fracture propagation. The toughness increasing is due to the increasing of the plastic effects inside the so-called Process Zone, i.e. the volume close to the crack-tip. The plastic effects increases with the crack propagation mainly because of decreasing of the ligament thickness: the stress field along the orthogonal direction to the crack plane becomes progressively less negligible while crack propagates into the test specimen. The J-R curve is a 2D graph which represents the J-Integral [KJ/m2] as a function of the extent of the crack length Δa [mm] as measured experimentally only

under stable fracture conditions. The material resistance to fracture initiation is evaluated with a single measurement point. Stable fracture is characterized by analyzing the entire J-R curve beyond the trigger point of crack initiation up to the point where the unstable fracture takes place. To measure material properties which are independent on specimen geometry and size, a pre-cracked bar with rectangular section referred as "Single-Edge Notched Beam (SENB)" was used in this work with sizes respecting the following relations:

$$\begin{cases} S = 4 \cdot W \\ 1 \leq \frac{W}{B} \leq 4; \\ B = 2a \end{cases}$$

where (S) is the distance (mm) between the two three-point bending supports; (B) is the thickness of the test specimen (mm); (W) is the specimen width (mm). Aiming to assure the accomplishment of data quality requirements, in our study, the following modifications were proposed for SENB test geometry:

$$\begin{cases} S \cong 2 \cdot W \\ \frac{W}{B} \cong 1 \\ B = 2.3 \cdot a \end{cases} \qquad \begin{cases} S = 90mm \\ W = 44mm \\ B = 44mm \\ a0 = 19mm \\ L = 100mm \end{cases}$$

The following four measurements were recorded simyultaneously

(1) Bending load, Pi[N]

(2) Displacement of load application point, in the next it is refereed as to **"v[mm]"**

(3) Vectorial Crack Extension, refereed as or **CEX**

(4) Vectorial Crack Mouth Opening Displacement, referred as to **CMOD**

Both CEX and CMOD were video captured during stable fracture using a high resolution 4K camera and measured by means of image and video analysis and using internal standard fixtures appropriately fixed on the W side of the test specimen near the fracture plane before mechanical tests. In the following layout configuration, CMOD was considered as the maximum vectorial distance between the two fracture surfaces. Crack-Tip Opening Displacement was also defined as the vectorial distance between the two fracture surfaces at a close distance from the crack tip. The two physical displacements, i.e. CTOD and CMOD, were not linearly related. CMOD increases

more rapidly with respect to CTOD as a function of the extent of the plastic strains. As a given time of fracture, the ratio between CTOD and CMOD can be used as a quantitiative measure of the cheese brittleness (or plasticity) related to the fracture initiation or propagation. CTOD (indicated as "δI") was estimated using alternatively one of the two following formulas:

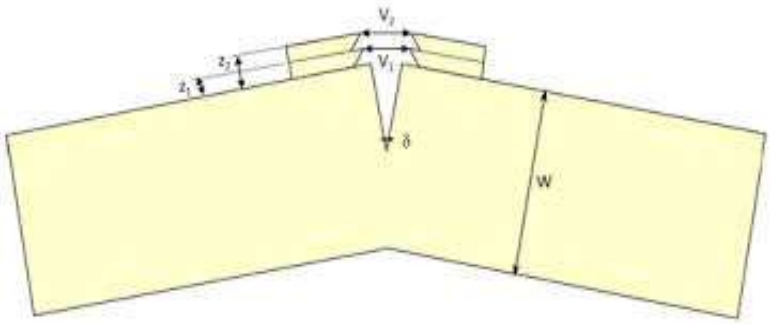

According to the basic multi-test procedure, the displacement (d) of the crack tip can be estimated using the following mathematical expression:

$$CTOD\ or\ \delta_i = \frac{K_i^2 \cdot (1-v^2)}{2 \cdot \sigma_{YS} \cdot E} + \frac{[r_p \cdot (W-a_o)] \cdot v_{pl}}{[r_p \cdot (W-a_{(0)}) + a_0 + z]} \quad (19)$$

According to the procedure based on the R-Curve with a single test geometry:

$$\text{CTOD or } \delta_i = \frac{K_i^2 \cdot (1-v^2)}{2 \cdot \sigma_{YS} \cdot E} + \frac{[r_p \cdot (W-a_i) + \Delta a] \cdot v_{pl(i)}}{[r_p \cdot (W-a_{(i)}) + a_{(i)} + z]} \quad (20)$$

where

a_i and a_0 are the length (mm) of the initial crack and crack during stable fracture
Δa is equal to $[a_i - a_0]$ indicates the crack extent (mm) during stable fracture
K_I is the stress intensity factor calculated considering $a_i = a_0$
v is the Poisson ratio, i.e. the ratio between the transverse εx to axial εy strain
σ_Y is the estimated yield stress at an arbitrary strain offset (0.2%)
E is the elastic modulus estimated at the test temperature
Vpl is the plastic component of the crack opening estimated at points vc, vi, va or vm of the load-displacement curve
Z is the distance of the fixture bottom edges from the fixture upper side
Rp is the plastic rotation factor of the specimen during flexion (it is equal to 0.4)

Cheese Resistance to the Crack initiation (or Fracture Toughness)

K_I expressed as MPa/$m^{0.5}$ was calculated at a given load Pi from experimental load-displacement data as in the following:

$$\begin{cases} K_{(i)} = \left[\frac{2P_{(i)} \cdot S}{B \cdot W^{3/2}}\right] \cdot f\left(\frac{a_i}{W}\right) \\ f\left(\frac{a_i}{W}\right) = \frac{3\left(\frac{ai}{W}\right)^{\frac{1}{2}} \cdot \left[2.15 - 3.93\left(\frac{ai}{W}\right) + 2.7\left(\frac{ai}{W}\right)^2\right]}{2\left(1+2\left(\frac{ai}{W}\right)\right) \cdot \left(1-\left(\frac{ai}{W}\right)\right)^{3/2}} \end{cases} \quad (21)$$

where

Pi if a given load from load-displacement curve (N);

S the span between bending supports (mm);

B, W the thickness and with oif the test specimen (mm);

ai is the extent of the crack during propagation (mm) (it correspond to the modulus of CEX vector);

f(ai/W) is the adimensional geometric factor required to make K_I as a material property independent on the geometry and size of the single-edge notched test specimen used for the fracture test. The algebraic coefficients required to calculate f(ai/W) are widely reported in literature and arise from FEM analysis of the stress field in the Process Zone, around the apex of a crack, under Elasto-Plastic Fracture Mechanics (EPFM) regime.

Since the proposed experimental conditions must be checked for their ability to consider negligible the large plastic deformation, thus providing evidence that the fracture process takes place both under plane-strain and small-scale yielding (SSY) conditions close to the crack-tip.

If both such conditions are accomplished, the cheese fracture toughness can be evaluated calculating the upper limit of the stress intensification factor K (next it is indicated with K_{IC}). In this case, K_{IC} can be estimated using the formulas for KI calculation under Linear-Elastic Fracture Mechanics (LEFM) regime; while the upper limit of Pi can be defined at interim as P_Q which in turn can be estimated following the next procedure:

1) build the load-displacement curve (or load-CTOD curve or load-CMOD curve)
2) construct the straight-line tangent to the linear part of the curve (with slope equal to P_0/V_0)
3) construct the secant line with a slope equal to 95% of the straight-line [$(P/V)_Q=0.95*(P_0/V_0)$]
4) estimate the load P_Q identifying the intersection point of the secant line with the load-displacement curve

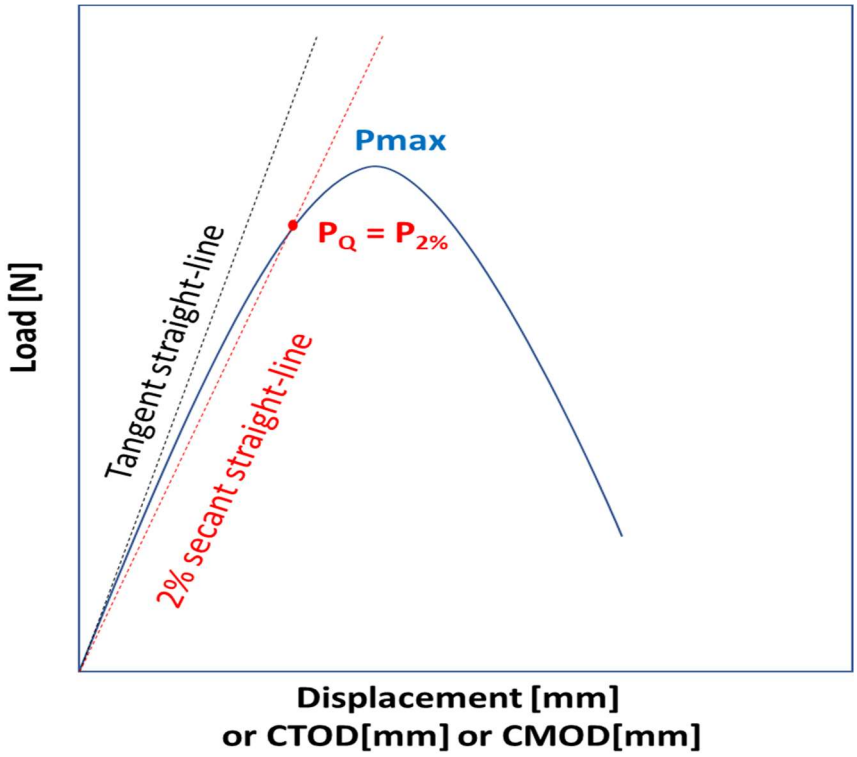

Values of K_Q were accepted as approximate descriptors of K_{IC} only when the following data qualification restrictions were satisfied:

$$\begin{cases} \dfrac{P_{max}}{P_Q} < 1.10 \\ 2.5 \cdot \left(\dfrac{K_Q}{\sigma_Q}\right)^2 < B \\ 2.5 \cdot \left(\dfrac{K_Q}{\sigma_Q}\right)^2 < (W - a_0) \end{cases}$$

The above boundary conditions allow considering both the **small-scale yielding (SSY) condition** close to the crack-tip and the **plane-strain condition** to be accomplished during fracture test.

Data qualification allows considering results obtained experimentally independent from the geometrical characteristics of the test specimens, and therefore the K_{IC} as a fundamental material property. However, the accuracy of the linear part of the load-displacement curce was previously cecked. Since non-linear relation between the applied load and displacement were always observed during mechanical tests, the first load-displacement data were discarded from derivative calculus.

Cheese Resistance to Crack Propagation (or Tearing Modulus)

The following mathematical expressions were used to evaluate both the elastic to plastic contributes during fracture propagation resistance:

$$\begin{cases} J_{tot} = J_{EL} + J_{PL} \\ J = \frac{K_I^2 \cdot (1-v^2)}{E} + J_{PL} \end{cases} \quad (22)$$

where J_{EL} and J_{PL} are respectively the elastic and plastic energy contribution (expressed in KJ/m^2) to the fracture propagation. In our study we followed both the two alternatives as suggested by ASTM guidelines for evaluating the J_{PL} plastic contribution to the Integral-J:

(1) Basic Procedure – requiring the independent measurement of loading, displacement and crack extension (multi test-specimens)

(2) J-R Curve procedure – requiring the independent measurement of load, displacement and crack extension (single test-specimen)

Basic Method

According to the basic procedure, an independent analysis of A_{PL} was performed through the analysis of an enough number of test specimens and the continuous acquisition of load, displacement as well as of both the initial and final crack extension. Cheese resistance associated with a given length of the initial notch (with different values of a0) was evaluated. Results was only used to evaluate the initiation of a stable fracture but not to construct the entire J-R resistance curve. The J integral was calculated with the following mathematical expression:

$$J = \frac{K^2 \cdot (1-v^2)}{E} + \frac{1{,}9 \cdot A_{PL}}{B \cdot (W - a_0)} \quad (23)$$

where A_{PL} is the plastic area obtained as difference between the whole area under load-displacement curve and the elastic area fraction, E is the elastic modulus, v is the Poisson ratio ($\sigma x/\sigma y$), 1,9 is a geometrical coefficient for SENB test geometry.

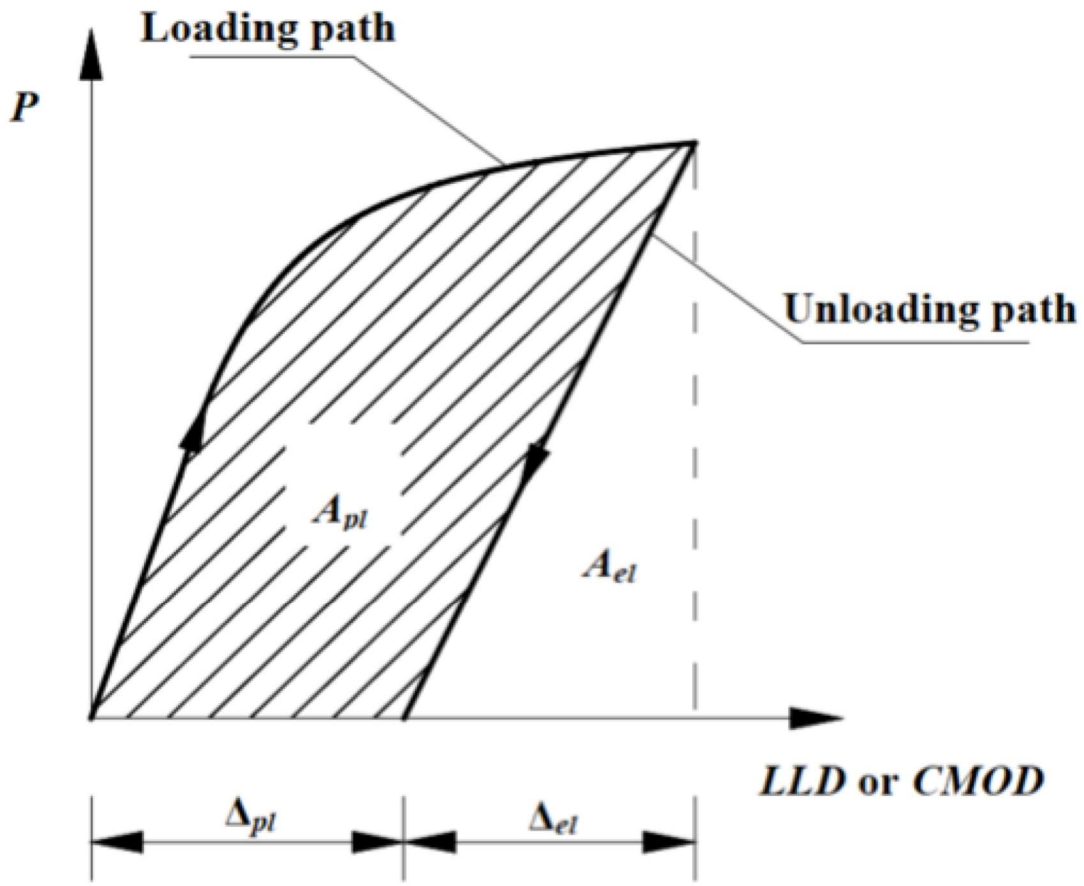

J-R Curve procedure

This procedure is based on the instantaneous estimation of the J-Integral and requires the use of the following mathematical expressions

$$\begin{cases} J_i(i) = J(i)_{EL} + J(i)_{PL} \\ J_{EL(i)} = \frac{K_i^2 \cdot (1-v^2)}{E} \\ J_{PL(i)} = \left[J_{J(i-1)_{PL}} + \left(\frac{\eta_{i-1}}{[W-a_i]_{i-1}} \right) \cdot \left(\frac{A_{PL(i)} - A_{PL(i-1)}}{B} \right) \right] \cdot \left[1 - (\gamma_{i-1}) \left(\frac{a_i - a_{i-1}}{(W-a_{i-1})} \right) \right] \end{cases} \quad (24)$$

where Ki

$$K_{(i)} = \left[\frac{2P_{(i)} \cdot S}{B \cdot W^{3/2}} \right] \cdot f\left(\frac{a_i}{W}\right)$$

$$f\left(\frac{a_i}{W}\right) = \frac{3\left(\frac{ai}{W}\right)^{\frac{1}{2}} \cdot \left[2.15 - 3.93\left(\frac{ai}{W}\right) + 2.7\left(\frac{ai}{W}\right)^2 \right]}{2\left(1+2\left(\frac{ai}{W}\right)\right) \cdot \left(1-\left(\frac{ai}{W}\right)\right)^{3/2}} \quad (25)$$

and

$$\begin{cases}\eta_{pl(i-1)}\\ \gamma_{pl(i-1)}\end{cases} \tag{26}$$

or

$$\begin{cases}\eta_{pl} = 3.667 - 2.199\cdot\left[\frac{a_{i-1}}{W}\right] + 0.437\cdot\left(\frac{a_{i-1}}{W}\right)^2\\ \gamma_{pl(i-1)} = 0.131 + 2.131\cdot\left[\frac{a_{i-1}}{W}\right] - 1.465\cdot\left(\frac{a_{i-1}}{W}\right)^2\end{cases} \tag{27}$$

The latter expressions were used when the crack-mouth opening displacement or crack-tip opening displacement were used to construct the load-displacement curves and to measure Apl.

Aiming to obtain an accurate estimate of J_{PL}, the strain rate was chosen relatively low, i.e. 5mm/min allowing small and uniform increments of the crack through the test specimens. Under these strain-controlled condition, the calculation of the incremental area [A_{PL}(i) - A_{PL}(i-1)] was made considering all the experimental load-displacement data. The incremental area was calculated as a function of the C_{LL} compliance (i) of the test specimen using the following formulas

$$A_{PL(i)} = A_{PL(i-1)} + \frac{[P_i + P_{i-1}]\cdot[V_{PL(i)} - v_{PL(i-1)}]}{2} \tag{28}$$

$$V_{PL(i)} = V_{(i)} - P_i \cdot C_{LL(i)} \tag{29}$$

The specimen complance was numerically estimated using the following formulas:

$$C_{LL(i)} = \left(\frac{\Delta v}{\Delta P}\right)_{(i)} \tag{30}$$

$$C_{LL(i)} = \frac{1}{E\cdot B}\cdot\left(\frac{S}{W-a_i}\right)^2\cdot\left[1.193 - 1.98\left(\frac{a_i}{W}\right) + 4.478\left(\frac{a_i}{W}\right)^2 - 4.442\left(\frac{a_i}{W}\right)^3 + 1.739\left(\frac{a_i}{W}\right)^4\right] \tag{31}$$

The experimental measurement of compliance was avoided because it would require a time-consuming experimental approach based on several partial loading-unloading cycles under quasi-elastic conditions for the entire test. In this case, the compliance can be estimated from the slope of the linear part of each partial loading and unloading cycle. Moreover, a preliminary verification of the reversibility limits is required for the individual load-unloading cycles as a function of the increase of the crack length, thus so high as possible precision and resolution of the load, displacement and lenght of crack must recorded experimentally.

In our study the values of Δai were calculated differently according to the reference method used to estimate the integral-J:

Δai according to the Basic Method

$$\Delta a_i = a_p - a_0$$

where a_p is the physical crack length at the end of fracture test, while a_0 is the starting crack length, both measured experimentally through image analysis

Δai according to the Resistance curve method

$$\Delta a_i = a_i - a_{0q}$$

where ai is the crack length as measured simultaneously with load and displacements

In this case, a correction was applied to the estimated Δa_i data to obtain an improved a_{oq}. This correction is intended to obtain the best value of a_{oq}, based on an initial set of crack size (ai data). All Ji and ai points were determined before the specimen reached the maximum force for the test. Moreover, this data set of points were used to calculate a revised a_{oq} by fitting the following equation

$$a = a_{0q} + \frac{J}{2\sigma_y} + BJ^2 + CJ^3 \quad (32)$$

The goodness-of-fit was evaluated by calculating the mean absolute relative error E% as follows:

$$E\% = \frac{100}{N}\sqrt{\frac{\left(a_{sper} - a_{calc}\right)^2}{a_{sper}}} \quad (33)$$

Calculation of an interim J_Q as descriptor of J_{IC} (Fracture initiation resistance)

The strain energy release at crack initiation, i.e. J_{IC} was estimate directly from the J-R resistance curve following the following steps according to the recommendations from ASTM. First step, a plot J versus Δa was constructed. Next step, a tangent line $J_{CL}(\Delta a)$ was constructed in accordance with the following equation:

$$J_{CL(0)} = 2 \cdot \sigma_Y \cdot \Delta a \quad (34)$$

Next, an exclusion line parallel to the tengent line and intersecting the abscissa at 1mm was constructed. With the following equation

$$J_{EL(1mm)} = 2 \cdot \sigma_Y \cdot \Delta a \quad (35)$$

Next, a second exclusion line parallel to the tangent line intersecting the abscissa at 2mm with the following equation

$$J_{EL(2mm)} = 2 \cdot \sigma_Y \cdot \Delta a \quad (36)$$

Plot all J − Δa data points that fall inside the area enclosed by these two parallel lines and capped by the J upper limit

$$J_{limit} = \frac{(W-a_0)\cdot\sigma_Y}{1.5} \quad (37)$$

Next, a line parallel to both the tangent and exclusion lines at an offset value of 5mm with the following equation

$$J_{EL(10mm)} = 2 \cdot \sigma_Y \cdot \Delta a \quad (38)$$

At least one J–Δa point shall lie between the 1mm exclusion line and a parallel line with an offset of 2mm from the construction line. At least five J−Δa point shall lie between this 2mm offset line and the 10mm exclusion line. Other J−Δa points can be anywhere inside the region of qualified data. J_{IC} wad determined by fitting the following power law to the qualified data falling in the region defined between 2mm and 10mm.

$$J = C_1 \cdot \left(\frac{\Delta a}{k}\right)^{C_2} \quad (39)$$

where k = 1.0 mm

Last step, to select the (Δa, J) data points to be used in determination of the power law coefficients, C1 and C2, and perform power law regression analysis using the method of least squares on all data points between 2mm and 10mm. The mean absolute relative error (E%) of the least squares fit must be greater than 0.95.

J_Q and Δa_Q are defined as the coordinates of the intersection between the power law regression line with the J-R curve.

Data qualifications and validity of J-R Resistance Curve

The maximum value of mechanical resistance as expressed by the J-Integral must respect the smallest value between the following data restrictions:

$$J_{max} = \frac{\sigma_Y\cdot(W-a_0)}{20} \quad (40)$$

or

$$J_{max} = \frac{B\cdot\sigma_Y}{20} \quad (41)$$

The maximum extension Δa_{max} of the crack under stable fracture must be below the following data restriction

$$\Delta a_{max} = 0.25 \cdot (W - a_0) \quad (42)$$

The maximum extension Δa_p of the crack under stable fracture required for J_Q (J_{IC}) calculation must be below the following data restriction

$$\Delta a_p > 0.1 \cdot a_0$$

The number of J-Da data points were 5 at least.

For test geometry thickness

$$B > 10 \cdot \frac{J_Q}{\sigma_Y}$$

For test geometry ligament ($W - a_0$)

$$(W - a_0) > 10 \cdot \frac{J_Q}{\sigma_Y}$$

Tearing Modulus calculation

The resistance to the fracture increases with growing crask size. The fracture propagation resistance under strain-controlled conditions (stable fracture) was evaluated by calculating the slope of the J-R curve in the stable propagation domain and using the following formula:

$$T_{SF} = \frac{E}{(\sigma_Y)^2} \frac{dJ_{SF}}{da} \quad (43)$$

Where T_{SF} is the Tear Modulus, the dimensionless material property able to quantufy the increase of plastic zone that opposes to the crack propagation

5.9.4. Kinematics of the Fracture Propagation

The entire fracture process, that includes crack initiation and propagation, has been video recorded using a full HD video camera (Lumix DMC-FZ 1000) equipped with a 4k memory card and previously synchronized to the mechanical fracture tests, enabling the video analysis off line (*Figure 63*). Time-course extent of crack propagation is required for the accurate construction of the

Resistance Curve (Integral-J versus Δa). Video analysis enables to identify with high precision the time position of the crack-tip during the crack propagation and at fracture initiation, which in turn takes place at the end of blunting. Crack blunting deals with the plastic deformation of the crack-tip before the stress intensity reach the upper limit for a crack to propagate. A mirror was used to virtualize the image corresponding to the notched side (B-side) of the test specimen, enabling to measure the crack mouth opening displacement (CMOD) during the fracture test. The mirror-image was video captured simultaneously with the image corresponding to the W-side of the test specimen where the crack-tip can be video captured while it propagates. Kinematics of the fracture process was based on both the first and second derivative calculus of the modulus of the two displacement vectors, the CEX vector related to the crack-tip extension on the W-side; and the CMOD vectorand to the crack-mouth opening on B-side. Both the x- and y- vector components were also analyzed in terms of first and second derivatives, aiming to evaluate the kinetic energy of the fracture process along with the crack plane direction (the preferred direction under strain plane condition) as well as the kinetic energy of the fracture process along the orthogonal direction to the crack plane. The greater the plastic effects, the greater the x-component of CEX vector.

Video processing analysis was performed by using TRACKER ver 5.05, an open source video analysis and modeling tool built on the Open Source Physics Java framework (web site https://physlets.org/tracker/). The software allows to apply special filters, manual or automatic tracking of objects and/or vectors as well as to export time and vectorial data in asci format for further numerical analysis using an Excel spreadsheet. Videos contained more than 1500 images (rate of acquisition was 25 frame per second) with a resolution of 1920 x 1080 pixels. A set of at least 250 images were selected for vector tracking analysis. Standard calipers were used to calibrate image objects and vectors.

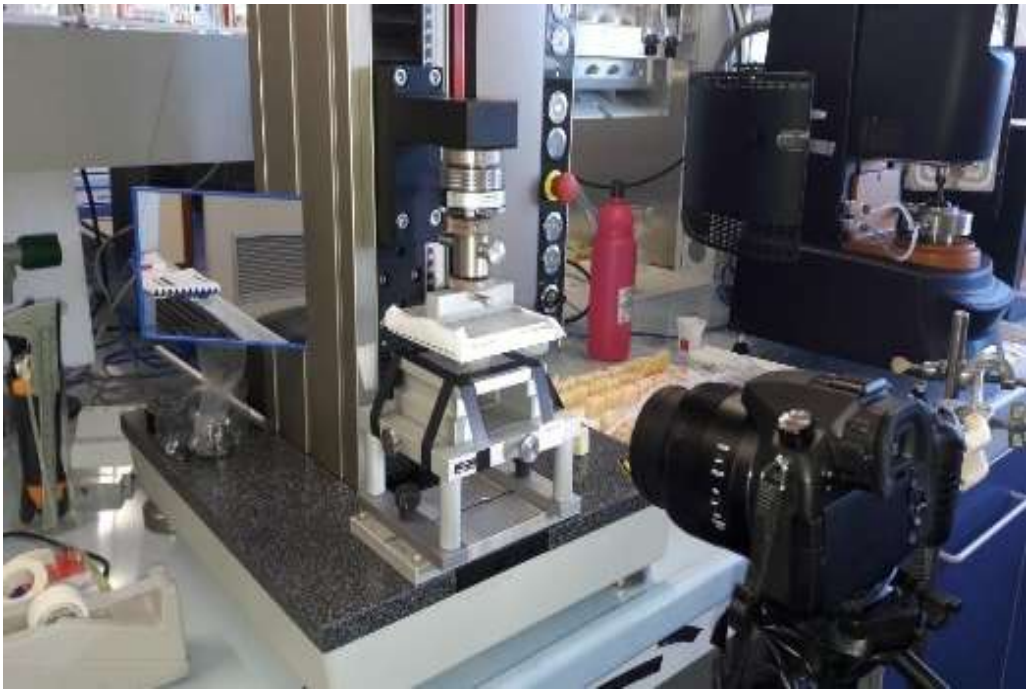

Figure 63 Full-HD 4K-Video recording of the mechanical tests

5.9.5. Numerical procedures for calculating new Fracture Properties

A series of algorithms based on the theory of fracture mechanics have been implemented on a spreadsheet to synchronize and process experimental video and mechanical data related to fracture testing.

After a preliminary verification of the quality of the data (respect of the geometric ratios B/L and a0/W), of the respect of the condition of plane deformation and of the small scale of deformation on the apex of the crack (SSY) and of the criteria of applicability of the equations that govern the mechanics of fracture (goodness-of-fit), it is possible to automatically determine and display in graphical form the Resistance Curve of the specimen together with the punctual variation of the thermodynamic and kinematic properties of the fracture process.

This information allows you to determine different material properties that include:

a) Density of the stress state on the apex of the fissure at the time of the triggering of the first fracture (stable or unstable) in conditions of plane deformation (FRACTURE TOUGHNESS, Kic). This property does not depend on the dimensional scale of the specimen and represents the minimum critical load to break the covalent bonds and responsible for the formation of new surfaces.

b) Minimum energy required to propagate the first stable or unstable fracture (INITIATION ENERGY, Jic). Also this property can be considered a material property, that is independent from the dimensional scale of the specimen provided that the criteria of applicability of the method, of the quality of the experimental data and of the mathematical models used to determine the basic mechanical properties are respected.

c) Energy release rate during stable fracture (FRACTURE ENERGY or TEAR MODULUS). Represents the energy released per unit of new surface formed during fracture propagation. It is inversely related to the average speed of fracture propagation and is a measure of the fragility of the material.

d) Elastic component (Jel) and plastic (Jpl) of the work promptly required for the propagation of the stable fracture through the ligament at any time following the triggering of the fracture. The Jel / Jpl report is a measure of the spontaneity of the fracture on a local scale along the natural direction of propagation of the fracture.

e) Number (Nuc) events of unstable fracture. Unstable fracture event means a short duration fracture event whose kinematic energy (propagation speed) is greater than the displacement point of the load application point.

f) Time required for the event of unstable fracture with greater kinematic energy (time to fracture).

g) Profile of fracture mechanisms. It is a qualitative and quantitative measure of the various mechanisms underlying the local fracture process. The profile is generated by estimating the local extension of the cracks generated by the breaking of the bonds (cracking and splitting) the extension of that generated by viscoelastic, plastic and friction deformation phenomena (slipping) that propagate at 45° with respect to the direction of the load applied.

h) Process area radius (plastic area at the apex of the crack measured before the first unstable or stable fracture propagation event). It is a measure of the plasticity and non-linearity of the mechanical behaviour of the material.

i) Stress, deformation and work corresponding to the propagation trigger.

6. RESULTS AND DISCUSSION

Fracture and yielding behavior of hard or semi-hard cheeses is an important quality mark, affecting aspect such as (i) eating quality, (ii) usage properties for example ease of cutting, grating, and spreading; (iii) product authenticity. Fracture and yielding properties of a cheese should be known under different conditions and time scales. During the first bite of eating, for example, cheese is quickly deformed until it fractures; the time scale of this deformation is less than a second. On the other hand, the time scale of shape retention for the whole cheese piece during storage (ripening) may be of the order of months or much longer. Fracture and yielding are properties concerned with large deformations. However, despite their importance, at the present non-conclusive description of the fracture and yielding exists that hold for all hard and semi-hard cheeses. In several cases there is no clear distinction between fracture and yielding. Both cause a sudden and significant change in the mechanical properties of the material placed under stress. General characteristics of macroscopic fracture are (i) simultaneous breacking of the bonds between the structural elements forming the network (atoms, molecules, particles) in one or more macroscopic planes; (ii) breack-down of the structure of the cheese over length-scales clearly larger than the structural elements, resulting in the formation of cracks, and (iii) ultimately, the falling apart of the cheese into pieces. The first characteristic applies also to the viscous flow, i.e. the bonds will break and reform within the time scale of the experiment. Yielding does not include the third characteristic. The initial processes leading to the fracture and yielding are the same. Sometimes yielding preceedes fracture, especially under slow deformation rates. In other cases, it may be unclear whether one can deal with fracture or yielding. For instance, this becomes evident during strongly deforming on even cutting of rennet-induced milk gels, an important step in PR cheese making. Then the protein network clearly fractures along with visible macroscopic planes, resulting in curd particles, but the whole remains continuous because of the abundance of the acqueous serum, which stems from the fast expulsion of it (syneresis) by the curd particles formed.

Next, various aspects of fracture and yielding of PR cheese were analyzed and discussed. The basic idea of our study was to clarify as the fracture and yielding mechanisms of PR cheese are related to the composition, microstructure, loading and temperature conditions. ESEM and X-Ray Tomography virtualized architecture details from macroscopic to microscopic scale, while the images were numerically processed aiming to clarify the cause-effect relationship between microstructure, material properties and fracture behavior. Rheological properties and fracture behavior were investigated under different external load conditions, which include uniaxial

compression, tensile and bending. To evaluate material properties dependence from both the external load and temperature, all rheological tests were firstly carried out under isothermal conditions by changing the level of the external load, then they were performed under non-isothermal conditions keeping constant the external load able to assure non destructive rheological responses. Results from thermorheological and DSC analysis were finally compared to separate the contribution of temperature from mechanical shear.

6.1. Compositional analysis

As shown in *Figure 64,* the content of moisture, proteins, lipids and salts (NaCl) varied among cheeses without an apparent direct relationship with the claimed ripening age. The major changes were observed in terms of water content just after 24 months of ripening: it decreased between from 30.66 to 22.35% in weight. The water mass transfer taking place outwards the cheese wheels during both salting and ripening operations was believed the most probable mechanism determining the water loss. Both proteolysis and lipolysis are expected to concur to the water activity lowering; they do not affect the total content of protein and lipid. Differences observed in lipids, proteins and salts content were attributed mainly to the initial gross composition of the milk used to produce the investigated cheeses.

6.2. Structure of the Fracture Surfaces

Both the grainy texture and surface complementarity for a 36-months ripened PR cheese can be easily detected at macroscopic scale through visual inspecting of the two fracture surfaces obtained after fracturing of the whole cheese wheel into two half-wheels as performed by the cheese vendors using the typical drop-knifes (*Figure 65*). As can be inferred from figure*,* the two new fracture surfaces appear with **very-high irregularity and partial complementarity at macroscopic scale**. However, grainy texture and surface complementarity can be better evaluated by analyzing the two fracture surfaces arising from standardized test specimens, such as geometry A (*Figure 66*) for DENT fracture test (*Figure 67*), SENB fracture test with geometry D (*Figure 68*), after mechanical fracture carried out under strain-controlled bending conditions (*Figure 69*). Fractured surfaces of the PR cheese sample coded to as “6B2DO” were reported in the *Figure 70* together with the bottom-surfaces of the notched specimen. Visual inspecting of the fracture surfaces provided clear evidence of the fact that the cheese sample behaves as an elastic-plastic material, and therefore, able

to recover partially the matrix architecture after mechanical fracture. The elastic properties are reasonably supposed the main cause of surface irregularity after fracture; the plastic properties the main cause of the permanent local strain and therefore of the loss of the complementarity of the fracture surfaces. Analyzing numerically both the digital images representing the two fracture surfaces at macroscopic scale provided compelling evidence of their partial complementarity. As showed in the *Figure 71*, in fact, the algebraic sum of the grey levels corresponding to the two original fracture surfaces allowed generating a new virtual and smoother surface able to test quantitatively the surface complementarity. Both the surface irregularity and complementarity appeared as scale invariant properties of the PR cheese because they were observed also at microscopic scale by ESEM. Right and left fracture surfaces of a 12-months ripened cheese sample were scanned by ESEM at different local sites and reported in the *Figure 72*. Sites with complementary architecture (indicated by yellow arrows) put on evidence the architecture recovery ability of the cheese matrix during fracture. Microscopic details on chemical phase distribution and architecture were imaged by ESEM coupled with a Solid-State Backscattered Electron Detector (SSD), while those on phase morphology by means of large-field detector (LFD). *Figure 73* shows the fracture surface morphology of a 30M PR sample as imaged at 2mm scale, with a detail at 300μm scale (*Figure 74*). According to what observed directly by visual inspection, different smooth **concave surfaces** appear dispersed inside a network of aggregated structural elements with brighter traits and rougher morphology. Smooth concave surfaces are consistent with the **inter-granular space**; the bright rough network with the **curd granule bulk** and **inter-granular junctions.** *Figure 75* shows the chemical phase distribution and architecture of the fracture surface of both 12-months and 72-months PR cheeses, as imaged at 50-micron scale. As can be inferred from data, PR cheese can be considered a multiphasic-dispersed matrix consisting of an irregular network of strands of aggregated casein micelles (PN) entrapping micropores (PO), free fat (DF) and aggregates of crystalline salts (SCA). As showed in the figure, crystal sizes are higher in the more ripened cheese. Casein and fat morphology as imaged at 100μm can be clearly observed in the *Figure 76*, showing the details of the fracture surface of a 30M PR sample, where the bright rough strands of **casein micelles are aggregated in a discontinuous three-dimensional network,** while the smoother **lipid are dispersed in the network discontinuities**. Data corroborating the above architecture description were provided by results from the x-ray energy dispersive analysis (EDAX) coupled with ESEM-LFD imaging of fracture surfaces of a 30-months ripened cheese are reported in the *Figure 77* and *Figure 78.* The main morphological details were x-ray focused to

extract information about their elemental composition supporting evidence of the lipid nature for the smooth areas and of the protein nature of bright and rough clupms. Carbon (C) and oxygen (O) are the only two chemical elements detected significantly in the smoth areas, that is consistent with the dispersed lipid phase. Carbon (C), oxygen (O), nitrogen (N), calcium (Ca) and phosphorus (P) are the main chemical elements detected inside the brigh and rough areas, that is consistent with the hydrated casein micelles linked together through calcium phosphate bridges. The *Figure 79* shows with high magnification the morphology of two concave surfaces, one of which showing **star-shaped microcracks extending through curd granule bulk**. Such architectures were routinely detected for all the investigated PR cheese samples after fracture under controlled strain conditions. Both the size and shape of the observed concave surfaces are compatible with the size of the partially fused curd granules reported in literature either in young and ripened PR cheese, usually ranging from 50microns to 500microns Annibal (1979). The concave surfaces are the walls of the thin **inter-granule space** and they were generated by granule detachment under strain-controlled fracture. The smooth ground of the concave surfaces is consistent with the lipid phase concentrated inside the external layers of the curd granules (the skin), because the inter-granule space is rich in aqueous serum phase and doesn't permit the fat syneresis. The discontinuous network of bright and rough strands is consistent with the casein micelles linked together through ***calcium phosphate bridges*** inside curd granule bulk and inter-granular junctions. Casein network discontinuity observed on the fracture surfaces clearly indicates that **cheese matrix is characterized by the so-called Shear Connections**: **the calcium phosphate bridges between the casein micelles are perpendicular to the loading direction**. Under mechanical standpoint, either the inter-granular spaces, microcracks inside the curd granule bulk and casein network discontinuity make the PR cheese a **Notch Sensitive Material** under fracture stress. This means that a stress applied on the end point of a discontinuous strand will be transferred to the adjacent strand (stress trajectories), resulting in stress concentration at the tip of microcracks to an extent that is a function of the crack tip lenght.

Further data corroborating the inter-granule nature of both the concave surfaces and star-shaped micro-cracks were provided by the presence of **microscopic crystals** with different surface morphology and with size close to 10microns on the concave surfaces of *Figure 79*. Data provided by ESEM-LFD coupled with EDAX (*Figure 80)* are very consistent with *Struvite, i.e. the magnesium ammonium phosphate hexahydrate* ($MgNH_4PO_4 \cdot 6H_2O$). Data provided by ESEM-LFD coupled with EDAX (*Figure 81*) and are very consistent with *Calcium Phosphate crystals*.

ESEM-LFD detail of the fracture surface of a 72-months PR sample clearly reveals that crystals nucleate on the casein-fat interface and growth towards the inter-granular space (*Figure 82)*: the extended lipolysis improves the phase contrast between inorganic crystals and casein network (*Figure 83*). Literature widely reported that calcium is a key factor controlling the rheological and fracture properties of ripened cheeses. The amount and the physical state of the retained calcium influences the physical characteristics of cheese during ripening, including fracture stress, fracture strain, and cheese firmness (Guinee et al., 2009). Acid development during cheese making dictates the loss of insoluble calcium (Johnson et al., 2006). Changes in the physical properties of cheese during ripening occur in two stages: one is governed by pH and changes to the insoluble calcium content and this may take hours, days or weeks to be fully realized; the other stage is governed by the extent of proteolysis of intact casein that occurs throughout cheese ripening. From that the importance of controlling the factors affecting insoluble calcium throughout cheese making chain including the ripening stage.

PR cheese microstructure observed in our study finds theoretical and experimental fundamentals on its artisanal making process history. During PR cheese production, the colloidal casein micelles undergo destabilization by combined effect of rennet and lactic acid bacteria to form a hydrated casein network entrapping fat globules and aqueous serum phase. Cheese makers cut by hand the casein curd to obtain free curd granules having a rice-like size, which in turn consist mostly of insoluble calcium-caseinate entrapping fat droplets. An insoluble curd mass of about 140kg precipitates at the bottom of the vat. The sites, where the granules close with each other, form the so-called inter-granule curd junctions. The patterns formed between inter-granule curd junctions became more complex because additional type of junctions develop when the curd mass is kept under serum and medium-high temperature (about 55°C for 10 minutes). Under these circumstances, the heat is transferred from surrounding serum towards the curd bulk allowing destabilization of the fat globules entrapped inside the casein network to form a viscous phase, mainly due to the partial melting of the triglycerides. At the meantime, the bulk stress induced by the curd mass under gravity causes the syneresis of both the melt lipids flowing from the bulk towards the skin of the curd granules and of the aqueous serum from curd granules towards the surrounding medium. Melted fat exerts a plasticizing role mainly on the external layers of the curd granules generating a partially fuse “skin” in a complex pattern of inter-granule junctions. Inter-granule spaces are depleted of fat and rich in organic and inorganic insoluble salts. Pressing and salting operations cause further extent of the serum syneresis and salts concentration within the

inter-granule spaces, allowing the curd granules to get closer one to each other and curd mass to strength. Proteolysis and lipolysis cause structure erosion and weakness of both casein network and plastic inter-granule junctions. In general, certain conditions promote the formation of crystals. The components of a crystalline entity must exceed the solubility of that entity (Rajbhandari and Kindstedt, 2005); nucleation sites must provide a place for crystal growth to begin (Swearingen et al., 2004); and physical space, in the form of an open structure or exposed surface, must provide room for the crystal deposit to grow.

Based on our experimental evidences about the fracture surfaces microstructure, two major structure-dependent mechanisms have been formulated for fracture initiation and propagation in PR cheese. An **inter-granule fracture mechanism** was hypothesized at fracture initiation that requires the concentration of the mechanical stress mainly around the deepest tips of the star-shaped micro-cracks, resulting in the detachment of the partially fused curd granules. Lesser-fused the curd granules, lesser deep the inter-granular junctions, deeper the star-shaped micro-cracks, lower the concentrated stress able to overcome the material resistance to the fracture initiation. An **intra-granule fracture mechanism** was hypothesized at fracture propagation as related to high strain gradients caused locally between protein bulk and lipid interfaces. Elastic resistance to the cheese deformation was hypothesized from the casein network, with stress relaxation times lower than those from plastic lipids. A strain gradient at protein-lipid interface may determine the bulk rupture of the curd granules, while plastic strain of lipids opposing to fracture propagation. The average size of the curd granules, the casein-lipid interfaces, and lipid content are expected to increase both the material resistance during fracture propagation as well as the overall time to propagate a fracture.

6.3. Bulk Microstructure

Figure 84 shows the two-dimensional virtualization of the bulk microstructure of a 30-months ripened cheese sample as observed on the sagittal, axial, and coronal planes in a volume of about 200mm^3. Due to the different density, the x-ray computed tomography was able to virtualize and quantify the spatial distribution of casein network, free fat, aggregated crystalline salts and air cells from micro to macro scale. The numerical reconstruction of the entire stack of the two-dimensional images allowed virtualizing of a cheese volume of 5.8cm^3 (*Figure 85*). The availability of a tree-dimensional array of bulk microstructure will enable further scientific investigation on both conceptual and mathematical planes aiming to develop models able to link microstructure to the material properties and composition. Quantitative analysis of the main four phases was performed

through segmentation and voxel count of stacks consisting of 200 2D-images (*Figure 86*). Results were consistent with those arising from both gross composition and data ESEM image analysis (data not showed).

Figure 87 shows 2D- and 3D virtualization of bulk microstructure of a 72-months ripened cheese sample. Data revealed the presence of four different phases. The brightest structures reveal the presence of very-high density crystals; the bright-diffused structures are linked to the high-density casein network entrapping the smooth lipid phase (lower density areas). Highly interconnected **micropores** are also detected, representing the lowest density phase dispersed inside the casein network. Micropores represent the result from mass balance between gas production through metabolic activity of surviving lactic acid bacteria and gas escaping from cheese matrix during the ripening. Coalescence mechanism was supposed to be caused by serum syneresis and cheese pressing. Protein and fat enzymatic hydrolysis during cheese ripening was supposed to cause structure erosion resulting into the spongy architecture of the porous phase. A series of **microcracks** also appear manly concentrated along with two fracture surfaces oriented along with the cheese rind. Such fracture surfaces were generated spontaneously during handling of this long-time ripened cheese specimen, more likely due to the high material fragility caused by very-extended proteolysis and lipolysis. As can be inferred from images, the fracture surfaces have very high complementary profile on macroscopic scale. Such microstructure layout suggests that cheese ripening is one of major factor causing the increasing of structure fragility, decreasing of fracture resistance and, therefore, a pronounced brittle and spontaneous behaviour during fracture propagation.

Numerical image processing allowed virtualization of space distribution of pores as reported in the *Figure 88*, thus enabling estimation of the volume size distribution as reported in the *Figure 89*. 72M showed a tyical four-polydispersed distribution of pores while 30M a typical three-polydispersed distribution with very wide distribution at lowest sizes. Coalescence mechanism progressing with ripening explains the observed differences in pore polydispersity. Major differences between 30M and 72M were found in terms of weighted average pore volume and total pore volume. The weighted average pore volume was about 1,42mm^3 for 30-months ripened cheese and 0,64mm^3 for 72M, respectively. The total pore volume was 230mm^3 for 30-months and 329mm^3 for 72-months respectively (*Table 2****Errore. L'origine riferimento non è stata trovata.***).

A key role of pore volume distribution can be supposed during fracture mechanics of the PR cheese. Higher levels of average pore volume will require higher dissipation of the mechanical energy

under strain as well as during fracture propagation. In other words, the 30-months cheese is expected to show a plastic behaviour more pronounced with respect to the 72-months cheese.

6.4. Thermal and Thermo-Rheological Analysis

The influence of fat crystallization, melting, and polymorphism upon the viscoelastic properties was investigated and demonstrated upon both heating and cooling. With this aim, thermal, rheological, and structural behaviours of PR cheese were studied by complementary techniques including DSC and rheology as a function of temperature. First-order transitions in cheese, i.e. crystallization and melting either of fat and inorganic salts, were monitored at a cooling rate of 10°C/min from -80°C to 350°C degrees C. Shearing tests were carried out under linear viscoelastic conditions, as validated by frequency- and amplitude-stress sweep experiments in the range of temperature of 0°C and 110°C.

6.4.1. First-order thermal transitions in “specks” and “spots” domains

The most probable crystallization and melting transitions occurring inside the “specks” and “spots”, the two typical different structured domains of the Parmigiano Reggiano cheese, were obtained under DSC conditions and then compared to that taking place inside the cheese matrix. For the sake of clarity, specks and spots withdraw from a 33-months ripened cheese are shown in *Figure 90*. A DSC profile of the cheese matrix is reported in *Figure 91* for 12, 20, 33, and 72-months ripened cheese samples. In the figures, “Exo Up” direction is reported to link thermal responses to crystallization (first-order transition) or other exothermal time-dependent events. As can be inferred, the total heat flux profile is characterized by multiple first-order transitions ranging from 13°C to over 60°C. According to results recently published in literature (Gliguem, 2009), endothermic first-order transitions are consistent to triglycerides melting events: saturated triacylglycerols melt close to 14°C, melting of unsaturated lipids continues beyond at 25°C, 37°C and 50°C. PR cheese showed a exothermic event as can be clearly detected within the range 15 - 25°C. According to Gliguem (2009), this “hot-crystallization” transition is consistent with the polymorphic conversion of the triple-chain length 3Lalpha (72 A) structure towards more thermodynamically stable crystalline structure.

From 0°C to 90°C, an endothermic well-shaped baseline was clearly detected that highlights the increasing plasticizing role of lipids in the cheese matrix softening, more pronounced in the samples

ripened beyond 20 months cheeses. The strength of casein-lipids network decreases during ripening as a function of the extent of both proteolysis and lipolysis. Supporting data have been provided by the DSC profiles as obtained in cyclic DSC runs as reported in the *Figure 92*: after the first heating cycle, the DSC profile shows only reproducible first-order transition events, suggesting the irreversible and complete loss of the original casein-lipids network.

Figure 93 shows a thermal spectrum of PR cheese paste whitout specks and spots, obtained with cooling and heating cycles performed at 2°C/min from -80°C to 300°C. *Figure 94* shows a complete DSC spectrum of a 12-months ripened cheese (paste, specks and spots togheter) in the temperature range between -80° and 300°C and a cooling rate of 10°C/min. Very-narrow melting transitions have been observed at the temperatures close to 134°C, 153°C and 168°C. Such these first-order events were attributed to the melting of inorganic crystalline structures. The last wide-endothermic event was registered around 222°C. Coupling DSC and ESEM-EDAX data it has been hypothesized the struvite, i.e. magnesium ammonium phosphate hexahydrate ($MgNH_4PO_4 \cdot 6H_2O$), as the most probable nature of crystal melting on DSC. The ammonium is omnipresent in milk/cheese: it is derived from the gases created by the surface microbes. Ramlogan et al. (2016) proved that the different thermal degradation products from struvite could be detected as a function of the applied analytical technique. X-ray diffraction to reveal that struvite ($MgNH_4PO_4 \cdot 6H_2O$) is stable at 55°C, partially decomposes to dittmarite ($MgNH_4PO_4 \cdot H_2O$) at 100-200°C, and forms an amorphous phase ($MgHPO_4$ and $Mg_2P_2O_7$) at 250-300°C. In our conditions, the four melting events could be associated to the thermal degradation products from struvite.

DSC analysis was also focused on both the “spots” (*Figure 95*) and “specks” (*Figure 97*) domains and results showed the same heat profile for each material domain, but quantitative differences were detected. In the *Figure 95,* DSC profile of a “spots” domain withdrawn from 12-months PR cheese shows clearly an endothermic event close to 240°C and an exothermic event close to 350°C, more likely due to the thermal degradation reactions of the cheese organic material inside the spot domain.

For the sake of the example, the DSC profile related to the speck samples withdrawn from 12M, 20M, 33M, and 72M PR cheeses was reported in the *Figure 97.* As can be inferred from data, a very-narrow and pronounced melting event is registered close to 296°C. Such thermal transition it is very consistent to the presence of **L-Tyrosin** into the speck domain. Moreover, it increases with ripening.

Coupling ESED-EDAX with DSC data, we hypothesize the presence of **Calcium Lactate** inside the spot domain able to undergo melting close to 240°C, very close to the theoretical melting temperature available for this organic salt (Lide, 2007). Literature reports data on crystal identification within the so-called "white particles" having macroscopic scale size on surfaces of ripened cheeses. Tuckey et al. (1938) provided evidence that such inorganic crystals can be identified as calcium lactate. Calcium lactate is formed as the cheese ages when lactic acid reacts with calcium in the cheese. In studies of Parmigiano-Reggiano and long-aged Gouda Tansman et al. (2015), powder x-ray diffractometry has confirmed that hard (crunchy) crystals that form abundantly within these cheeses consist of tyrosine. Furthermore, the authors have tentatively identified the presence of an unusual form of crystalline leucine in large (up to 6 mm in diameter) spherical entities, or "pearls", that occur abundantly in 2-year-old Parmigiano Reggiano and long-aged Gouda cheeses, and on the surface of rindless hard Italian-type cheese. Fltickiger and Schilt (1963) found **tyrosine crystals** in Swiss cheese by light microscopy. Using chromatography, SEM, and energy dispersive spectrometry, Blanc et al. (1979) identified calcium **tyrosinate crystals** in Swiss cheese with secondary fermentation.

Different inorganic salts have been detected in different hard and ripened cheeses that include calcium phosphate and calcium lactate, struvite, brushite, ikaite and calcite (Tansman, 2014, 2017). The white powdery smear found on many aged cheddars are crystals of the compound calcium lactate. Calcium lactate is formed as the cheese ages when lactic acid reacts with calcium in the cheese. They don't have any flavor themselves, but usually signify a piece of well-aged cheese that will be flavorful. The crystals found in aged Italian, Dutch, and Swiss cheese varieties are usually the amino acids tyrosine (distinct specks) and/or leucine (powdery smear, diffuse spots). These are formed as the cheese ages when the protein breaks down into its constituent amino acids. They can build up to high concentrations and crystallize out. Crystals cause the gritty mouthfeel associated with washed rind cheese. Ikaite is a calcium carbonate crystal, and struvite is a magnesium ammonium phosphate crystal. The mineral components are omnipresent in milk/cheese, the carbonate and ammonium is derived from the gases created by the surface microbes. One of the earliest reports on crystals of inorganic and organic origin is from Steinegger (1901). Aggregates of **calcium lactate crystals** are irregular in shape, may measure up to 80microns in diameter, and consist of randomly arranged bundles of slightly curved, needle-like crystals (Bottazzi et al., 1982; Brooker, 1979). Calcium phosphate and lactate crystals are most common. **Calcium phosphate crystals** are abundant and are present in cheese in the form of aggregates up to 30microns in

diameter. Sodium phosphates react with calcium in the cheese and produce insoluble **calcium phosphate** (Kosikowski, 1982). Because of their insolubility, calcium phosphate crystals withstand the processing of cheese and are found in the finished product. Specific staining for calcium makes was used to characterize **calcium phosphate crystals** by optical microscopy (Caric et al., 1985). Anhydrous phosphates absorb water and form large aggregates (Kosikowski, 1982). Small white crystals occasionally develop on the surface of process cheese. Morris et al. (1985) reported their development as early as a week after manufacture. The crystals were identified to be **calcium citrate** and eliminating citrate from the emulsifying agent prevented their incidence. Another kind of crystal was found in process cheese slices by Klostermeyer et al. (1984). The crystals were characterized by the Debye-Scherrer x-ray ana1ysis and were chemically identified as a new tertiary **sodium calcium citrate**.

DSC melting transitions and hot-crystallization coincide with thermal events observed in the two-steps increase in the rheological moduli G' and G".

6.4.2. Loading effects on Viscoelastic and Yielding behaviour

Fundamental rheological properties are material properties, i.e. physical properties that do not depend on experimental conditions used for their determination but only on their composition and microstructure, which in turn depend on their technology history and temperature. Fundamental properties can be measured only when the applied mechanical solicitations (stress, strain, or strain rate) have not permanent effects on material microstructure, i.e. when rheological test is carried out under the so-called “Linear Viscoelastic Regime” or LVR.

Aiming to explore the load range for reversible (linear) and irreversible (non linear) rheological responses, at least three replicates of 18-months, 24-months and 30-months ripened PR cheeses were analyzed under to loading (creep) - unloading (recovery) experiments. Creep was carried out at environmental temperature (25°C) applying an external constant load ranging from 10 to 70N with an increasing step of 10N by using the universal testing machine. After creep a recovery step was also analyzed where the external load was completely removed. For tha sake of example, *Figure 98* shows creep and recovery data for 18-months PR cheese obtained applying a constant load of 50N on a cubic specimen under uniaxial mode. As can be inferred from creep results, the load-point displacement moves on time through three different steps. First, it increases linearly with time as indicated by the instantaneous deformation of the cheese structure. Second, it increases with time according to a long-time stretched exponential law, indicating retarded viscoelastic

mechanisms underlying structure deformation. Third, it increases with time according to a linear law, indicating a steady-state plastic (irreversible) deformation rate. The first step of recovery was able to full recover the instantaneous deformation previously observed under creep conditions. Long-time stretched exponential displacement indicated viscoelastic relaxation mechanisms underlying structure recovery. However, both retarded and steady state recovery were not able to full recover the starting load-point displacement before creep, suggesting hysteretic relaxation mechanisms during structure recovery. The *load-point displacement curves* were registered for all constant loads and numerically analyzed through derivative calculus aiming to evaluating the following rheologial properties:

- **initial elastic modulus** Ge[MPa]. It was estimated by calculating the first derivative of the load-point displacement curve with the creep time going towards zero. The inverse of initial elastic modulus represents the instantaneous compliance, i.e. the ability of specimen to deform reversibly under constant stress.
- **Steady-state deformation rate, dL/dt min** [1/s]. It represents the apparent viscosity of the investigated cheese specimen. It was estimated by calculating the minimum level for the first derivative of the load-point displacement curve with creep time going towards the end of creep.
- **maximum compliance 1/G**[1/MPa] = It was defined as the inverse value of the elastic modulus as calculated at the end of creep (or equivalently, calculated as ratio between the last deformation to the constant stress);
- **residual deformation** ε_f[mm]. It was defined as the last deformation registered at the end of the recovery step.

Results from creep inspired us to hypothesize a key role of the main microstructural elements to the overall deformation mechanism in the investigated cheese. The hydrated protein network, porosity and lipid phase are expected to contribute in a significant way. Under a rheological perspective, PR cheese was pictured as a multiphasic and hierarchical matrix mainly consisting of a viscoelastic network of casein micelles linked through elastic calcium phosphate briges, entrapping plastic components that include globule fat, free fat, star-shaped micro discontinuities and polydispersed microporosity. A **microstructure-based creep model has been developed to describe the time-dependent relaxation under constant load and to measure both elastic and inelastic moduli of the cheese components.** With this aim, a six-parameter model Burger's model consisting of a

Maxwell element, i.e. a spring connected in series with a dashpot, which in turn is connected in series with three Voigth elements has been elaborated (*Figure 99*). Each of Voight element consists of a spring and a dashpot connected in a paraller fashion able to describe the viscoelastic retarded repsonse. In our rheological model, the Maxwell spring ideally represents the instantaneous elastic strain of the hydrated casein network; the Maxwell dashpot ideally models the steady-state viscous flow (or apparent viscosity) of the free fat; the first Voight element describes the viscoelastic respoinse of star-shaped micro-cracks; the second Voight element represents the microvoids, like shown in *Figure 100*. The equation governing the creep behavior of the cheese under constant stress was the following:

$$\varepsilon(t) = \left(\frac{\sigma 0}{E0}\right) + \left(\frac{\sigma 0}{E1}\right)\left[1 - \exp\left(-\frac{t}{\tau 1}\right)\right] + \left(\frac{\sigma 0}{E2}\right)\left[1 - \exp\left(-\frac{t}{\tau 2}\right)\right] + t\left(\frac{\sigma 0}{\eta 1}\right) \qquad (44)$$

Where: σ_0 = applied stress [Pa or N/m^2]

Material properties for the Maxwel element (indicated with the apper case 1):

E_1 = instantaneous elastic modulus [MPa]

η_1 = apparent viscosity [MPa*s]

Material properties represented by the first and second Voight elements (indicated with the number 2, 3 respectively) are the following:

$E_{2,3}$ = elastic modulus [MPa]

$\tau_{2,3}$ = characteristic retardation time [s]

The proposed creep model was fitted to the experimental data (*Figure 101*) under the specified boundary conditions:

1) $E_1>0$;
2) $E_1>E_2>E_3$;
3) $0<\tau_1<\tau_2<\tau_3<t_{max}$.

In *Table 3, Table 4* and *Table 5* are reported model-creep parameters for PR 18M, 24M and 30M.

The Steady-state deformation rate (de/dt) was modelled as a function the applied load using a two-parameters power law equation:

$$de/dt = B * (e)^n \qquad (45)$$

where B and n were treated as fitting parameters. *The parameter "n" was considered as a quantitative measure of the degree of deviation from the liner viscoelastic regime*. For the sake of example, *Figure 102* shows loading and unloading cycles in displacement [mm] versus load [N].

Figure 103 shows the steady-state strain rate dL/dt [1/min] as under loading – unloading cycles in 18-months ripened cheeses. The linear viscoelastic regime can be clearly detected under the limit of 10-40N, after which a loss of linearity takes place with the rate of deformation increasing according to the power law. In the range 10-40N the bulk elastic properties dominate. Over about 40N the frictional and plastic properties becomes dominant on the elastic ones, and rheological behavion becomes non linear. Under medium-high loads the cheese yields because of the decreasing of the friction coefficients, which in turn is caused by the oiling-off phenomenon, i.e. the liquid fat migrates through the cheese specimen towards the surface favoring strain mechanisms. The values "B" and "n" for PR 18M, 24M and 30M were reported in the *Table 3, Table 4* and *Table 5.* Under rheological standpoint, one can conclude that the PR cheese as a soft material showing an instantaneous, time-dependent and steady-state plastic (or viscous) relaxation only under non-destructive loading conditions. The yielding behavior under non-linear regime increases with the cheese ripening, more likely due to the greater extent of proteolysis. A major contribution of the discontinuities and pore phase of the more ripened cheeses was believed to affect their creep behavior: the more ripened the cheese, greater material discontinuities and porosity, the more pronounced the non-linear regime for the cheese deformation.

6.4.3. Temperature effects on Viscoelastic and Yielding behaviour

The effect of temperature on viscoelastic properties was evaluated carrying out creep tests at in the range of temperature sweeping from 0°C to 110°C and using the strain-controlled Rheometer under shearing conditions. Preliminary tests were performed to individuate the stress range able to assure the linear viscoelastic response at each investigated temperature. 3Pa was chosen as a non-destructive stress to be used during all temperature-sweep creep tests. For the sake of example, *Figure 104* shows creep-recovery curves of 12M PR cheese and *Figure 105* PR 33M creep-recovery curves. As can be inferred from curves, temperature affects more in depth the recovery response, suggesting hysteretic mechanisms from structure relaxation. The six-parameter model previously tested on isothermal data was used also to model the creep behavior under temperature sweep. Steady-state relaxation representing the yielding behavior under each isothermal creep step was discussed accounting for the casein network discontinuities and plastic relaxation of the lipid phase inside the cheese matrix. The linear relationship between the logarithm value of the steady-state strain rate was analyzed for PR 12M, 30M and 60M cheeses against the reciprocal temperature (for an easier reading of results, it was expressed in Kelvin degree and multiplied per 10^3/T[K])

using the Arrhenius linearized model (*Figure 106)*. *Two apparent creep activation energies suggest two main mechanisms for yielding response as measured by the steady-state strain rate*. The first relaxation mechanism (in the figure E1, ranging from 74 to 81J/Kmol) has been mainly attributed to the dislocation/coalescence (buckling) of macro-discontinuities and micro-porosity up to the point where such discontinuities disappear. The second relaxation mechanism (in the figure E2, ranging from 10 to 45J/Kmol) suggested a softening response of the cheese matrix. Such relaxation mechanism was mainly attributed to the sliding or slippage of the interfaces between the strands of casein micelles (harder regions) and free fat (soft regions). The transition point was indicated as ***Softening Transition Temperature (Ts)*** or *Plastic Transition Temperature*: it appeared strictly related to the cheese ripening, i.e. close to 324K (51°C), 317K (44°C), and 315K (42°C) for 12, 60 and 30-months respectively. In *Figure 107* is shown the plastic transition temperature of 12M PR cheese. Softening temperature can be considered as a physical marker of cheese yielding (plastic) behavior. The lower the softening temperature, the greater the plastic contribute of fat component on cheese yielding. A role of the shear forces has been postulated on melting events under creep, resulting in transition temperatures lower those estimated under DSC conditions. Both the creep activation energies and transition temperatures show the minor temperature dependence of structure relaxation for both 30- and 60-months cheeses. These results have been attributed to the plasticizing role of water and fat. The longer the time of ripening, the more extent of water evaporation and the naturally occurring lipolysis, i.e. triglycerides hydrolysis and free fatty acid degradation to a low-molecular weight compounds all acting as impurities that hinder and limit the crystallization processes. DSC data provide compelling evidence the minor extent degree of fat melting.

For practical purposes, we also analyzed the apparent activation energy (E2) related to the relaxation mechanism upon softening temperature agains the length of cheese ripening ranging between 12 months to 60 months (*Figure 108*). The lower the E2, the higher the yielding response under creep. As can be inferred from the figure, a well-shaped relation with a minimum close to 36M was detected between yielding behavior and ripening. However, the yielding response was statistically different ($p<0,05$) among among 16M, 18M, 24M, 28M, 36M but the differences between 14M and 16M, between 12M and 24M, and between 28M, 30M and 46M were not significant ($p<0.05$). An intermediate softening was observed for 12-month ripened cheese, more likely due to the plasticizing contribute from the water content relatively high in this cheese. The increasing of softening was attributed to the extend of both proteolysis and lipolysis in the range of 16M and 36M, over which the lipolysis dominates on ripening. Proteolysis causes the shortness of

the strands of casein micelles, while the lipolysis causes the splitting of triglycerides into free fatty acids and glycerol.

However, a role of the pH increase was hypothesized over 36M causing the increase of th strain resistance and lowering of softening.

Both the Softening Temperature and the Activation Energy (E2) can be considered as new physical markers of plastic behavior of the PR cheese and therefore they can be used to quantify the difference in brittle behavior. The greater the softening temperature or E2, the lower the brittle and higher response. Pastic mechanisms oppose to the elastic strain and can stop the propagation of a facture.

6.4.4. Volume distribution of Viscoelastic and Yielding properties

Aiming to evaluate the distribution of the viscoelastic and yielding properties, isothermal creep and recovery tests were carried out under different constant loads (from 10N to 100N) applied on cubic test specimens (10mm x10mm x10mm). Seven slabs were obtained by cutting the cheese cloves along direction parallel to the cheese radius (they are referred as to “radially-oriented slabs” from “radial-oriented cut”). Five slabs were obtained by cutting the cheese cloves along direction orthogonal to the cheese radius (they are referred as to “axially-oriented slabs” from “axially-oriented cut”). At least five test specimens from the axially oriented slabs were “axially loaded” and indicated with the letter “ai”. In both the cases the “I” represent the position of the specimen on the slab. In particular, the slabs indicated as “a1” were the closer to the diameter of the cheese wheel; while the slabs indicated as “a6” were the closer to the rind at the bottom of the cheese wheel. On the other hand, the slabs indicated as “r1” were the closer to the axial rind of the cheese wheel; while the slabs indicated as “r7” were the closer to the axis of the cheese wheel. At least five test specimens from radially oriented slabs were “radially loaded” and indicated wth the petter “ri”. The instantaneous elastic modulus (MPa) was treated as a marker for the viscoelastic response, whereas both the steady-state deformation rate (mm/min) and residual deformation after recovery step were considered as measure of the yielding response. In the *Figure 109*, the scheme of cutting of the slabs from the cheese cloves was reported. Results from ANOVA were also reported in the figure. The major differences were observed in terms of elastic modulus and residual deformation, irrespectively of the load applied. Radial loading was on average greater than the axial one, while the residual deformation was greater for axial loading. This means that, both the viscoelastic and the yielding response of the PR cheese are anisotropically distributed inside the cheese wheel. The

number of the elastic bonds is higher and/or oriented preferentially along with the cheese radius, where the lower yielding response was consequently observed. Such physical distribution of the elastic bonds is consistent with the of the PR cheese making history. In fact, the fresh caseous mass become slowly a cheese wheel through a strong deforming operation which take place inside typical cylindrical tools having convex lateral surfaces, while a flat tool placed on the top of the mass assures the formation of the two flat surfaces of the cheese wheel. Under these particular strain conditions, the caseous mass undergoes anisotropic stress status, with a radially oriented stress greater than the axially oriented one. Such stress may cause a major number of intermolecular interacions and interatomic bonds along the axial direction. Smaller but significant differences in terms of the steady-state deformation rate can be appreciated in the *Figure 110*. The effect of different loads on the steady-state deformation rate was reported. It was possible to recognize that the yielding behavior dominates over 50N on the linear viscoelastic response. However, such rheological property was also distributed locally according to the slab orientation. In particular, the axially oriented slabs close to the diameter of the cheese wheel behave on average more plastic than those close to the flat rind. Moreover, the radially oriented slabs close to the central axis of the cheese wheel behave on average more plastic than those close to the convex rind. As showed the *Figure 111* (top) the yielding behavior described by the permanent residual deformation takes place only over the 70N. The upper limit for the load was greater that that observed for the steady-state deformation rate, suggesting that the elastic bonds involved for the structure recovery dominate over the viscous ones, while the viscous bonds dominate under creep yielding. More likely hysteretic mechanisms underpin viscoelastic deformation and relaxation steps. Permanent deformation was also distributed locally, more pronounced into the slabs close to the flat and convex rinds. Finally, the instantaneous elastic modulus can be analyzed according to the data reported in the *Figure 112*. A well-shaped trend was observed as a function of the applied load, with a maximum level close to 70N. This result was consistent with the canges observed in the permanent deformation, providing compelling evidence that the elastic bonds dominate on the viscoelastic response enabling the cheese structure to recover upon relatively high loading. However, the instantaneous elastic modulus was distributed locally: it reduces on average to the half from the diameter of the cheese wheel to the flat rind as well as from the central axis to the convex rind. More in dept knowledge of the loading and position dependence of the viscoelastic and yielding properties can be gained analyzing data reported in the *Figure 113, Figure 114* and *Figure 115*. ANOVA were performed to analyze the difference using the load level, loading direction and

slab position as grouping factors. As can be observed, the characteristics distribution profiles can be recognized, irrespective of both the slab position and loading direction.

6.4.5. Temperature effects on viscoelastic behaviour

The effect of temperature on viscoelastic behavior was also evaluated under dynamic shearing conditions. Small-amplitude oscillatory shear (SAOS) tests were carried out under linear viscoelastic regime (non destructive conditions). Stress amplitude and frequency sweep tests were preliminarly carried out aiming to find the range of stress and frequency delimiting the linear viscoelastic response in the range of temperature from 0°C to 70°C (*Figure 116* for 60°C and *Figure 119* for 100°C). The storage modulus G'(Pa) and the loss modulus G'' (Pa) analyzed at 3Pa and 1Hz were reported in the *Figure 118* for 12M, 33M, and 72M cheeses. As can be inferred from figure, cheese with 33 months of ripening behave more hard respect to both the 12M and 72M cheeses, with an intermediate behavior of the 12M cheees in the temperature range of 10-35°C. Differences between 33M and 72M cheese were attributed to the different extent of the proteolysis. The latter causes the rupture of casein strands, causing the decreasing of the elastic bond to be solicited during shear. The modulus is given by the ratio of the stress over the strain. Thus, for a constant strain, the stress will be proportional to the number of bonds that are deformed in the material. This implies that the modulus will decrease only proportionally to the number of bonds that become elastically inactive as a result of ripening. The intermediate solid behavior of th 12M cheese in the temperature range of 10-35°C was explained accounting for its relatively higher water content. Furthermore, G1 of the 12M and 33M reaches a maximum level in the range of temperature of 15-20°C, but this maximum was hardly to detect for 72M more likely due to the very extend of ripening. The maximum of G1 in this temperature range was attributed to the crystallization of the unsaturated lipids in the cheese matrix. Most hydrolyzed lipids of the 72M cheese cannot more crystallize. However, G' for 33M and 72M cheeses followed a whell-shaped trend with a minimum in the range to 40-50°C, providing compelling evidence that the cheese undergoes softening close to this temperature range before to undergo hardening due to the casein denaturation and cross-linking towards 70°C. However, the G' in 12M cheese followed a monotonic decreasing trend beyond 25°C until to 70°C, suggesting the loss of the water due to the evaporation and that the higher water content protected the cheese matrix from casein degradation and structure hardening. The hardening effect was not detected during creep experiments more likely because of the difference of time length of the experiments: the creep holds for 120s, while

the SAOS hold for 300s at each of investigated temperature. The ratio between G'' and G1, called "tan delta", deals with the solid or liquid-like behavior. Tan delta for 12M, 33M, and 72M were reported in *Figure 119.* As can be observed from data, G''/G' undergoes a step-change close to 45°C indicating the softening of the cheese matrix for all the investigated cheeses. Comparing the G' and Tan Delta profiles one can conclude that the investigated cheeses behave as a hard solid in the temperature range of 10°C and 40°C with the harder response in the range 15-20°C. Temperature induced hardening, more likely due to the loss of the free water and casein degradation more pronounced for the 33M cheese.

Figure 120 shows results from dynamic tests under cyclic steps of temperature changing in the range of 0°C and 35°C (with a rate of 10°C/min) for 12M cheese. Data indicate clearly hysteretic changes of both the storage and loss moduli (G' and G'') with a decreasing trend of both the moduli. However, an increasing trend of Tan Delta was registered, indicating the progressive loss of the solid-like behavior. Such behavior was attributed to the changes in lipid crystalline status. Cyclic heating-cooling allow the crystalline lipid fraction to disappear so that its contribute in terms of elastic bonds to the elastic modulus decreases.

6.5. Fracture Behavior Analysis

The way in which a hard or semi-hard cheese fractures may be different. In general, two fracture modes may be distinghished, viz. fracture in tension and in shear mode. However, fracture mode is not always unequivocally related to the way in which the test piece is stressed. Both in a tension and in a uniaxial compression test the test piece may fracture either in tension or in shear. In the frequently applied uniaxial compression test, fracture always starts at the outside if it occurs in tension, while it normally starts in the interior of the test piece if it occurs in shear. In compression, the tensile stress is caused by the increase in circumference of the test piece. General characteristics of macroscopic fracture are (i) simultaneous breacking of the bonds between the structural elements forming the network (atoms, molecules, particles) in one or more macroscopic planes; (ii) breack-down of the structure of the cheese over length-scales clearly larger than the structural elements, resulting in the formation of cracks, and (iii) ultimately, the falling apart of the cheese into pieces.

As provided from ESEM and X-Ray tomography, microcracks are naturally occurring into the PR cheese bulk. However, one or more notches can be volountarily applied on the macroscopic scale on a test specimen when the cheese is recnognized as a crack-length sensitive material aiming to standardize its fracture dynamics. As known from the fracture mechanical theory, microcracks

and/or notches will start to growth (fracture initiated) if the local stress at the crack tip exceed the strength of the bonds between the structural elements giving the solid-like properties to the cheese. In general, fracture propagation could follow different mechanisms, one of which would dominate as a function of cheese structure, composition, loading conditions and time scale. Size and shape distribution of micro-cracks and pores, the extent of casein-fat interfaces and temperature must be considered as critical factors affecting fracture and yielding properties.

6.5.1. Compression test

The compression tests were carried out to evaluate the extent of the "overshoot" for comparative purposes among the investigated cheeses, as shown in *Figure 121a*. The overshoot is conventionally interpreted as being due to a limited breakown of the physical structure of the sample. In our study, the overshoot was evaluated only qualitatively being related to the tixotropic properties the cheese, i.e the time-dependent structure relaxation. Moreover, the region of the macroscopic fracture was also analyzed qualitatively. Finally, the elastic modulus, the maximum load and the corresponding limiting deformation were calculated. For the sake of example*, Figure 121a* shows the fracture profile obtained from uniaxial compression tests for 12M, 24M, 30M, 36M and 72M cheeses together with the images of the test specimens. As can be inferred from data, all the investigated cheeses show non-linear relation between the load and load line displacement with the load going to zero. Therefore, the Young modulus was detected accounting as the maximum of first derivative load-displacement data, which corresponds to the slope of the straight line passing through the inflexion point of the load-displacement curve. Ripened cheeses showed higher resistance to the elastic deformation as suggested by the higher levels of the elastic modulus. The cheese with 72months ripening showed a maximum load of about 10 time greater than that of 12months cheeses, while the 36months cheeseswas about four times greater. Cheees with 12M and 24M cheeses show very similar characteristics. More young cheeses showed yielding behavior, more pronounced respect to the more ripened ones, as suggested by the more extended region of plastic fracture. The fracture process occurs from the interior of the test specimen due to tension stress along with the equatorial plane. Overshooting after the maximum stress was directly related to the ripening extent and inversely related to extent of the observed oiling-off. More ripened cheeses allow the liquid fat to migrate towards the surfaces of the test specimens during fracture tests. Under uniaxial compression conditions, it is not possible to predict exactly where a microcrack will start and propagate inside the test specimen. Uniaxial compression tests were

carried out also to investigate the yielding behavior of the cheese. In *Figure 122* is shown the cheese bulk structure after 75% uniaxial compression. *Figure 123*a and b show both the load-time and the load-displacement curves for a 12-months ripened cheese. Cubic specimens were compressed until 30% with a constant displacement rate of 5mm/min for load and unload steps. Under such conditions, the test specimens were not fractured but only yielded. *Figure 124* compare the maximum load, the corresponding displacement, and the work to yielding among the cheeses having 12, 24, 30, 36, 42, 48, 54, and 60 months of ripening. Data showed that, the "Work to Yielding" reaches a minimum level for 24M nd 30M cheeses.

6.5.2. Double-edge notched tensile test (DENT)

Creep tests were carried out also to investigate fracture properties. After an initial elastic and viscoelastic response, the cheese deforms plastically under constant stress to reach an upper limit of time where the fracture initiate, then it resists to the fracture propagation, and finally breaks in two pieces. For each curve, the time for fracture initiation, time of end fracture, duration of the fracture, time of maximum speed of fracture propagation were calculated by means of the first and second derivative calculus. The slope of the straight-line tangent to the initial part of the displacement-time curve (**tg1**) represents the initial elastic modulus; the slope of the straight-line tangent to the inflection point (**tg2**) represents the steady-state plastic deformation rate. They were indicated as to "**m1"** and "**m2"**, respectively. The adimensional ratio m2/m1 was used as a measure of the elastoplastic behavior that opposes to the fracture initiation. In *Figure 125* and in *Figure 126* are shown the tensile fracture curve of PR 30M sample 3B1AV. *Table 6* shows tensile parameters calculated for 18M and 30M PR samples. Results were compared and reported in the *Figure 127* and *Figure 128.* As can be inferred from data, cheesewith 18months of ripening showed undergo to the frature initiation in a time more than double respect to the 30months cheese. The elastioplastic ratio decreases according to a power law as a function of time to fracture initiation. The structure relaxation times required for fracture to initiate is inversely relatd to m2/m1. The lower the deformation rate, the greater the cheese resistance to fracture initiation.

6.5.3. Single-edge notched bending test (SENB)

Since fracture propagation from a notch follows the crack plane direction if the Small-scale yielding (SSY) and the Plane-Strain conditions are both accomplished, preliminar data qualification was

performed. As can be observed in the *Figure 129*, the stress was not negligible in the direction orthogonal to the crack plane, as suggested by the fracture profile of the two new fractuer surfaces changing direction at 45°, for test specimens for which the relations between length, thickness, with, and crack length do not accomplish the required specifications:

$$\begin{cases} \dfrac{P_{max}}{P_Q} < 1.10 \\ 2.5 \cdot \left(\dfrac{K_Q}{\sigma_Q}\right)^2 < B \\ 2.5 \cdot \left(\dfrac{K_Q}{\sigma_Q}\right)^2 < (W - a_0) \end{cases}$$

Another preliminary test was performed aiming to evaluate the notch sensivity of PR cheese (
Figure 130). Four types of test specimens having rectangular cross-section, two whitout notch (sample B and D) (
Figure 131) and two with notch (sample A and C) (
Figure 132), having different relations between length, width, thickness and notch size, were compared under three-point bending test conditions. Results clearly showed that fracture in a test specimen without notch propagtes from a random point through an unpredictable pattern. Plastic deformation was not negligible inside the sample A, allowing to resist to the fracture initiation and propagation. In this case, cheese flows to such an extent that part of the deformation is lasting after removal of the stress already before fracturing initiate (before the maximum load). The applied load concentrates on a randomly distributed discontinuity of the cheese bulk, thus the work to fracture is governed by the plastic behavior across the specimen tickness. The extent of flow increases with the time scale as well as with the ligament, i.e the uncracked specimen portion. Load concentrates on a notch previously generated on the cheese surface, allowing to reduce drastically the plastic strain close to the crack-tip. In fact, sample B and D having the same ligament showed the same plasticization before fracture initiation (the same deformation at the maximum load), with sample D showing lower resistance, like shown in *Figure 133*, and more detailed in *Figure 134*. Such behavior was explained because of the greater ligament, i.e. higher number of strain connections within the sample B that can bear the applied load before a fracture initiate. The notched sample B has the same ligament of the unnotched sample C, thus they showed very similar load resistance but different yielding behavior, with the sample C more undergoing more plastic deformation before fracture initiation.

Aiming to construct affordable resistance curves (J-R curves) each investigated cheese was analyzed for uncertainty of its geometrical properties. *Figure 135* shows the uncertainty associated to the geometrical properties of the test specimens. In particular, the 95% of the investigated cheese specimens showed a ratio between notch length and with ranging between 0.4 and 0.44: the relative uncertainty was less than 10% respect to the standardized specification, i.e. a0/W equal to 0,41. Ligament calculated as difference between specimen with and notch length varied between 25mm and 27mm for the 95% of the investigated cheese samples: the relative uncertainty was lower 5% respect to the test geometry specifications, i.e. a0 = 18mm and W = 44mm. All test specimens outside that ranges were discarded from further analysis.

Load, load-line and crack-mouth opening displacements, and crack extent under controlled strain has been registered simultaneously and then analysed aiming to characterize the cheese resistance to both the fracture initiation and propagation. For tha sake of the example, load-line displacement, crack mouth opening displacement together with the video recorded track of crack propagation in 18months cheese were reported in the *Figure 136*. The integral-J was calculated as a function of the stress intensity factor during crack initiation and propagation so that the J-R curves were constructer for each investigated cheese sample. Moreover, the kinetic energy released during fracture propagation was also calculated by means of the first and second derivative calculus of the time - crack extent data. Energy kinetic profiles allow to characterize the brittle events underpinning cheese fracture under strain-controlled fracture (quasi-stable fracture). The main results from Integral-J and kinetic analysis are the following:

- Load, load-line displacement and crack extent profiles
- Elastic (Jel), Plastic (Jpl) energy releasing and energy kinetic profiles
- Elastoplastic relation between crack-mouth opening displacement (CMOD) and crack extension (CEX)
- Geometrical distribution of the elastic (Jel) and plastic (Jpl) energy releasing inside the test specimen
- Fracture surface profile as calculated numerically
- J-R Resistance Curve

For the sake of example, results from I-Integral and kinematic analysis for 18months cheese were reported in *Figure 137*, *Figure 138* , *Figure 139* and *Figure 140*.

A computer program was finally developed in visual basic language, able to calculate strain, stress, elastic modulus, the work to fracture, as well as elastic and plastic energy released at crack initiation

and propagation together with the kinetic energy of the main brittle events underpinning the quasi-stable fracture process. Material properties obtained from J-integral and kinematic analisis where new fracture properties were defined and calculated starting from the basic measurements:

1) Jic (Jq) (KJ/m^2) = Energey released for fracture initiation
2) T_{EF} (KJ/m^2) = Tearing Modulus, energy released during fracture propagation (it was calculated as $T_{SF} = \frac{E}{(\sigma_Y)^2}\frac{dJ_{SF}}{da}$
3) CEX(K)max (Joule, J) = Kinetic Energy under crack extension
4) Δa(UCi)max (mm) = Maximum fracture extent inside the test specimen
5) Σ(Δa(UCi) (mm) = Cumulative extent of unstable fracture (only the brittle evente)
6) J_{UC1} (KJ/m^2) = Energy released for the unstable fracture event with the highest kinematic energy
7) (Jel/Epl)UCimax (adimensional) = elastoplastic energy involved under the unstable fracture event with the highest kinematic energy
8) Σ(JEL)/ Σ(EPL) = elastoplastic energy involved during the whole fracture process
9) Jtot Δa (mm1) (KJ/m^2) = Energy released when the fracture progresses 1 mm
10) Jtot Δa (mm5) (KJ/m^2) = Energy released when the fracture progresses 5 mm
11) Jtot Δa (mm10) (KJ/m^2) = Energy released when the fracture progresses 10 mm
12) Wf Pmax (KJ/m^2) = work of fracture, area under the curve
13) εUTS/εE_Bmax (adimensional) = ratio between the ultimate strain and strain at the end of the linear elastic response

Figure 141 shows J-R curves of PR 12M, 18M, 24M, 30M and 37M cheese samples and material properties were summarized in the *Table 7.* The J-R curve two steps can be clearly distinguished:

1. PRE-CRACK (or BLUNTING step) terminating at the maximum deceleration of the J-R curve. A first quantity of energy (elastic and plastic energy) must be supplied for the elastoplastic notch-mouth opening before fracture intitiation.

2. CRACK PROPAGATION step represented by the steady-state growing part of the J-R curve (the asymptotic linear section of the curve). The rate of growing of the energy releasing is due to the increase of plastic processes close to the tip of the notch during fracture propagation.

As can be inferred from Resistnce Curve, tearing modulus, indicated decreasing of the plastic zone with the following order: 12M, 18M, 30M. The brittle fracture follows the inverse order. The more ripened the cheese, more brittle the fracture behavior. However, some unexpected behavior was

observed for the 36months cheese. Fracture properties as defined and calculated from the three basic experimental measurements (load, displacement, crack extension) were statistically grouped into “Kinetic” and “Energy” based classes (*Figure 142*), then the most significant of them were used as input variables for Principal component Analysis (PCA). Results from PCA were showed in the *Figure 143* and *Figure 144*. As can be inferred from data, three new independent factors were individuated all explaining more than 81% of the experimental variance, which enable us to classify all the investigated cheese samples according to their material properties related to the crack initiation and fracture propagation resistance. More than 50 cheese specimens were fully classified with respect to their ripening time, using a Tree Classification algorithm to find the split value for the fracture properties used as input variables (*Figure 145*).

CONCLUSIONS

Why the Frattura a Scaglie is one of the most important texture properties for Parmigiano Reggiano cheese? It is strictly related to artisan manufacturing process and product authenticity. The cheese structure takes origin during the manufacturing process. Firstly, casein proteins undergo liquid-to-gel transition entrapping serum and fat. Then a semi-solid grainy structure is obtained through an artisan operation, cutting curd by-hand to obtain fine granules. Finally, cooking, serum syneresis, salt curing, enzymatic proteolysis and lipolysis all make the cheese structure hard throughout an extended ripening period (minimum 12 months). The simplest way to prove both the artisan process and cheese authenticity is by evaluating to what extent fine granules split into brittle slivers.
The goal of my research was to evaluate the relationships between structure and fracture mode, under both theoretical and experimental viewpoints. The aim was to provide an engineering definition of the "Frattura a Scaglie" and an instrumental method for its quantitative measurement. With this aim. the PR cheese has been studied over a wide of scale size and scale time, using instrumental techniques all giving very-high level of data.

Microstructure virtualization and analysis indicated that casein micelles are aggregated in a discontinuous three-dimensional network, while the smoother lipid are dispersed in the network discontinuities. Inter-granular space, curd granule bulk and inter-granular junctions are clearly distinguishable. Morover, star-shaped microcracks extend through curd granule bulk and granule junctions. Data corroborating the inter-granule nature of both the concave surfaces and star-shaped micro-cracks were provided by the presence of microscopic crystals with different surface morphology and with size close to 10microns on the concave surfaces. Magnesium ammonium phosphate hexahydrate (Struvite), Calcium Phosphate, tyrosine crystals, and Calcium Lactate crystals were detected into the inter granular space. Casein network discontinuity observed on the fracture surfaces clearly indicates that cheese matrix is characterized by the so-called Shear Connections: the calcium phosphate bridges between the casein micelles are perpendicular to the loading direction. Under mechanical standpoint, either the inter-granular spaces, microcracks inside the curd granule bulk and casein network discontinuity make the PR cheese a Notch Sensitive Material under fracture stress. This means that a stress applied on the end point of a discontinuous strand will be transferred to the adjacent strand (stress trajectories), resulting in stress concentration at the tip of microcracks to an extent that is a function of the crack tip lenght. Based on our experimental evidences about the fracture surfaces microstructure, two major structure-dependent

mechanisms have been formulated for fracture initiation and propagation in PR cheese. An inter-granule fracture mechanism was hypothesized at fracture initiation that requires the concentration of the mechanical stress mainly around the deepest tips of the star-shaped micro-cracks, resulting in the detachment of the partially fused curd granules. Lesser-fused the curd granules, lesser deep the inter-granular junctions, deeper the star-shaped micro-cracks, lower the concentrated stress able to overcome the material resistance to the fracture initiation. An intra-granule fracture mechanism was hypothesized at fracture propagation as related to high strain gradients caused locally between protein bulk and lipid interfaces. Elastic resistance to the cheese deformation was hypothesized from the casein network, with stress relaxation times lower than those from plastic lipids. A strain gradient at protein-lipid interface may determine the bulk rupture of the curd granules, while plastic strain of lipids opposing to fracture propagation. The average size of the curd granules, the casein-lipid interfaces, and lipid content are expected to increase both the material resistance during fracture propagation as well as the overall time to propagate a fracture. A key role of pore volume distribution can be supposed during fracture mechanics of the PR cheese. Higher levels of average pore volume will require higher dissipation of the mechanical energy under strain as well as during fracture propagation.

The influence of fat crystallization, melting, and polymorphism upon the viscoelastic properties and yielding properties was investigated and demonstrated upon both heating and cooling, suggesting hysteretic mechanisms for structure relaxation in the range of 0°C and 50°C.

Under a structural standpoint, PR cheese was pictured as a multiphasic and hierarchical matrix mainly consisting of a viscoelastic network of casein micelles linked through elastic calcium phosphate briges, entrapping plastic components that include globule fat, free fat, star-shaped micro discontinuities and polydispersed microporosity. Under a rheological standpoint, PR cheese behaves as a soft material showing an instantaneous, time-dependent and steady-state plastic (or viscous) relaxation only under non-destructive loading conditions. The yielding behavior under non-linear regime increases with the cheese ripening, more likely due to the greater extent of proteolysis. A major contribution of the discontinuities and pore phase of the more ripened cheeses was believed to affect their creep behavior: the more ripened the cheese, greater material discontinuities and porosity, the more pronounced the non-linear regime for the cheese deformation. A **microstructure-based creep model** has been developed to describe the both viscoelastic and yielding behavior under constant load. With this aim, a six-parameter model Burger's model consisting of a Maxwell element, i.e. a spring connected in series with a dashpot, which in turn is

connected in series with three Voigth elments, has been hypothesized. Each of Voight element consists of a spring and a dashpot connected in a paraller fashion able to describe the viscoelastic retarded repsonse. In our rheological model, the Maxwell spring ideally represents the instantaneous elastic strain of the hydrated casein network; the Maxwell dashpot ideally models the steady-state viscous flow (or apparent viscosity) of the free fat; the first Voight element describes the viscoelastic response of star-shaped micro-cracks; the second Voight element represents the microvoids.

Two apparent creep activation energies suggest two main mechanisms for yielding response as measured by the steady-state strain rate. The first relaxation mechanism (in the figure *Figure 106*, E1, ranging from 74 to 81J/Kmol) has been mainly attributed to the dislocation/coalescence (buckling) of macro-discontinuities and micro-porosity up to the point where such discontinuities disappear. The second relaxation mechanism (in the *Figure 106*, E2, ranging from 10 to 45J/Kmol) suggested a softening response of the cheese matrix. Such relaxation mechanism was mainly attributed to the sliding or slippage of the interfaces between the strands of casein micelles (harder regions) and free fat (soft regions). The transition point was indicated as Softening Transition Temperature (Ts): it appeared strictly related to the cheese ripening, i.e. close to 324K (51°C), 317K (44°C), and 315K (42°C) for 12, 60 and 30-months respectively. Softening temperature can be considered as a physical marker of cheese yielding (plastic) behavior. The lower the softening temperature, the greater the plastic contribute of fat component on cheese yielding. Both the creep activation energies and transition temperatures show the minor temperature dependence of structure relaxation for both 30- and 60-months cheeses. These results have been attributed to the plasticizing role of water and fat. The longer the time of ripening, the more extent of water evaporation and the naturally occurring lipolysis, i.e. triglycerides hydrolysis and free fatty acid degradation to a low-molecular weight compounds all acting as impurities that hinder and limit the crystallization processes. Both the Softening Temperature and the Activation Energy (E2) can be considered as new physical markers of plastic behavior of the PR cheese and therefore they can be used to quantify the difference in brittle behavior. The greater the softening temperature or E2, the lower the brittle and higher response. Pastic mechanisms oppose to the elastic strain and can stop the propagation of a fracture.

Both the viscoelastic and the yielding properties of the PR cheese are anisotropically distributed inside the cheese wheel. The number of the elastic bonds is higher and/or oriented preferentially along with the cheese radius, where the lower yielding response was consequently observed. Such

physical distribution of the elastic bonds is consistent with the PR cheese making history. In fact, the fresh caseous mass become slowly a cheese wheel through a strong deforming operation which take place inside typical cylindrical tools having convex lateral surfaces, while a flat tool placed on the top of the mass assures the formation of the two flat surfaces of the cheese wheel. Under these particular strain conditions, the caseous mass undergoes anisotropic stress status, with a radially oriented stress greater than the axially oriented one. Such stress may cause a major number of intermolecular interacions and interatomic bonds along the axial direction. The coalescence of voids does not stop the crack propagation across the whole cheese matrix.

Based on empirical evidences and fracture mechanic theory, an engineering definition for the law requirement “FRATTURA A SCAGLIE” has been provided as follows “the ability to initiate and propagate a crack under strain-controlled conditions whitout significant plastic deformation”. It will be used to modify the PDO disciplinary aiming to solve the actual criticism in sensory evaluating of this product characteristics. “Fracture toughness” and “Tear Modulus” define and quantify the fracture resistance of the PR cheese. The fracture toughness quantifies the initiation of stable crack growth. The dimensionless tearing modulus quantifies the increase of plastic zone that opposes to the crack propagation. Lower Fracture Toughness and Tear Modulus corresponds to more brittle fracture behavior. The resistance to the fracture increases with growing crack size, because a «plastic zone» develops at the tip of the crack because of coalescence of microvoids. These two fracture parameters have been proposed as a measure of the law requirement “FRATTURA A SCAGLIE”. Fracture resistance was measured by the so-called J-Integral theory requiring only four experimental measurements, i.e. load, crack-mouth opening displacement, load-line displacements, crack extension. J-Integral defined as the energy releasing rate per unit crack area of a pre-cracked test specimens with standardized geometry. A rising resistance curve can be obtained by plotting J-Integral versus crack extension. According to the generalized theory of fracture mechanics, a minimum of energy is required for a crack to start and propagate. However, temperature, loading direction and specimen size all affect the measurement of fracture resistance. Therefore, either the geometrical characteristics of cheese test specimens, instrumental specification for fracture testing as well as quality requirements for evaluable data have been standardized according to the American Society for Testing and Materials (ASTM) guidelines. A computer program was finally developed in visual basic language, able to calculate strain, stress, elastic modulus, the work to fracture, as well as elastic and plastic energy released at crack initiation and propagation together with the kinetic energy of the main brittle events underpinning the quasi-stable fracture process.

Tearing modulus, indicated decreasing of the plastic zone with the following order: 12M, 18M, 30M. The brittle fracture follows the inverse order. The more ripened the cheese, more brittle the fracture behavior. However, some unexpected behavior was observed for the 36months cheese. Moreover, new other fracture properties were calculated from the three basic experimental measurements (load, displacement, crack extension). They were grouped into Kinetic and Energy based classes of material properties and used as input variables for Principal component Analysis (PCA). Results from PCA allowed to find three new independent factors, all explaining more than 81% of the experimental variance, enabling to classify all the investigated cheese samples according to their material properties related to the crack initiation and fracture propagation resistance. More than 50 cheese specimens were fully classified with respect to their ripening time, using a Tree Classification algorithm to find the split value for14 fracture properties used as input variables.

The experimental setup and theoretical criteria from this study set the basis to codify a uniform, industry-recognized measurement of the quality that can be useful to certify the authenticity of Parmigiano Reggiano cheese

ACKNOWLEDGEMENTS

I thank Prof. Pasquale Massimiliano Falcone (Università Politecnica delle Marche, Italy) for its scientific supervising; Dr. Marco Nocetti, Dr. Aldo Bianchi and Dr.ssa Valentina Pizzamiglio (Consorzio del Parmigiano Reggiano, Italy) for their help in cheese recruitment and evaluating cheese fracture properties; Ing. Marco Moscatti (EurotecLab, Montegalliano, Modena, Italy) for imaging by microtomography, as well as Dr.ssa Laura Valentini and Prof. Pietro Gobbi (Università di Urbino, Italy) for ESEM measurements.

FIGURES AND TABLES

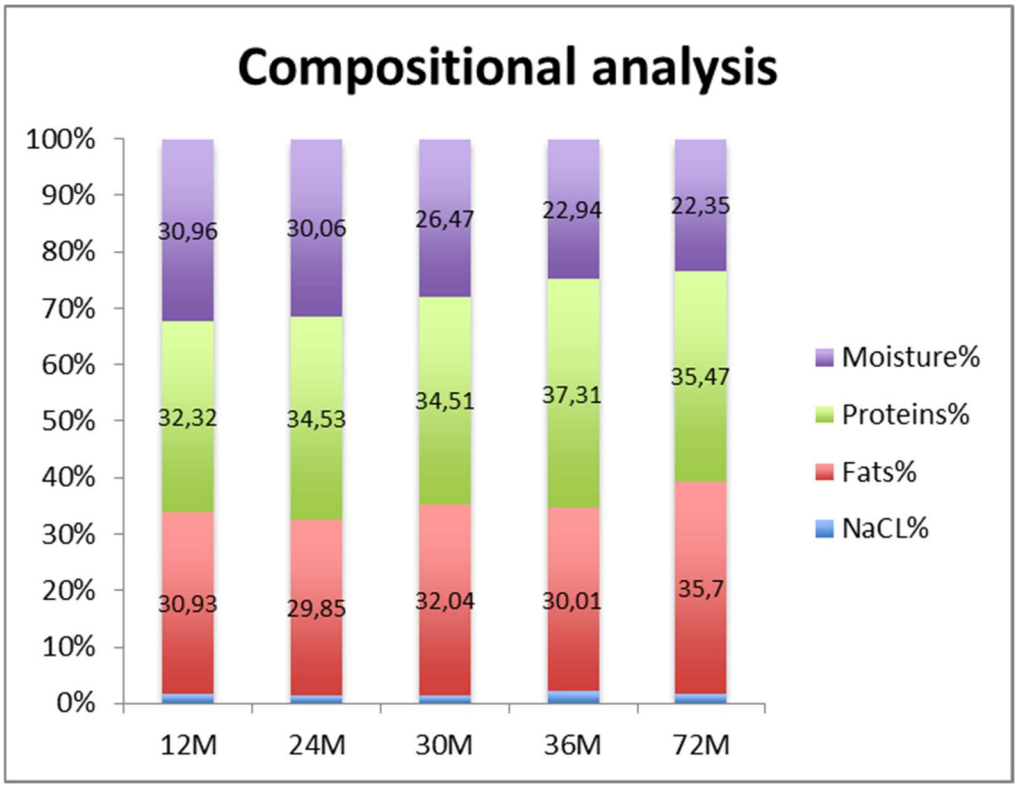

Figure 64 Gross composition of PR cheese with different ripening ages. Total humidity, proteins, fat and inorganic salts are reported as average of 5 replicates (the relative uncertainty was below 5% for each measurement at p-level of 0.05)

Figure 65 Grainy Texture of Fracture Surfaces for a 36-months Parmigiano Reggiano cheese

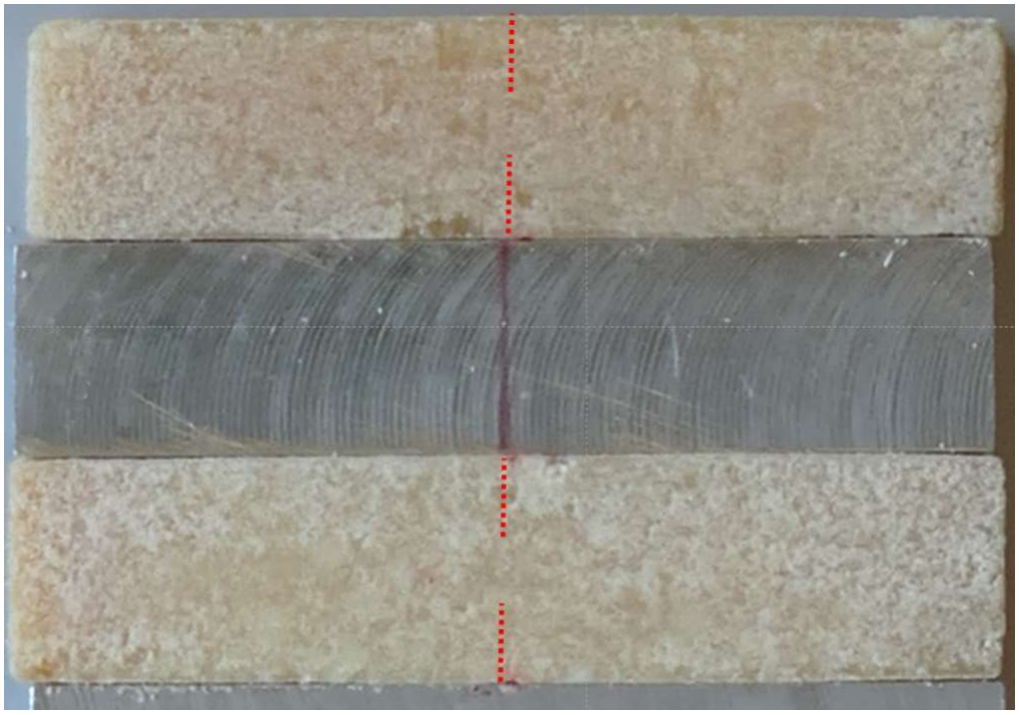

Figure 66 Test geometry A for DENT fracture test [detail of 18-months ripened PR cheese]

Figure 67 Fracture surfaces after DENT fracture test [detail of 18-months ripened PR cheese]

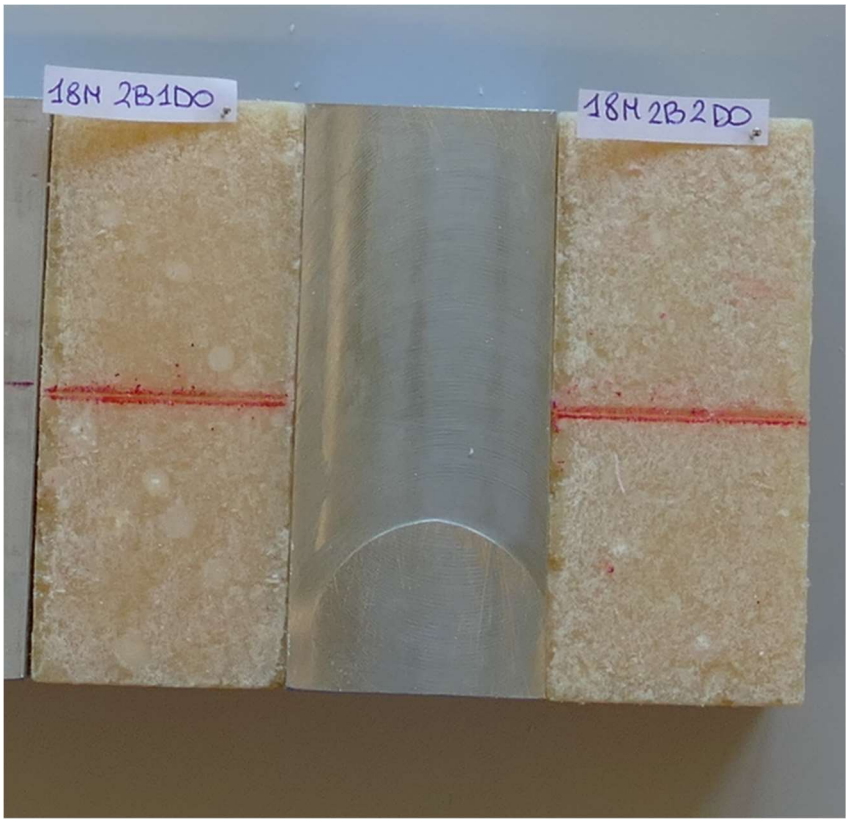

Figure 68 Test geometry D for SENB fracture test [18-months ripened PR cheese]

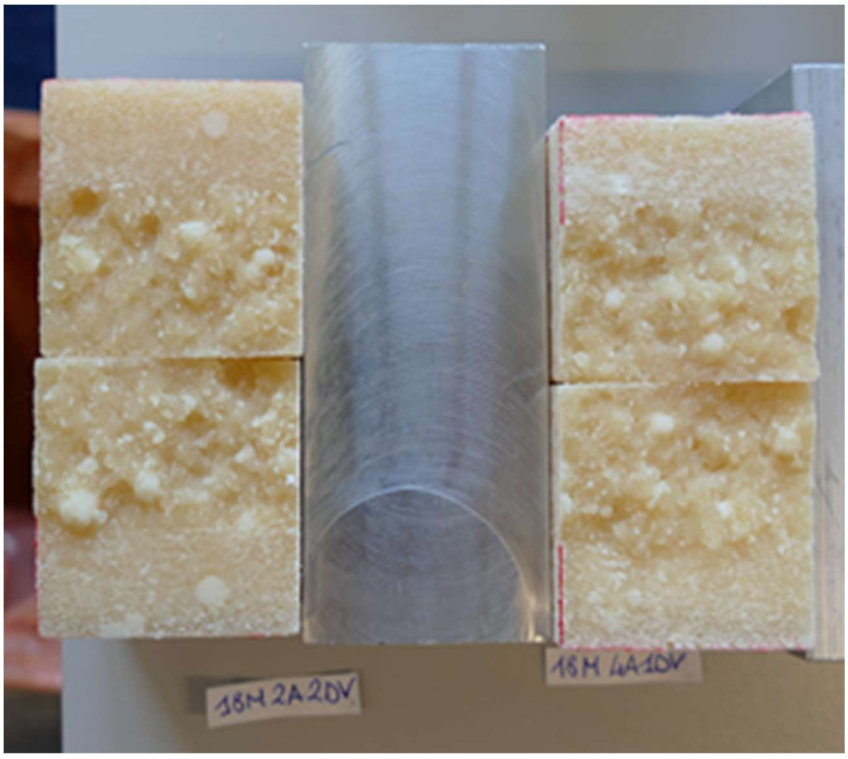

Figure 69 Fracture surfaces after SENB fracture test [18-months ripened PR cheese]

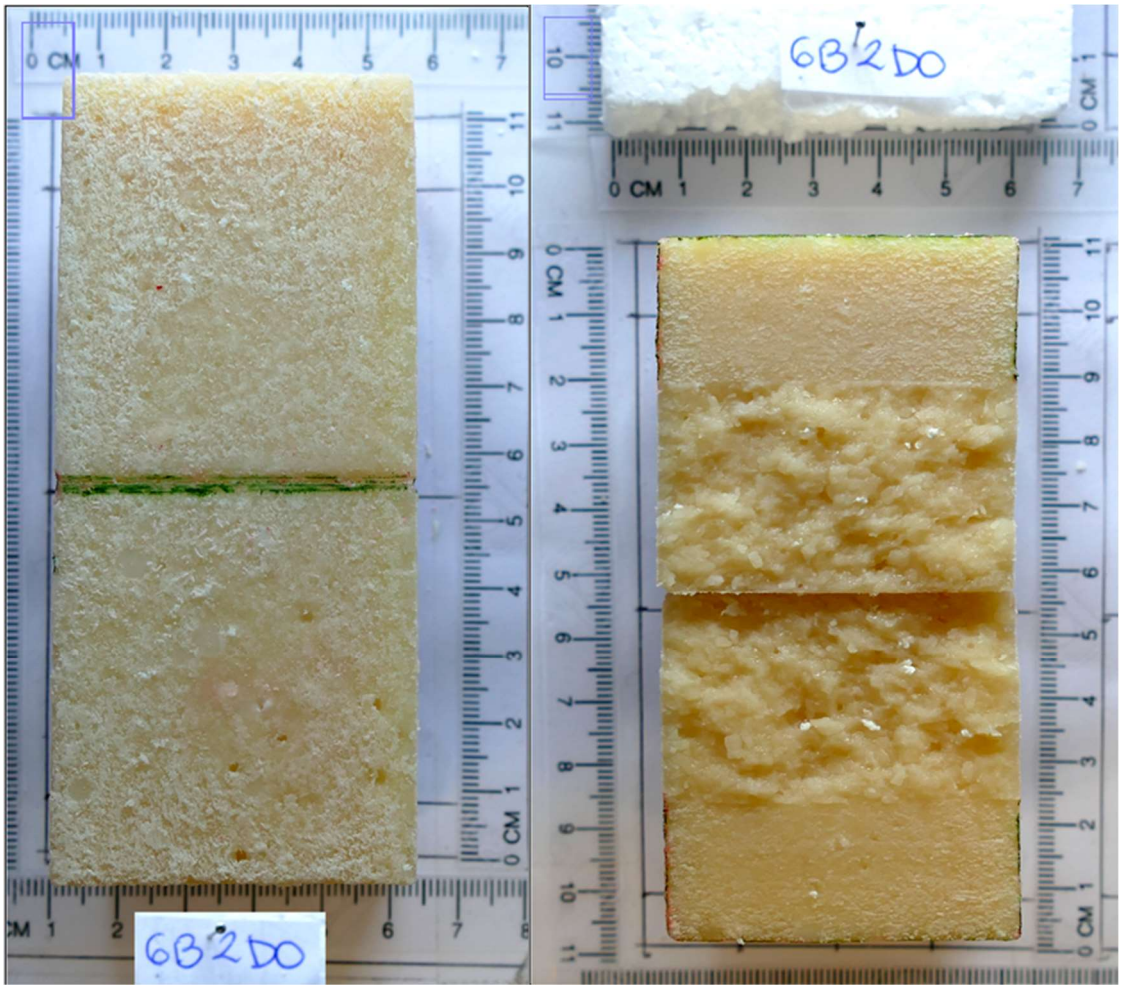

Figure 70 Test geometry D before and after SENB fracture test [12-months ripened PR cheese]. The fracture surfaces are grainy and partially complementary

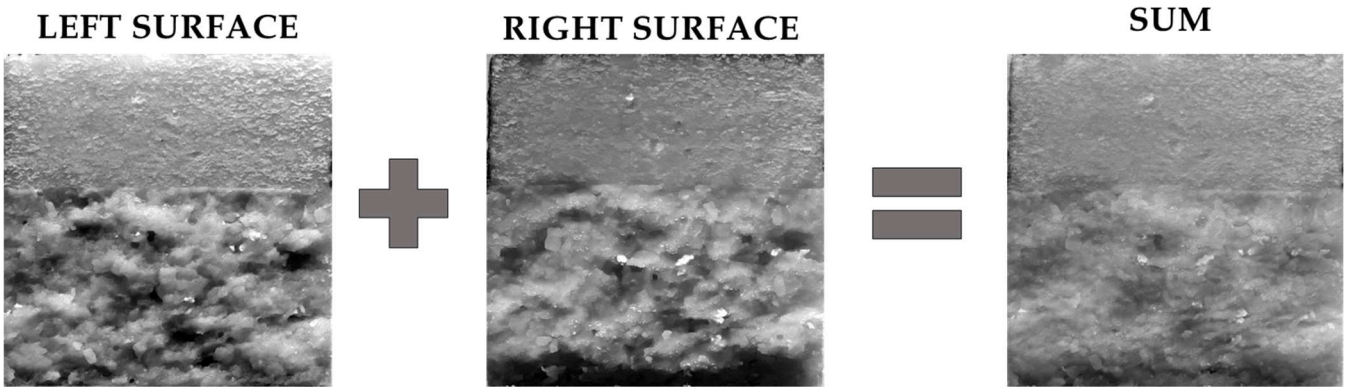

Figure 71 Test for complementarity of fracture surface profiles originated under strain-controlled conditions. Lower surface intensity profiles indicate higher complementarity between the two fracture surfaces

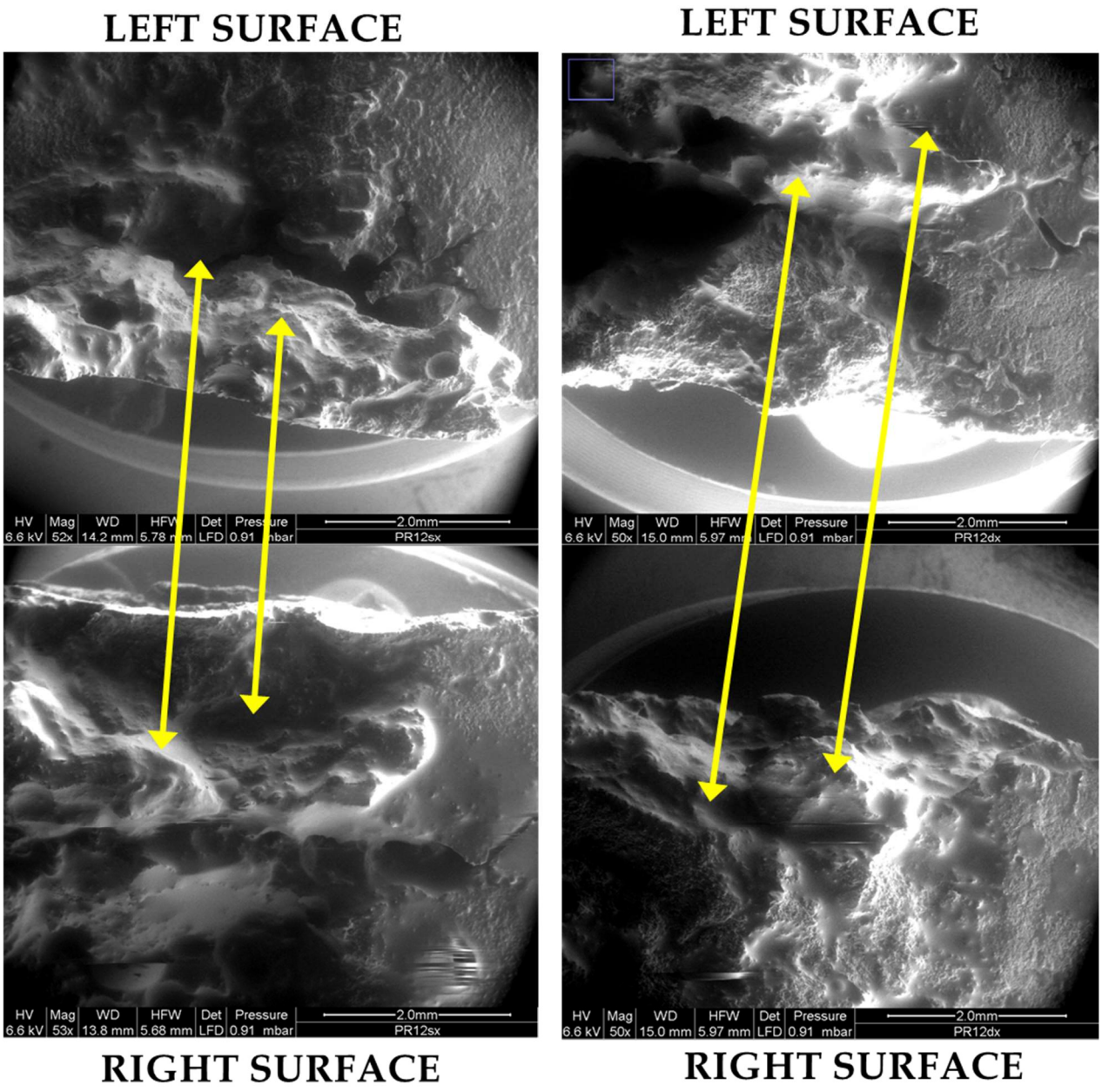

Figure 72 ESEM-LFD images of left and right fracture surfaces of a 12-month PR cheese as pictured at mesoscopic scale (scale bar of 2.0mm). Fracture surface complementarity is scale-invariant property.

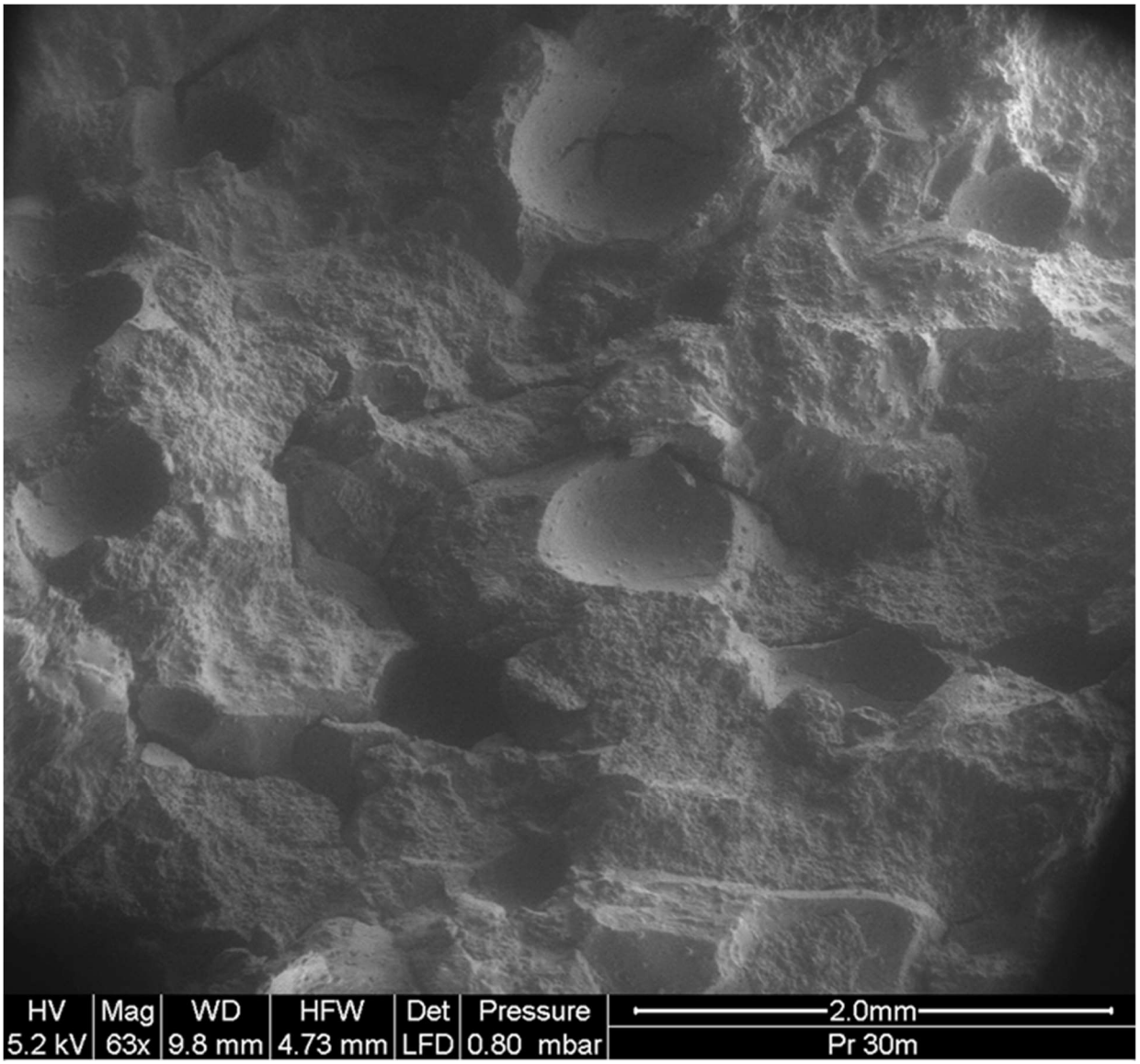

*Figure 73 ESEM-LFD detail of the fracture surface of a 30M PR sample (scale bar 2mm). Smooth concave surfaces are consistent with the **inter-granule space**; the bright rough network is consistent with the **curd granule bulk** and **inter-granular junctions***

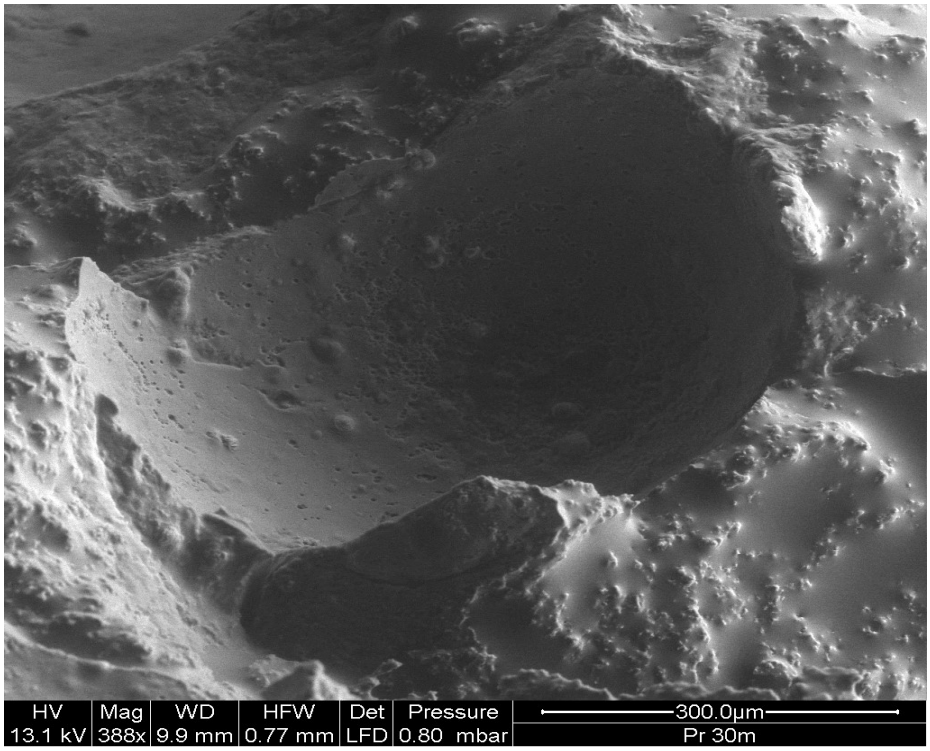

Figure 74 ESEM-LFD detail of the fracture surface of a 30M PR sample (scale bar 300µm)

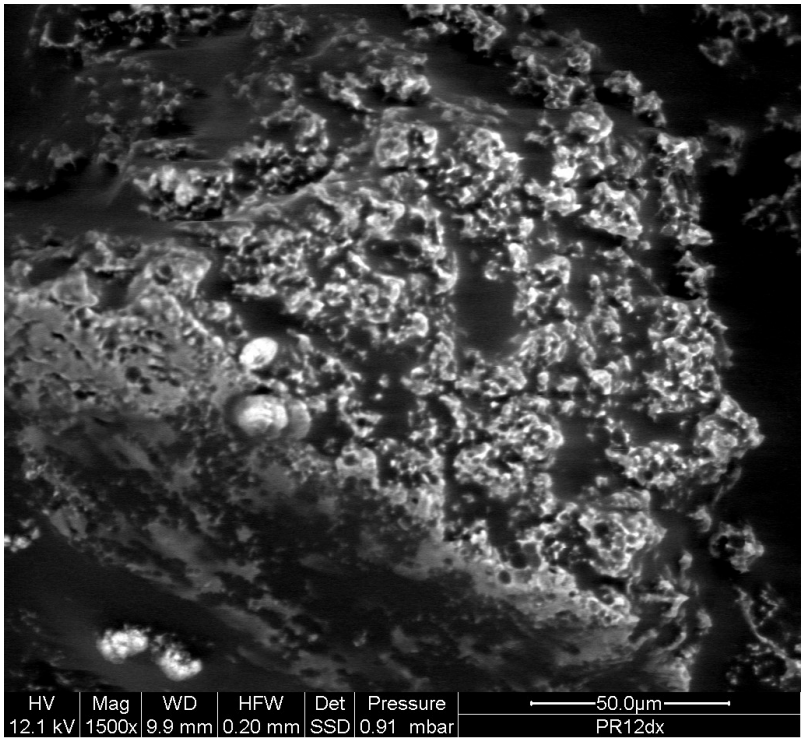

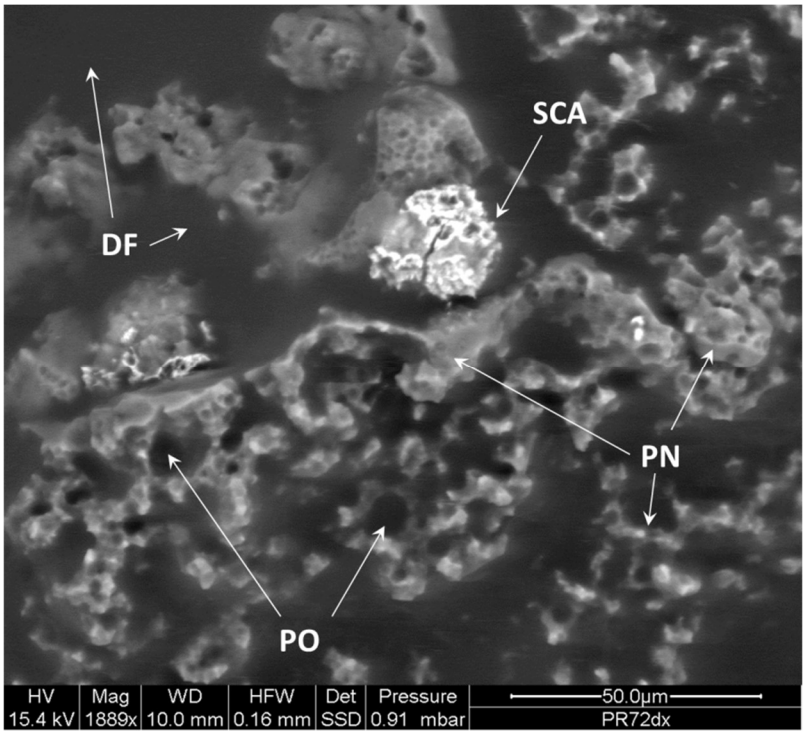

Figure 75 ESEM-SSD phase detail (scale bar of 50µm) of fracture surface of a 12-months PR cheese (Top) and 72-months PR cheese (Bottom). Phases detected: discontinuous Network of hydrated Casein Micelles (PN), Dispersed Fat (DF), Porosity (PO) and Salt Crystals Aggregates (SCA). Crystals' size growths with ripening.

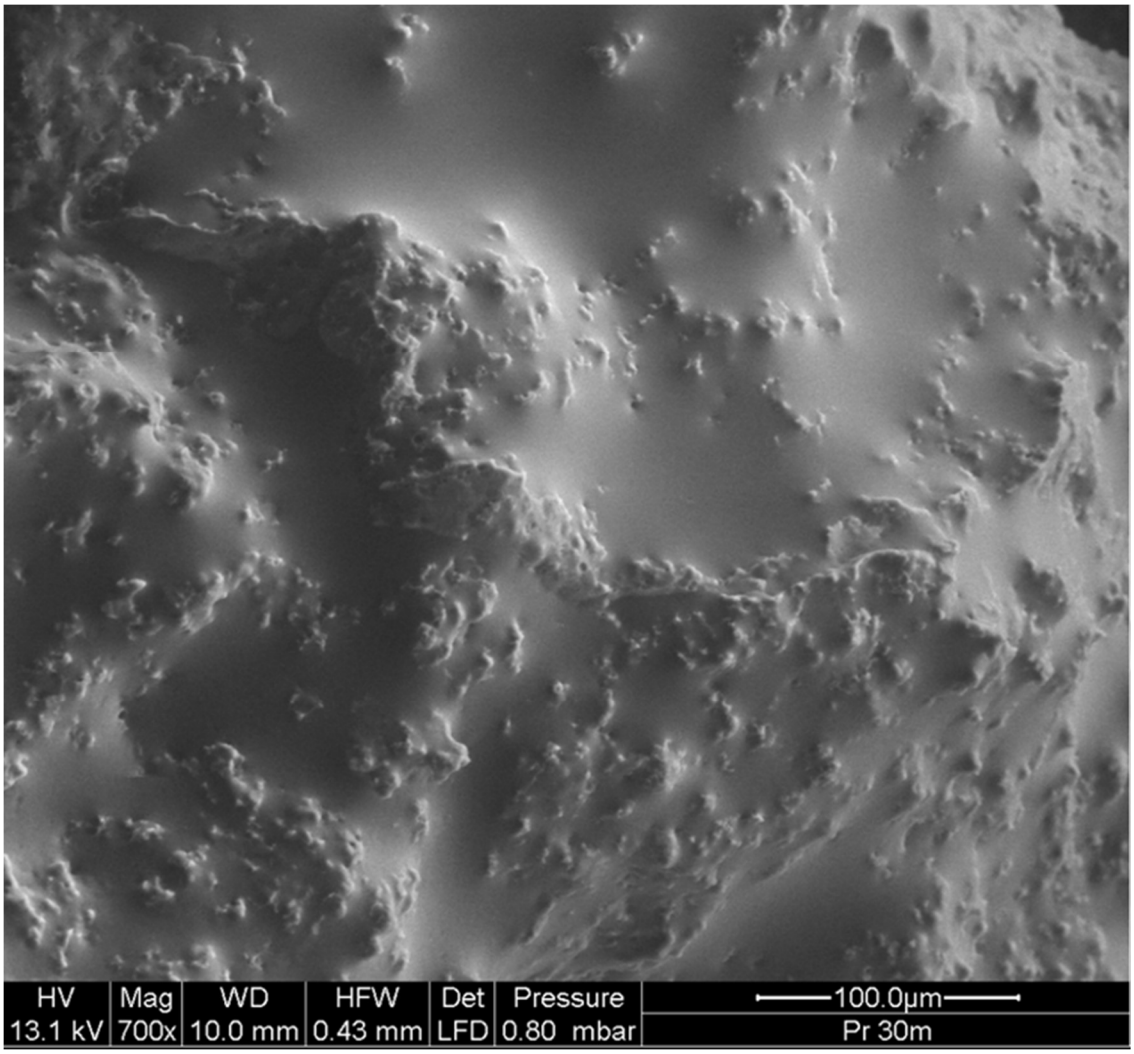

Figure 76 ESEM-LFD detail of the fracture surface of a 30M PR sample (scale bar 100µm). The bright rough clumps represent the ***discontinuous Network of hydrated Casein Micelles****; the smoother phase indicates the* ***dispersed lipid phase***

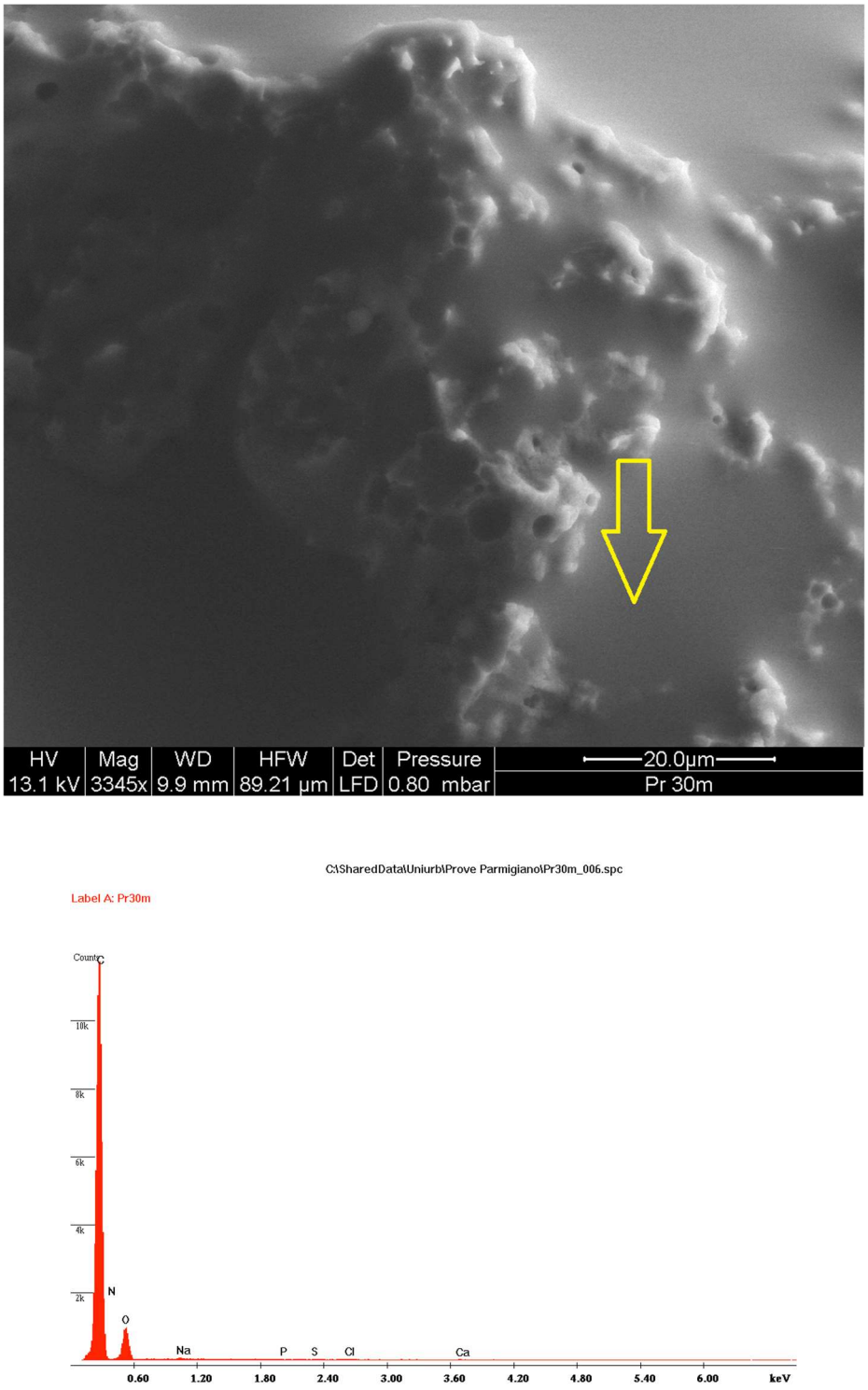

Figure 77 Top: ESEM-LFD image of a 30-months PR cheese (scale bar of 20µm). Bottom: smooth morphology and EDAX spectrum are consistent with the ***dispersed lipid phase****. Nitrogen, calcium and phosphorus are not significant*

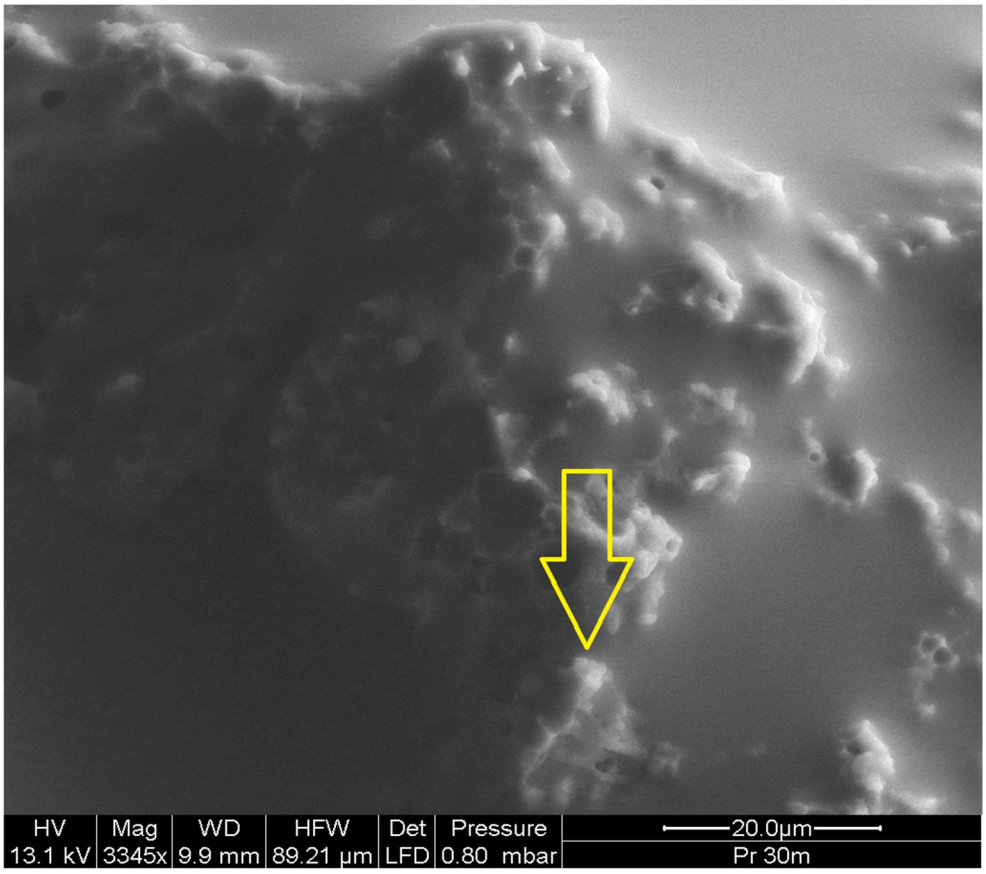

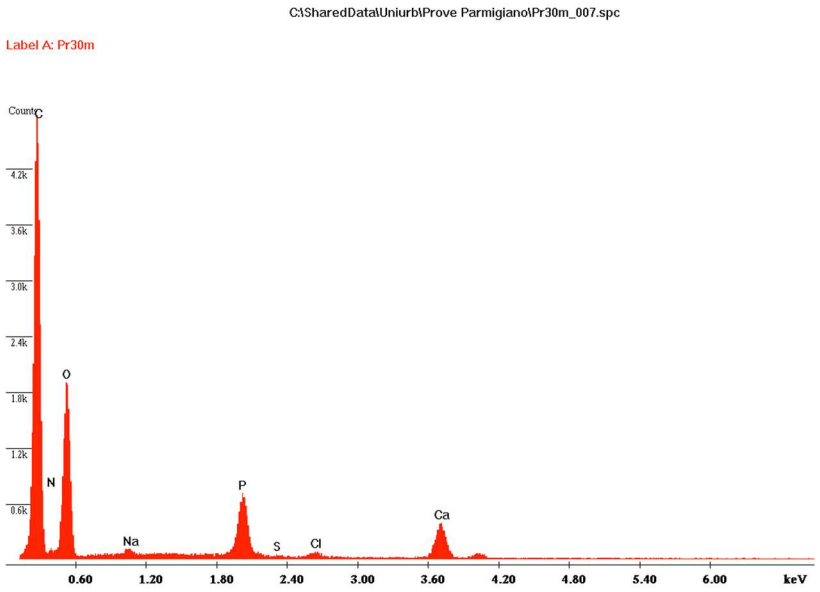

Figure 78 ESEM-LFD image of a 30-months PR cheese (scale bar of 500µm). Bottom: Brighter area and its EDAX spectrum are consistent with the ***discontinuous Network of hydrated Casein Micelles aggregates through calcium phosphate bridges***

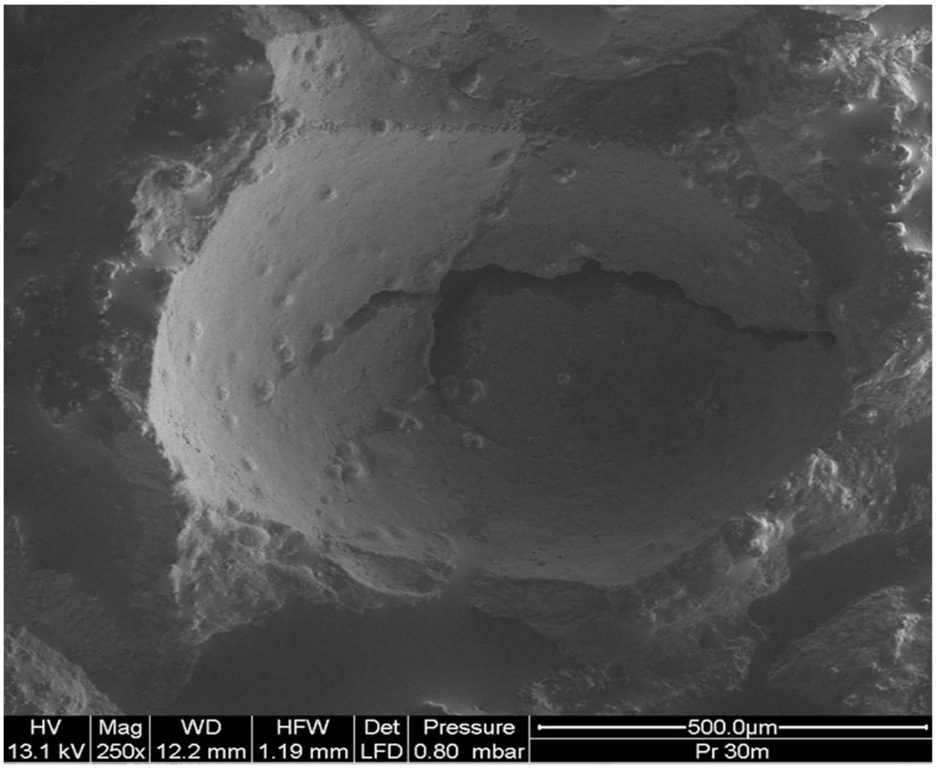

Figure 79 ESEM-LFD detail of the fracture surface of a 30M PR sample (scale bar of 500µm Top). ***Star-shaped microcrack*** *and* ***crystalline structures dislocation*** *indicate that the concave site represents the* ***inter-granule space*** *that was generated after curd granule detachment under strain-controlled fracture (scale bar of 300µm Bottom).*

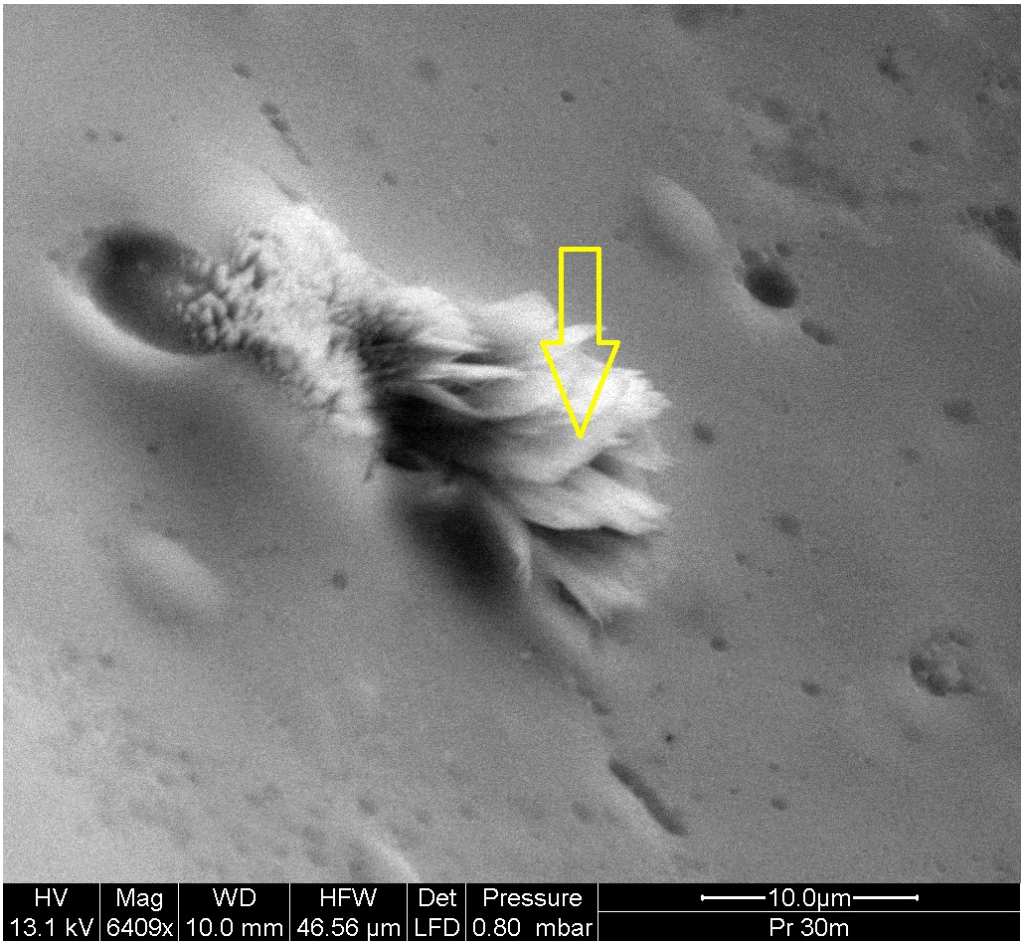

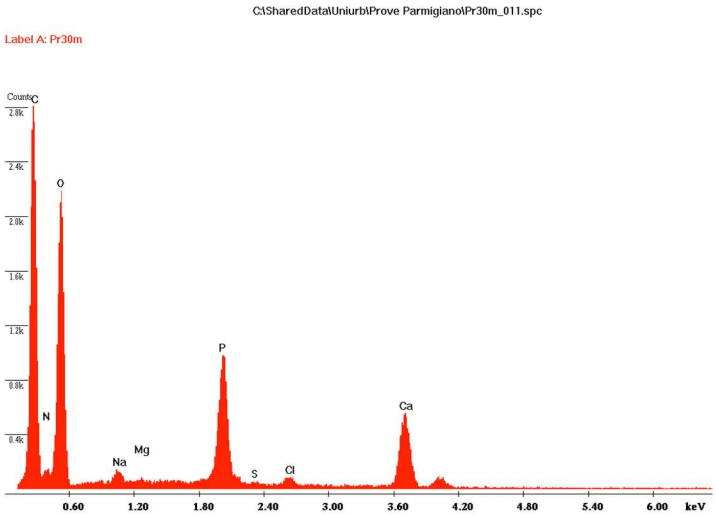

Figure 80 ESEM-LFD detail of the fracture surface of a 30-months PR cheese (scale bar of 300µm). Bottom: Crystalline structure and EDAX chemical spectrum are consistent with Struvite, i.e. the magnesium ammonium phosphate hexahydrate (MgNH4PO4·6H2O).

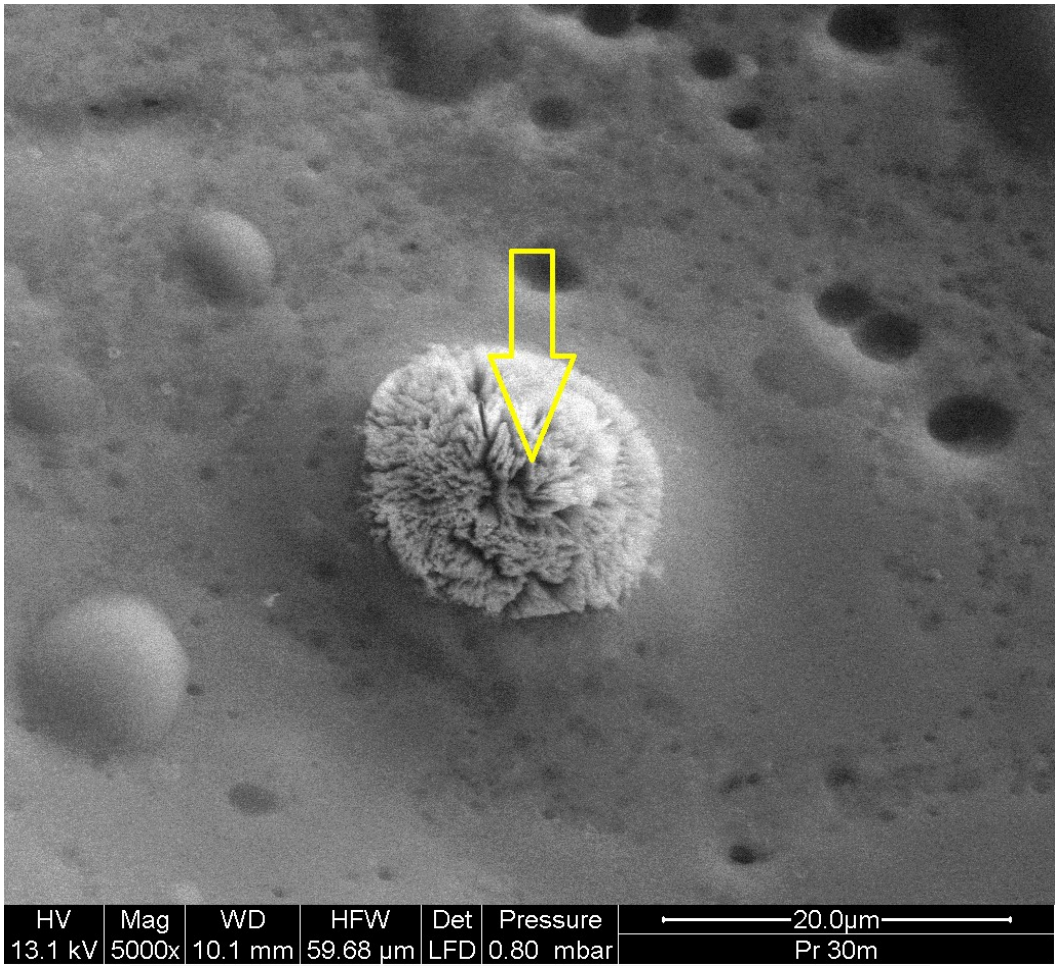

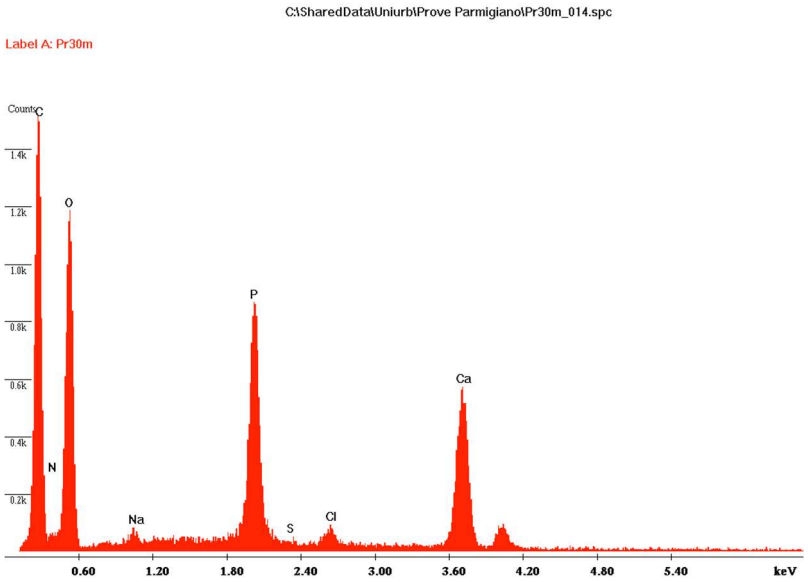

Figure 81 Top: ESEM-LFD detail of the fracture surface of a 30-months PR cheese (scale bar of 300µm). Bottom: Crystalline structure and EDAX chemical spectrum are very consistent with calcium phosphate crystals

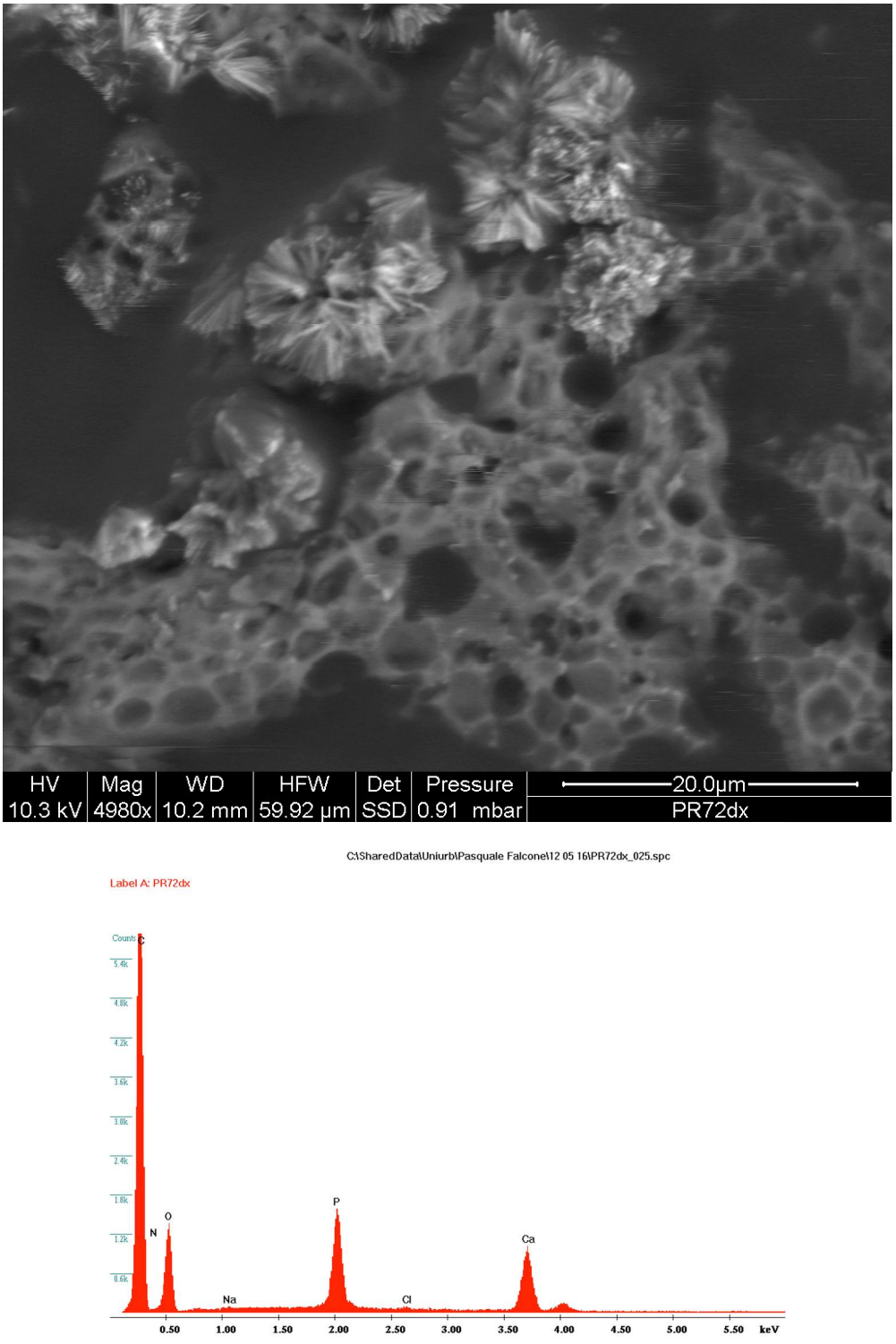

Figure 82 Top: ESEM-LFD detail of the fracture surface of a 72-months PR cheese (scale bar of 20µm). Bottom: Crystalline structure and EDAX chemical spectrum are very consistent with ***calcium phosphate crystals****. Crystals are nucleate on the casein-fat interface and growth towards the inter-granular space*

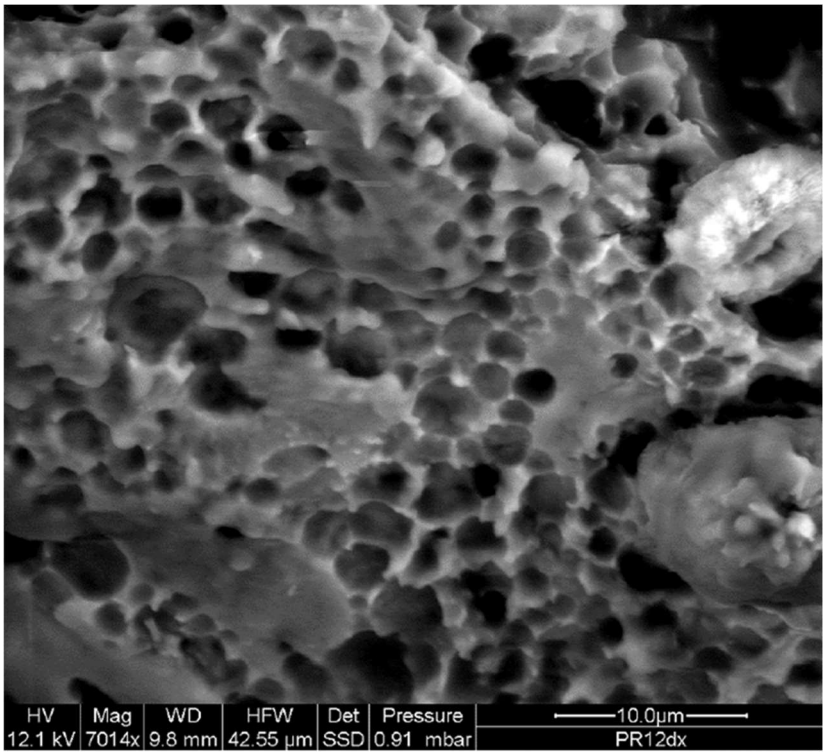

Figure 83 Cellular Architecture of the Hydrated Casein Network of a 12-months PR cheese

Figure 84 2D Axial, Radial and Sagittal and 3D tomographic virtualization of 30M PR cheese. Pixel of 20µm - 50mm cross-section

.

PR72M

[Risolution 50µm] VOLUME = 5.8cm^3

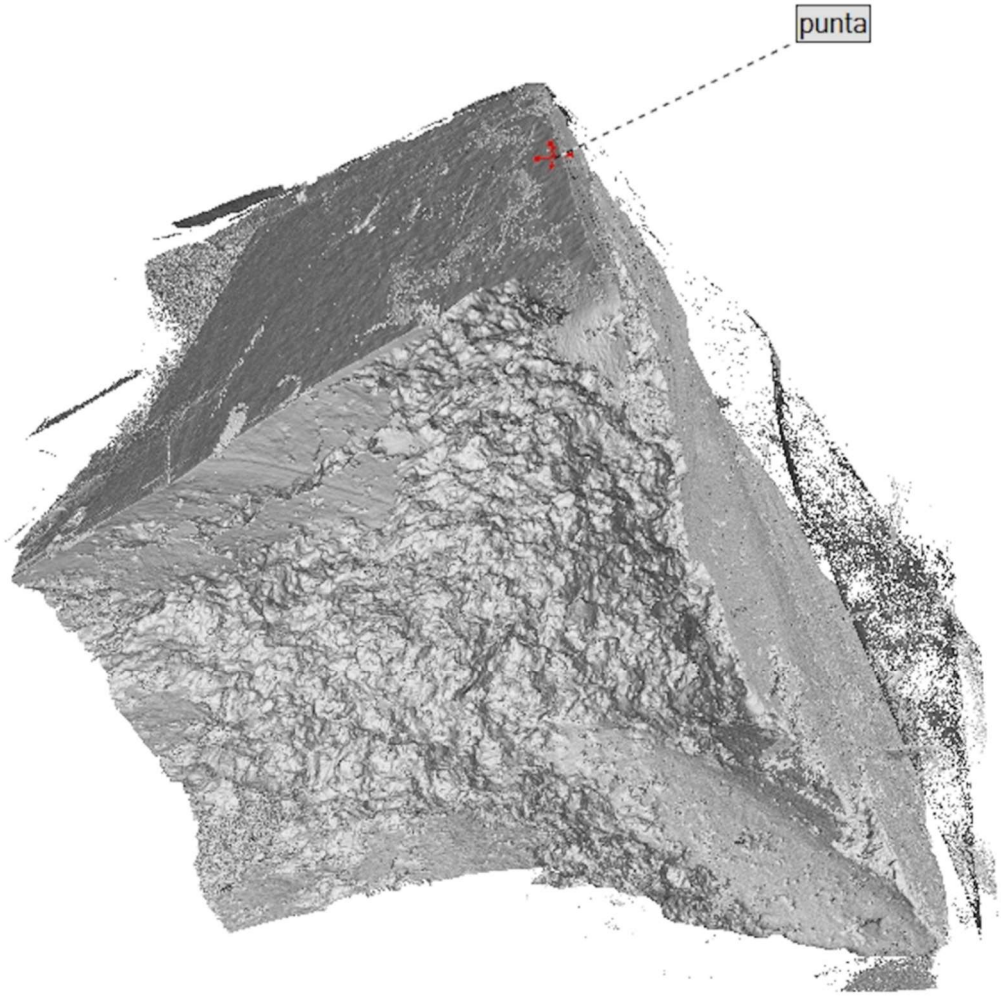

Figure 85 3D tomographic virtualization of 30M PR cheese (volume of 5.8 cm^3)

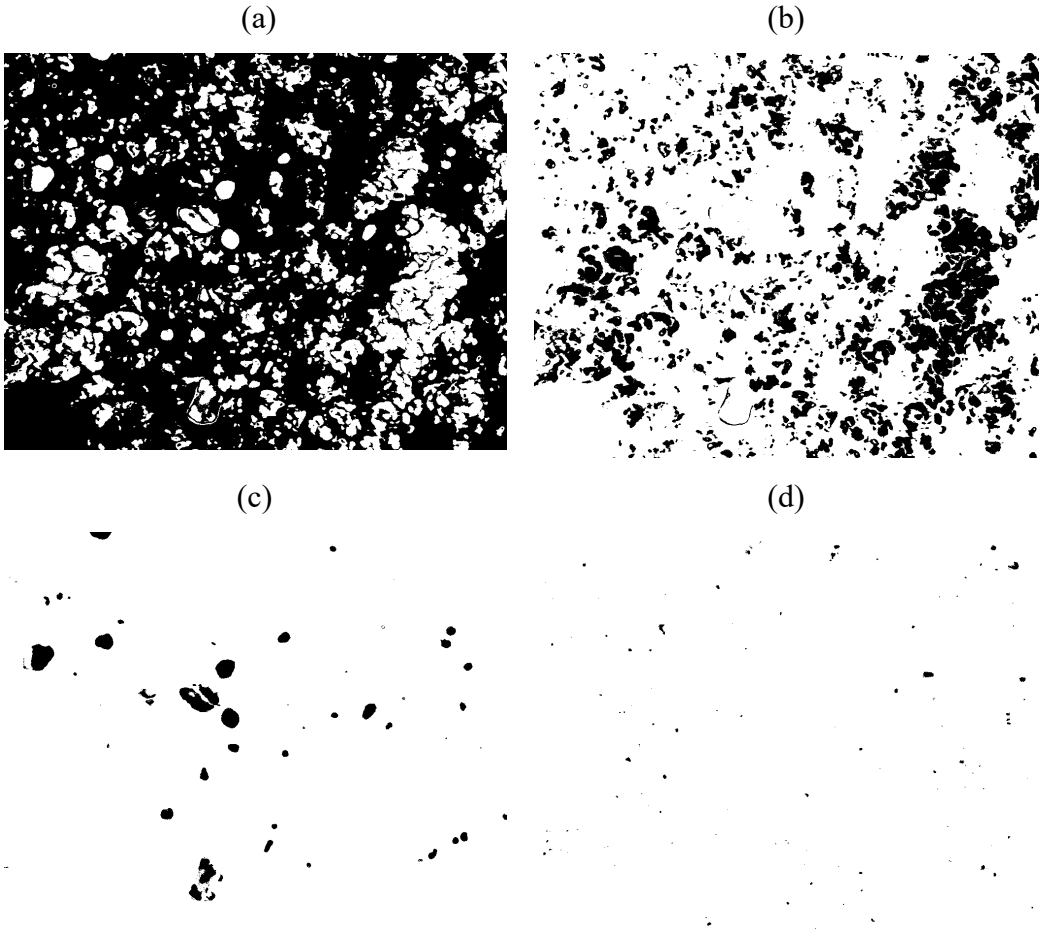

Figure 86 Results from segmentation of 2D tomographic image of 30M PR cheese (white is the background; 10mm cross-section): 61% of hydrated casein network (a), 34% of dispersed fat (b), air cells (c), and salt crystal aggregates (d) are showed.

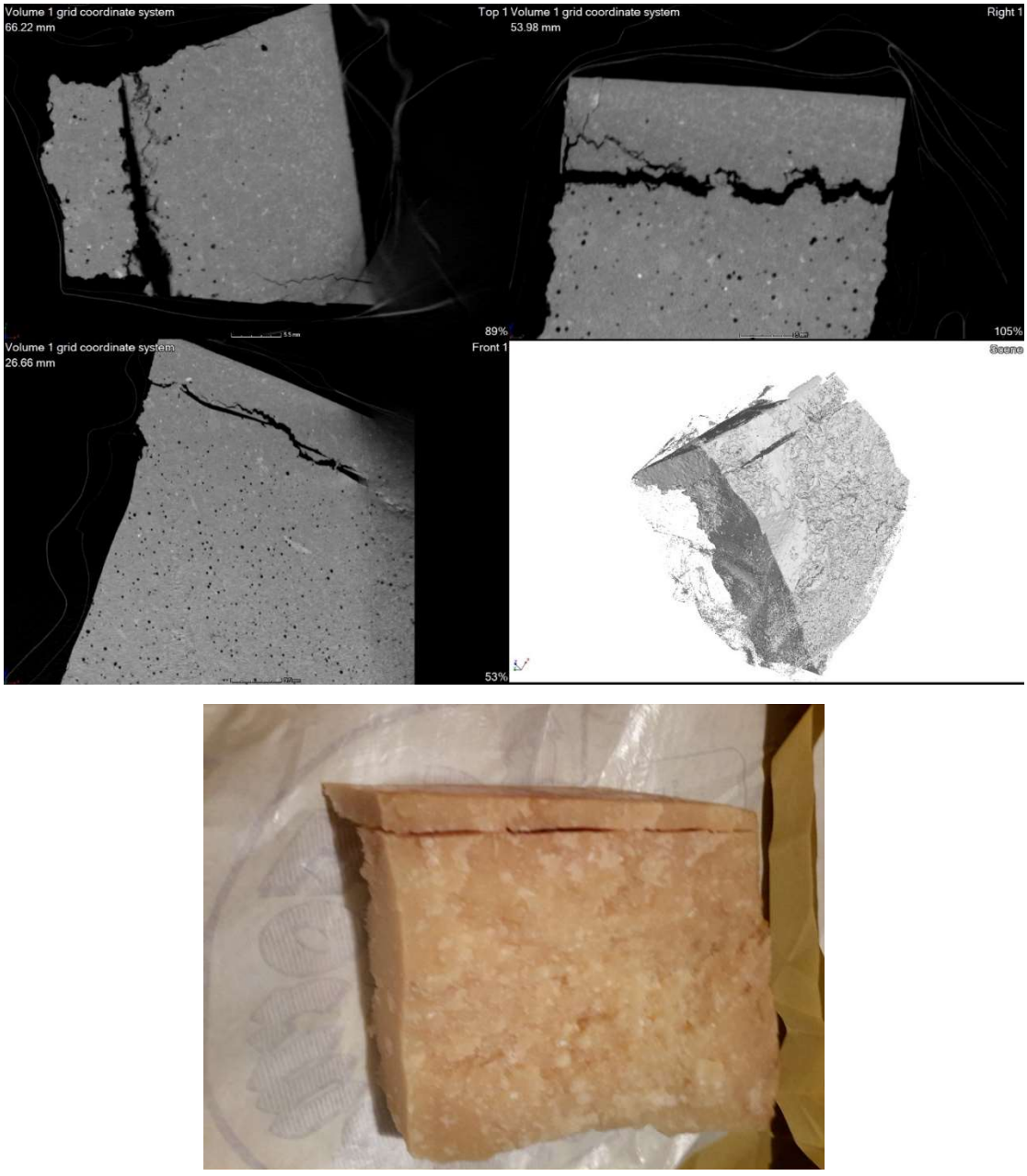

Figure 87 2D Axial, Radial and Sagittal and 3D tomographic virtualization of 72M PR cheese. Pixel of 50μm - 50mm cross-section.

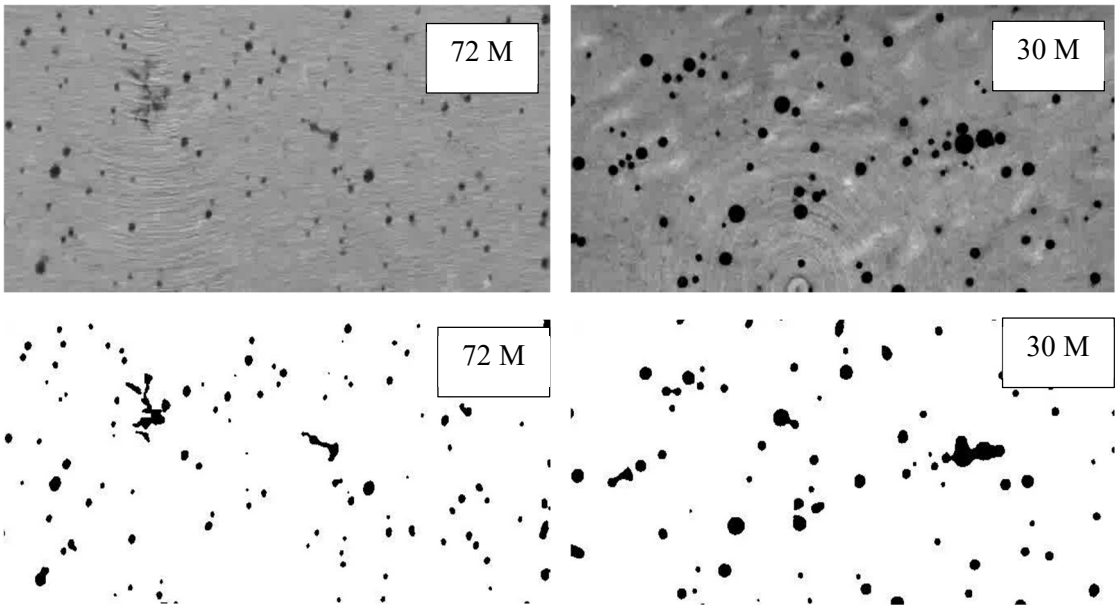

Figure 88 Porosity segmentation of 2D-staks of 72-months and 30-months-ripened PR cheese

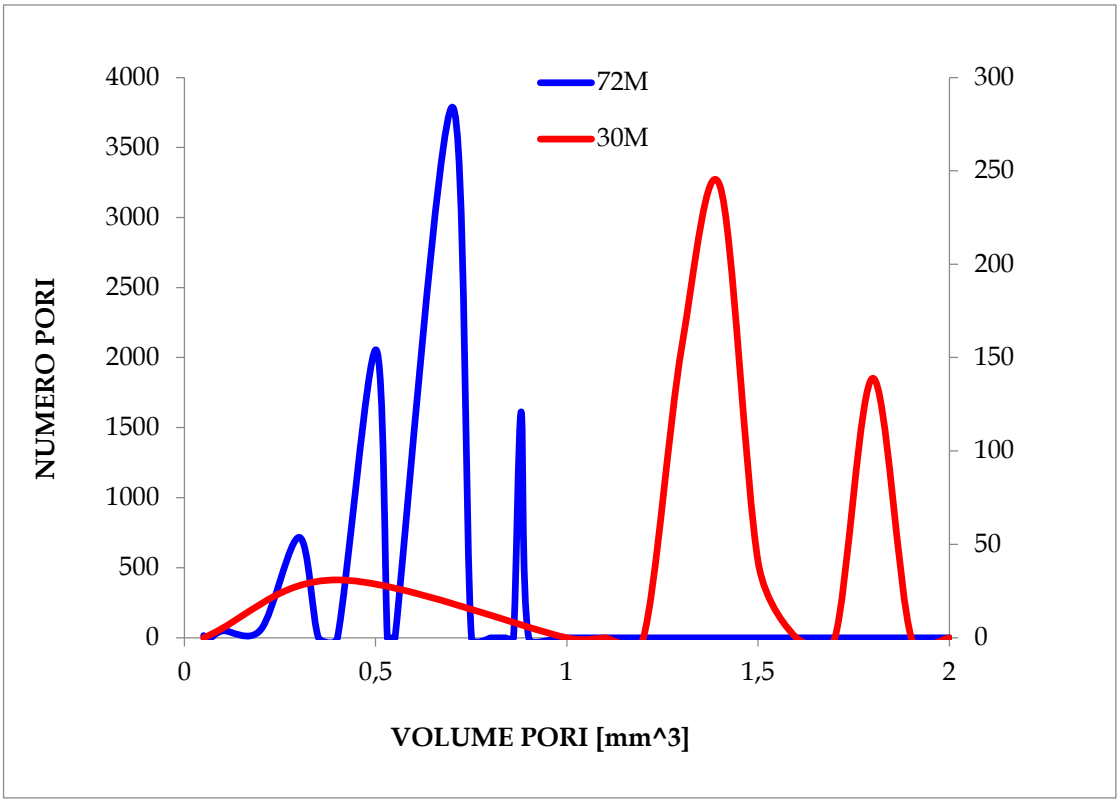

Figure 89 Three-dimensional distribution of voids in 30M and 72M PR samples

Table 2 Volume of voids in 30M and 72M PR cheese

	Volume totale	Volume totale Pori	Volume medio ponderato Pori	Porosità
	VT [mm^3]	VP [mm^3]	VPm [mm^3]	%
30M	10521,72	230,15	**1,42**	**2,18**
72M	10396,28	329,01	**0,64**	**3,16**

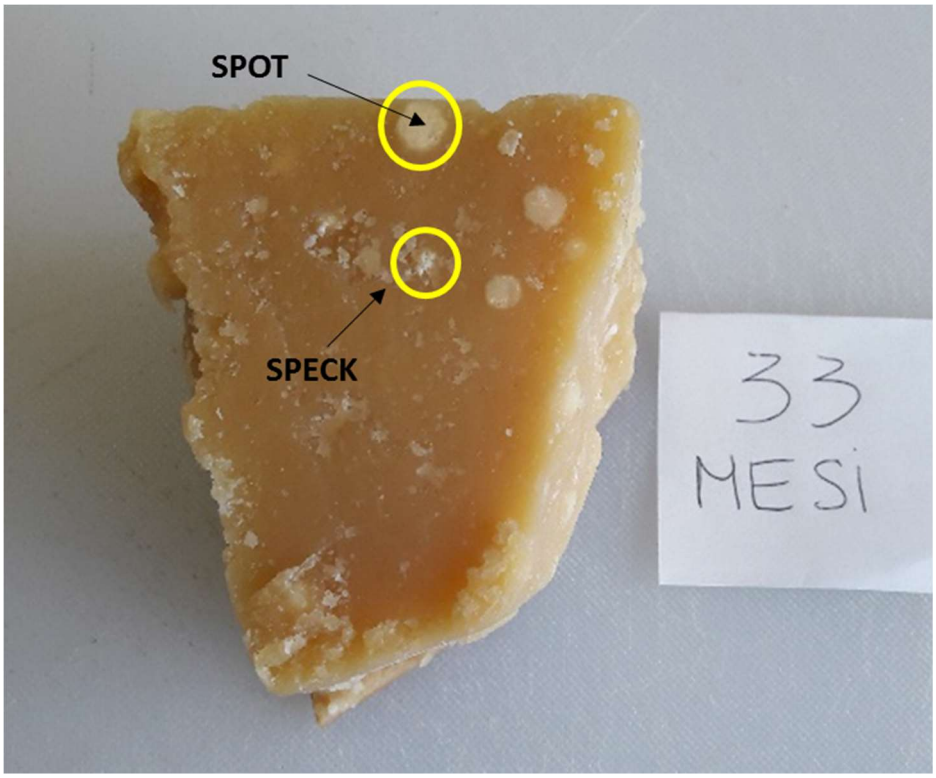

Figure 90 Specks and spots in PR 33M

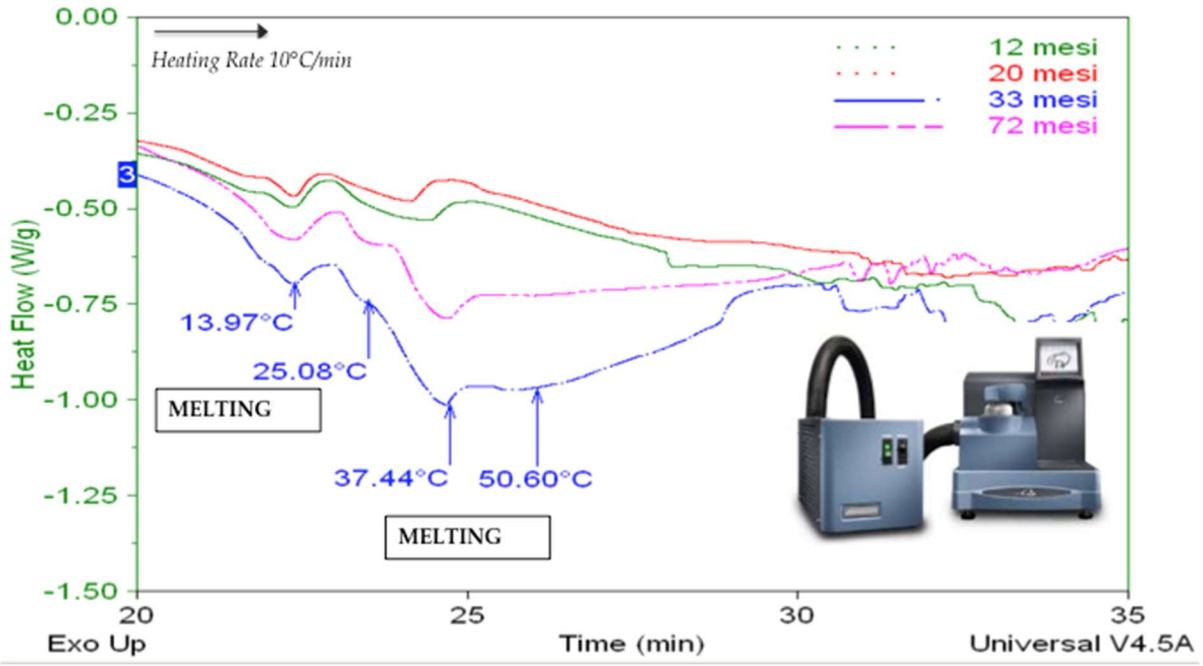

Figure 91 Saturated lipids melt at 12.5°C - Melting of unsaturated lipids continues over 50°C

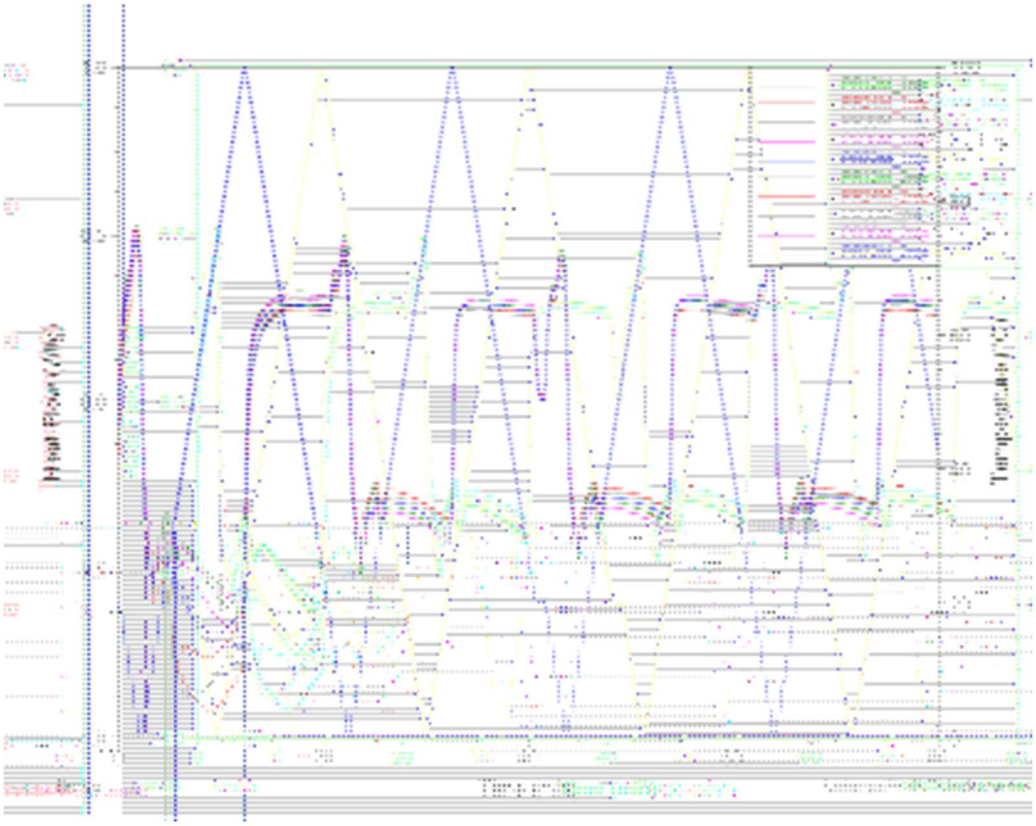

Figure 92 Cyclic thermal spectra of PR 12, 24, 30, 36, 72M from 0°C to 100°C. Proteolysis and lipolysis on ripening affect cheese matrix architecture

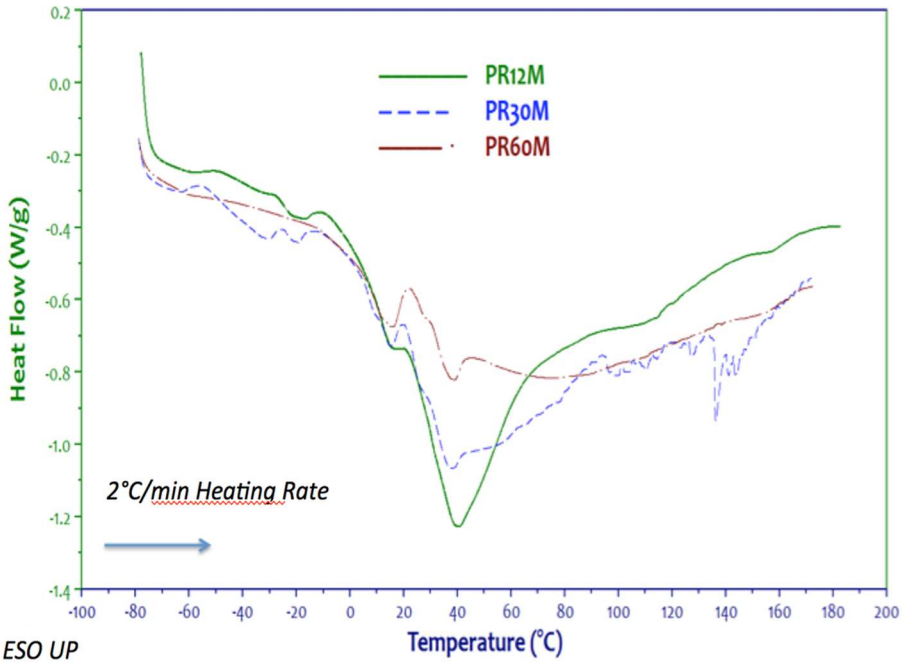

Figure 93 Thermal spectrum of PR cheeses paste (deprived of spots and specks domains). Cooling and Heating cycles were performed at 2°C/min from -80°/300°C.

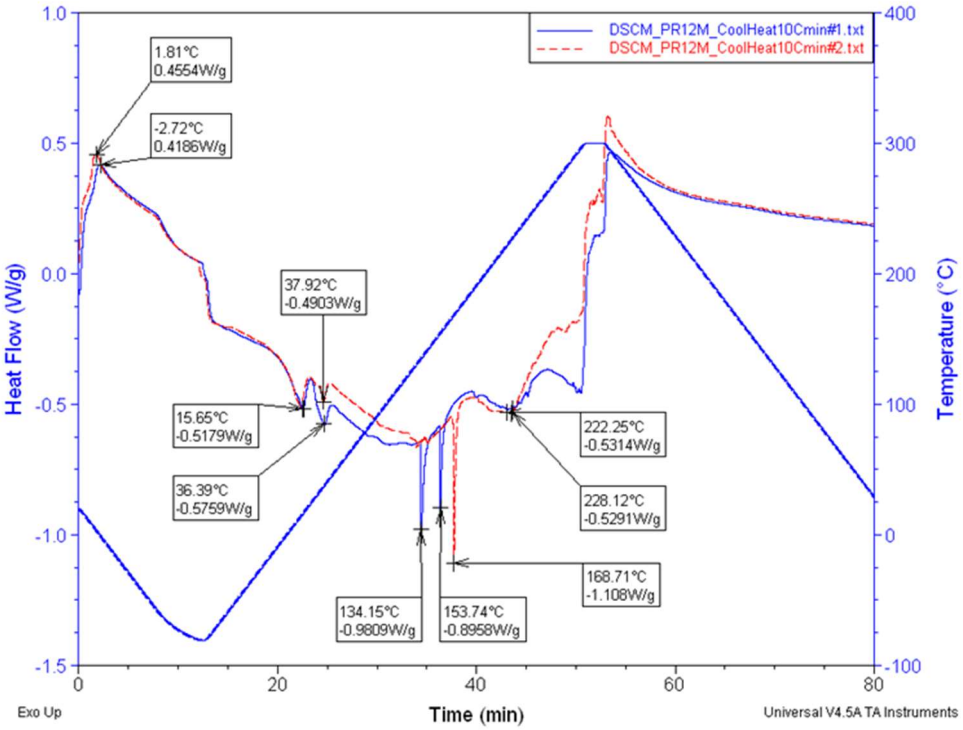

Figure 94 DSC spectrum of PR 12M under the thermal cycle -80 / 300 °C with cooling-heating rate of 10°C/min

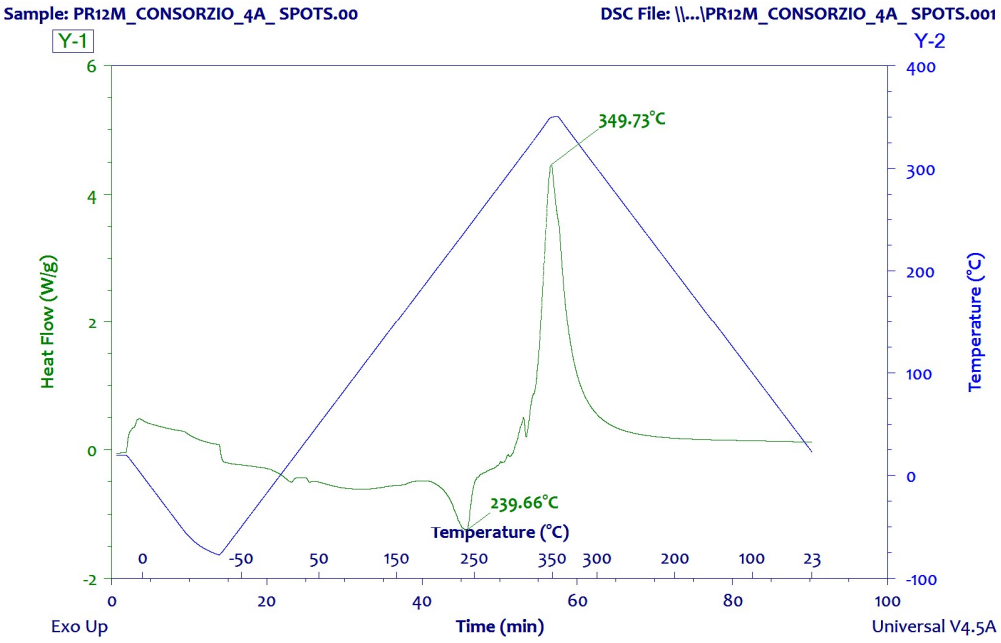

Figure 95 DSC spectrum of "spot" domain of PR 12-months under the thermal cycle -80°/350 °C with cooling-heating rate of 10°C/min

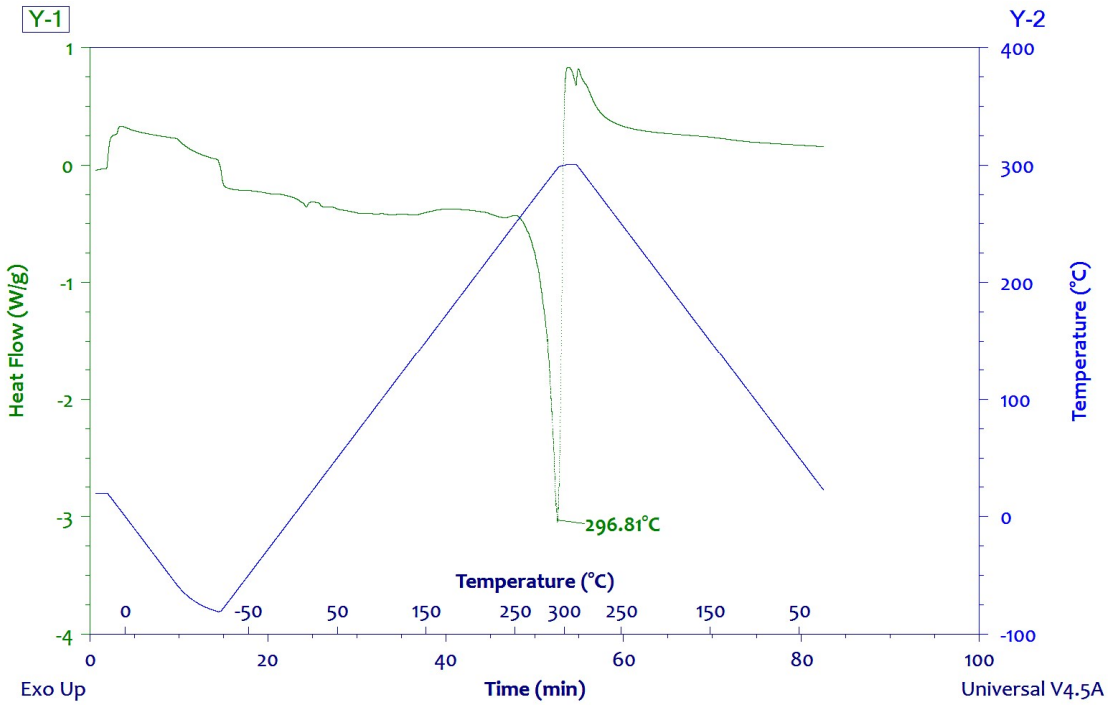

Figure 96 DSC spectrum of "specks" domain in 20-months PR cheese under the thermal cycle -80°/300 °C with cooling-heating rate of 10°C/min

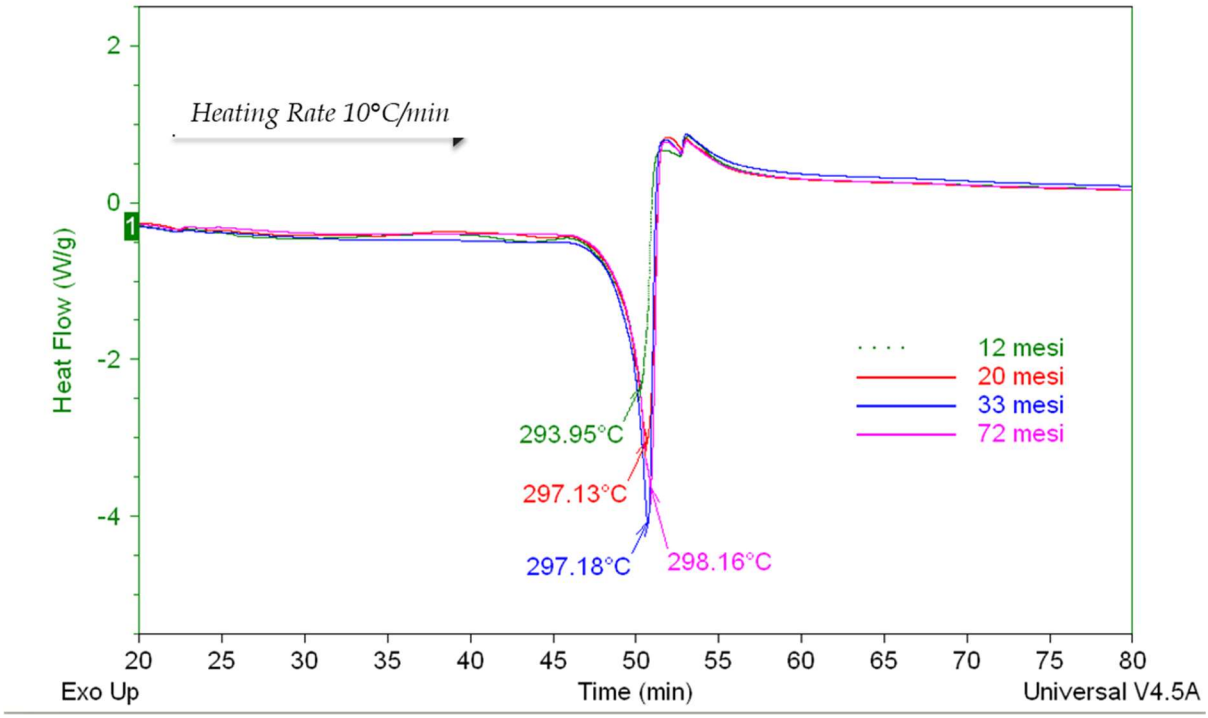

Figure 97 Overlay of DSC spectra of "specks" in 12M, 20M, 33M, and 72M PR cheese (samples were cooled from 20°C to -80°, next heated to 300°C). Crystals of the specks domains increase with ripening.

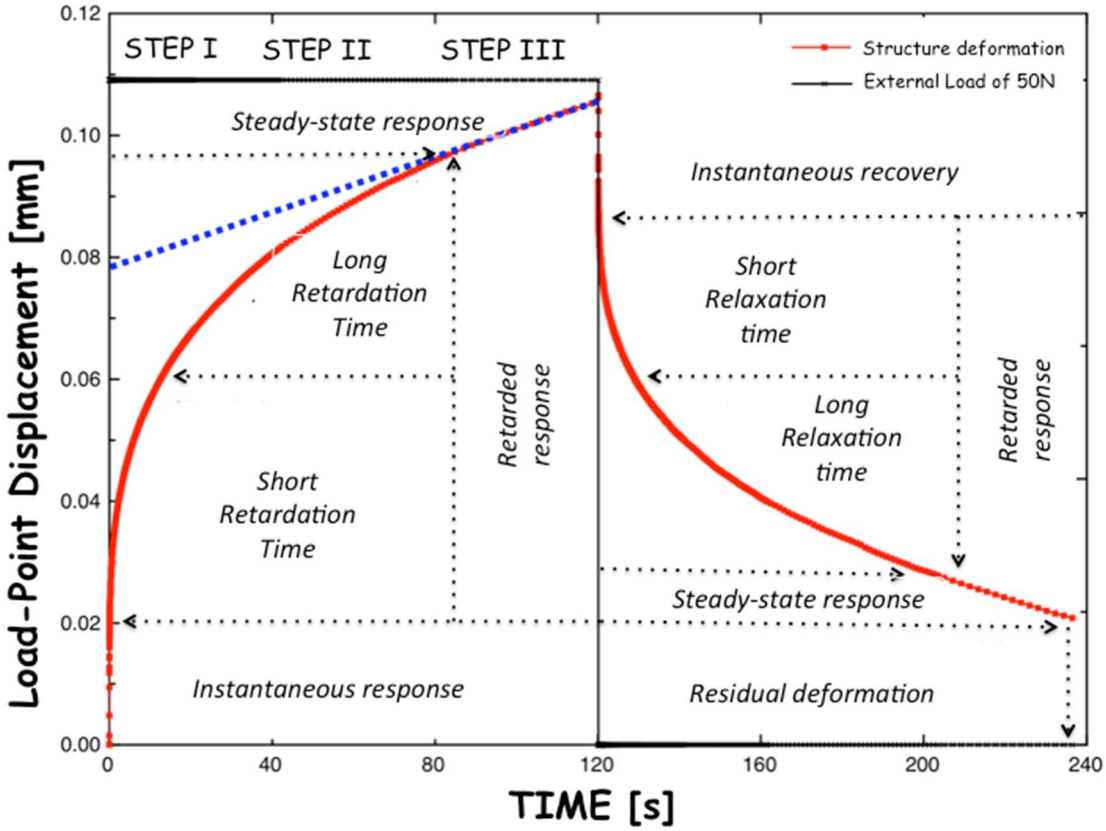

Figure 98 Creep curve of PR 18M at 50N load

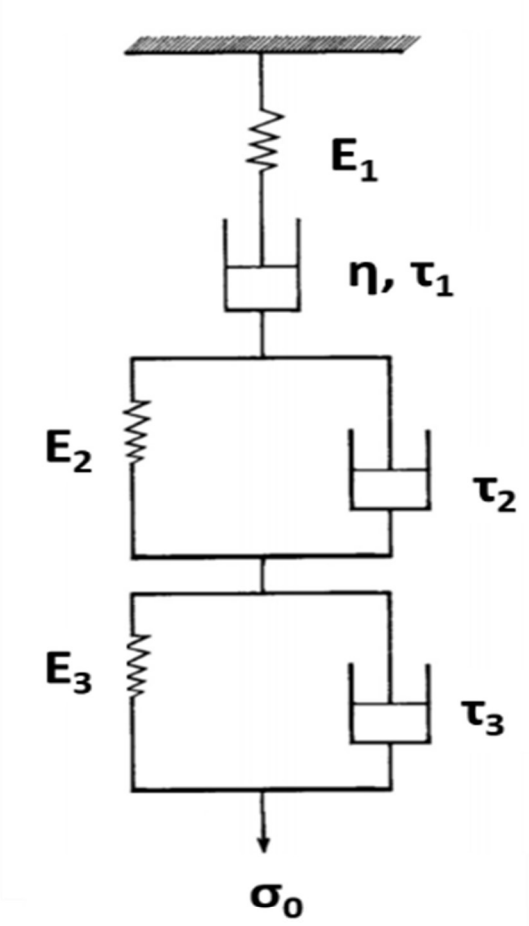

CHEESE MICROSTRUCTURAL ELEMENTS	MODEL CREEP ELEMENT	RHEOLOGICAL PROPERTIES
HYDRATED-CASEIN NETWORK	Maxwell	Instantaneous Elastic Modulus (E1)
CURD-GRANULE INTERSPACE	Voigth	t1 (time-dependent relaxation) E2 (retarded elastic modulus)
MICROVOID PHASE	Voigh	t1 (time-dependent relaxation) E2 (retarded elastic modulus)
LIPID PHASE	Maxwell	Steady-state plastic strain (h1)

Figure 99 Six-parametesr Burgers'model used to describe the Visco-Elastic and Visco-Plastic properties of PR cheese under creep

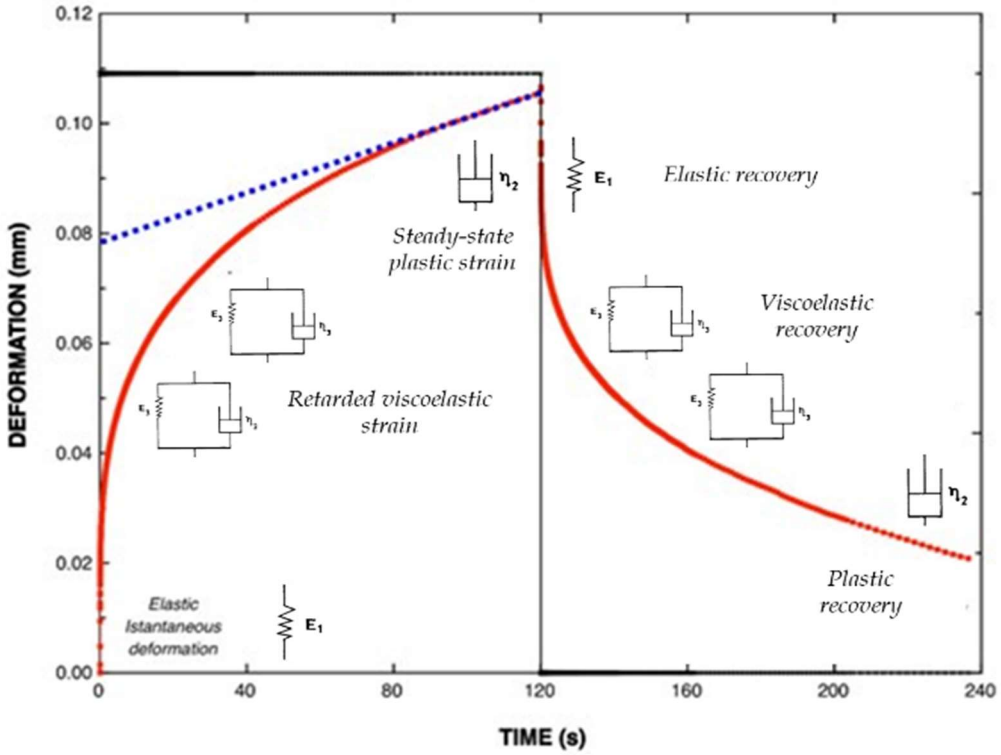

Figure 100 Creep curve and microstructure-elements for modeling

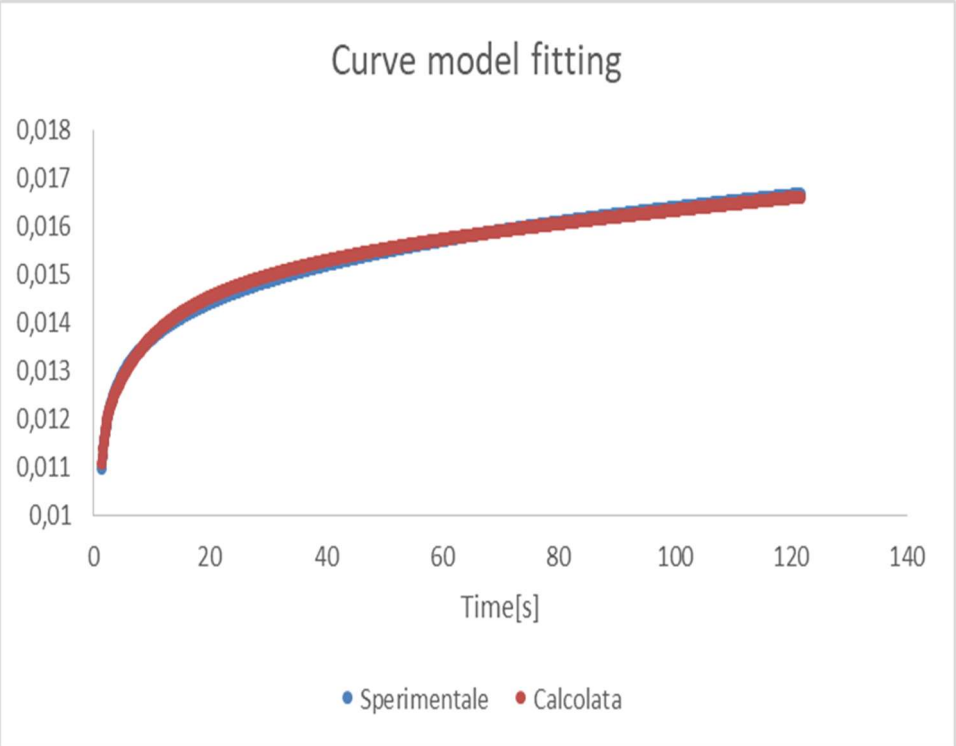

Figure 101 Goodness-of-fit of the six-parameter Burgers' model

Table 3 Burgers 'Model parameters for PR 18M under creep

RIPENING AGE	SAMPLE	Load [N]	dL/dt min	Residual Deformation [mm]	Compliance max [1/Mpa]	Instant Elastic Modulus [Mpa]	E1 [Mpa]	τ_1[s]	E2 [Mpa]	τ_2 [s]	E3 [Mpa]	τ_3 [s]	η_1 [Mpa*s]	η_2 [Mpa*s]	η_3 [Mpa*s]	η(inf) [Mpa*s]	B	n
18M	1B1DO-4	10	1,2E-05	0,010	0,84	1,75	1,80	0,57	9,90	5,70	11,00	24,00	1,03	56,43	-13,00	1681,82	1E-05	0,025
18M	1B1DO-16	10	2,0E-05	0,012	1,13	1,43	1,48	0,65	5,00	6,60	8,30	60,00	0,96	33,00	-51,70	1017,01	2E-05	0,022
18M	1B2DO-4	10	1,1E-05	0,007	0,60	2,58	2,86	0,50	7,30	6,00	17,80	76,00	1,43	43,80	-58,20	1930,55	8E-06	0,026
18M	1B2DO-16	10	1,7E-05	0,014	1,38	1,07	1,10	0,70	4,50	8,50	9,00	55,00	0,77	38,25	-46,00	1209,71	1E-05	0,025
18M	2B1DO-4	10	1,3E-05	0,015	1,16	1,15	1,24	0,40	5,20	6,85	17,00	75,00	0,50	35,62	-58,00	1574,99	1E-05	0,029
18M	2B1DO-16	10	1,3E-05	0,015	1,18	1,11	1,18	0,55	7,00	5,00	11,00	65,00	0,65	35,00	-54,00	1589,56	1E-05	0,030
18M	2B2DO-4	10	1,3E-05	0,009	0,79	1,94	2,18	0,54	6,00	4,50	11,20	68,00	1,18	27,00	-56,80	1560,23	1E-05	0,023
18M	2B2DO-16	10	1,9E-05	0,015	1,42	1,07	1,10	0,65	4,20	8,50	8,50	52,00	0,72	35,70	-43,50	1047,10	2E-05	0,024
18M	4B1DO-4	10	1,4E-05	0,023	1,65	0,75	0,84	1,00	5,00	4,80	8,00	62,00	0,84	24,00	-54,00	1456,72	1E-05	0,030
18M	4B1DO-16	10	1,8E-05	0,011	1,06	1,46	1,60	0,55	5,00	5,60	9,00	50,00	0,88	28,00	-41,00	1151,48	1E-05	0,024
18M	4B2DO-4	10	1,2E-05	0,009	0,83	1,84	2,00	0,45	4,60	9,50	26,00	95,00	0,90	43,70	-69,00	1734,17	1E-05	0,023
18M	4B2DO-16	10	2,2E-05	0,012	1,29	1,34	1,34	0,70	4,30	10,00	7,00	45,00	0,94	43,00	-38,00	906,52	2E-05	0,024
18M	5B1DO-2	10	4,3E-06	0,003	0,25	5,83	6,20	0,60	20,00	6,00	32,00	115,00	3,72	120,00	-83,00	4731,67	3E-06	0,023
18M	5B1DO-14	10	3,9E-06	0,003	0,24	6,34	6,80	0,60	18,00	7,50	35,00	115,00	4,08	135,00	-80,00	5260,32	3E-06	0,024
18M	5B2DO-1	10	5,3E-06	0,003	0,32	5,52	6,30	0,62	12,20	5,00	20,00	56,00	3,91	61,00	-36,00	3836,84	4E-06	0,021
18M	5B2DO-14	10	6,8E-06	0,005	0,41	3,84	4,40	0,60	9,50	5,50	19,00	75,00	2,64	52,25	-56,00	2991,83	6E-06	0,015
18M	7B1DO-2	10	3,7E-06	0,002	0,21	7,23	8,10	0,50	19,00	8,20	39,00	120,00	4,05	155,80	-81,00	5545,34	3E-06	0,027
18M	7B1DO-14	10	4,2E-06	0,003	0,26	5,77	6,80	0,25	14,00	6,00	42,00	118,00	1,70	84,00	-76,00	4857,46	4E-06	0,026
18M	7B2DO-2	10	4,8E-06	0,003	0,32	5,06	5,50	0,70	13,00	7,00	22,50	110,00	3,85	91,00	-87,50	4239,33	4E-06	0,026
18M	7B2DO-14	10	6,5E-06	0,003	0,33	5,47	6,20	0,70	10,50	6,00	18,50	90,00	4,34	63,00	-71,50	3129,97	6E-06	0,017
18M	8B1DO-2	10	4,7E-06	0,003	0,29	5,28	6,00	0,40	14,00	5,50	35,00	100,00	2,40	77,00	-65,00	4272,65	4E-06	0,026
18M	8B1DO-14	10	4,4E-06	0,004	0,30	5,00	5,20	0,65	18,00	7,00	28,00	98,00	3,38	126,00	-70,00	4620,10	4E-06	0,025
18M	8B2DO-2	10	4,3E-06	0,003	0,27	5,71	6,50	0,50	15,50	5,30	26,00	99,00	3,25	82,15	-73,00	4713,49	4E-06	0,026
18M	8B2DO-14	10	3,7E-06	0,003	0,24	6,29	7,50	0,50	15,00	5,50	28,00	98,00	3,75	82,50	-70,00	5424,53	3E-06	0,024
	Average		1,0E-05	0,008	0,70	3,53	3,93	0,58	10,28	6,50	20,37	80,04	2,16	65,55	-59,68	2936,81	8E-06	0,024
	St.dev.		6E-06	0,006	0,47	2,23	2,54	0,14	5,38	1,50	10,88	26,81	1,41	37,40	17,77	1680,60	5E-06	0,003
	Var.coeff.		61%	71%	68%	63%	65%	25%	52%	23%	53%	33%	65%	57%	-30%	57%	66%	14%
	Err.st.		1,23E-06	0,001	0,10	0,45	0,52	0,03	1,10	0,31	2,22	5,47	0,29	7,63	3,63	343,05	1,10E-06	0,001

Table 4 Burgers 'Model parameters for PR 24M under creep

RIPENING AGE	SAMPLE	Load [N]	dL/dt min	Residual Deformation [mm]	Compliance max [1/Mpa]	Instant Elastic Modulus [Mpa]	E1 [Mpa]	τ_1[s]	E2 [Mpa]	τ_2 [s]	E3 [Mpa]	τ_3 [s]	η_1 [Mpa*s]	η_2 [Mpa*s]	η_3 [Mpa*s]	η(inf) [Mpa*s]	B	n
24M	5B1DO-1	10	1,87E-05	0,016	1,42	1,06	1,40	1,20	2,50	6,00	7,00	40,00	1,68	15,00	-33,00	1084,45	1,E-05	0,030
24M	5B1DO-4	10	1,93E-05	0,016	1,37	1,13	1,25	0,62	3,60	6,20	8,00	38,00	0,78	22,32	-30,00	1053,10	1,E-05	0,040
24M	5B1DO-7	10	1,87E-05	0,018	1,48	0,98	1,00	0,70	5,00	8,00	7,20	48,00	0,70	40,00	-40,80	1084,65	1,E-05	0,040
24M	5B1DO-10	10	3,28E-05	0,022	2,24	0,89	0,91	0,82	1,80	9,00	4,00	40,00	0,75	16,20	-36,00	618,02	2,E-05	0,031
24M	5B1DO-13	10	1,58E-05	0,010	0,87	1,87	2,00	0,60	5,00	7,50	15,00	55,00	1,20	37,50	-40,00	1284,97	1,E-05	0,031
24M	6B1DO-1	10	1,53E-05	0,012	1,09	1,36	1,50	0,50	4,50	7,00	11,50	50,00	0,75	31,50	-38,50	1321,70	1,E-05	0,032
24M	6B1DO-4	10	2,83E-05	0,023	1,98	0,80	0,90	0,50	2,10	7,50	8,00	40,00	0,45	15,75	-32,00	717,20	2,E-05	0,018
24M	6B1DO-7	10	1,56E-05	0,019	1,43	0,94	1,12	0,30	3,50	4,50	8,00	30,00	0,34	15,75	-22,00	1298,91	1,E-05	0,037
24M	6B1DO-10	10	1,73E-05	0,007	0,86	1,97	2,00	0,66	6,00	9,49	16,00	40,00	1,32	56,93	-24,00	1174,13	1,E-05	0,028
24M	6B1DO-13	10	1,61E-05	0,014	1,37	1,06	1,25	0,35	3,00	4,50	9,00	45,00	0,44	13,50	-36,00	1260,97	1,E-05	0,027
24M	6B2DO-1	10	1,35E-05	0,010	0,89	1,68	1,80	0,55	6,00	6,00	11,00	60,00	0,99	36,00	-49,00	1497,68	1,E-05	0,026
24M	6B2DO-4	10	1,55E-05	0,012	1,15	1,28	1,40	0,55	4,50	6,50	9,20	55,00	0,77	29,25	-45,80	1310,87	1,E-05	0,024
24M	6B2DO-7	10	1,52E-05	0,011	1,01	1,52	1,60	0,60	4,50	8,20	17,80	58,00	0,96	36,90	-40,20	1334,23	1,E-05	0,030
24M	6B2DO-10	10	1,49E-05	0,010	0,93	1,71	2,00	0,35	4,40	5,50	10,00	55,00	0,70	24,20	-45,00	1358,39	7,E-06	0,054
24M	6B2DO-13	10	1,52E-05	0,012	1,04	1,43	1,50	0,72	6,00	8,00	11,00	45,00	1,08	48,00	-34,00	1330,21	1,E-05	0,018
24M	7B1DO-2	10	7,74E-06	0,011	0,85	1,57	1,60	0,60	7,90	8,00	25,00	90,00	0,96	63,20	-65,00	2618,72	6,E-06	0,020
24M	7B1DO-14	10	1,03E-05	0,009	0,79	1,84	2,00	0,52	6,00	7,20	17,00	70,00	1,04	43,20	-53,00	1977,97	1,E-05	0,013
24M	7B2DO-2	10	1,48E-05	0,008	0,83	1,91	2,00	0,60	6,10	8,00	14,00	61,00	1,20	48,80	-47,00	1370,12	1,E-05	0,027
24M	7B2DO-14	10	1E-05	0,012	1,06	1,26	1,30	0,72	7,00	8,00	13,00	60,00	0,93	56,00	-47,00	2023,94	8,E-06	0,019
24M	8B1DO-2	10	1,01E-05	0,010	0,82	1,76	1,80	0,60	7,00	8,00	18,00	70,00	1,08	56,00	-52,00	2005,04	8,E-06	0,019
24M	8B1DO-14	10	2,19E-05	0,022	1,99	0,76	0,88	0,50	2,00	5,50	8,00	58,00	0,44	11,00	-50,00	926,82	2,E-05	0,010
24M	9B1DO-2	10	7,4E-06	0,007	0,58	2,43	2,70	0,30	7,80	6,50	22,00	100,00	0,81	50,70	-78,00	2739,35	6,E-06	0,018
24M	9B1DO-14	10	1E-05	0,008	0,79	1,83	2,00	0,55	6,00	6,20	14,00	78,00	1,10	37,20	-64,00	2025,48	9,E-06	0,013
24M	9B2DO-2	10	7,33E-06	0,007	0,59	2,45	2,63	0,62	8,00	7,00	23,00	88,00	1,63	56,00	-65,00	2765,71	6,E-06	0,024
24M	9B2DO-14	10	7,03E-06	0,007	0,59	2,41	2,60	0,55	9,00	5,50	20,00	70,00	1,43	49,50	-50,00	2885,83	6,E-06	0,020
	Average		1,5E-05	0,013	1,12	1,52	1,65	0,58	5,17	6,95	13,07	57,76	0,94	36,42	-44,69	1562,74	7E-06	0,026
	St.dev.		6E-06	0,005	0,45	0,51	0,53	0,18	2,02	1,31	5,60	17,73	0,35	16,24	13,44	642,93	4E-06	0,010
	Var.coeff.		41%	39%	40%	33%	32%	31%	39%	19%	43%	31%	38%	45%	-30%	41%	59%	39%
	Err.st.		1,24E-06	0,001	0,09	0,10	0,11	0,04	0,40	0,26	1,12	3,55	0,07	3,25	2,69	128,59	7,96E-07	0,002

Table 5 Burgers 'Model parameters for PR 30M under creep

RIPENING AGE	SAMPLE	Load [N]	dL/dt min	Residual Deformation [mm]	Compliance max [1/Mpa]	Instant Elastic Modulus [Mpa]	E1 [Mpa]	τ_1[s]	E2 [Mpa]	τ_2 [s]	E3 [Mpa]	τ_3 [s]	η_1 [Mpa*s]	η_2 [Mpa*s]	η_3 [Mpa*s]	$\eta_{(inf)}$ [Mpa*s]	B	n
30M	3B1DO-2	10	4,02E-06	0,003	0,23	6,77	7,70	0,50	17,80	6,00	25,00	102,00	3,85	106,80	-77,00	5038,94	3,E-06	0,026
30M	3B1DO-14	10	4,82E-06	0,003	0,31	4,88	5,55	0,42	14,50	5,00	22,00	102,00	2,33	72,50	-80,00	4206,09	4,E-06	0,027
30M	3B2DO-2	10	3,48E-06	0,004	0,31	4,38	5,30	0,30	13,00	3,60	23,00	108,00	1,59	46,80	-85,00	5833,44	3,E-06	0,031
30M	3B2DO-14	10	3,9E-06	0,002	0,23	7,05	8,30	0,80	16,20	4,50	25,00	109,00	6,64	72,90	-84,00	5196,48	3,E-06	0,030
30M	4B1DO-2	10	4,88E-06	0,002	0,27	6,13	7,60	0,44	13,00	4,60	19,00	96,00	3,34	59,80	-77,00	4152,56	4,E-06	0,025
30M	4B1DO-14	10	3,51E-06	0,003	0,28	5,24	6,40	0,10	13,20	4,00	26,00	105,00	0,64	52,80	-79,00	5778,46	3,E-06	0,029
30M	4B2DO-2	10	5,54E-06	0,004	0,35	4,54	5,20	0,60	11,80	5,00	19,00	85,00	3,12	59,00	-66,00	3661,58	4,E-06	0,026
30M	4B2DO-14	10	3,54E-06	0,003	0,28	5,15	6,20	0,47	14,00	3,80	23,00	98,00	2,91	53,20	-75,00	5726,53	3,E-06	0,031
30M	5B1DO-2	10	1,46E-05	0,016	1,29	1,10	1,36	0,30	3,70	3,50	6,00	35,00	0,41	12,95	-29,00	1390,83	1,E-05	0,031
30M	5B1DO-14	10	1,49E-05	0,016	1,20	1,15	1,43	0,30	3,50	3,50	10,00	45,00	0,43	12,25	-35,00	1359,21	1,E-05	0,028
30M	5B2DO-2	10	1,29E-05	0,009	0,88	1,74	2,00	0,42	5,00	5,00	10,00	60,00	0,84	25,00	-50,00	1572,36	1,E-05	0,032
30M	5B2DO-14	10	1,47E-05	0,011	1,01	1,50	1,76	0,40	3,90	4,80	11,00	85,00	0,70	18,72	-74,00	1380,67	1,E-05	0,027
30M	6B1DO-2	10	1,16E-05	0,016	1,19	1,10	1,22	0,50	6,00	3,50	9,00	45,00	0,61	21,00	-36,00	1753,38	9,E-06	0,026
30M	6B1DO-14	10	1,53E-05	0,010	0,87	1,79	2,00	0,55	6,00	4,50	10,00	40,00	1,10	27,00	-30,00	1329,55	1,E-05	0,026
30M	6B2DO-2	10	1,39E-05	0,010	0,91	1,63	1,95	0,40	4,50	4,50	12,50	46,00	0,78	20,25	-33,50	1459,85	1,E-05	0,030
30M	6B2DO-14	10	1,48E-05	0,012	1,09	1,37	1,50	0,50	5,00	5,00	8,00	48,00	0,75	25,00	-40,00	1367,96	1,E-05	0,032
30M	7B1DO-2	10	1,91E-05	0,012	1,18	1,40	1,74	0,32	3,00	5,00	7,90	38,00	0,56	15,00	-30,10	1061,98	2,E-05	0,019
30M	7B1DO-14	10	1,55E-05	0,013	1,06	1,44	1,50	0,62	4,80	7,80	12,80	63,00	0,93	37,44	-50,20	1305,28	1,E-05	0,023
30M	7B2DO-2	10	1,72E-05	0,012	1,19	1,36	1,50	0,70	3,60	7,00	9,20	42,00	1,05	25,20	-32,80	1177,85	1,E-05	0,026
30M	7B2DO-14	10	4,28E-06	0,003	0,74	2,05	2,30	0,55	5,20	6,00	12,00	45,00	1,27	31,20	-33,00	4738,84	5,E-06	0,042
30M	8B1DO-2	10	3,29E-06	0,003	0,29	4,89	5,50	0,43	15,30	5,00	26,00	95,00	2,37	76,50	-69,00	6156,57	3,E-06	0,020
30M	8B1DO-14	10	3,26E-06	0,004	0,29	4,80	5,60	0,45	14,30	4,00	27,00	100,00	2,52	57,20	-73,00	6217,75	3,E-06	0,018
30M	8B2DO-2	10	4,05E-06	0,003	0,29	5,27	5,80	0,55	17,00	5,00	25,00	82,00	3,19	85,00	-57,00	5008,31	3,E-06	0,018
30M	8B2DO-14	10	3,24E-06	0,002	0,20	7,74	8,75	0,55	22,00	5,00	32,00	103,00	4,81	110,00	-71,00	6267,81	3,E-06	0,022
30M	10B1DO-2	10	3,06E-06	0,004	0,30	4,35	4,90	0,35	16,80	4,80	30,00	105,00	1,72	80,64	-75,00	6627,09	3,E-06	0,025
30M	10B1DO-14	10	3,42E-06	0,003	0,26	5,44	6,20	0,45	17,00	4,50	30,00	105,00	2,79	76,50	-75,00	5924,48	3,E-06	0,020
30M	10B2DO-1	10	3,86E-06	0,003	0,25	6,36	6,80	0,60	17,70	6,00	32,00	98,00	4,08	106,20	-66,00	5248,20	3,E-06	0,019
30M	10B2DO-13	10	4,54E-06	0,003	0,29	5,27	6,10	0,45	14,00	5,50	26,00	98,00	2,75	77,00	-72,00	4470,85	4,E-06	0,014
	Average		8,3E-06	0,007	0,61	3,78	4,36	0,47	10,78	4,87	18,87	77,96	2,07	52,28	-59,09	3764,75	6E-06	0,026
	St.dev.		6E-06	0,005	0,41	2,18	2,52	0,14	5,87	1,02	8,58	27,33	1,55	30,46	19,91	2066,12	4E-06	0,006
	Var.coeff.		68%	73%	67%	58%	58%	30%	54%	21%	45%	35%	75%	58%	-34%	55%	66%	23%
	Err.st.		1,07E-06	0,001	0,08	0,41	0,48	0,03	1,11	0,19	1,62	5,16	0,29	5,76	3,76	390,46	7,90E-07	0,001

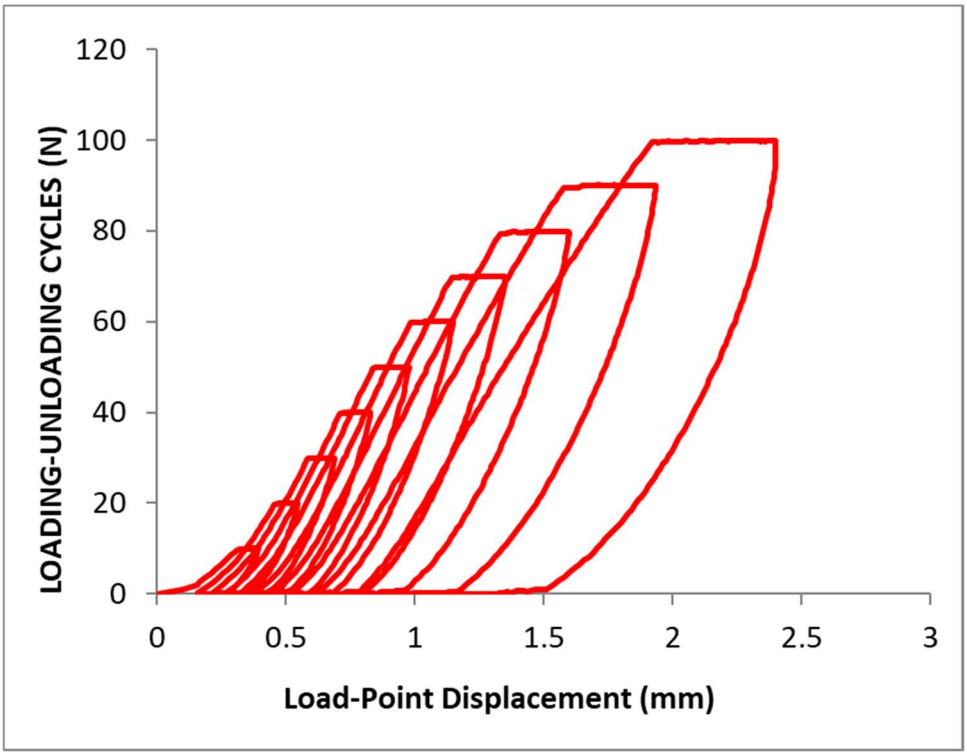

Figure 102 Loading - Unloading cycles

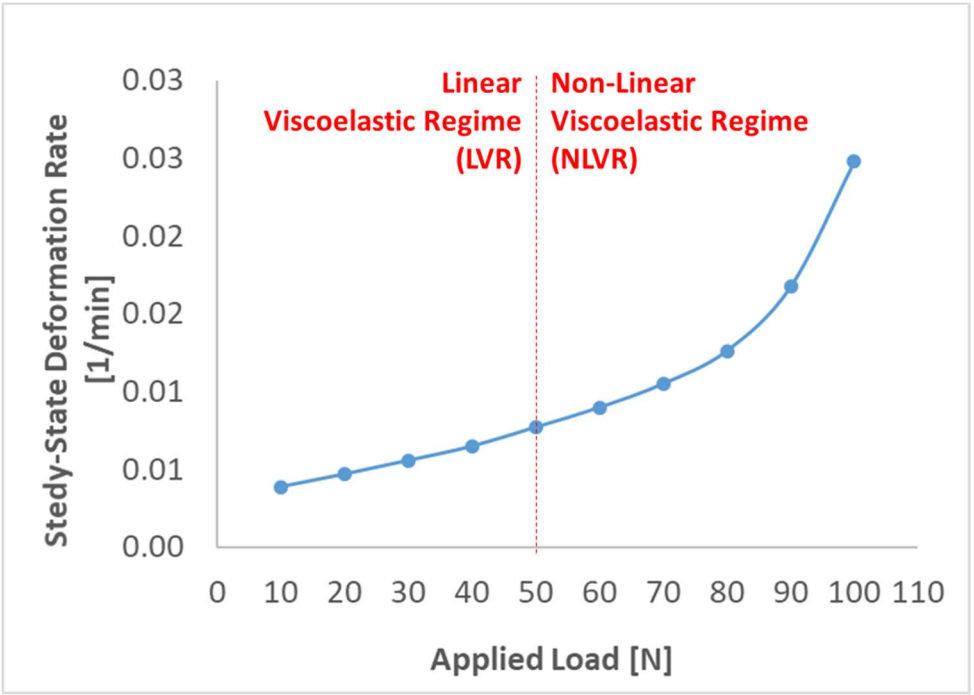

Figure 103 Linear and Non-Linear Viscoelastic Regime of PR 18M cheese as evaluated by steady-state deformation rate (dL/dt [1/s] measured under isothermal creep at different loading conditions (from 10 to 70 N)

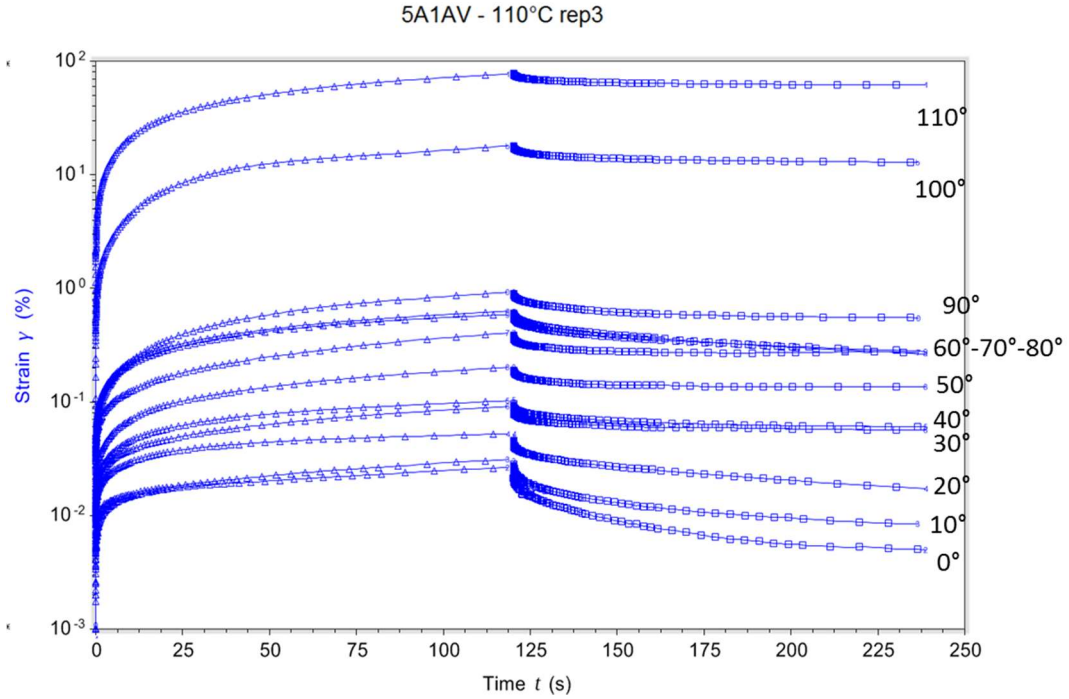

Figure 104 Sweep-temperature in Creep-Recovery tests of PR 12M cheese [from 0°C to 110 °C, under constant stress of 3 Pa]

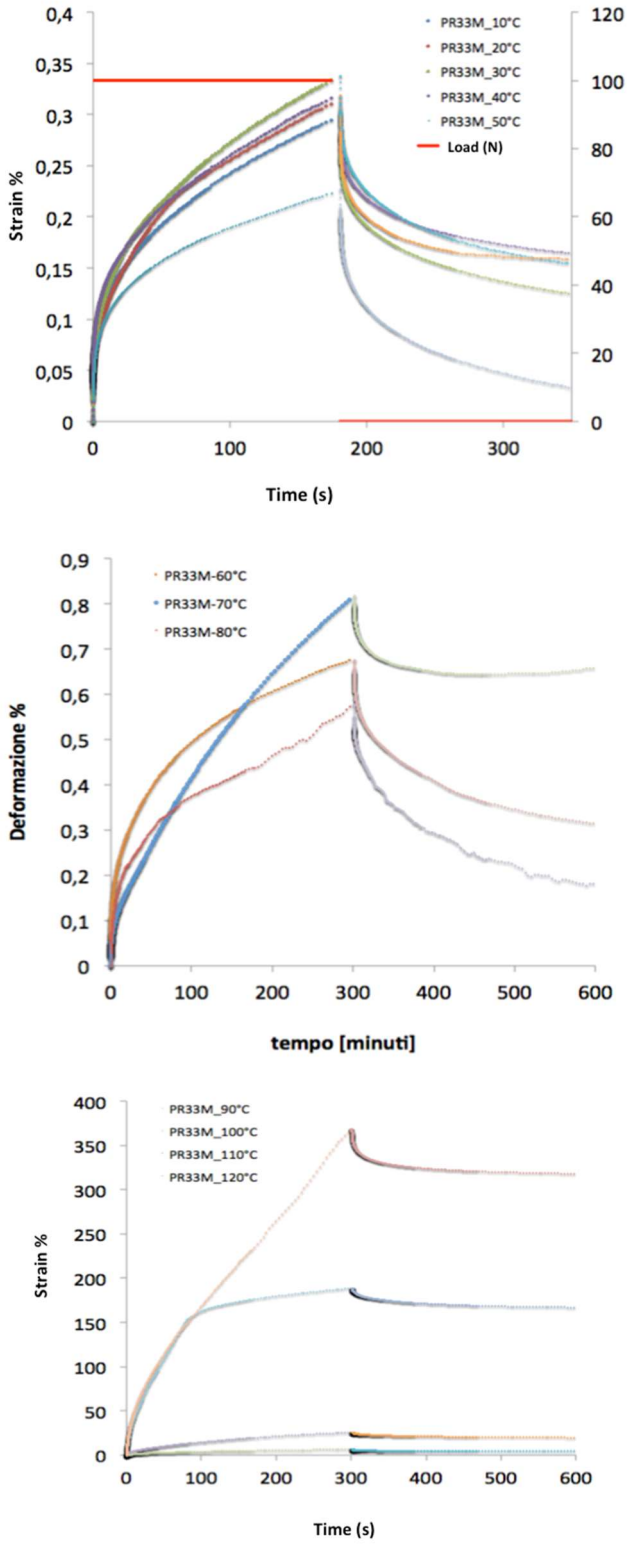

Figure 105 Creep-Recovery of PR 33M cheese under sweep-temperature from 0°C to 110 °C, (constant stress of 3 Pa). Instantaneous modulus decreases and maximum compliance increase with temperature with a step-change above the softening temperature, i.e. close to 51°

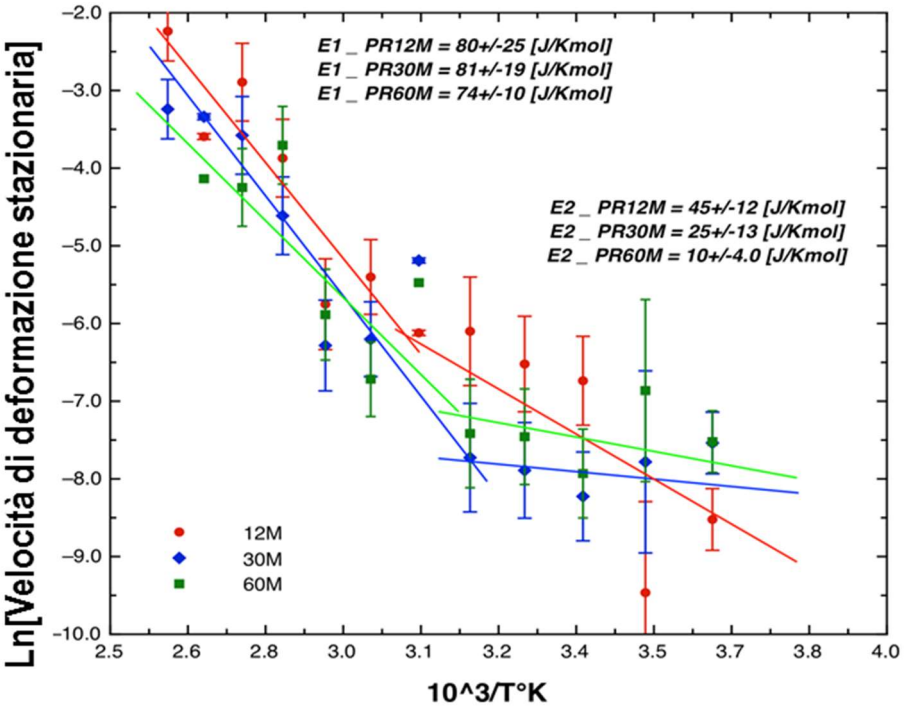

Figure 106 Arrhenius model for creep behavior, in PR 12M, 30M and 60M. Two apparent creep activation energies ranging from 10 to 81J/Kmol suggest two main mechanisms for steady-state structure relaxation across the softening temperature, i.e. close to 55°C

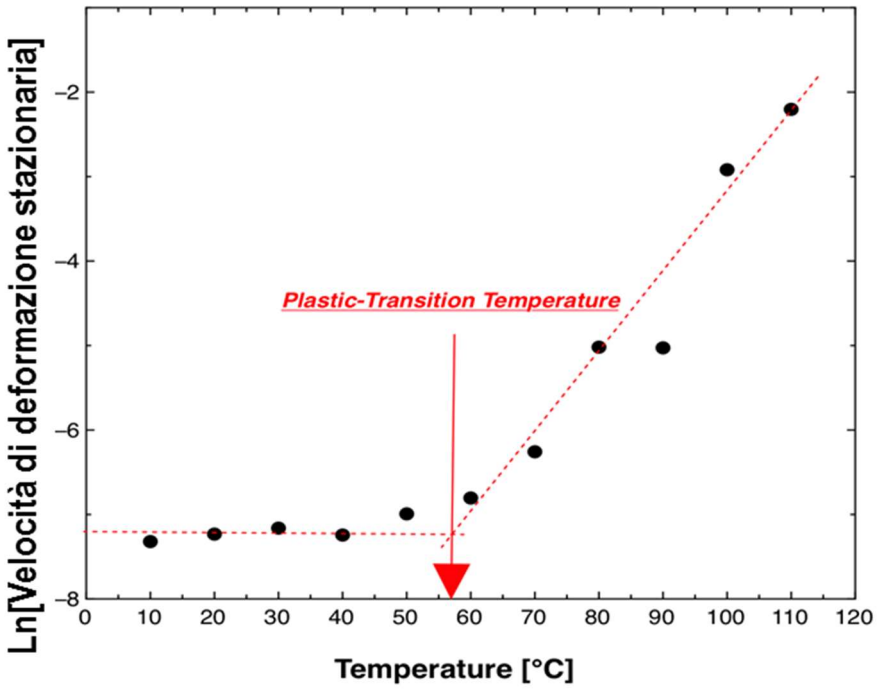

Figure 107 Softening transition temperature in 12M PR sample

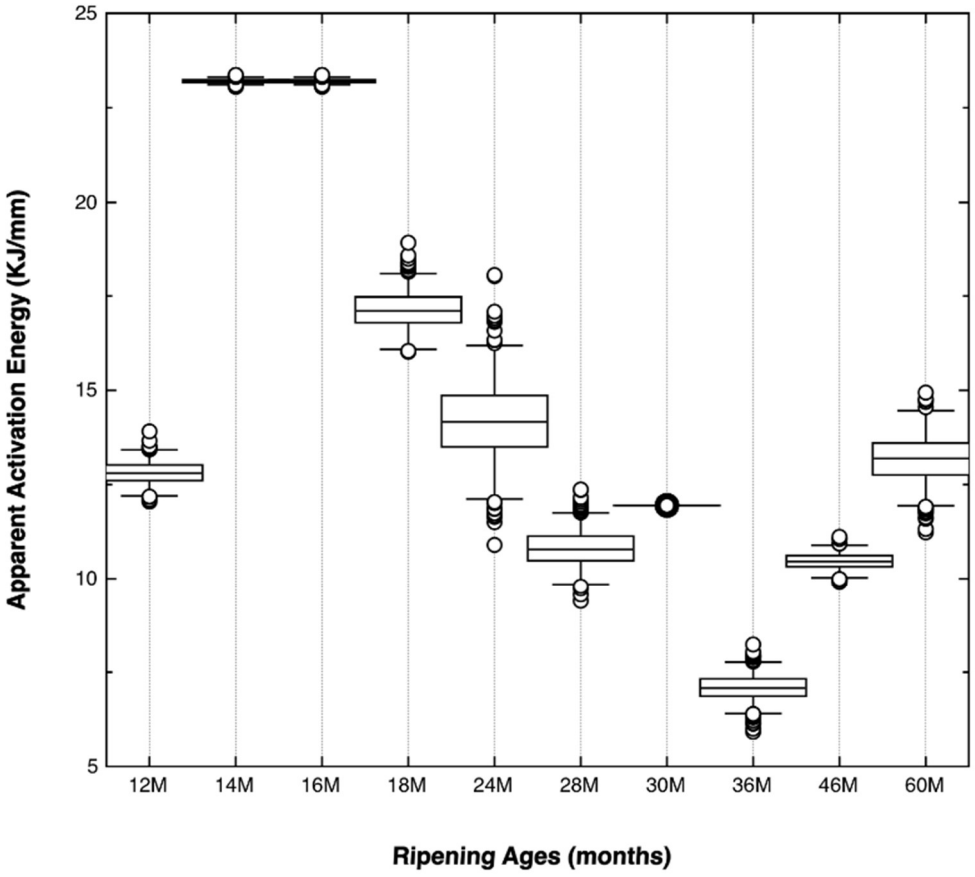

Figure 108 The apparent activation energy (E2) for softening mechanism as a function of cheese ripening. A well-shaped relation with a minimum close to 36M can be detected between yielding behavior and ripening.

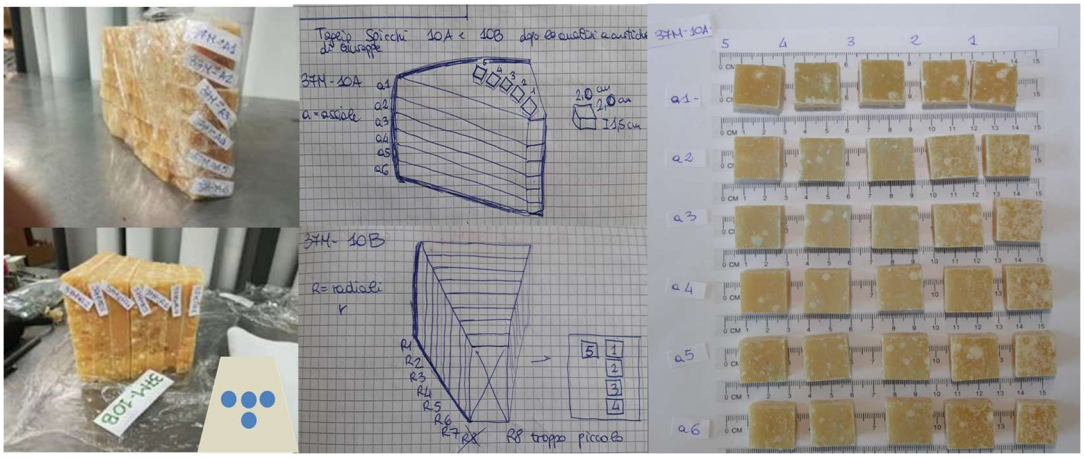

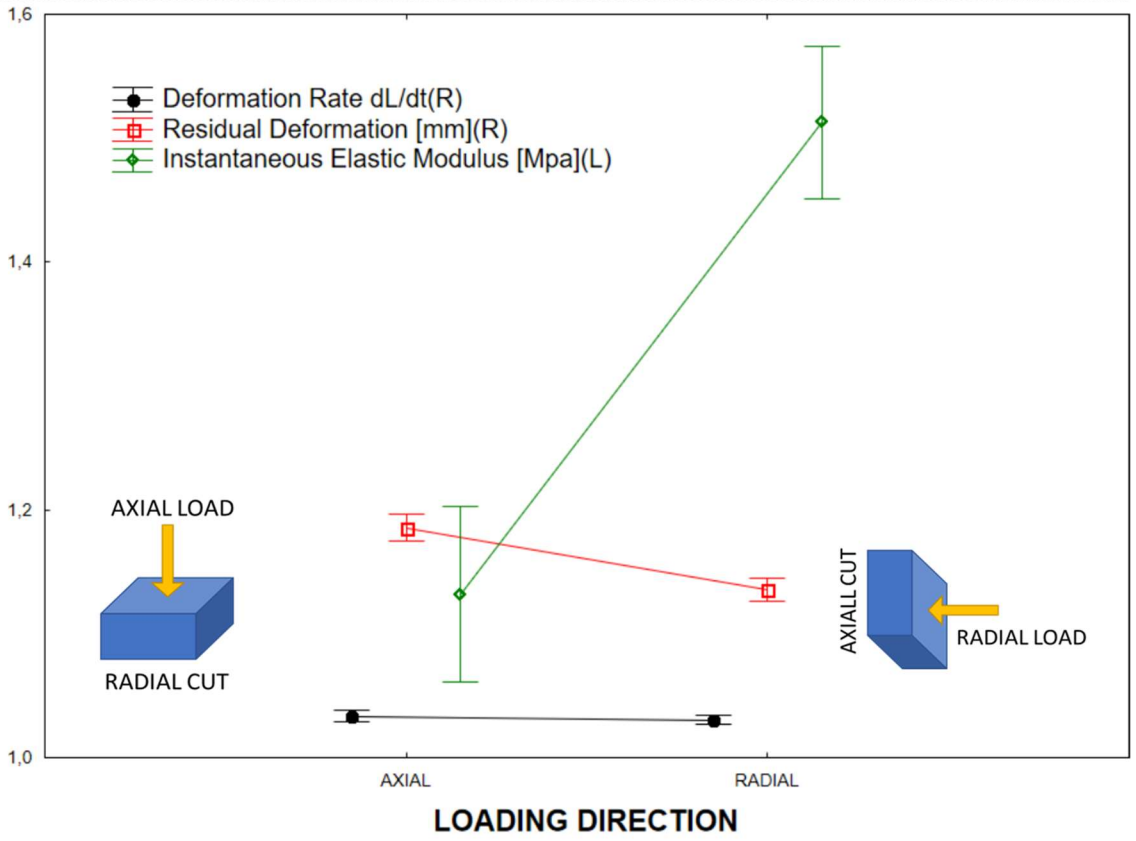

Dependent Variable	Test of SS Whole Model vs. SS Residual (Axial and Radial Rheological Properties.sta)								
	Multiple R	Multiple R^2	Adjusted R^2	SS Model	df Model	MS Model	SS Residual	df Residual	MS Residual
dL/dt	0,108433	0,011758	-0,006977	0,0	12	0,00	0,1	633	0,0001
Deformazione residua [mm]	0,348474	0,121434	0,104779	0,0	12	0,00	0,3	633	0,0005
Compliance max [1/Mpa]	0,260472	0,067845	0,050174	12,1	12	1,01	166,4	633	0,2628
Modulo Elastico Istantaneo [Mpa]	0,409212	0,167455	0,151672	24,0	12	2,00	119,2	633	0,1884

Figure 109 Top: Cubic test specimens oriented axially or radially respect to the cheese wheel. Bottom: Loading Direction effect on both the viscoelastic and yielding properties

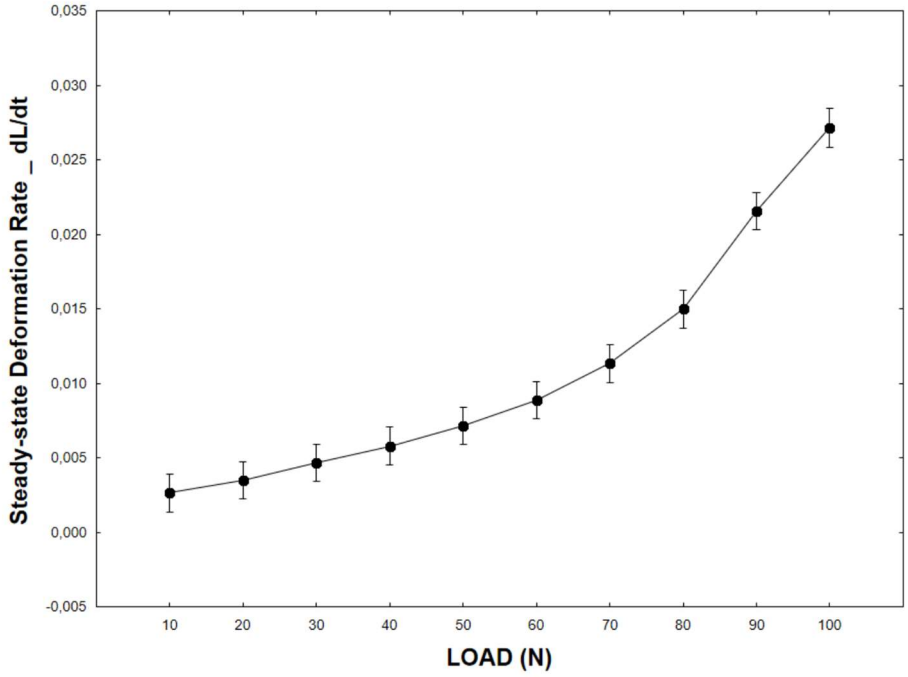

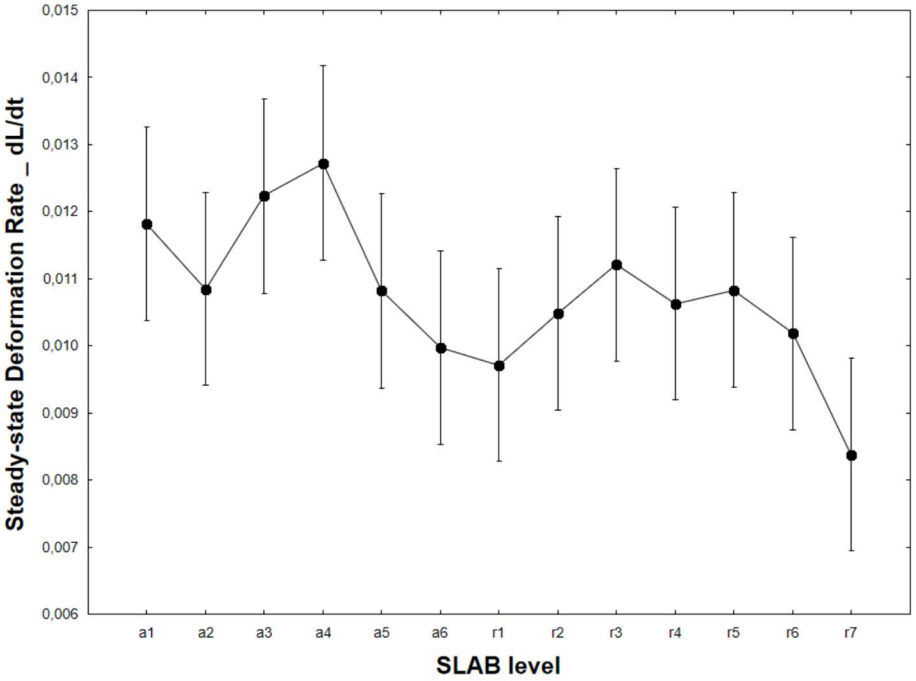

Dependent Variable	Test of SS Whole Model vs. SS Residual (Axial and Radial Rheological Properties.sta)								
	Multiple R	Multiple R^2	Adjusted R^2	SS Model	df Model	MS Model	SS Residual	df Residual	MS Residual
dL/dt	0,850102	0,722673	0,653341	0,0400	129	0,000310	0,01534	516	0,000030
Deformazione residua [mm]	0,816828	0,667208	0,584010	0,2248	129	0,001742	0,11210	516	0,000217
Compliance max [1/Mpa]	0,858598	0,737191	0,671489	131,5649	129	1,019883	46,90297	516	0,090897
Modulo Elastico Istantaneo [Mpa]	0,823289	0,677805	0,597256	97,0801	129	0,752559	46,14707	516	0,089432

Figure 110 Top: Loading effect on the Creep Plastic Response. Bottom: Axial and Radial Slab Distribution of the Yielding Response

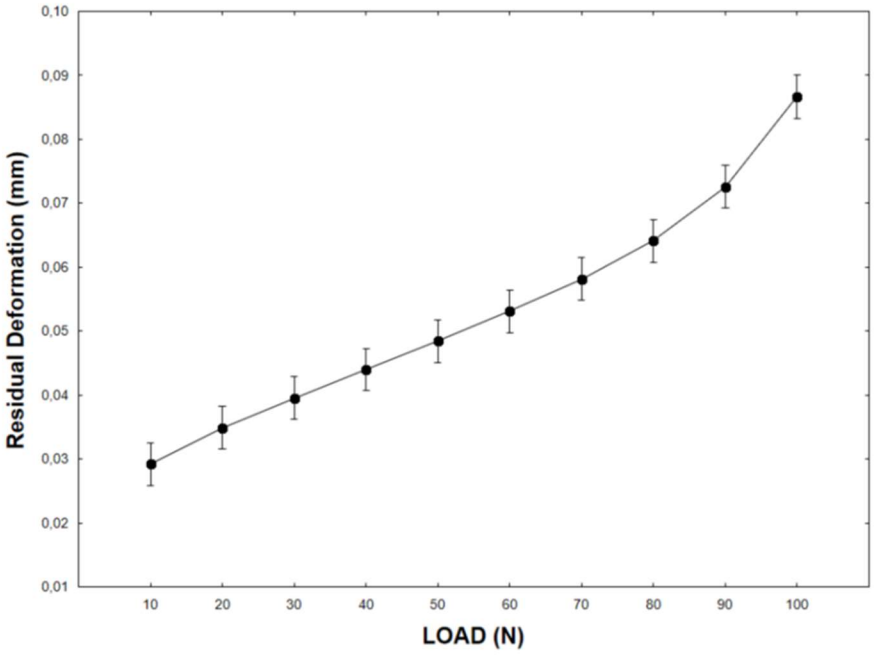

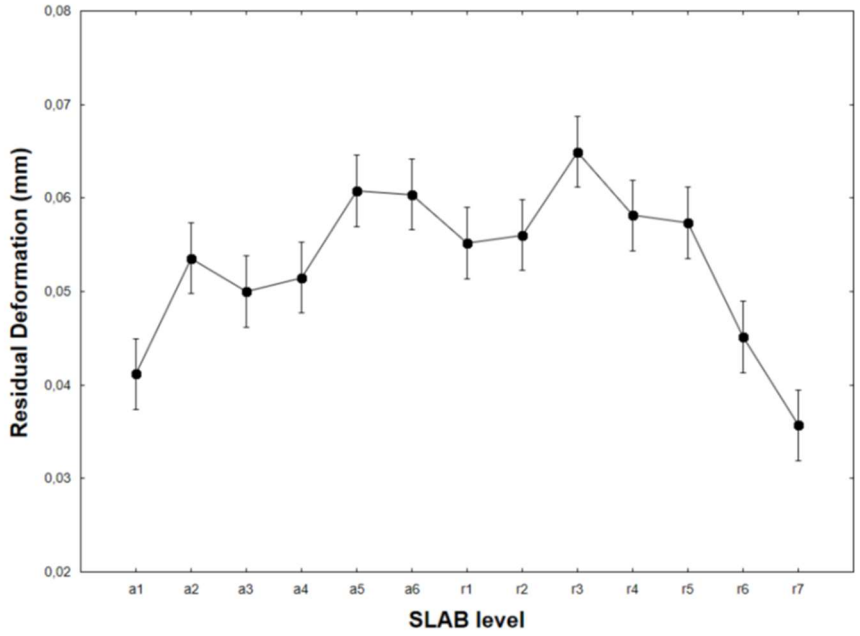

	Test of SS Whole Model vs. SS Residual (Axial and Radial Rheological Properties.sta)								
Dependent Variable	Multiple R	Multiple R^2	Adjusted R^2	SS Model	df Model	MS Model	SS Residual	df Residual	MS Residual
dL/dt	0,850102	0,722673	0,653341	0,0400	129	0,000310	0,01534	516	0,000030
Deformazione residua [mm]	0,816828	0,667208	0,584010	0,2248	129	0,001742	0,11210	516	0,000217
Compliance max [1/Mpa]	0,858598	0,737191	0,671489	131,5649	129	1,019883	46,90297	516	0,090897
Modulo Elastico Istantaneo [Mpa]	0,823289	0,677805	0,597256	97,0801	129	0,752559	46,14707	516	0,089432

Figure 111 Top: Loading effect on the Residual Deformation after Creep and Recovery . Bottom: Axial and Radial Distribution of the Residual Deformation after Creep and Recovery

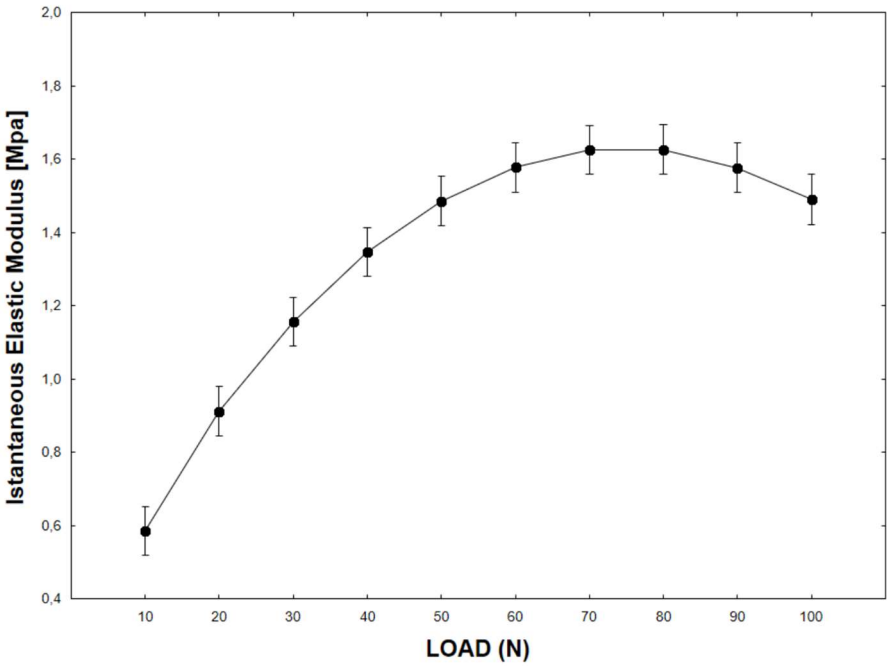

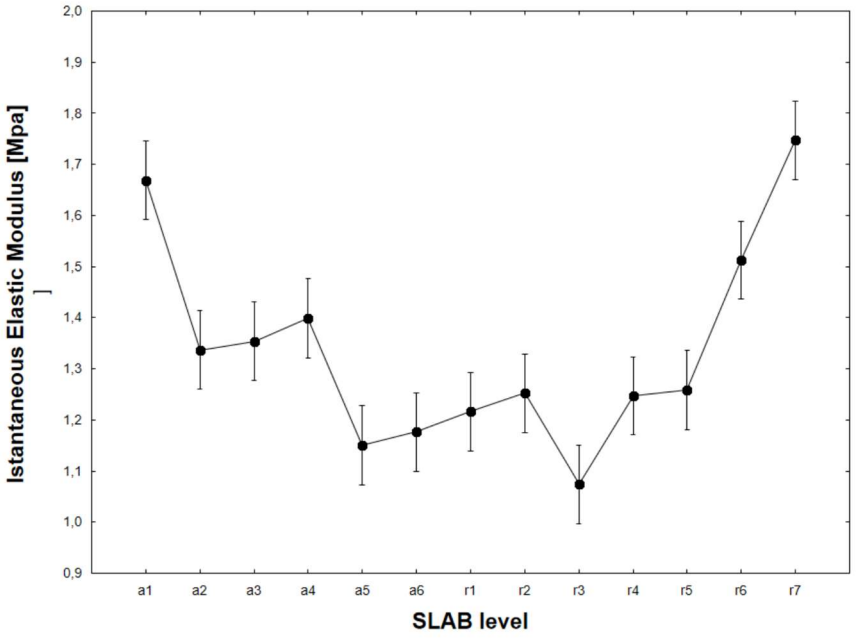

Dependent Variable	Test of SS Whole Model vs. SS Residual (Axial and Radial Rheological Properties.sta)								
	Multiple R	Multiple R^2	Adjusted R^2	SS Model	df Model	MS Model	SS Residual	df Residual	MS Residual
dL/dt	0,850102	0,722673	0,653341	0,0400	129	0,000310	0,01534	516	0,000030
Deformazione residua [mm]	0,816828	0,667208	0,584010	0,2248	129	0,001742	0,11210	516	0,000217
Compliance max [1/Mpa]	0,858598	0,737191	0,671489	131,5649	129	1,019883	46,90297	516	0,090897
Modulo Elastico Istantaneo [Mpa]	0,823289	0,677805	0,597256	97,0801	129	0,752559	46,14707	516	0,089432

Figure 112 Top: Loading effect on the Instantaneous Elastic Modulus under Creep. Bottom: Cheese Clove Distribution Profile of the Instantaneous Elastic Modulus under Creep

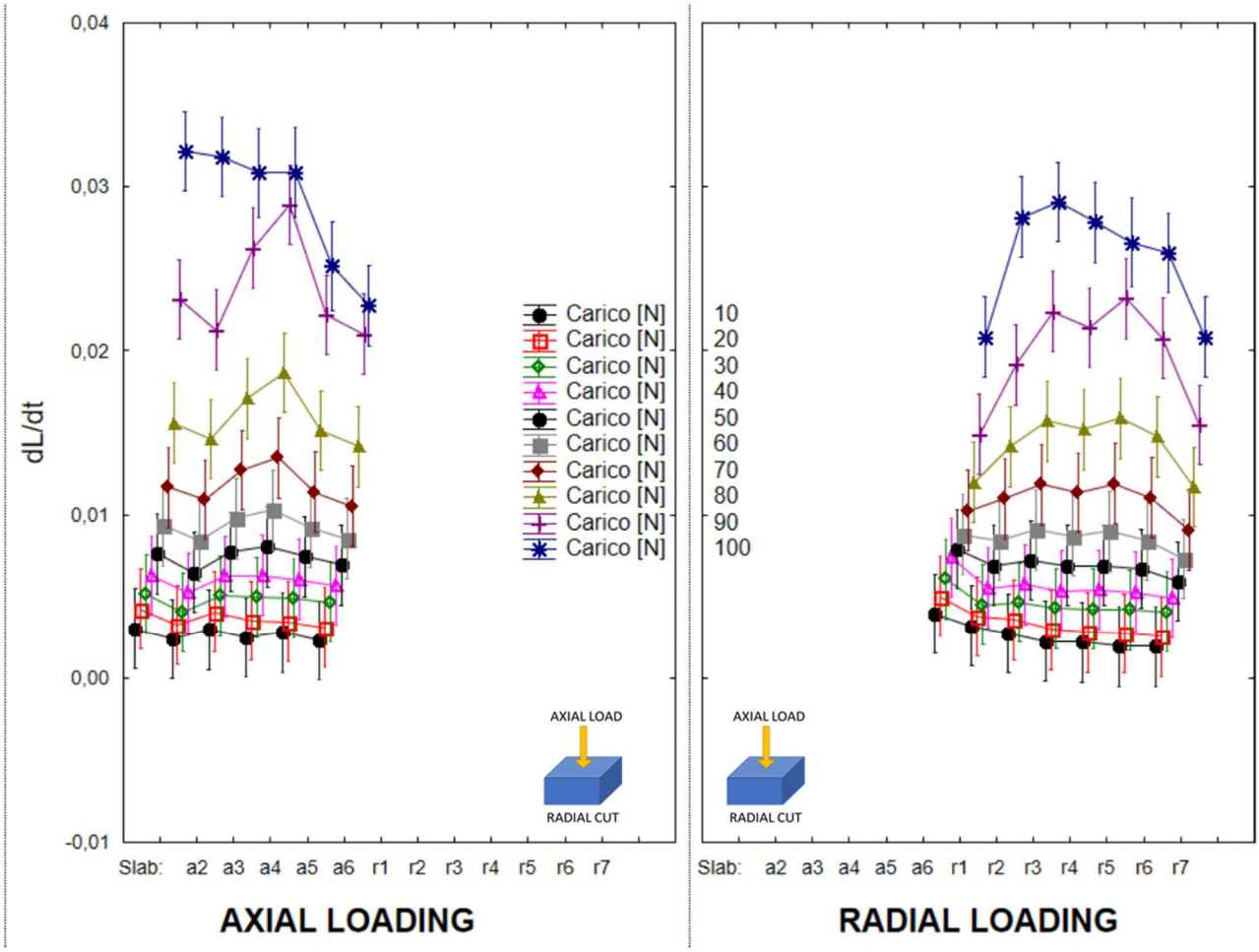

Dependent Variable	Test of SS Whole Model vs. SS Residual (Axial and Radial Rheological Properties.sta)								
	Multiple R	Multiple R^2	Adjusted R^2	SS Model	df Model	MS Model	SS Residual	df Residual	MS Residual
dL/dt	0,850102	0,722673	0,653341	0,0400	129	0,000310	0,01534	516	0,000030
Deformazione residua [mm]	0,816828	0,667208	0,584010	0,2248	129	0,001742	0,11210	516	0,000217
Compliance max [1/Mpa]	0,858598	0,737191	0,671489	131,5649	129	1,019883	46,90297	516	0,090897
Modulo Elastico Istantaneo [Mpa]	0,823289	0,677805	0,597256	97,0801	129	0,752559	46,14707	516	0,089432

Figure 113 Anisotropic distribution of the Steady-state deformation rate under different creep loads

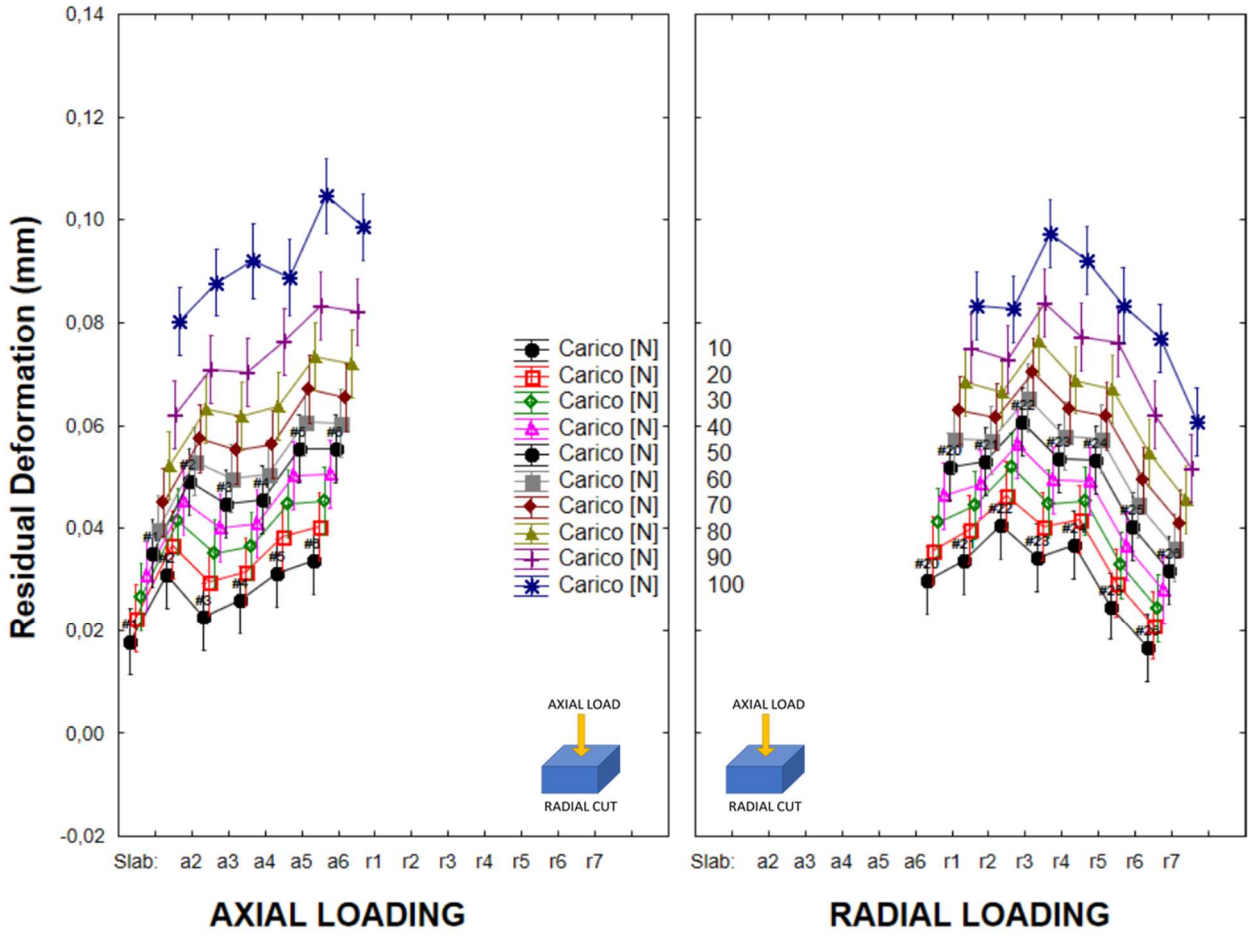

Dependent Variable	Test of SS Whole Model vs. SS Residual (Axial and Radial Rheological Properties.sta)								
	Multiple R	Multiple R^2	Adjusted R^2	SS Model	df Model	MS Model	SS Residual	df Residual	MS Residual
dL/dt	0,850102	0,722673	0,653341	0,0400	129	0,000310	0,01534	516	0,000030
Deformazione residua [mm]	0,816828	0,667208	0,584010	0,2248	129	0,001742	0,11210	516	0,000217
Compliance max [1/Mpa]	0,858598	0,737191	0,671489	131,5649	129	1,019883	46,90297	516	0,090897
Modulo Elastico Istantaneo [Mpa]	0,823289	0,677805	0,597256	97,0801	129	0,752559	46,14707	516	0,089432

Figure 114 Anisotropic distribution of Residual Deformation after Creep and Recovery

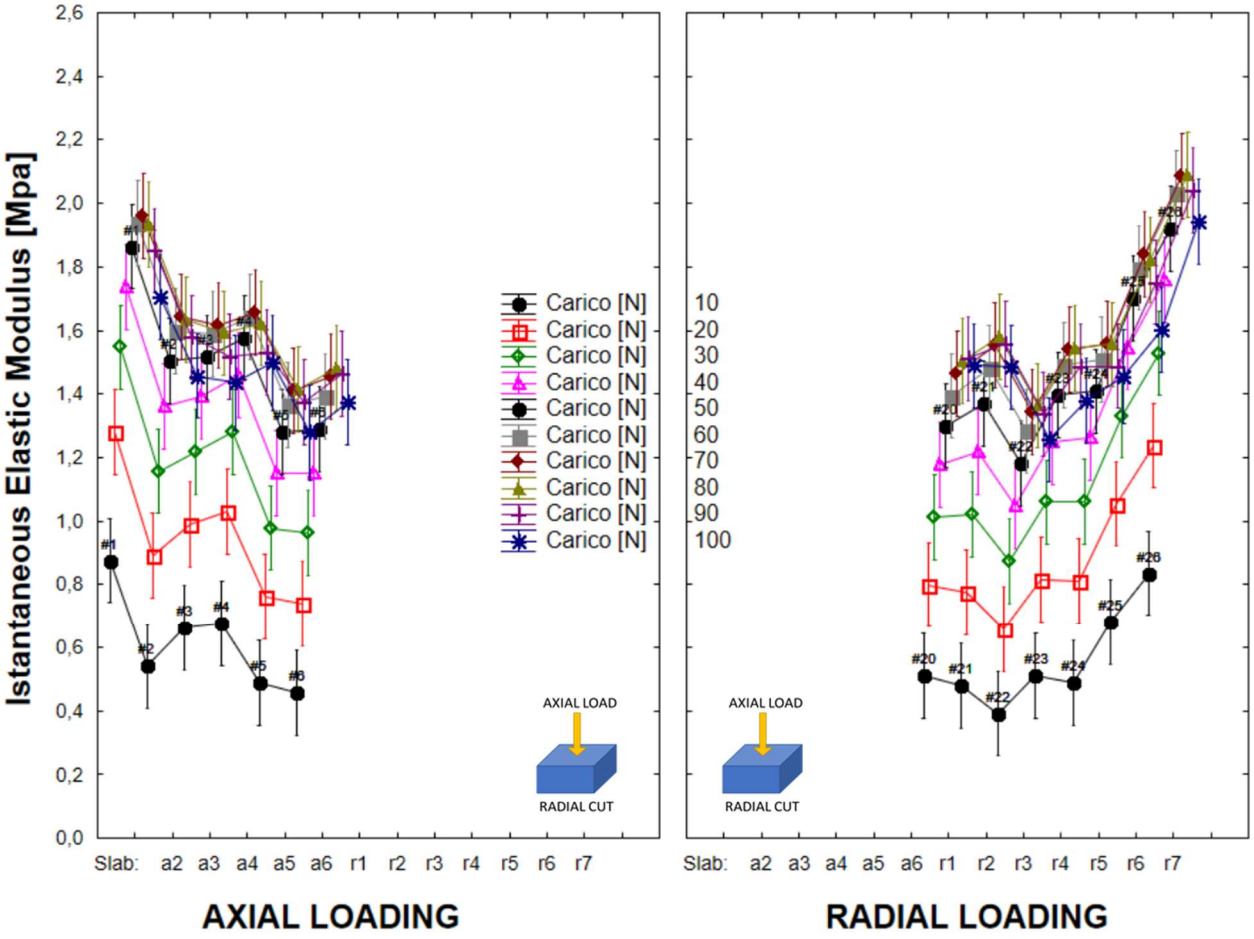

Dependent Variable	Test of SS Whole Model vs. SS Residual (Axial and Radial Rheological Properties.sta)								
	Multiple R	Multiple R^2	Adjusted R^2	SS Model	df Model	MS Model	SS Residual	df Residual	MS Residual
dL/dt	0,850102	0,722673	0,653341	0,0400	129	0,000310	0,01534	516	0,000030
Deformazione residua [mm]	0,816828	0,667208	0,584010	0,2248	129	0,001742	0,11210	516	0,000217
Compliance max [1/Mpa]	0,858598	0,737191	0,671489	131,5649	129	1,019883	46,90297	516	0,090897
Modulo Elastico Istantaneo [Mpa]	0,823289	0,677805	0,597256	97,0801	129	0,752559	46,14707	516	0,089432

Figure 115 Anisotropic distribution of the instantaneous Elastic Modulus under Creep

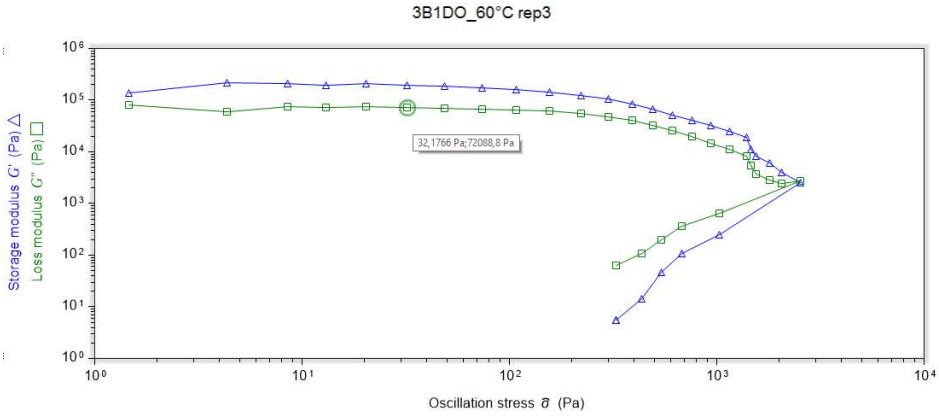

Figure 116 Linear viscoelastic region at 60°C in 37M PR samples

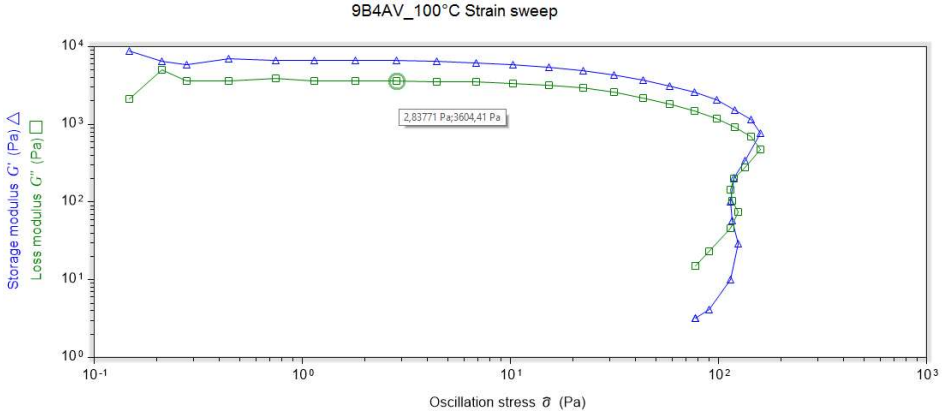

Figure 117 Linear viscoelastic region at 100°C in 37M PR samples

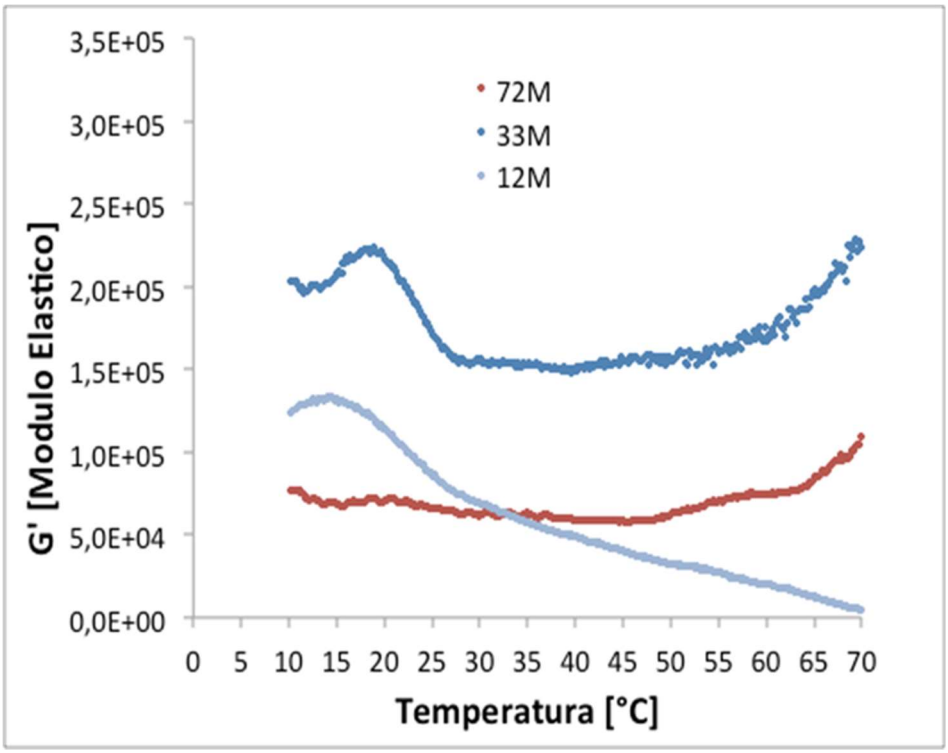

Figure 118 Temperature sweep test: elastic component (G') versus temperature, in PR 12M, 33M, 72M.

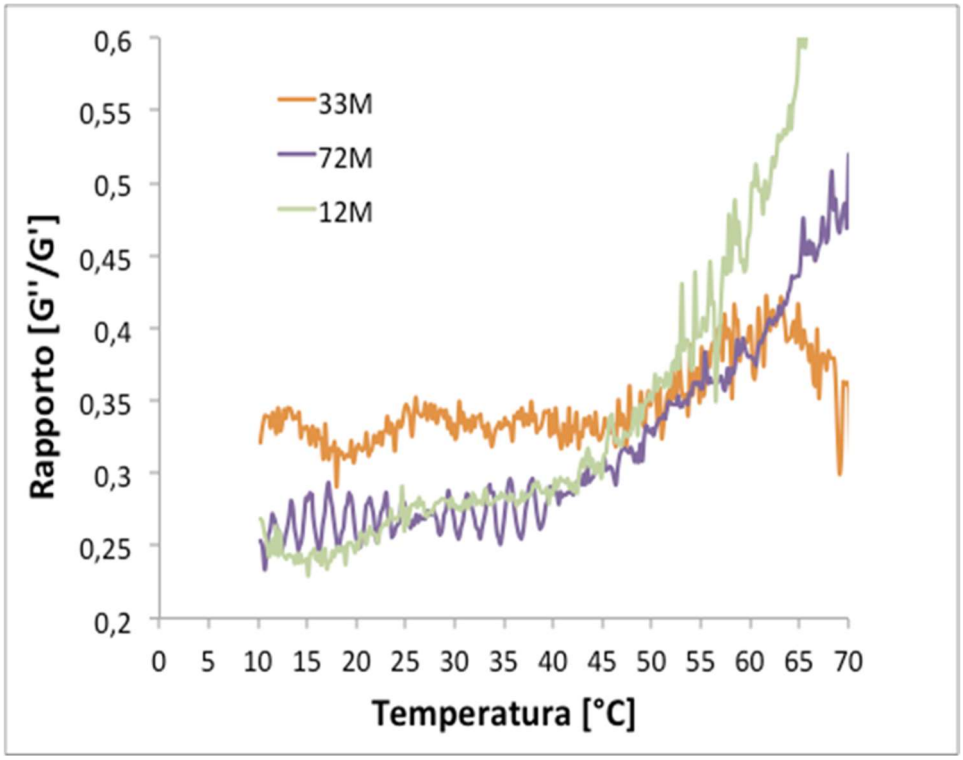

Figure 119 Temperature sweep test: G''/G' (Tan delta) versus temperature, in PR 12M, 33M, 72M

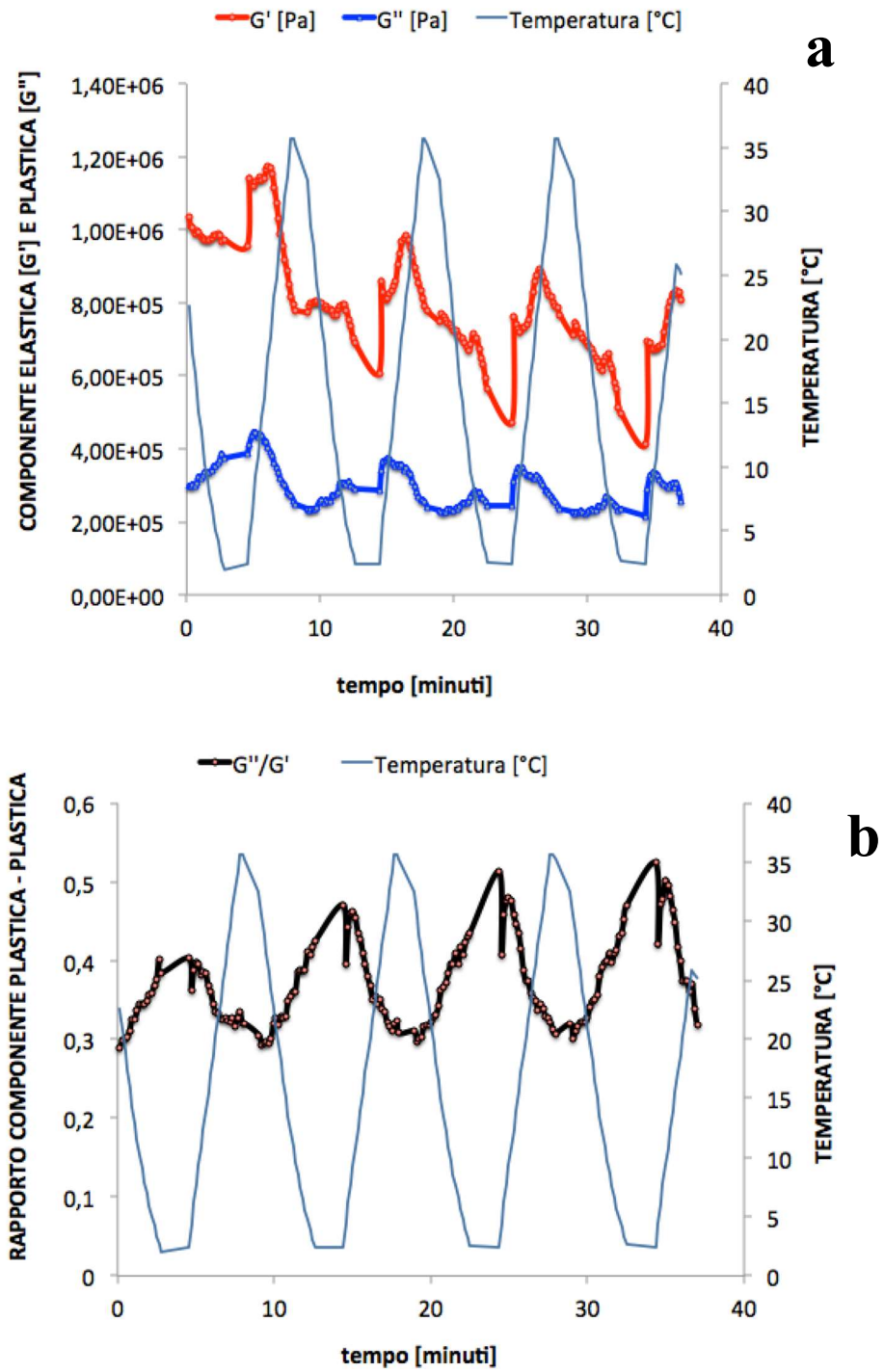

Figure 120 a-b Hysteretic changes in Storage and Loss Moduli as a function of temperature in the range 0°C – 35°C (with a rate of 10°C/min) for a 12M cheese

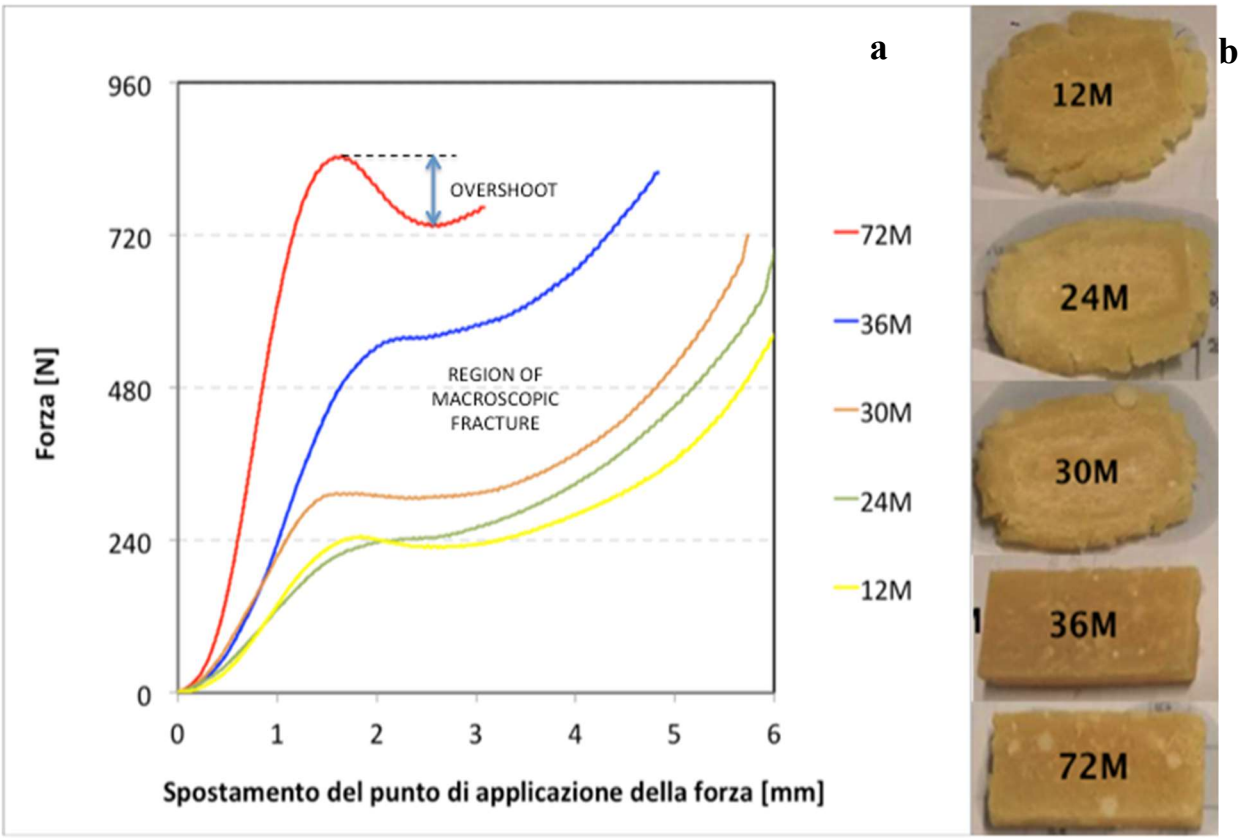

Figure 121 a) Load-displacement curves for PR 12M, 2M, 30M, 36M and 72M. b) Fracture of test specimen occur from the interior due to tension stress along with the circumference. Overshooting after the maximum stress was inversely related to the oiling-off phenomena

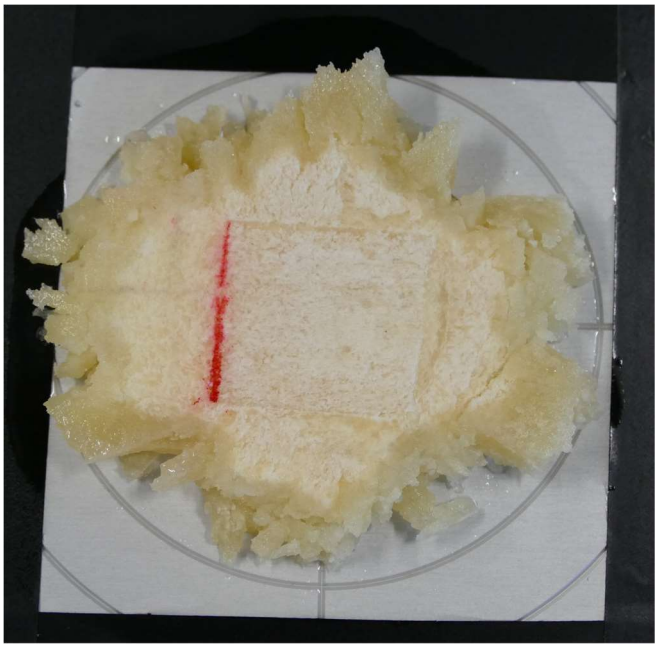

Figure 122 Bulk structure after 75% uniaxial compression

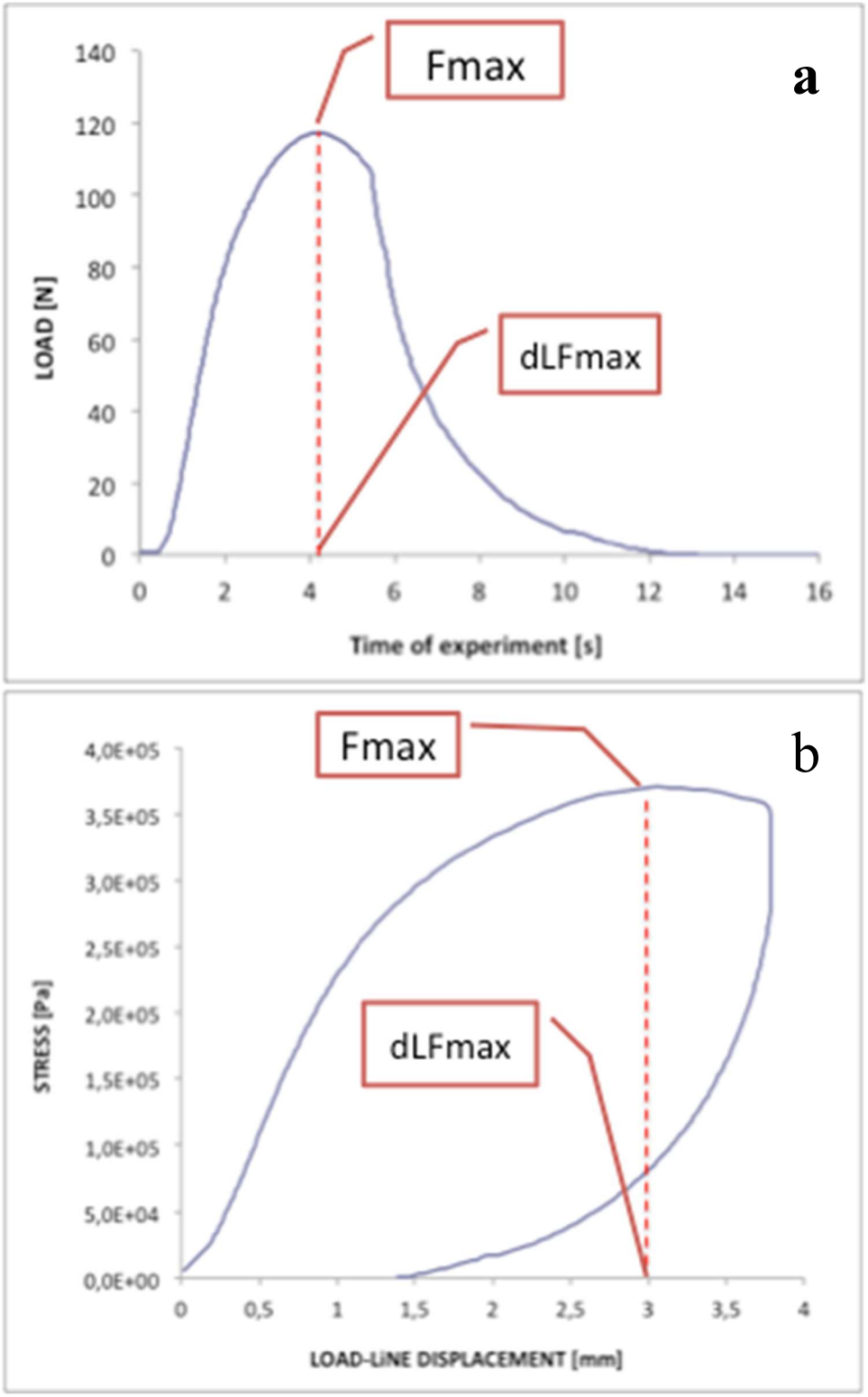

Figure 123 a-b. Yielding behavior under uniaxial compression test for 12M cheese. Cubic specimens were compressed until 30% with a constant displacement rate of 5mm/min for load and unload steps.

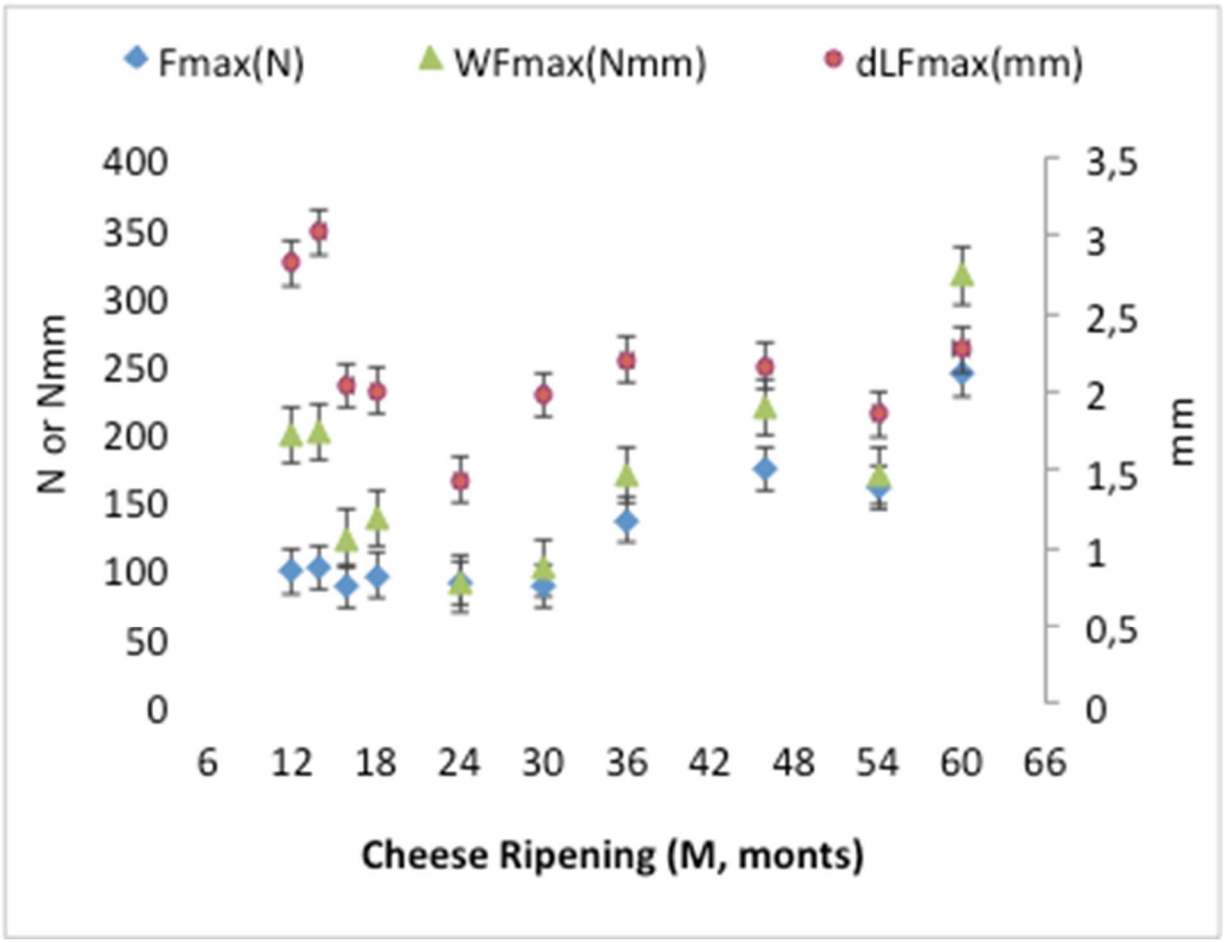

Figure 124 Comparison of Yielding properties for PR cheese with different ripening ages. Error bars represent the standard deviation for nine test specimens at least. The "Work to Yielding" reaches a minimum level for 24M nd 30M cheeses.

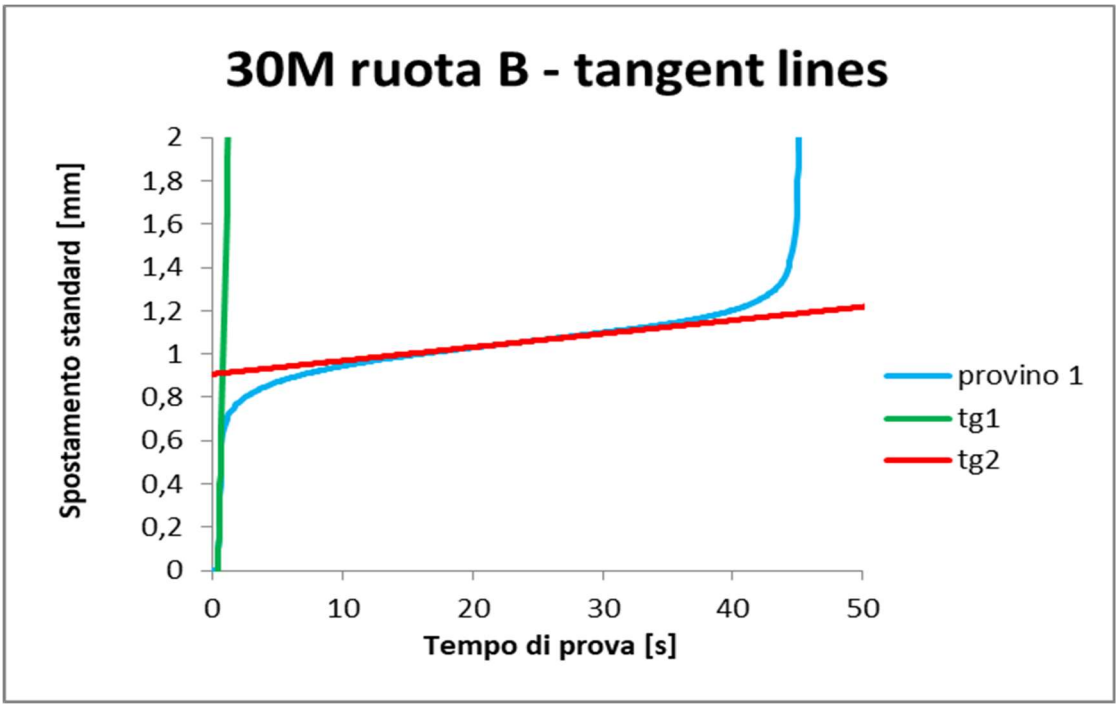

Figure 125 Tensile Creep curve of PR30M 3B1AV (SENT test specimen). The slope of tangent lines tg1 and tg2 represents the instantaneous elastic modulus (E0) and the steady-state strain rate (dL/dt), respectively

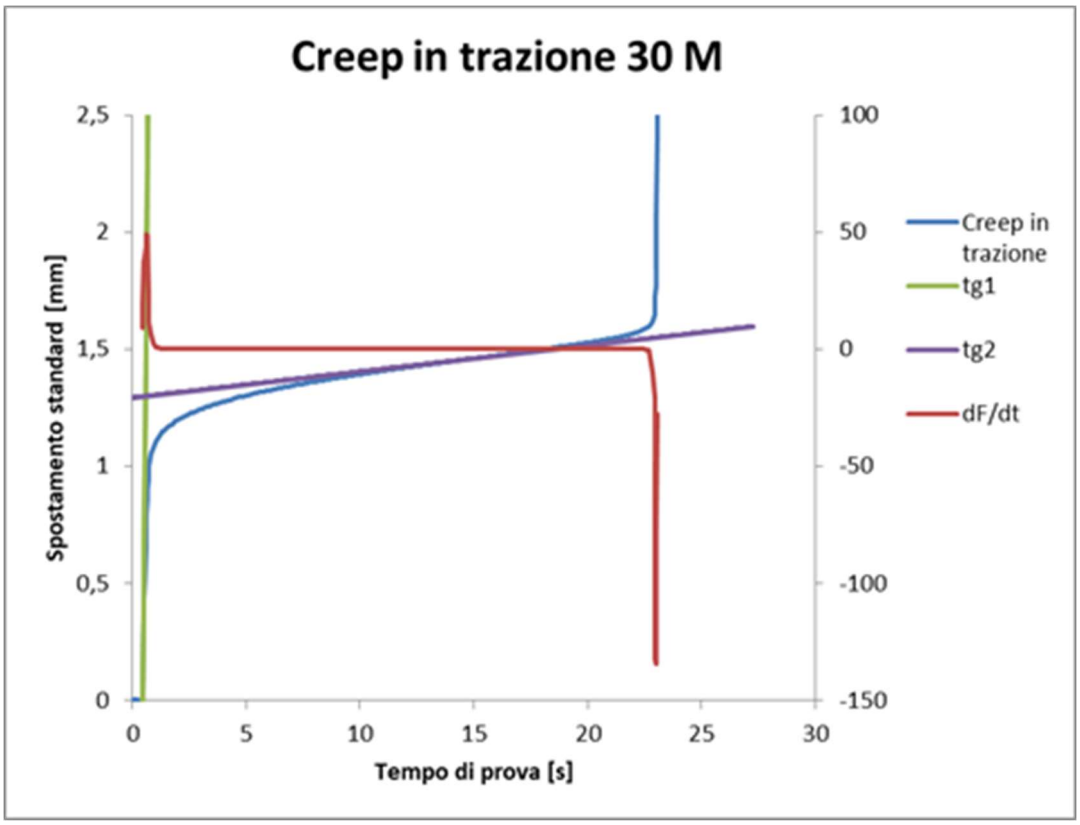

Figure 126 Tensile curve of PR30M 3B1AV sample: derivative analysis of the load versus time

Table 6 Fracture properties under tension of 18M and 30M PR test specimens

Samples	Time of start fracture [s]	Time of end fracture [s]	Duration of the fracture [s]	Time of maximum speed of breaking [s]	m1	m2
18M 1B2AV	14,19	14,68	0,49	14,27	5,62	0,03
18M 1B3AV	23,55	24,00	0,45	23,61	3,92	0,01
18M 2B1AV	15,61	16,10	0,49	15,65	3,68	0,03
18M 2B3AV	99,68	100,18	0,50	99,73	3,43	0,00
18M 4B3AV	77,80	78,25	0,45	77,85	4,13	0,00
18M 7B3AV	81,50	81,87	0,37	81,56	2,76	0,00
18M 8B1AV	45,53	45,99	0,46	45,59	2,83	0,01
18M 8B2AV	5,91	6,30	0,39	5,97	8,74	0,07
18M 8B3AV	63,40	63,79	0,39	63,47	4,52	0,00
30M 3B1AV	44,92	45,36	0,44	45,00	2,48	0,01
30M 3B2AV	17,95	18,31	0,36	18,00	2,55	0,02
30M 3B3AV	4,13	4,40	0,27	4,18	4,09	0,06
30M 3B4AV	9,19	9,55	0,36	9,24	3,86	0,03
30M 3B5AV	27,48	27,94	0,46	27,53	4,21	0,01
30M 3B6AV	27,05	27,42	0,37	27,10	2,82	0,01
30M 4B5AV	67,53	67,86	0,33	67,59	2,69	0,00
30M 5B1AV	2,31	2,69	0,38	2,36	5,06	0,13
30M 5B2AV	1,58	1,95	0,37	1,63	7,96	0,33
30M 5B3AV	25,42	25,78	0,36	25,48	2,98	0,01
30M 6B1AV	21,22	21,62	0,40	21,29	4,27	0,01
30M 6B2AV	4,73	5,11	0,38	4,78	6,25	0,05
30M 7B1AV	2,09	2,56	0,47	2,16	3,86	0,13
30M 7B2AV	18,36	18,77	0,41	18,43	4,69	0,01
30M 7B3AV	22,94	23,28	0,34	22,98	10,73	0,01
30M 8B3AV	4,55	4,93	0,38	4,59	8,40	0,05
10B2AV	51,64	51,99	0,35	51,67	8,32	0,00
10B3AV	6,54	7,24	0,70	6,63	4,46	0,06

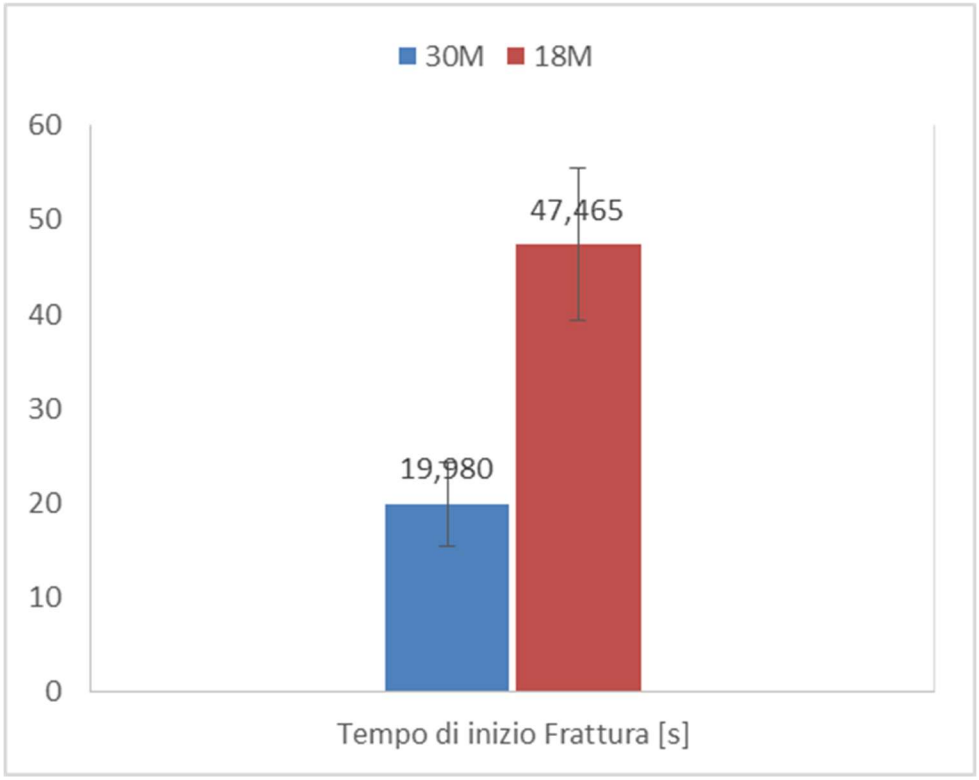

Figure 127 Average time for the fracture initiation in 18 M and 30 M cheeses

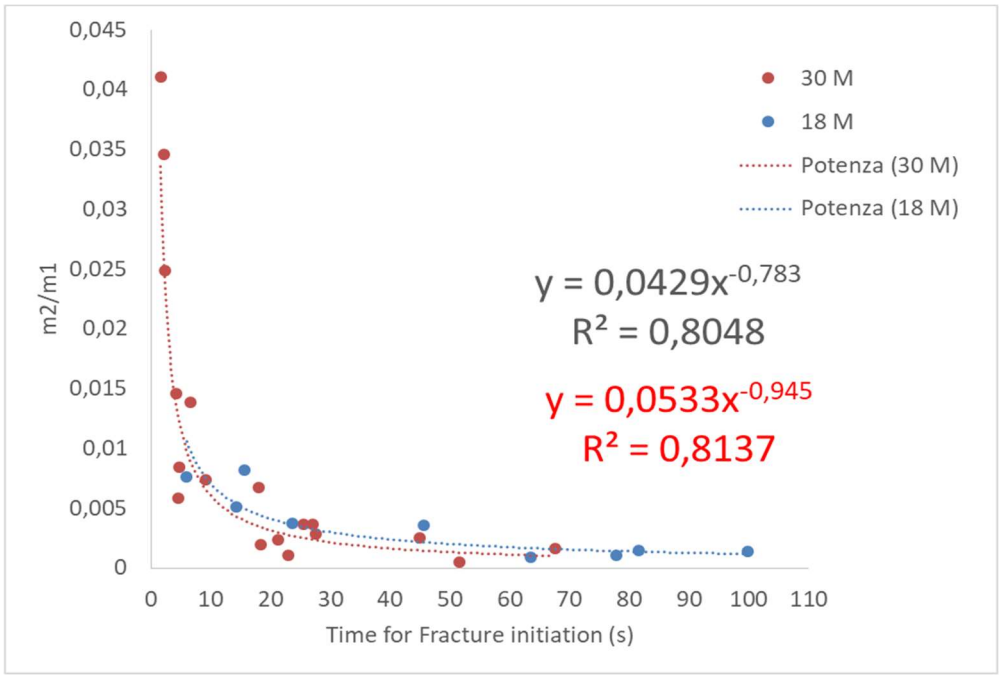

Figure 128 Elastoplastic ratio (m2/m1) is related to fracture initiation according to a power law

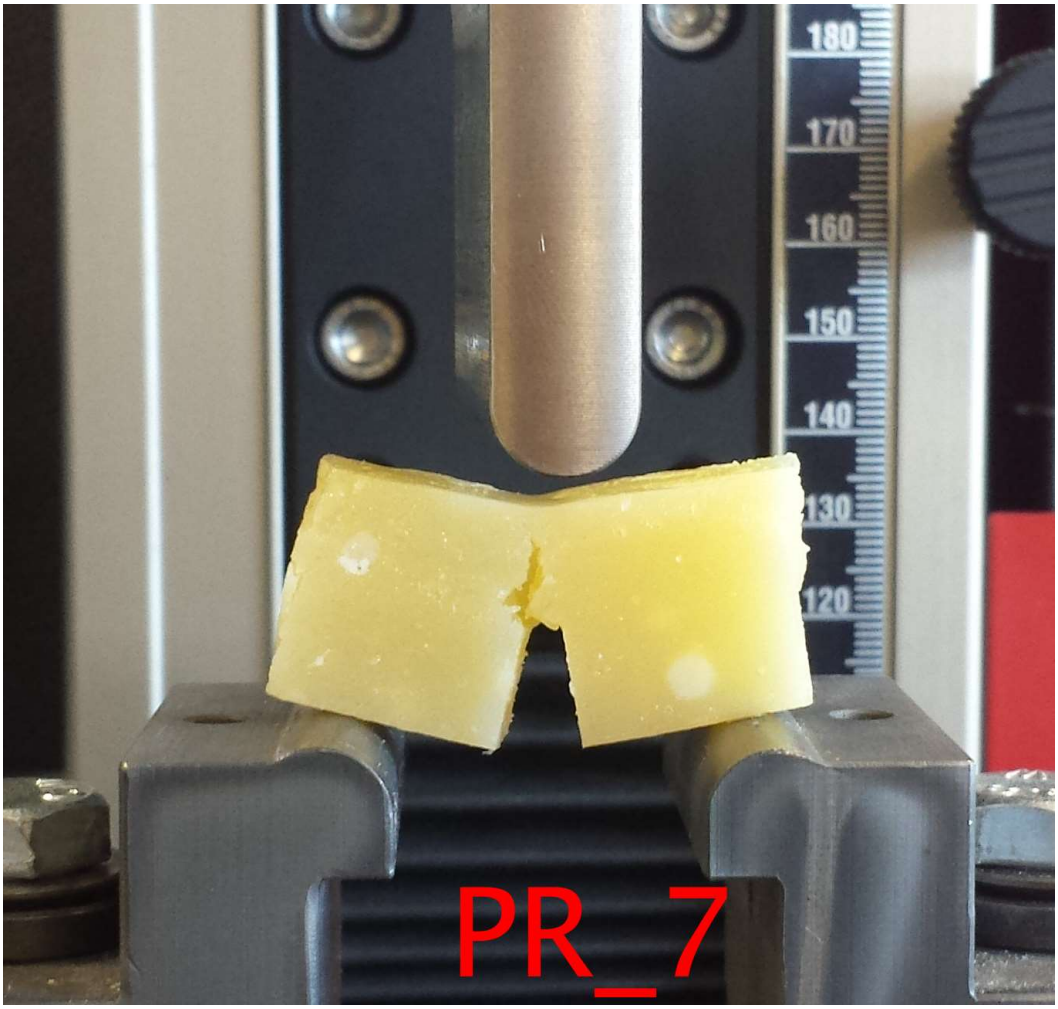

PR20M – IN ASSE ***PR20M – FUORI ASSE***

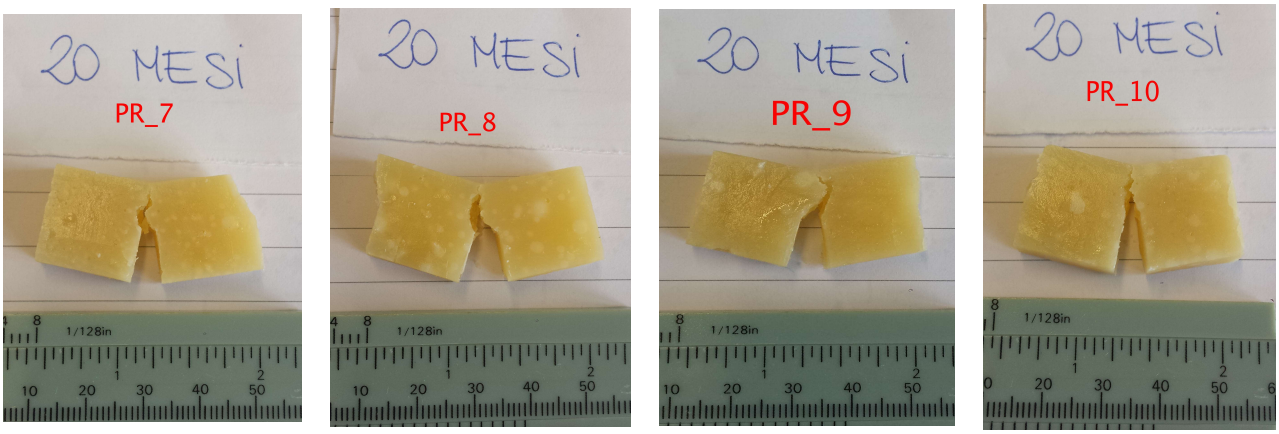

Figure 129 Small-scale yielding (SSY) and the Plane-Strain conditions are not accomplished: the stress was not negligible in the direction orthogonal to the crack plane as suggested by the fracture profile of the two new fracture surfaces changing direction at 45°

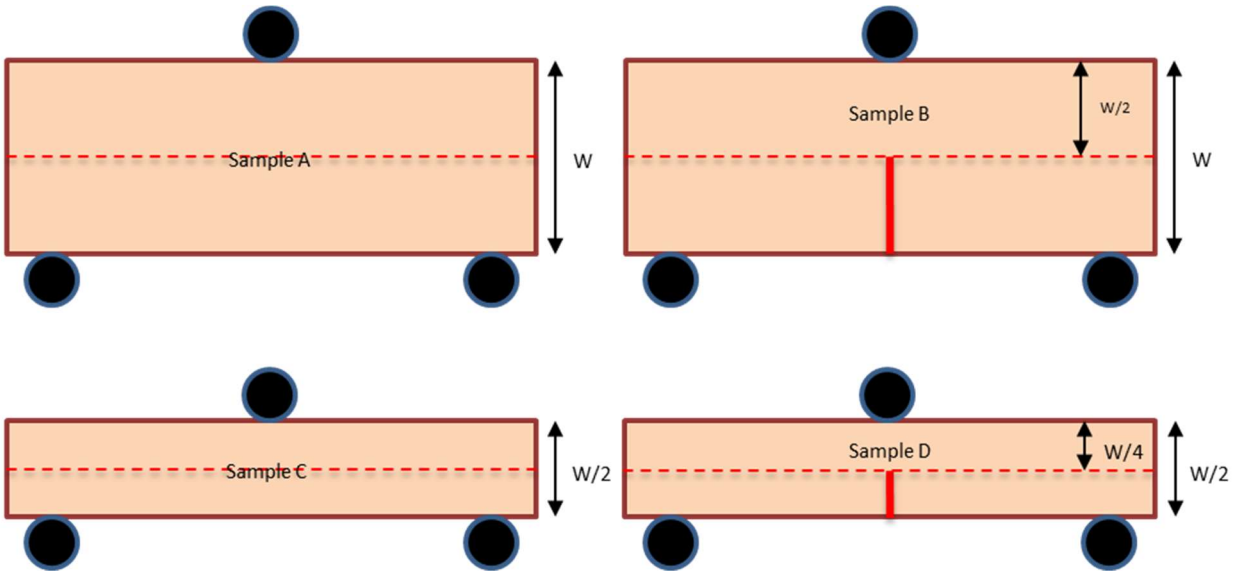

Figure 130 Notch-sensivity test for PR cheese: thre-point bending test with and without notch for two scale sizes of the cheese test geometry

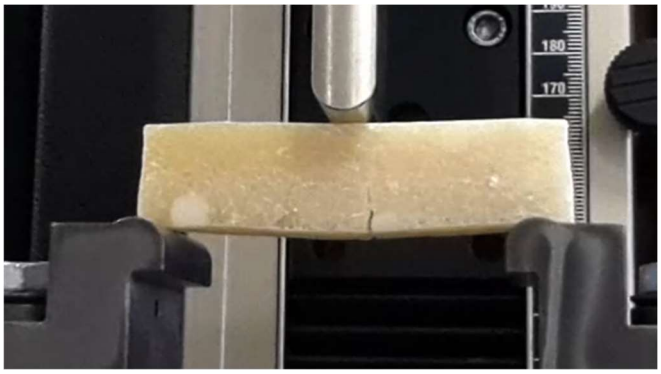

Figure 131 Fracture propagation form a spontaneous initiation follow an unpredictable pattern

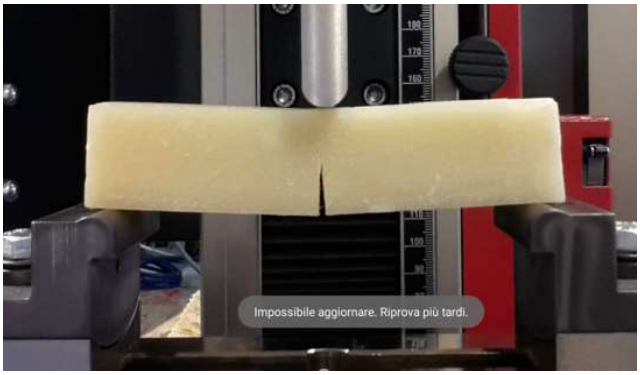

Figure 132 Fracture propagation from a notch follows the crack plane direction if the Small-scale yielding (SSY) and the Plane-Strain conditions are both accomplished

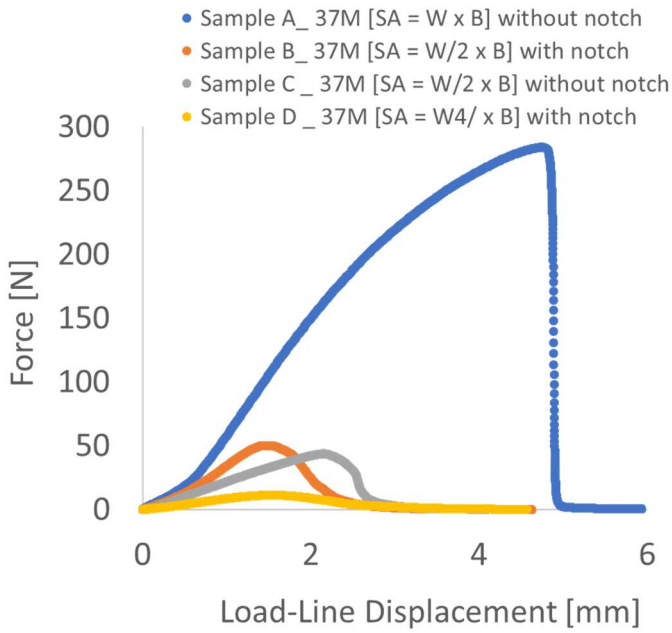

Figure 133 Load concentrates on a randomly distributed discontinuity of the cheese bulk. The work to fracture is governed by the plastic behavior across the specimen tickness

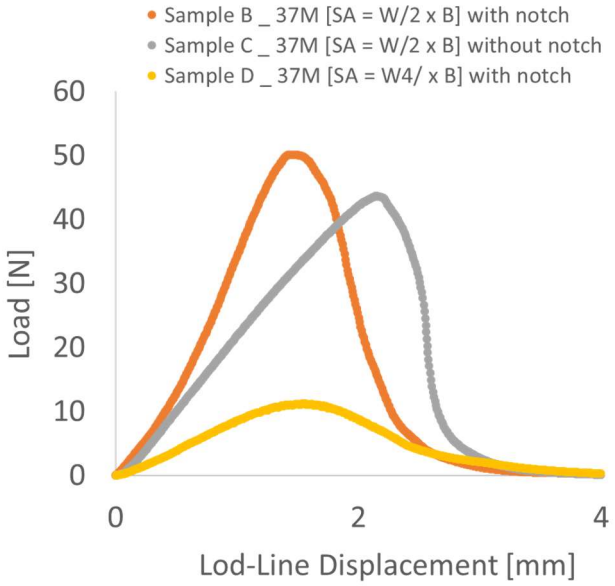

Figure 134 Load concentrates on a notch previously generated on the cheese surface, allowing to reduce drastically the plastic strain close to the crack-tip

	W [m]	B [m]	L [m]	S [m^2]	a/W	a_0 [m]	f(a/W)	Fmax [N]	E [Mpa]	σ_{US} [Mpa]	Wf [J/m^2]	Kic [Mpa*m^0.5]	ry [µm]	Small-scale yielding	Plane Strain
Sample A	0,05	0,04	0,09	0,0020	0,00	0,00	0,00	284,10	1,98	0,14	194,76	0,00	0,00	Verified!	Verified!
Sample B	0,04	0,04	0,09	0,0014	0,50	0,02	2,66	50,07	2,11	0,03	12,61	2,55	282,73	Verified!	Verified!
Sample C	0,02	0,04	0,09	0,0010	0,00	0,00	0,00	43,63	2,17	0,05	25,37	0,00	0,00	Verified!	Verified!
Sample D	0,02	0,04	0,09	0,0009	0,49	0,01	2,59	11,23	2,09	0,01	5,31	0,20	13,93	Verified!	Verified!

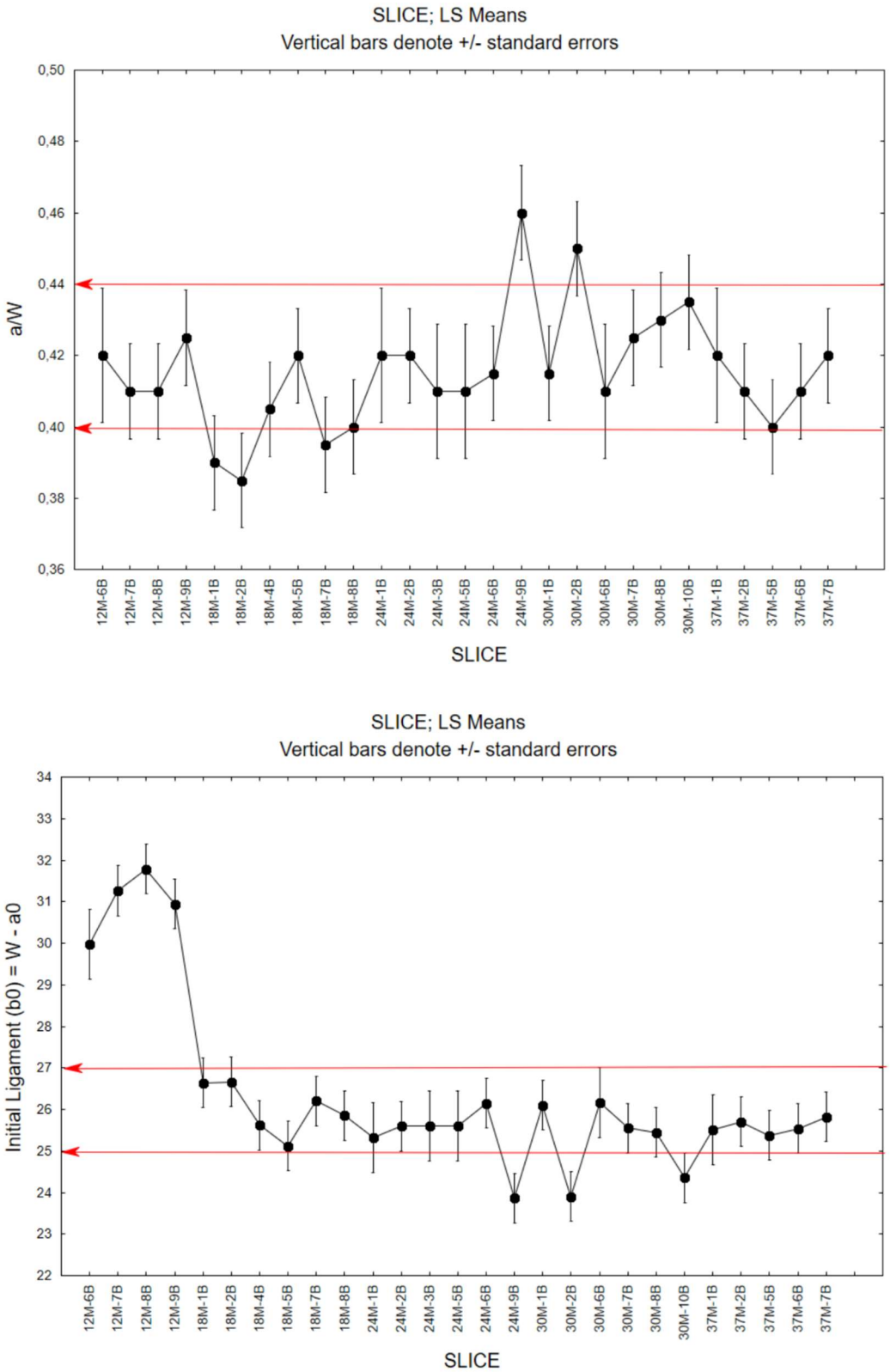

Figure 135 Uncertainty associated to the geometrical properties of the test specimens. Top: ratio between notch length and with. Bottom: Ligament calculated as difference between specimen with and notch length

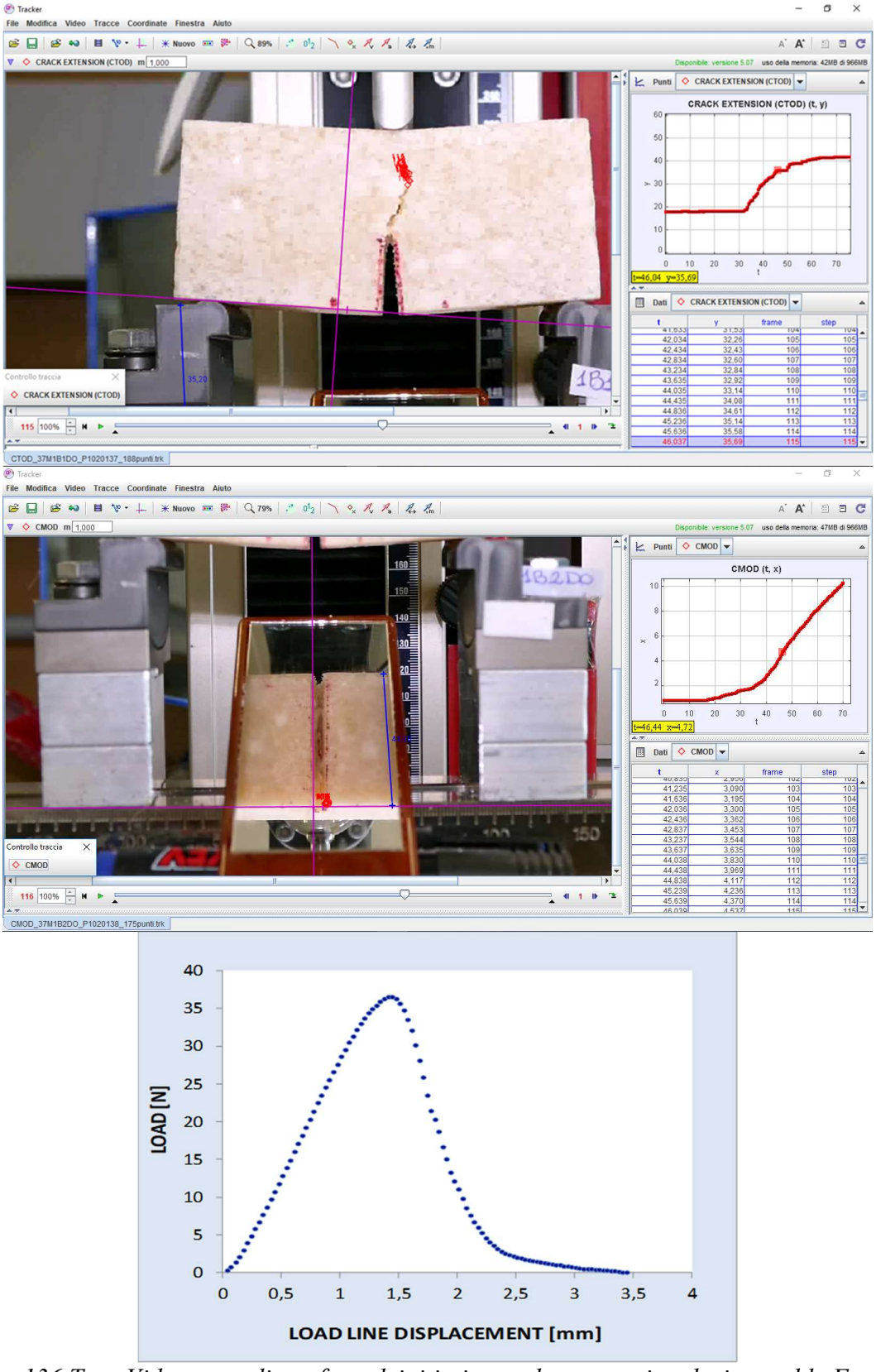

Figure 136 Top: Video recording of crack initiation and propagation during stable Fracture. Bottom: Load-displacement curve

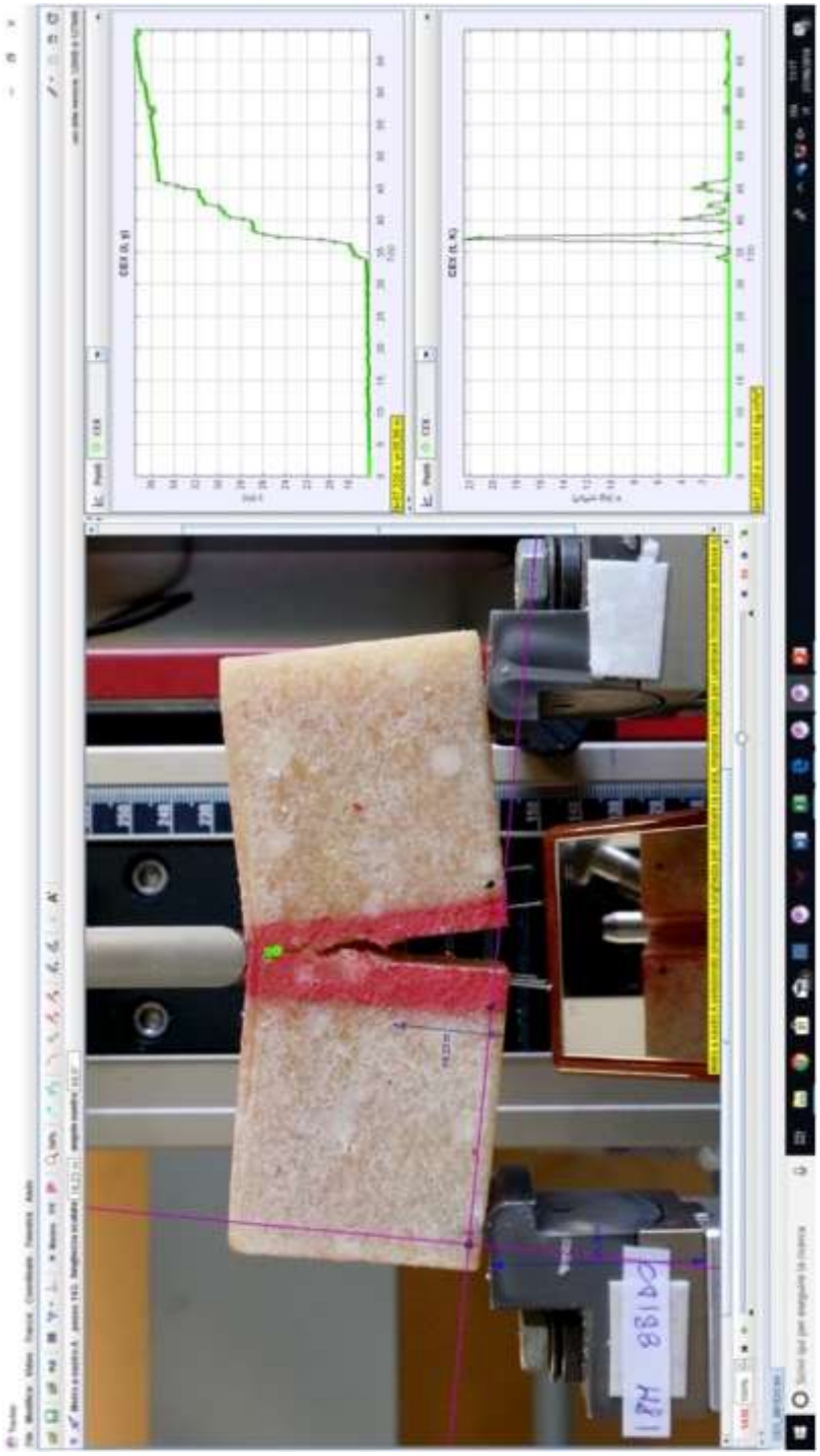

Figure 137 Kinetic Energy released during Fracture Propagation in 18-months cheese. First and second derivative calculus of the crack propagation kinetics allows to characterize the brittle events underpinning cheese fracture under strain-controlled fracture (stab)

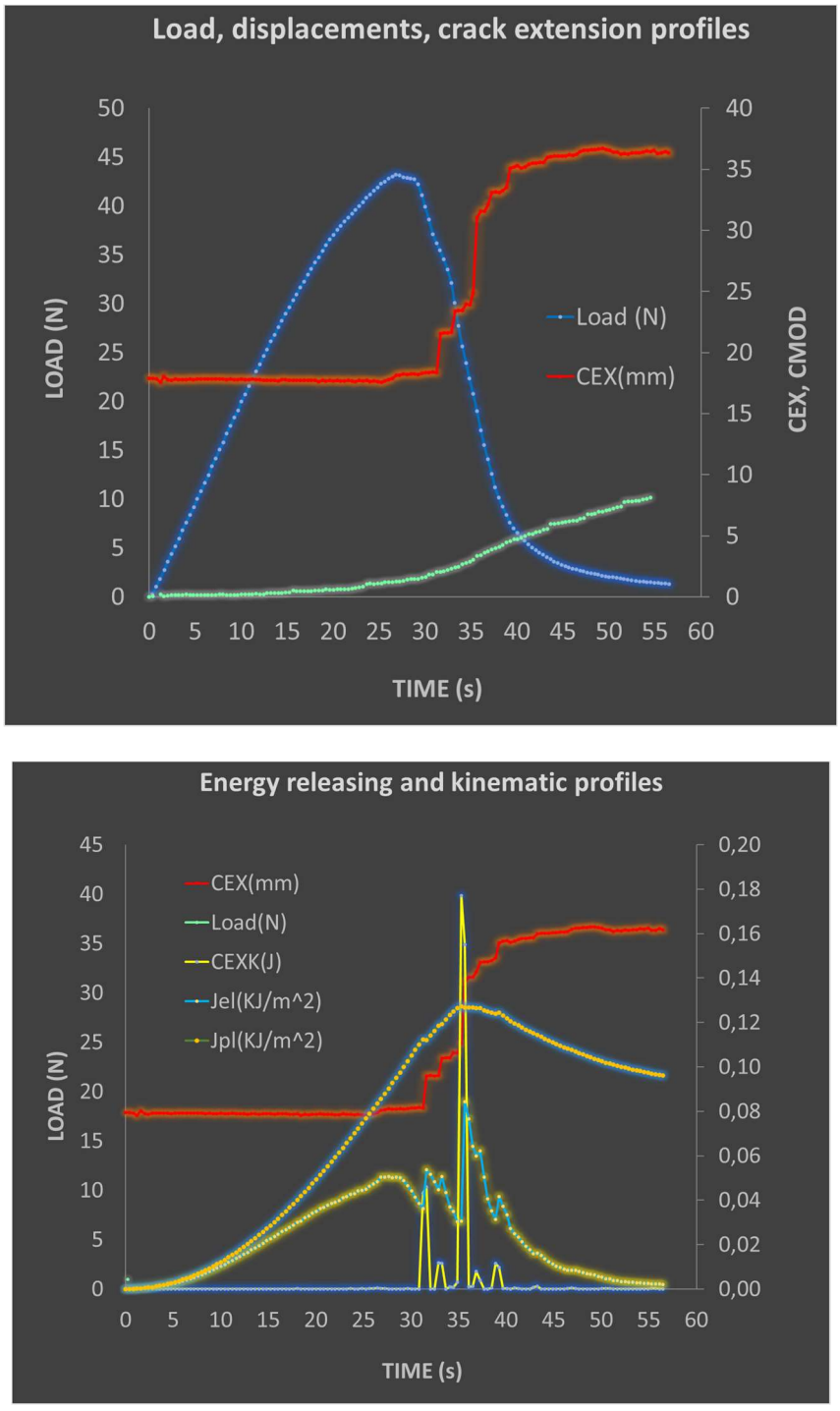

Figure 138 Top: Load, displacements, and crack extent profile. Bottom: Elastic (Jel), Plastic (Jpl) Energies underpinning the brittle events taking place with a kinetic energy CEX(K) during strain-controlled fracture for a 12-months ripened PR cheese

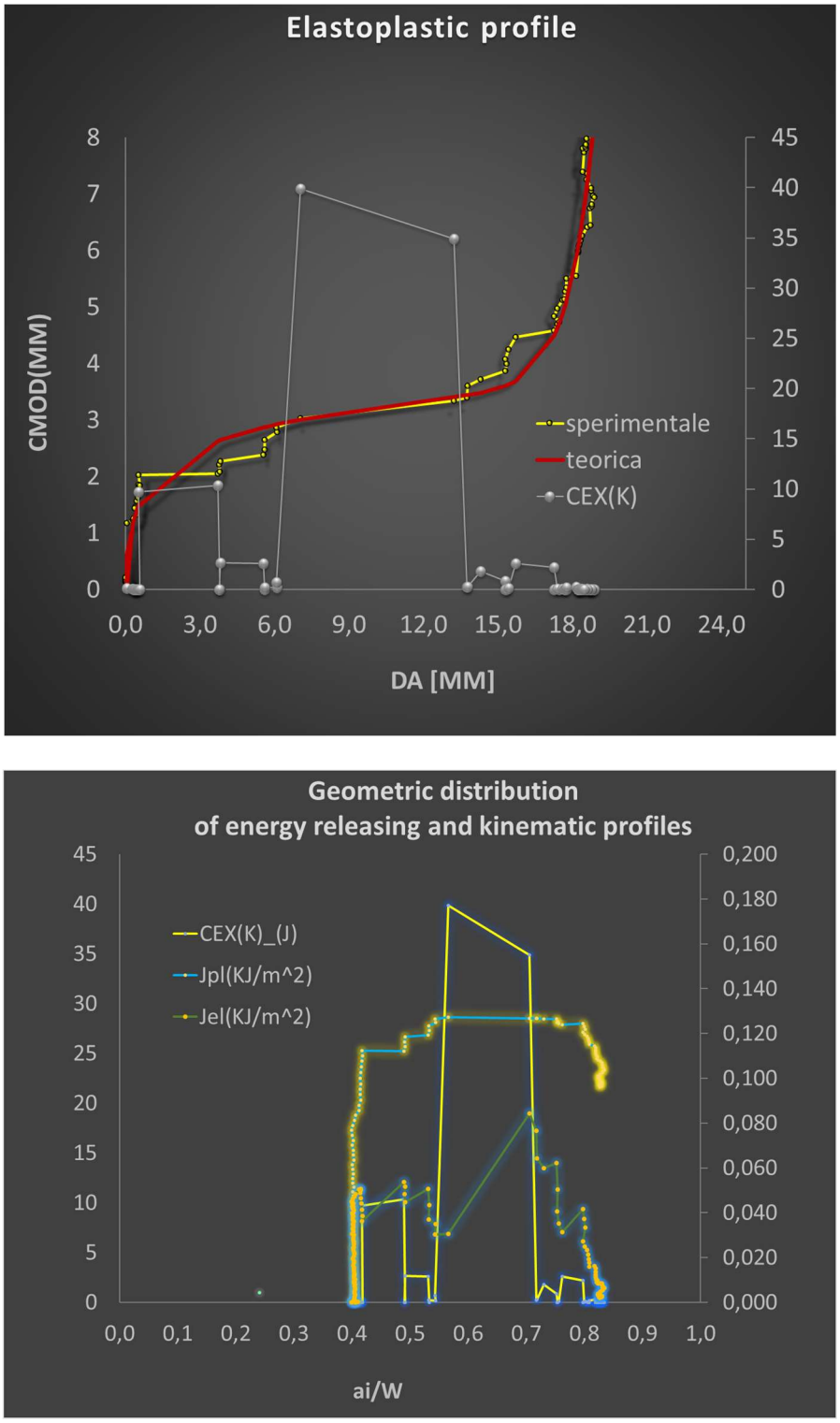

Figure 139 Top: Elastoplastic relation between crack-mouth opening displacement (CMOD) and crack extension (CEX). Bottom: Geometrical distribution of the elastic (Jel) and plastic (Jpl) energy releasing during fracture taking place with a kinetic energy CEX(K) in 18months cheese

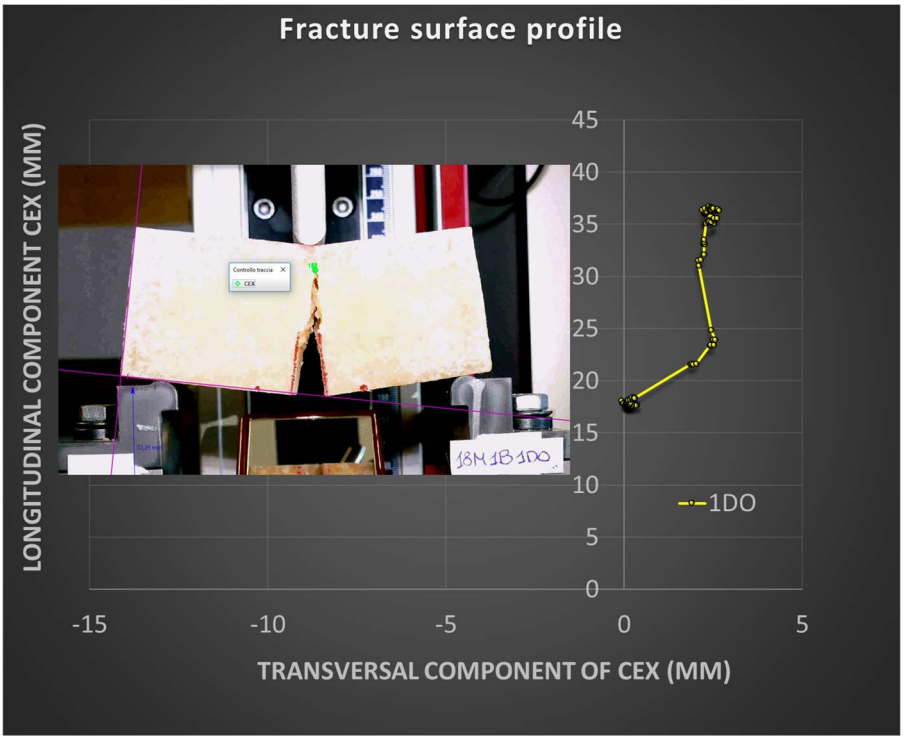

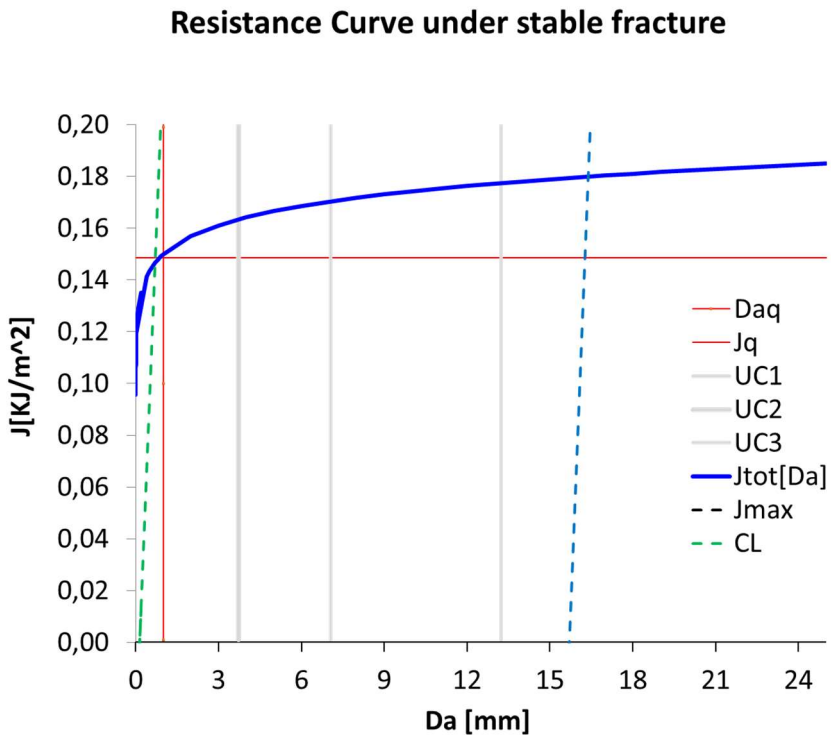

Figure 140 Top: Comparison between the fracture surface profile as calculated numerically and the corresponding digital data. Bottom: J-R Resistance Curve for 18months cheese

Table 7 14 Energetic and kinematic fracture properties for PR 18M cheese

12 M											
symbol	**unit of measure**	**6B1DO**	**6B2DO**	**7B1DO**	**7B2DO**	**8B1DO**	**9B1DO**	**9B2DO**	**Media 12M**	**Dev.st.**	**Coeff.Var.**
E_B	MPa	4,203	3,171	4,283	5,054	13,786	9,310	12,397	7,458	4,334	0,581
CEX(K)_media	(mm/s)^2	3,709	3,706	3,425	2,095	1,927	3,375	4,061	3,185	0,834	0,262
CEX(K)_max	(mm/s)^2	6,060	7,674	5,698	4,612	3,933	12,167	7,026	6,739	2,719	0,404
Δa(UCi)max	mm	3,585	4,218	4,225	3,911	8,693	6,368	4,670	5,096	1,824	0,358
$\Sigma\lvert\Delta a(UCi)$	mm	19,198	14,748	19,401	18,323	34,601	20,902	23,124	21,471	6,325	0,295
J_{IC} (J_Q)	KJ/m^2	0,070	0,070	0,100	0,100	0,170	0,140	0,143	0,113	0,039	0,340
J_{UC1}	KJ/m^2	0,084	0,180	0,119	0,099	0,174	0,251	0,202	0,158	0,060	0,381
$(JEL/EPL)_{Uci\_MAX}$	adimensionale	1,962	5,820	0,894	0,592	0,468	1,571	1,135	1,777	1,859	1,046
$\Sigma(JEL)/\Sigma(EPL)\_t_{last}$	adimensionale	0,891	3,023	0,706	0,390	0,387	1,089	0,793	1,040	0,911	0,876
Jtot_Δa(mm1)	KJ/m^2	0,070	0,081	0,115	0,100	0,170	0,140	0,143	0,117	0,036	0,309
Jtot_Δa(mm5)	KJ/m^2	0,105	0,102	0,132	0,104	0,176	0,186	0,182	0,141	0,039	0,279
Jtot_Δa(mm10)	KJ/m^2	0,124	0,123	0,158	0,105	0,178	0,209	0,202	0,157	0,041	0,261
$Wf_{\_Pmax}$	KJ/m^2	0,014	0,018	0,018	0,015	0,026	0,028	0,029	0,021	0,007	0,307
$\varepsilon_{UTS}/\varepsilon(EB)_{max}$	adimensionale	0,056	0,069	0,030	0,003	0,037	0,192	0,008	0,057	0,064	1,137

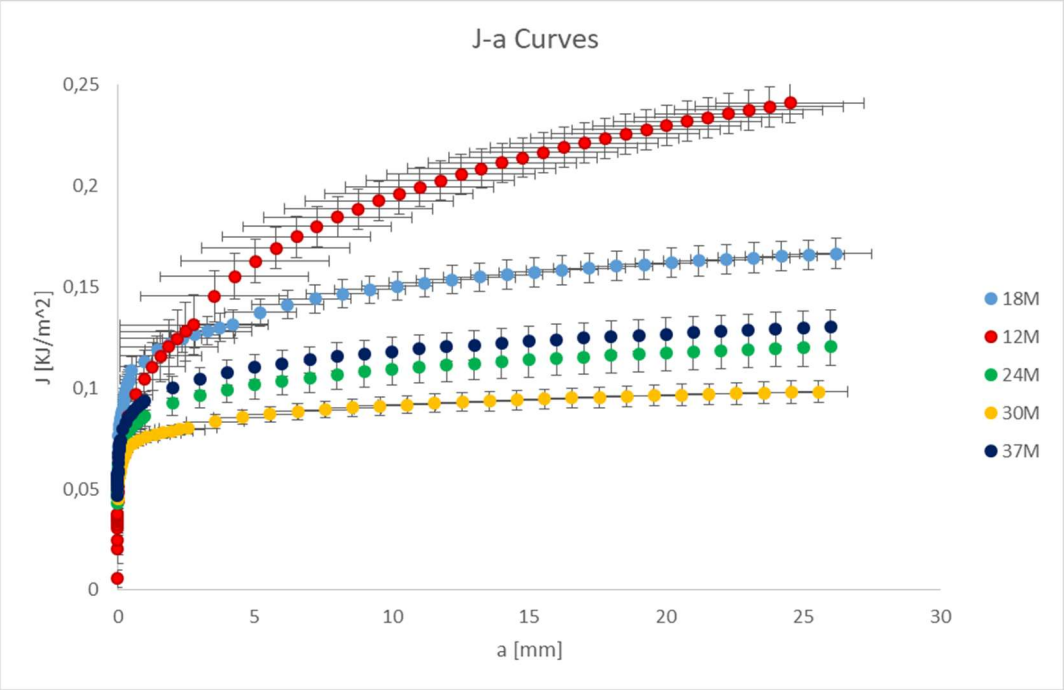

Figure 141 Fracture resistance (J-R curve) of PR 12M, 18M, 24M, 30M and 37M cheeses

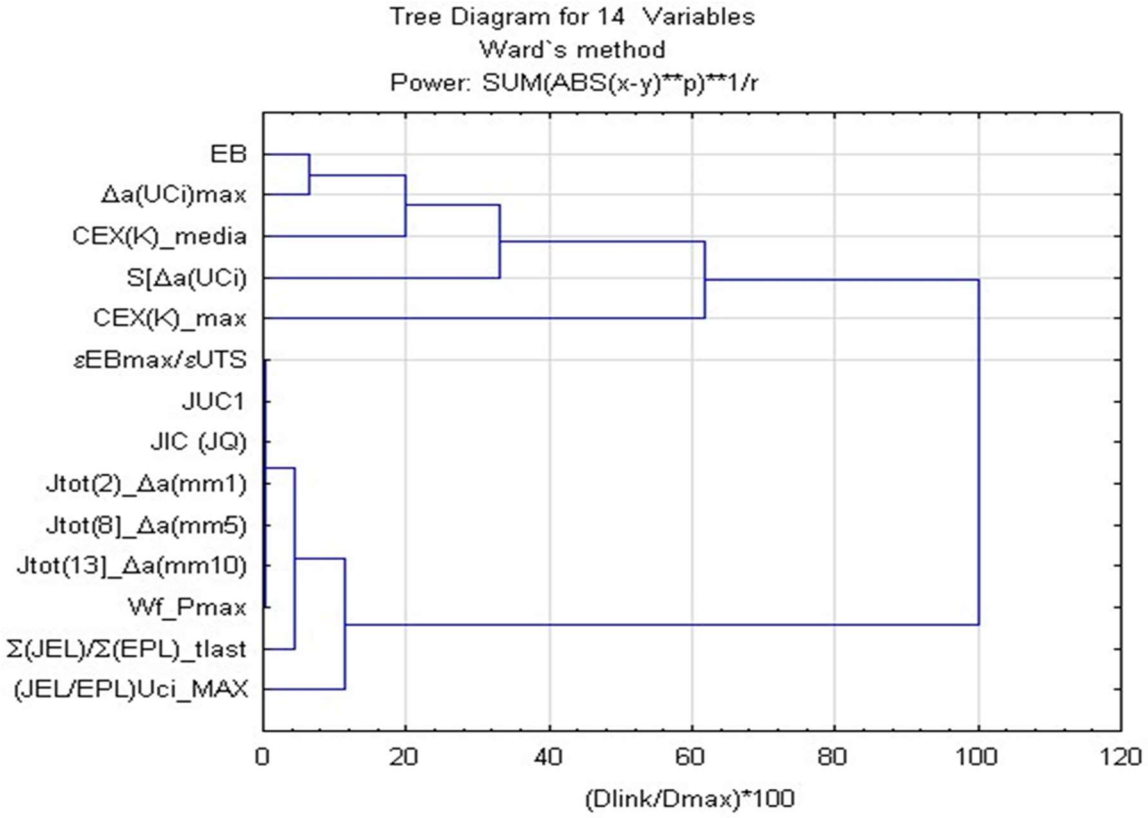

Figure 142 New 14 Fracture Properties as defined and calculated from the three basic experimental measurements (load, displacement, crack extension). They were grouped into Kinetic and Energy based classes of material properties

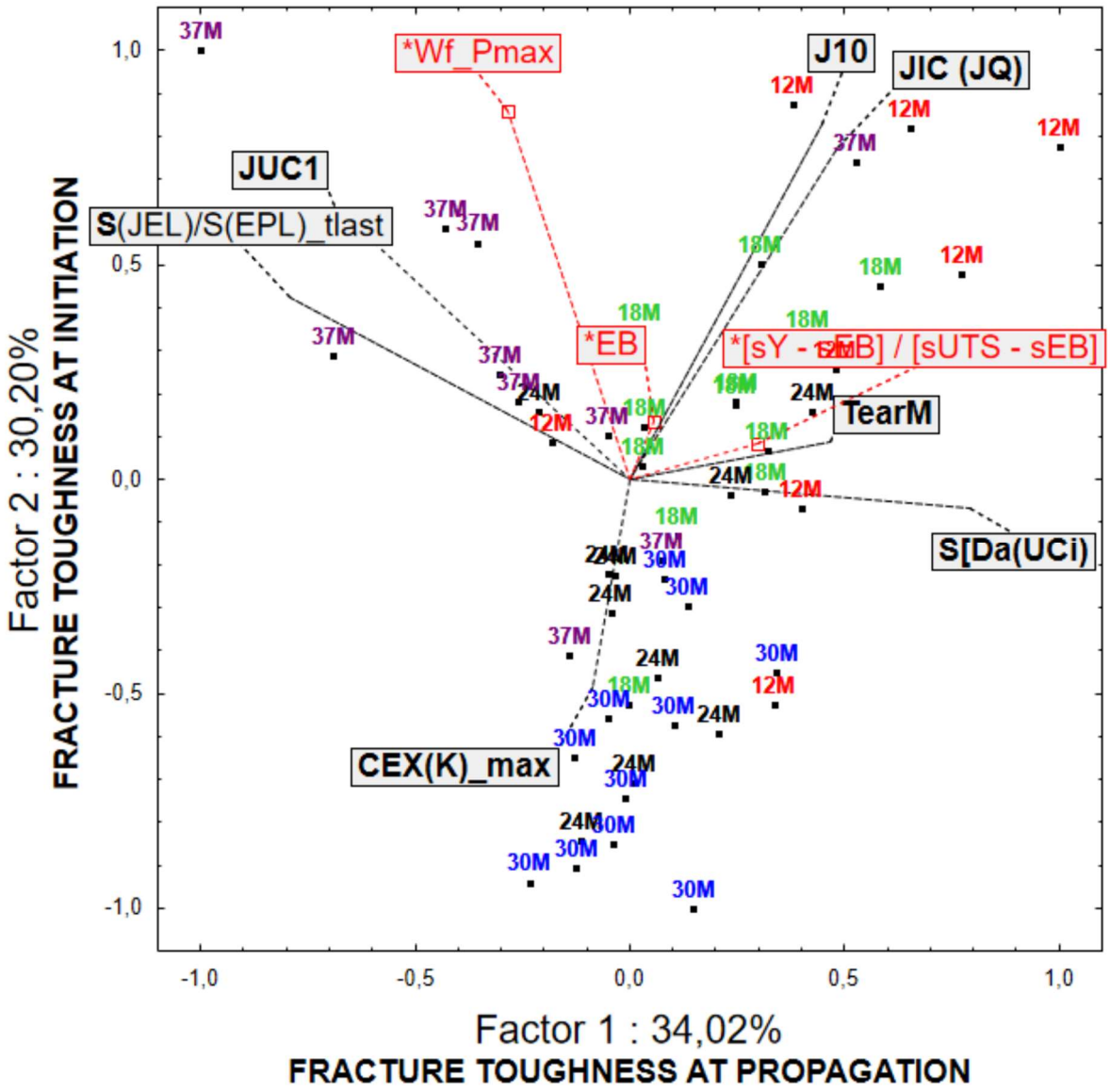

Figure 143 Factor and Score coordinates on the F1 vs F2 plane

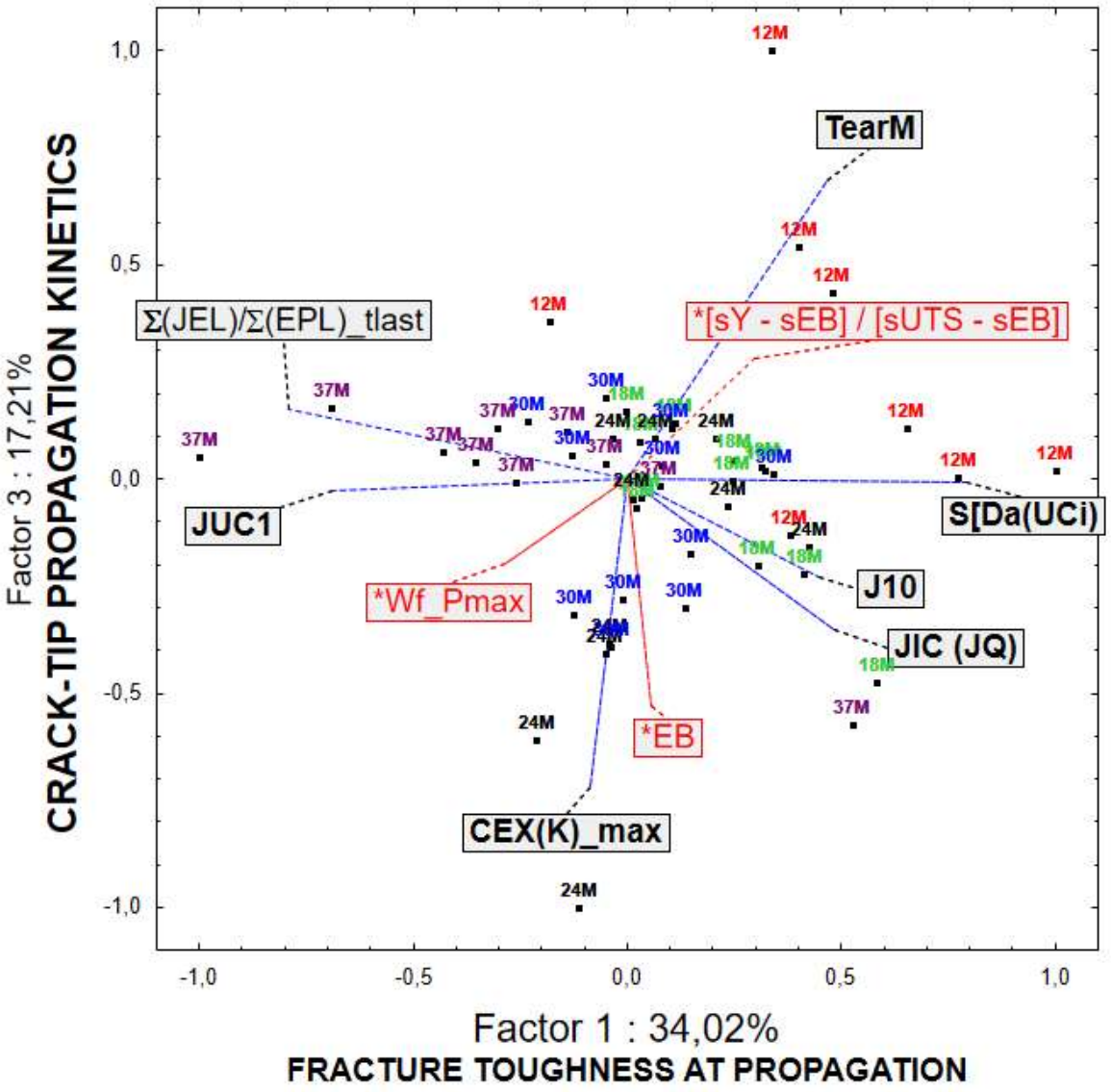

Figure 144 Factor and Score coordinates on the F1 vs F3 plane

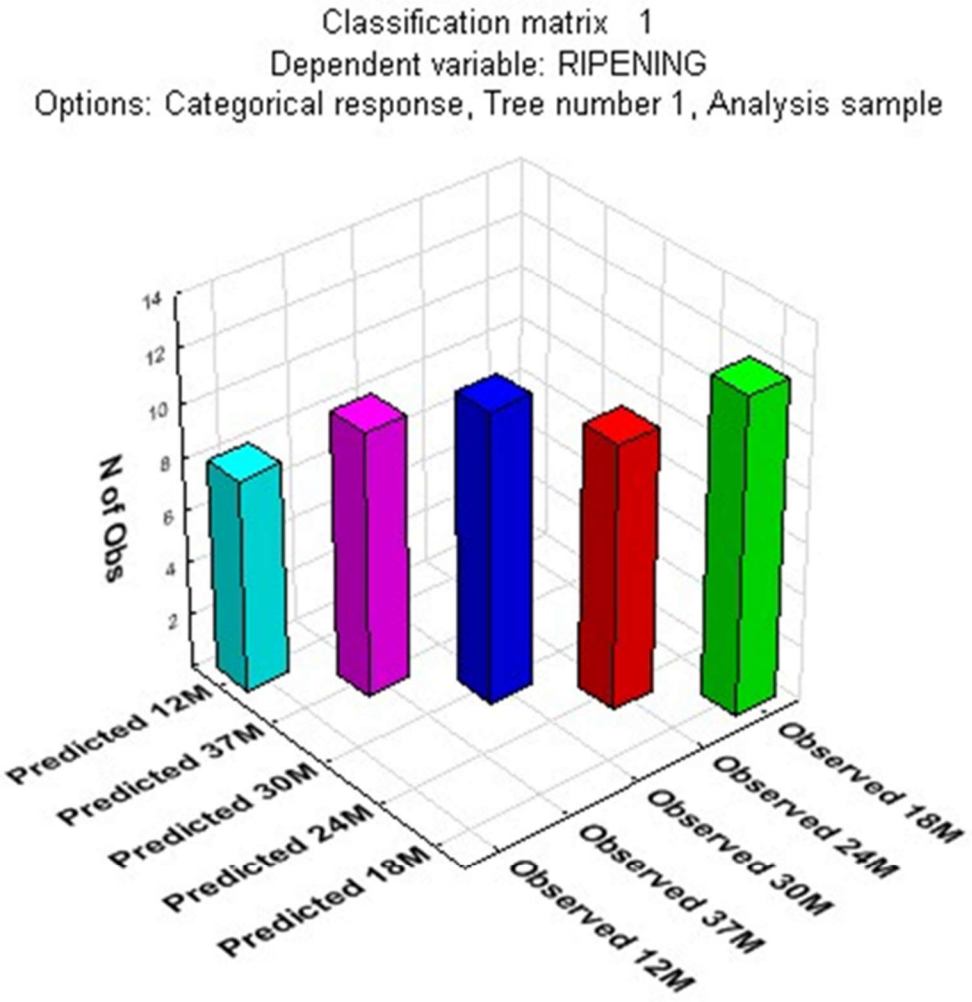

Figure 145 More than 50 cheese specimens were fully classified with respect to their ripening time, using a Tree Classification algorithm to find the split value for each of the new 14 fracture properties

ANNEX I

Disciplinary of Production

From the official gazette n.185 of 10-08-2006

Disciplinare di produzione
del formaggio Parmigiano-Reggiano
Regolamento di alimentazione delle bovine

Art. 1.
Campo di applicazione

Il presente regolamento stabilisce le modalità per l'alimentazione degli animali destinati a produrre latte per la trasformazione in Parmigiano-Reggiano e, se non diversamente specificato, si applica alle vacche in lattazione, alle vacche in asciutta ed alle manze dal sesto mese di gravidanza compreso. Negli articoli seguenti gli animali appartenenti alle predette categorie verranno denominati «bovine da latte».

Art. 2.
Principi generali per il razionamento

Il razionamento delle bovine da latte si basa sull'impiego di foraggi del territorio di produzione del formaggio Parmigiano-Reggiano. Nella razione giornaliera, almeno il 50% della sostanza secca dei foraggi deve essere apportata da fieni.

La razione di base, costituita dai foraggi, deve essere convenientemente integrata con mangimi in grado di bilanciare l'apporto dei vari nutrienti della dieta. La sostanza secca dei mangimi nel loro complesso non deve superare quella globalmente apportata dai foraggi (rapporto foraggi/mangimi non inferiore a 1).

Non debbono essere somministrati alle bovine da latte alimenti che possono trasmettere aromi e sapori anomali al latte e alterarne le caratteristiche tecnologiche, alimenti che

rappresentano fonti di contaminazione e alimenti in cattivo stato di conservazione.

Art. 3.

Origine dei foraggi

Nell'alimentazione delle bovine da latte:

almeno il 50% della sostanza secca dei foraggi utilizzati deve essere prodotta sui terreni aziendali, purche' ubicati all'interno del territorio di produzione del formaggio Parmigiano-Reggiano; almeno il 75% della sostanza secca dei foraggi deve essere prodotta all'interno del territorio di produzione del formaggio Parmigiano-Reggiano.

Art. 4.

Foraggi ammessi

Possono essere somministrati alle bovine da latte:

i foraggi freschi ottenuti da prati naturali, da prati stabili polifiti e da prati di erba medica e di erba di trifoglio;

gli erbai di loietto, di segale, di avena, di orzo, di frumento, di granturchino, di sorgo da ricaccio, di panico, di erba mazzolina (Dactilis), di festuca, di fleolo (Phleum), di sulla, di lupinella, somministrati singolarmente o associati tra loro;

gli erbai di pisello, veccia e favino, purche' associati con almeno una delle essenze foraggere di cui al punto precedente;

i fieni ottenuti a mezzo dell'essiccamento in campo o mediante ventilazione forzata (aeroessiccazione con temperature inferiori a 100°C) delle essenze foraggere predette;

il foraggio trinciato ottenuto dalla pianta intera del mais a maturazione latteo-cerosa o cerosa, somministrato immediatamente dopo la raccolta;

le paglie di cereali, con esclusione di quella di riso.

Possono, altresi', essere utilizzati per l'alimentazione delle bovine da latte i foraggi delle essenze sopraindicate, ad esclusione del trinciato di mais, trattati termicamente con temperatura pari o superiore a 100°C, nella dose massima di 2 kg/capo/giorno. Tale apporto non può essere cumulato con la quota di foraggi disidratati eventualmente fornita con i mangimi.

Art. 5.

Foraggi e sottoprodotti vietati

Per evitare che gli insilati, anche attraverso il terreno ed i foraggi, possano contaminare l'ambiente di stalla, negli allevamenti delle vitelle, delle manze fino al sesto mese di gravidanza e delle bovine da latte, sono vietati l'uso e la detenzione di insilati di ogni tipo.

L'eventuale allevamento di animali da carne deve avvenire in ambienti distinti e separati da quelli degli animali della filiera latte.

E', comunque, vietata anche la semplice detenzione in azienda di insilati di erba e di sottoprodotti, quali le polpe di bietola, le buccette di pomodoro, ecc., conservati in balloni fasciati, trincee, platee o con altre tecniche.

Nell'alimentazione delle bovine da latte e' vietato:

a) l'impiego di:

foraggi riscaldati per fermentazione;

foraggi trattati con additivi;

foraggi palesemente alterati per muffe e/o altri parassiti,imbrattati oppure contaminati da sostanze tossiche o comunque nocive;

b) l'impiego di:

colza, ravizzone, senape, fieno greco, foglie di piante da frutto e non, aglio selvatico e coriandolo;

stocchi di mais e di sorgo, brattee e tutoli di mais, paglia, di riso, nonche' quelle di soia, di medica e di trifoglio da seme;

ortaggi in genere ivi compresi scarti, cascami e sottoprodotti vari allo stato fresco e conservati;

frutta fresca e conservata nonche' tutti i sottoprodotti freschi della relativa lavorazione;

barbabietole da zucchero e da foraggio, ivi compresi le foglie ed i colletti;

melasso in forma liquida (fatto salvo l'utilizzo previsto all'art.6), lieviti umidi, trebbie di birra, distiller, borlande, vinacce, vinaccioli, graspe ed altri sottoprodotti agroindustriali;

tutti i sottoprodotti della macellazione, ivi compreso il contenuto del rumine;

tutti i sottoprodotti dell'industria lattiero-casearia.

Art. 6.

Materie prime per mangimi

Nell'alimentazione delle bovine da latte possono essere utilizzate, nelle forme indicate nell'allegato, le seguenti materie prime:

cereali: mais, sorgo, orzo, avena, frumento, triticale, segale,
farro, miglio e panico;

semi di oleaginose: soia, lino, girasole;

semi di leguminose: fava, favino e pisello proteico;

foraggi: farine delle essenze foraggere ammesse;

polpe secche di bietola;

concentrato proteico di patate.

Possono inoltre essere utilizzati nei mangimi complementari composti:

la carruba, in quantita' non superiore al 3%;

il melasso, in quantita' non superiore al 3%.

E' consentito l'uso di mangimi in blocchi melassati, anche in forma frantumata, nella dose massima giornaliera di 1 kg a capo. In ogni caso, l'impiego dei blocchi melassati non e' compatibile con l'impiego di mangimi contenenti melasso.

Sono ammesse, inoltre, preparazioni zuccherine e/o a base di glicole propilenico e glicerolo, in forma liquida o disperse nei mangimi, nella dose massima complessiva di 300 grammi capo/giorno.

Fatto salvo quanto previsto dall'art. 8, possono essere, inoltre, utilizzati i prodotti e gli alimenti consentiti dalla legislazione vigente per le bovine da latte previa sperimentazione del Consorzio del Formaggio Parmigiano-Reggiano che, verificata la compatibilita', ne' da comunicazione agli organi preposti.

Art. 7.

Uso dei mangimi complementari semplici e composti, integrati e non

La somministrazione dei mangimi deve avvenire nel rispetto delle indicazioni di seguito riportate nell'allegato.

I mangimi devono essere corredati da «cartellini» in cui siano indicate le singole materie prime in ordine decrescente di quantita'.

E' vietato l'impiego di polpe secche di bietola se umidificate.

I mangimi non possono essere conservati all'interno della stalla.

La quantita' complessiva di grasso greggio apportata da prodotti e sottoprodotti della soia, del lino, del girasole del germe di mais e del germe di frumento non deve superare i 300 grammi/capo/giorno.

Art. 8.

Materie prime per mangimi e prodotti vietati

Non possono essere impiegati nell'alimentazione delle bovine da latte:

tutti gli alimenti di origine animale: farine di pesce, carne, sangue, plasma, penne, sottoprodotti vari della macellazione nonche' i sottoprodotti essiccati della lavorazione del latte e delle uova;

i semi di cotone, veccia (comprese le svecciature), fieno greco, lupino, colza, ravizzone e vinaccioli;

il riso e i suoi sottoprodotti;

i tutoli e gli stocchi di mais trinciati e/o macinati;

le farine di estrazione, i panelli e gli expeller di arachide, colza, ravizzone, cotone, vinaccioli, semi di pomodoro, girasole con meno del 30% di proteine, babassu, malva, neuk, baobab, cardo mariano, cocco, tabacco, papavero, palmisto, olive, mandorle, noci e cartamo;

la manioca, le patate e i derivati, ad eccezione del concentrato proteico di patata;

gli alimenti disidratati ottenuti da ortaggi, frutta ed i sottoprodotti della loro lavorazione nonche' gli alimenti disidratati ottenuti da trinciati di mais e da insilati di ogni tipo;

le alghe, ad eccezione di quelle coltivate ed impiegate quali integratori di acidi grassi essenziali, nella dose massima di 100 grammi/capo/giorno;

tutti i sottoprodotti delle birrerie (trebbie essiccate) e dell'industria dolciaria o della panificazione;

i terreni di fermentazione;

l'urea e i derivati, i sali di ammonio;

il concentrato proteico di bietole (CPB), le borlande e i distiller di ogni tipo e provenienza. Non possono essere somministrati alle bovine da latte, ne' direttamente, ne'come ingredienti dei mangimi i saponi e tutti i grassi (oli, seghi, strutti, burri) siano essi di origine animale o vegetale. Possono

essere usati lipidi di origine vegetale solo come supporto e protezione di micronutrienti, nella dose massima di 100 grammi/capo/giorno.

Non possono essere somministrati alle bovine da latte mangimi che contengano:

additivi appartenenti al gruppo degli antibiotici;

gli antiossidanti butilidrossianisolo, butilidrossitoluolo ed etossichina.

Come supporto per gli integratori minerali e vitaminici, non possono essere utilizzati prodotti non ammessi dal presente Regolamento.

Non possono essere somministrati alle bovine da latte mangimi rancidi, ammuffiti, infestati da parassiti, deteriorati, imbrattati oppure contaminati da sostanze tossiche o comunque nocive. Non possono essere somministrati, alle bovine da latte, mangimi che contengano foraggi dei quali non si conosca la provenienza, tagliati in modo grossolano.

In ogni caso i foraggi eventualmente presenti nei mangimi complementari in farina o in pellet non possono superare la lunghezza di 5 mm

Art. 9.

Animali provenienti da altri comparti produttivi

Le bovine da latte provenienti da filiere produttive diverse da quella del Parmigiano-Reggiano, possono essere introdotte negli ambienti delle vacche in lattazione ed in asciutta dopo non meno di quattro mesi dall'introduzione nell'azienda. In tale periodo le bovine da latte devono essere alimentate conformemente alle norme del presente Regolamento e il latte, eventualmente prodotto, non puo' essere conferito in caseificio.

Le aziende agricole non appartenenti alla filiera Parmigiano-Reggiano sono autorizzate al conferimento del latte dopo non meno di quattro mesi dalla visita ispettiva.

Art. 10.

Alimentazione con Piatto Unico

Gli alimenti possono essere somministrati alle bovine da latte mediante la tecnica del «Piatto Unico», che consiste nella preparazione di una miscela omogenea di tutti i componenti della razione prima di distribuirli agli animali.

La preparazione della miscela deve avvenire nell'allevamento che la utilizza.

Inoltre:

non e' consentita la miscelazione di foraggi verdi, nemmeno nel caso in cui si impieghi il trinciato fresco di mais. Se si utilizzano foraggi verdi, questi vanno somministrati a parte;

le operazioni di preparazione non possono essere eseguite all'interno della stalla;

se si procede all'umidificazione della massa, la miscelazione deve essere effettuata almeno due volte al giorno e la distribuzione deve seguire immediatamente la preparazione;

anche se non si procede all'umidificazione della massa, la conservazione della stessa deve essere effettuata al di fuori della stalla e la distribuzione in greppia della miscelata deve essere effettuata almeno una volta al giorno.

Art. 11.

Nuovi prodotti e tecnologie

L'eventuale impiego di alimenti non contemplati dal presente Regolamento, cosi' come le variazioni delle dosi utilizzabili e l'introduzione di modalita' di preparazione e di somministrazione non previste, sono condizionate dall'esito favorevole delle sperimentazioni e degli studi valutati dal Consorzio del Parmigiano-Reggiano e, in caso di esito positivo, potranno costituire oggetto di richiesta di modifica del Disciplinare di produzione.

Standard di produzione del formaggio

La D.O.P. Parmigiano-Reggiano e' un formaggio a pasta dura, cotta e a lenta maturazione, prodotto con latte crudo, parzialmente scremato, proveniente da vacche la cui alimentazione e' costituita prevalentemente da foraggi della zona d'origine. Il latte non puo' essere sottoposto a trattamenti termici e non e' ammesso l'uso di additivi.

Tutto il latte introdotto in caseificio deve essere conforme ai Regolamenti di produzione del Parmigiano-Reggiano.

Per l'intero allevamento il tempo di mungitura di ciascuna delle due munte giornaliere consentite deve essere contenuto entro le quattro ore.

Il latte della mungitura della sera e quello della mungitura del mattino sono consegnati integri al caseificio entro due ore dalla fine di ciascuna mungitura. Il latte non puo' essere sottoposto a processi di centrifugazione.

Il latte puo' essere raffreddato immediatamente dopo la mungitura e conservato ad una temperatura non inferiore a 18°C.

Il latte della sera viene parzialmente scremato per affioramento naturale del grasso in vasche di acciaio a cielo aperto. Il latte del mattino, dopo la consegna in caseificio, viene miscelato con il latte parzialmente scremato della sera precedente; puo' anche essere sottoposto ad una parziale scrematura per affioramento naturale del grasso.

E' possibile conservare un'aliquota di latte del mattino, fino a un massimo del 15%, per la caseificazione del giorno successivo. In tal caso il latte deve essere conservato in caseificio in appositi recipienti di acciaio; se raffreddato, la temperatura non puo' risultare inferiore a 10°C.

Al latte e' addizionato il siero-innesto, una coltura naturale di fermenti lattici ottenuta dall'acidificazione spontanea del siero residuo della lavorazione del giorno precedente.

La coagulazione del latte, ottenuta con l'uso esclusivo di caglio di vitello, e' effettuata nelle caldaie tronco-coniche di rame per ottenere fino a due forme per ciascuna caldaia.

Le caldaie devono essere utilizzate una sola volta al giorno. E' possibile riutilizzare il 15% delle caldaie per una seconda caseificazione.

Alla coagulazione seguono la rottura della cagliata e la cottura.

Si lasciano quindi sedimentare i granuli sul fondo della caldaia in modo da ottenere una massa compatta. Tali operazioni debbono avvenire entro la mattinata.

Dopo la sedimentazione, la massa caseosa e' trasferita negli appositi stampi per la formatura.

Dopo alcuni giorni, si procede alla salatura per immersione in una soluzione salina. La maturazione deve protrarsi per almeno 12 mesi, a partire dalla formatura del formaggio. In estate la temperatura del magazzino di stagionatura non puo' essere inferiore a 16°C.

Il Parmigiano-Reggiano presenta le seguenti caratteristiche:

forma cilindrica a scalzo leggermente convesso o quasi diritto, con facce piane leggermente orlate;

dimensioni: diametro delle facce piane da 35 a 45 cm., altezza dello scalzo da 20 a 26 cm.;

peso minimo di una forma: kg 30;

aspetto esterno: crosta di colore paglierino naturale;

colore della pasta: da leggermente paglierino a paglierino;

aroma e sapore della pasta caratteristici: fragrante, delicato,
saporito ma non piccante;

struttura della pasta: minutamente granulosa, frattura a

scaglia;

spessore della crosta: circa 6 mm.;

grasso sulla sostanza secca: minimo 32%.

Per quanto non specificato, si fa riferimento alla prassi consacrata dagli usi locali, leali e costanti. Come gia' previsto dal decreto del Presidente del Consiglio dei Ministri 4 novembre 1991, la denominazione di origine del formaggio «Parmigiano Reggiano» e' estesa alla tipologia grattugiato, ottenuta esclusivamente da formaggio intero avente diritto alla denominazione di origine di cui trattasi, a condizione che le operazioni di grattugia siano effettuate nell'ambito della zona di produzione del formaggio medesimo e che il confezionamento avvenga immediatamente senza nessun trattamento e senza aggiunta di sostanze atte a modificare la conservabilita' e le caratteristiche organolettiche originarie.

La tipologia della denominazione in parola e' riservata al formaggio grattugiato avente i parametri tecnici e tecnologici sottospecificati:

additivi: assenti;

umidita': non inferiore al 25% e non superiore al 35%;

aspetto: non pulverulento ed omogeneo, particelle con diametro inferiore a 0,5 mm non superiori al 25%;

quantita' di crosta: non superiore al 18%;

composizione amminoacidica: specifica del «Parmigiano Reggiano».

La zona di produzione comprende i territori delle province di Bologna alla sinistra del fiume Reno, Mantova alla destra del fiume Po, Modena, Parma e Reggio nell'Emilia.

Il condizionamento del formaggio Parmigiano-Reggiano grattugiato e in porzioni con e senza crosta deve essere effettuato all'interno della zona di origine, al fine di garantire la qualita', la tracciabilita' e il controllo.

E' consentito il confezionamento di porzioni di Parmigiano-Reggiano, destinato alla vendita immediata, nell'esercizio dove e' stato preparato.

I prodotti per la cui preparazione e' utilizzata la D.O.P. Parmigiano-Reggiano, anche a seguito di processi di elaborazione e di trasformazione, possono essere immessi al consumo in confezioni recanti il riferimento alla detta denominazione senza l'apposizione del logo comunitario, a condizione che:

il prodotto a denominazione protetta, certificato come tale, costituisca il componente esclusivo della categoria merceologica di appartenenza;

gli utilizzatori del prodotto a denominazione protetta siano autorizzati dai titolari del diritto di proprieta' intellettuale conferito dalla registrazione della D.O.P. riuniti in Consorzio incaricato alla tutela dal Ministero delle politiche agricole e forestali. Lo stesso consorzio incaricato provvedera' anche ad iscriverli in appositi registri e a vigilare sul corretto uso della denominazione di origine protetta.

Regolamento di marchiatura

CAPITOLO I

Disposizioni generali e definizioni

Art. 1.

I marchi

1. I segni distintivi del formaggio Parmigiano-Reggiano sono rappresentati dai marchi d'origine e dai marchi di selezione.

2. La marchiatura d'origine e' eseguita a cura dei singoli caseifici mediante:

a) l'apposizione di una placca di caseina recante la scritta «Parmigiano-Reggiano» o «CFPR» ed i codici identificativi della forma;

b) l'impiego di apposite matrici (fasce marchianti) imprimenti sulla superficie dello scalzo di ogni forma la dicitura a puntini «Parmigiano-Reggiano» (cfr. immagine n. 1), nonche' la matricola del caseificio produttore, l'annata e il mese di produzione.

3. La marchiatura di selezione e' effettuata dal Consorzio del formaggio Parmigiano-Reggiano mediante l'apposizione di marchi indelebili, come riportato nei successivi articoli 4, 5, 6, 7 e 8, dopo l'effettuazione delle operazioni di controllo da parte dell'Organismo di controllo autorizzato.

Art. 2.

Compiti del Consorzio del formaggio Parmigiano-Reggiano

1. Il Consorzio, ai sensi della legge n. 526/99, stabilisce le modalita' per l'impiego dei marchi, nel rispetto del Disciplinare di produzione e vigila sul loro corretto utilizzo presso i caseifici. In caso di uso non corretto dei marchi di origine o di altra inosservanza al disciplinare depositato ai sensi del Regolamento 2081/92, verificato dagli Organi a cio' preposti, il Consorzio dispone il ritiro delle matrici marchianti e delle placche e/o l'applicazione di una misura sanzionatoria secondo le norme vigenti;

2. il Consorzio assegna ad ogni caseificio produttore di Parmigiano-Reggiano un numero di matricola, che viene anche comunicato all'Organismo di controllo ed inserito nel sistema di controllo;

3. l'uso sulle forme di altri contrassegni non previsti dal presente Regolamento deve essere espressamente autorizzato dal Consorzio, che ne fissa le caratteristiche e le modalita' applicative, in quanto gli stessi non possono sovrapporsi ai marchi DOP e devono assicurare la prevalenza di questi ultimi.

Art. 3.

Obblighi dei caseifici

1. I caseifici che intendono produrre Parmigiano-Reggiano, almeno quattro mesi prima dall'inizio dell'attivita', debbono inoltrare domanda al Consorzio comunicando che sono inseriti nel sistema di controllo per l'assegnazione del numero di matricola e per la richiesta delle matrici marchianti e delle placche di caseina, al fine di effettuare la marchiatura di origine;

2. i caseifici sono responsabili del corretto uso e della conservazione delle fasce marchianti e delle placche di caseina, che sono loro fornite in dotazione fiduciaria;

3. i caseifici debbono tenere quotidianamente aggiornato il Registro di Produzione, vidimato dal Consorzio, che sara' a disposizione dell'Organismo di controllo per l'espletamento della sua attivita', e delle competenti Autorita';

4. i caseifici hanno l'obbligo di mantenere il rendiconto di tutta la produzione.

In caso di non corretta tenuta della rendicontazione, saranno applicate le sanzioni previste dalla normativa vigente;

5. i caseifici hanno l'obbligo di mettere o di far mettere a disposizione del Consorzio il formaggio per le operazioni di classificazione, apposizione dei bolli e annullamento dei marchi previste dagli articoli 4, 5, 6, 7, 8 e 9. In caso di inadempienza, il Consorzio dispone, secondo le modalita' previste dal piano di controllo, il ritiro delle matrici marchianti e delle placche e/o l'applicazione di una misura sanzionatoria;

6. i caseifici sono tenuti a fornire al Consorzio ed ai suoi incaricati tutti gli elementi utili per l'applicazione del presente regolamento.

Art. 4.

Definizione dei lotti produttivi e operazione di espertizzazione

1. La produzione del caseificio e' divisa in lotti e piu' precisamente:

a) 1° lotto: il formaggio prodotto nei mesi da gennaio ad aprile;

b) 2° lotto: il formaggio prodotto nei mesi da maggio ad agosto;

c) 3° lott: il formaggio prodotto nei mesi da settembre a dicembre.

2. Prima della marchiatura di selezione, tutte le forme di Parmigiano-Reggiano sono esaminate da una Commissione composta da almeno due esperti nominati dal Consorzio, iscritti in un elenco tenuto dallo stesso e comunicato all'Organismo di controllo.

3. Le operazioni di espertizzazione e di apposizione dei marchi devono avvenire all'interno della zona di origine.

CAPITOLO II

Procedure

Art. 5.

Espertizzazione

Le operazioni di espertizzazione sono espletate per i tre lotti di produzione in tre periodi, secondo il seguente calendario:

a) il formaggio del primo lotto e' espertizzato a partire dal 1° dicembre dello stesso anno;

b) il formaggio del secondo lotto e' espertizzato a partire dal 1° aprile dell'anno successivo;

c) il formaggio del terzo lotto e' espertizzato a partire dal 1° settembre dell'anno successivo.

Art. 6.

Classificazione del formaggio

1. L'espertizzazione del formaggio avviene attraverso la valutazione dell'aspetto esterno, della struttura e delle caratteristiche olfattive della pasta, avvalendosi dell'esame con

il martello e con l'ago in riferimento agli usi ed alle consuetudini, secondo la classificazione riportata in allegato;

2. al fine di approfondire l'oggettivita' dell'espertizzazione, le commissioni devono procedere al taglio di almeno una forma per lotto e, comunque, non meno di una ogni mille o frazione di mille, per valutarne le caratteristiche strutturali ed organolettiche. Ai caseifici e' fatto obbligo di mettere a disposizione le forme indicate dagli esperti da sottoporre al taglio e di consentire l'eventuale prelievo di una porzione delle stesse.

Art. 7.

Apposizione dei bolli ad inchiostro

Contestualmente alle operazioni di espertizzazione, di cui all'art. 6, alle forme sono applicati bolli provvisori ad inchiostro indelebile per caratterizzare le seguenti categorie definite nell'allegato:

a) prima categoria, costituita dalle forme classificate come formaggio Parmigiano-Reggiano «scelto sperlato», «zero» ed «uno»;

b) seconda categoria, costituita dalle forme classificate come formaggio Parmigiano-Reggiano «mezzano» o «prima stagionatura»;

c) terza categoria, costituita dalle forme classificate come formaggio «scarto» e «scartone».

Art. 8.

Apposizione dei bolli a fuoco

1. Sulle forme di prima e di seconda categoria, si appone un bollo ovale a fuoco imprimente la dicitura «Parmigiano-Reggiano Consorzio Tutela» e l'anno di produzione (cfr. immagine n. 2);

2. il formaggio di seconda categoria e' sottoposto all'identificazione mediante un contrassegno indelebile da applicarsi solo sullo scalzo della forma;

3. l'applicazione del bollo a fuoco puo' essere effettuata dopo sette giorni dall'avvenuta espertizzazione, su indicazione dell'Organismo di controllo.

Art. 9.

Annullamento marchi d'origine

Sulle forme di terza categoria, unitamente a quelle con gravi difetti strutturali che non ne hanno consentito la stagionatura ed a quelle che hanno subito correzioni tali da compromettere l'estetica della forma e/o la qualita' della pasta e/o i contrassegni identificativi del mese, dell'anno di produzione e della matricola del caseificio, saranno asportati i marchi di origine a cura degli addetti del Consorzio, o le stesse dovranno essere consegnate ad una o piu' strutture di trasformazione convenzionate con il Consorzio.
Per tali forme, il caseificio dovra' conservare la documentazione prodotta dalle suddette strutture da cui risulti l'avvenuto annullamento dei marchi di origine. L'annullamento dei marchi e' effettuato anche per le forme sulle quali non sono stati correttamente applicati i marchi di origine.

Art. 10.

Redazione dei verbali

Per le operazioni di espertizzazione, di identificazione e bollatura a fuoco delle forme di prima e di seconda categoria e di annullamento dei marchi di origine, per ognuno dei lotti o per le frazioni di lotto della partita, e' redatto un verbale che deve essere sottoscritto dal personale preposto a svolgere tali operazioni e dal legale rappresentante del caseificio o da persona da esso espressamente incaricata.

Art. 11.

Ricorsi

1. I caseifici possono ricorrere avverso l'esito della espertizzazione inviando apposita notifica al Consorzio entro quattro giorni dal termine della stessa, a mezzo lettera raccomandata;

2. I ricorsi sono esaminati da una Commissione di appello che disporra' l'eventuale riesame del formaggio entro quindici giorni dal ricevimento della notifica. Tale Commissione e' nominata dal Consorzio ed e' composta da almeno tre membri non facenti parte delle Commissioni di espertizzazione di cui all'art. 4.

CAPITOLO III

Altre disposizioni

Art. 12.

Richiesta correzione dei marchi di origine

Per le forme che nel corso della maturazione presentassero difetti di crosta tali da richiedere un intervento di correzione nella zona della placca, il caseificio dovra' richiedere al Consorzio l'applicazione di un bollo indelebile a fuoco sostitutivo della placca stessa. Il caseificio dovra' conservare e consegnare al Consorzio le placche asportate.

Art. 13.

Richiesta di annullamento marchi di origine

Per le forme che nel corso della maturazione presentassero gravi difetti tali da non consentirne la prosecuzione della stagionatura, i caseifici avranno la facolta' di richiedere, prima dell'espertizzazione, l'annullamento dei marchi di origine a cura del Consorzio o la consegna come indicato all'art. 9.

Art. 14.

Cessione di forme prima del 12° mese

Nel caso di cessione di forme prima del compimento del 12° mese di stagionatura, ma comunque in zona di produzione, anche se riportanti il bollo a fuoco, le bolle di consegna e le fatture dovranno riportare la seguente dizione, gia' sottoscritta dal Legale Rappresentante del caseificio sui verbali di espertizzazione e di marchiatura: «Il formaggio non puo' essere immesso al consumo con la denominazione tutelata Parmigiano-Reggiano prima del compimento del 12° mese».

Art. 15.

Marchi «Export» e «Extra»

A partire dal compimento del 18° mese di maturazione, i detentori di Parmigiano-Reggiano possono richiedere al Consorzio l'apposizione del marchio «Parmigiano-Reggiano Export» (cfr. immagine n.3) o «Parmigiano-Reggiano Extra» (cfr. immagine n. 4).

Il formaggio, per potersi fregiare dei suddetti marchi, deve presentare le caratteristiche merceologiche previste per il Parmigiano-Reggiano «scelto sperlato» di cui all'art.7. Le forme certificate che abbiano compiuto la stagionatura di 18 mesi, possono acquisire l'idoneita' a fregiarsi dei marchi sopra indicati anche se la stagionatura e' proseguita in locali situati al di fuori della zona di produzione; in quest'ultimo caso, dovranno essere stipulate apposite convenzioni con il Consorzio di tutela al fine di consentirgli l'esercizio delle attivita' di vigilanza.

Le spese relative alle operazioni di marchiatura sono a carico dei richiedenti.

Art. 16.

Costi

1. Per la consegna delle matrici marchianti e delle placche di caseina, a garanzia dell'adempimento degli obblighi relativi, e' facolta' del Consorzio di richiedere ai caseifici un deposito

cauzionale nella misura che sara' dallo stesso annualmente fissata;

2. per il servizio di annullamento dei marchi per le forme di terza categoria di cui agli articoli 9 e 13 e per l'apposizione del bollo a fuoco sostitutivo delle placche di cui all'art. 12, ai caseifici sara' richiesto un rimborso spese per forma, nella misura che sara' stabilita dal Consorzio;

3. per la sostituzione delle matrici marchianti usurate anzitempo, o comunque deteriorate, verra' richiesto ai caseifici un rimborso spese.

CLASSIFICAZIONE MERCEOLOGICA DEL FORMAGGIO

1. Parmigiano-Reggiano «scelto sperlato».

Tale qualifica viene attribuita a quelle forme immuni da qualsiasi difetto sia interno che esterno (pezzatura, crosta, martello, ago, struttura della pasta, aroma, sapore) in qualsiasi modo rilevabile, sia alla vista sia al collaudo dell'ago e del martello.

2. Parmigiano-Reggiano «zero(0) e uno(1)».

Tale qualifica comprende:

a) zero: le forme che, pur rispondendo alle caratteristiche di scelto, presentano sulla crosta fessure superficiali, piccole erosioni, spigoli leggermente rovinati e qualche piccola correzione senza che la forma risulti deformata.

b) uno: le forme aventi leggere anomalie di struttura ed in particolare:

uno o due vescicotti (cavita' di forma circolare od oblunga creatasi nella pasta) di diametro non superiore ai 3-4 cm e sempre che, sondato il vescicotto con l'ago, questo non riveli difetti olfattivi;

vespaio localizzato (zona di pasta spugnosa) di pochi centimetri senza difetti olfattivi;

alcune «bocche di pesce» e cioe' occhi di forma oblunga, non superiori ai 3-4 cm;

leggere sfoglie, costituite da alcune fessurazioni della pasta, di lunghezza non superiore ai 3-4 cm;

occhi radi e non eccessivamente ripetuti;

le forme cosidette «lente», e cioe' quelle che alla percussione con il martello rivelano un suono sordo.

3. Parmigiano-Reggiano «mezzano» o «prima stagionatura» (uno lungo).

In questa classe sono comprese le forme con:

vescicotti di diametro superiore ai 3-4 cm immuni da difetti olfattivi;

vespai immuni da difetti olfattivi;

occhiatura diffusa nella forma (occhi lucidi, rotondi, di diametro medio-piccolo);

alcune fessurazioni e spacchi disposti orizzontalmente;

fessurazioni e spacchi orizzontali localizzati in prossimita' di un piatto e/o interessanti parte dello scalzo;

correzioni in scalzo o in piatto in assenza di difetti olfattivi eseguite a regola d'arte, di entita' tale da non compromettere significativamente l'aspetto esteriore della forma.

4. Formaggio «scarto».

In questa classe sono comprese le forme con:

bombatura molto accentuata dei piatti della forma;

pasta spugnosa con grande e diffusa occhiatura;

fessurazioni orizzontali multiple e diffuse con conformazione a «libro»;

grosse fenditure e spacchi diffusi su gran parte della forma;

grossa cavita' localizzata al centro o in zona sub-centrale a forma sferica od oblunga con o senza pasta spugnosa;

correzioni in scalzo e/o in piatto profonde ed estese;

forme con evidenti difetti olfattivi.

5. Formaggio «scartone».

A questa classe appartengono tutte le forme nelle quali si nota la presenza di numerosi e gravi difetti e cioe' tutte quelle che non possono, per la loro qualita', essere comprese nelle categorie sopra specificate.

BIBLIOGRAPHY

Ayyash M.M., Sherkat F., Francis P., Williams R.P.W., Shah N.P. The effect of sodium chloride substitution with potassium chloride on texture profile and microstructure of Halloumi cheese. (2011). *Journal of Dairy Science*. Vol.94 (1), 37-42.

Annibaldi S., Nanni M. Osservazioni preliminari sulla microstruttura del formaggio Parmigiano-Reggiano. (1979). *Sci. Tecn. Latt.-Cas*. Vol.3, 191-198.

Benedito J., Gonzalez R., Rossello C., Mulet A. Instrumental and expert assessment of Mahon cheese texture. (2000). *Journal of Food Science*. Vol.65 (7), 1170-1174.

Blanc B., Ruegg M., Baer A., Casey M., Lukesch A. Comparative tests on Emmental cheese with and without late fermentation. IV. Biochemical and physico-chemical comparison. (1979). *Schweiz.Milchw. Forschung.* Vol.8, 27-36.

Bonazzi G., Manghi E. Il formaggio Parmigiano-Reggiano ed il controllo della denominazione di origine protetta. (2005). *Ann. Fac. Medic. Vet. Di Parma*. Vol.25, 231-246.

Bottazzi V., Battistotti B., Bianchi F. The microscopic crystalline inclusions in Grana cheese and their X- ray microanalysis. (1982). *Milchwissenschaft*. Vol.37 (10), 577- 580.

Bowland E.L., Foegeding E.A. Small strain oscillatory shear and microstructural analyses of a model processed cheese. (2001). *Journal of Dairy Science*. Vol.84 (11), 2372-2380.

Brooker B.E. The crystallization of calcium phosphate at the surface of mould-ripened cheeses. (1987). *Food Structure*. Vol.6 (1), 25-33.

Brooker B.E. (1979). Milk and its products. *Food Microscopy*. J.G. Vaughan (ed.), Academic Press, New York, USA, 273- 311.

Brown J.A. Cheese texture. (2002).

Caric M., Gantar M., Kalab M. Effects of emulsifying agents on the microstructure and other characteristics of process cheese - A Review. (1985). *Food Structure*. Vol.4 (2), 13.

D'Incecco P., Limbo S., Faoro F., Hogenboom J., Rosi V., Morandi S., Pellegrino L. New insight on crystal and spot development in hard and extra-hard cheeses: Association of spots with incomplete aggregation of curd granules. (2016). *Journal of dairy science*. Vol.99 (8), 6144-6156.

De Man S., Dhaene J., De Schryver T., Van Hoorebeke L., & De Block J. Use of X-ray tomography in aerated dairy food and cheese research. (2015). In 2nd UGCT seminar. Ghent University. Centre for X-ray Tomography (UGCT).

De Roest K. The production of Parmigiano-Reggiano cheese – The force of an artisanal system in an industrialised world. (2000). ISBN n.90-5808-298-9.

Del Nobile M.A., Chillo S., Falcone P.M., Laverse J., Pati S., Baiano A. Textural changes of Canestrello Pugliese cheese measured during storage. (2007). *Journal of Food Engineering*. Vol. 83 (4), 621-628.

Disciplinare di Produzione del formaggio Parmigiano Reggiano. Consorzio di tutela Parmigiano Reggiano. (Documento Unico del 29/08/2011).

Drake M.A., Truong V.D., Daubert C.R. Rheological and sensory properties of reduced-fat processed cheeses containing lecithin. (1999a). *Journal of Food Science*. Vol.64 (4), 744-747.

Drake M.A., Gerard P.D., Truong V.D., Daubert C.R. Relationship between instrumental and sensory measurements of cheese texture. (1999b). *Journal of Texture Studies*. Vol.30 (4), 451-476.

El-Bakry M., Sheehan J. Analysing cheese microstructure: a review of recent developments. (2014). *Journal of Food Engineering*. Vol.125, 84-96.

El-Nour A.A., Scheurer G.J., Buchheim W. Use of rennet casein and milk protein concentrate in the production of spread-type processed cheese analogue. (1998). *Milchwissenschaft.* Vol.53 (12), 686-690.

Everett D.W., Auty M.A. Cheese structure and current methods of analysis. (2008). *International Dairy Journal*. Vol.18 (7), 759-773.

Falcone P.M., Baiano A., Zanini F., Mancini L., Tromba G., Dreossi D.M.A.D., Nobile M.A.D. Three-dimensional quantitative analysis of bread crumb by X-ray microtomography. (2005). *Journal of Food Science*. Vol.70 (4), E265-E272.

Flilckiger E., Schilt P. Formation of salt crystals in Swiss cheese. (1963). *Milchwissenschaft*. Vol.18, 437- 442.

Formaggioni P., Malacarne M., Summer A., Franceschi P., Pecorari M., Tambini A., Vecchia P., Mariani P. The “maturation” of milk for Parmigiano-Reggiano cheesemaking: effects on mineral equilibria and technological properties. (2010). *Italian Journal of Animal Science*. Vol.6 (1s), 427-429.

Fossa E., Sandri S., Tosi F., Franceschi P., Summer A. Caratteristiche chimico-fisiche e microbiologiche della salamoia ad immersione totale con ricircolo per Parmigiano-Reggiano. (2002). *Sci. Tecn. Latt.-Cas*. Vol.53, 383-397.

Fox P.F., McSweeney P.L., Cogan T.M., Guinee T.P. (Eds.). (2004). Cheese: Chemistry, Physics and Microbiology, Volume 1: General Aspects. *Elsevier*.

Giese J. Measuring physicalproperties of food. (1995). Food Technology. Vol.19, 54-63.

Gliguem H., Ghorbel D., Lopez C., Michon C., Ollivon M., Lesieur P. Crystallization and polymorphism of triacylglycerols contribute to the rheological properties of processed cheese. (2009). *Journal of agricultural and food chemistry*. Vol.57 (8), 3195-3203.

Grufferty M.B., Fox P.F. Effect of added NaCl on some physicochemical properties of milk. (1985). *Irish Journal of Food Science and Technology*. Vol.1 (9).

Guggisberg D., Schuetz P., Winkler H., Amrein R., Jakob E., Fröhlich-Wyder M.T., Irmler S., Bisig W., Jerjen I., Plamondon M., Hofmann J., Flisch A., Hofmann, J. Mechanism and control of the eye formation in cheese. (2015). *International dairy journal*. Vol.47, 118-127.

Guggisberg D., Frohlich-Wyder M.R., Irmler S., Greco M., Wechsler D., Schuetz P. Eye formation in semi-hard cheese: X-ray computed tomography as a non-invasive tool for assessing the influence of adjunct lactic acid bacteria. (2013). *Dairy Science & Technology*. Vol.93 (2), 135-149.

Guinee T.P., O'Kennedy B.T. The effect of calcium content of Cheddar-style cheese on the biochemical and rheological properties of processed cheese. (2009). *Dairy Science & Technology*. Vol.89 (3-4), 317-333.

Gunasekaran S., & Ak M.M. Cheese rheology and texture. CRC press. (2002).

Gunasekaran S., Ding K. Three-dimensional characteristics of fat globules in cheddar cheese. (1999). *Journal of dairy science*. Vol.82 (9), 1890-1896.

Herremans E., Chassagne-Berces S., Chanvrier H., Atoniuk A., Kusztal R., Bongaers E., Nicolai B. Possibilities of X-ray nano-CT for internal quality assessment of food products. (2011). In ICEF, Date: 2011/05/22-2011/05/26.

Huc D., Mariette F., Challois S., Barreau J., Moulin G., Michon C. Multi-scale investigation of eyes in semi-hard cheese. (2014). *Innovative Food Science & Emerging Technologies*. Vol.24, 106-112.

Huc D., Moulin G., Mariette F., Michon C. Investigation of curd grains in Swiss-type cheese using light and confocal laser scanning microscopy. (2013). *International Dairy Journal*. Vol.33 (1), 10-15.

Huc D., Mariette F., Challois S., Barreau J., Moulin G., Michon C. Multi-scales investigation of eyes in Swiss-type cheese. (2013, April). *In Food Symposium 2013* (p. 6). Nicolai, B. and Piazza Eds.

Jenness R. Composition of Milk. (1988). In: Wong N.P., Jenness R., Keeney M., Marth E.H. (eds) Fundamentals of Dairy Chemistry. Springer, Boston, MA.

Johnson M.E., Lucey, J.A. Calcium: a key factor in controlling cheese functionality. (2006). *Australian journal of dairy technology*. Vol.61 (2), 147.

Kim E.H-J., Corrigan V.K., Wilson A.J., Waters I.R., Hedderley D.I. and Morgenstern M.P. Fundamental fracture properties associated with sensory hardness of brittle solid foods. (2011). *Journal of Texture Studies*. Vol.43, 49-62.

Klostermeyer H., Uhlmann G., Merkenich K. Formation of crystals in processed cheese. II. Identification of a new citrate. (1984). *Milchwissenschaft*. Vol.39, 195- 197.

Kosikowski F.V. Cheese and Fermented Milk Foods. (1982). Edwards Brothers, Inc., Arm Arbor, Michigan, USA, 382- 401.

Kota K., & Langrish T. A. G. Fluxes and patterns of wall deposits for skim milk in a pilot-scale spray dryer. (2006). *Drying technology*. Vol.24 (8), 993-1001.

Imbeni V., Atkins A.G., Heronimidis G., Yeo J. Rate and temperature dependence of the mechanical properties of Cheddar cheese. (2001). *In ICF10, Honolulu (USA) 2001*.

Lavanchy, P. Guida per la valutazione sensoriale della struttura dei formaggi a pasta dura o semidura. (1994). *Institut national de la recherche agronomique*.

Laverse J., Mastromatteo M., Frisullo P., & Del Nobile M. A. X-ray microtomography to study the microstructure of cream cheese-type products. (2011a). *Journal of Dairy Science*. Vol.94 (1), 43-50.

Laverse J., Mastromatteo M., Frisullo P., Albenzio M., Gammariello D., & Del Nobile M. A. Fat microstructure of yogurt as assessed by x-ray microtomography. (2011b). *Journal of Dairy Science*. Vol.94 (2), 668-675.

Lee K., Uegaki K., Nishii C., Nakamura T., Kubota A., Hirai T., & Yamada K. Computed tomographic evaluation of gas hole formation and structural quality in Gouda-type cheese. (2012). *International journal of dairy technology*. Vol.65 (2), 232-236.

Lide, D.R. CRC Handbook of Chemistry and Physics 88TH Edition 2007-2008. *CRC Press, Taylor & Francis, Boca Raton,* FL 2007, p. 3-320.

Luyten, Hannemieke. The rheological and fracture properties of Gouda cheese. (1988). PhD Thesis. Luyten.

Malacarne M., Summer A., Panari G., Pecorari M., Mariani P. Caratterizzazione chimico-fisica della maturazione del Parmigiano-Reggiano. (2006). *Sci. Tecn. Latt.-Cas*. Vol.57 (4), 215-228.

Marschoun L.T., Muthukumarappan K., Gunasekaran S. Thermal properties of cheddar cheese: Experimental and modeling. (2001). *International Journal of Food Properties*. Vol.4 (3), 383-403.

Mendoza F., Verboven P., Mebatsion H. K., Kerckhofs G., Wevers M., & Nicolaï B. (2007). Three-dimensional pore space quantification of apple tissue using X-ray computed microtomography. *Planta*. Vol.226 (3), 559-570.

Meullenet J.F., Carpenter J.A., Lyon B.G., Lyon C.E. Bi-cyclical instrument for assessing texture profile parameters and its relationship to sensory evaluation of texture. (1997). *Journal of Texture Studies*. Vol.28 (1), 101-118.

Michalski M.C., Camier B., Briard V., Leconte N., Gassi J.Y., Goudédranche H., Michael F., Fauquant J. The size of native milk fat globules affects physico-chemical and functional properties of Emmental cheese. (2004). *Le lait*. Vol.84 (4), 343-358.

Mora R., Nanni M., Panari G. Variazioni chimiche, fisiche e microbiologiche nel formaggio Parmigiano-Reggiano durante le prime 48 ore. (1984). *Sci. Tecn. Latt.-Cas*. Vol.35, 20-32.

Morris H.A., Guinee T.P., Fox P.F. Salt diffusion in Cheddar cheese. (1985). *Journal of Dairy Science*. Vol.68 (8), 1851-1858.

Mucchetti G., Gatti M., Nocetti M., Reverberi P., Bianchi A., Galati F., Petroni A. Segmentation of Parmigiano Reggiano dairies according to cheese-making technology and relationships with the aspect of the cheese curd surface at the moment of its extraction from the cheese vat. (2014). *J. Dairy Sci.* Vol.97 (3), 1202-1209.

Mucchetti G. Le peculiarità qualitative dei formaggi tradizionali ed a denominazione di origine: caratterizzazione e strumenti per la salvaguardia. (2004). *Sci. Tecn. Latt.-Cas*. Vol.55, 5-24.

Mucchetti G., Addeo F., Neviani E. Evoluzione storica della produzione di formaggi a denominazione di origine protetta DOP. Pratiche di produzione, utilizzo e composizione dei sieroinnesti nella caseificazione a formaggi Grana Padano e Parmigiano-Reggiano: considerazioni sulle relazioni tra sieroinnesto e DOP. (1998). *Sci. Tecn. Latt.-Cas.* Vol.49, 281-311.

Mucchetti G., Locci F., Mazzucotelli L., Neviani E. Evoluzione del processo di acidificazione del formaggio grana padano nelle prime 24 ore: influenza delle diverse condizioni di temperatura misurate all'interno della forma. (1995). *Atti del II Congresso italiano di Scienza e tecnologia degli Alimenti (CISETA)*. Cernobbio (pp. 21-22).

Nanni M., Annibaldi S. Osservazioni sulla microstruttura del formaggio Parmigiano-Reggiano: i granuli caseosi. (1982). *Sci. Tecn. Latt.-Cas*. Vol.33 (2), 81-94.

Noël Y., Ardö Y., Pocher S., Hunter A., Lavanchy P., Luginbuhl W., Pellegrino L. Characterisation of protected denomination of origin cheeses: relationships between sensory texture and instrumental data. (1998). *Le Lait*. Vol.78 (5), 569-588.

Noël Y., Zannoni M., Hunter E.A. Texture of Parmigiano Reggiano cheese: Statistical relationships between rheological and sensory variates. (1996). *Le Lait*. Vol.76 (3), 243-254.

Norma, F. I. L. 99A: 1987. Evaluación sensorial de Productos Lácteos, 4(1).

Noronha N., Duggan E., Ziegler G.R., Stapleton J.J., O'riordan E.D., O'sullivan M. Comparison of microscopy techniques for the examination of the microstructure of starch-containing imitation cheeses. (2008). *Food research international*. Vol.41 (5), 472-479.

Panari G., Pecorari M. Peculiarità qualitative e sicurezza igienica del Parmigiano-Reggiano. (2004). *Sci. Tecn. Latt.-Cas*. Vol.55, 443-448.

Panari G., Mariani P., Summer A., Guidetti R., Pecorari M. Variazioni della composizione e andamento della proteolisi del Parmigiano-Reggino nel corso della maturazione in riferimento al profilo (centro e periferia) della forma. (2003). *Sci. Tecn. Latt.-Cas*. Vol.54 (3), 199-212.

Panari G., Pecorari M., Fossa E., Menozzi P. Il Parmigiano-Reggiano: la macrocomposizione in relazione alla tecnologia ed ai fattori di produzione. (1988). Atti della Giornata di Studio "Ricerca triennale sulla composizione e su alcune peculiari caratteristiche del formaggio Parmigiano-Reggiano". Ed.Consorzio del Parmigiano-Reggiano, pp 73-83.

Parisi O. Il formaggio grana. (1951). Società tipografica modenese.

Pearse M.J., Mackinlay A.G. Biochemical aspects of syneresis: a review. (1989). *Journal of Dairy Science*. Vol.72 (6), 1401-1407.

Pecorari M., Panari G. La produzione di Parmigiano-Reggiano tra innovazione e tradizione. (2005). *Sci. Tecn. Latt.-Cas*. Vol.56, 85-103.

Pecorari M., Fossa E., Sandri S., Mariani P. Andamento della proteolisi nel corso della maturazione del Parmigiano-Reggiano. (1997). *Sci. Tecn. Latt.-Cas*. Vol.48, 61-72.

Pecorari M., Sandri S., Fossa E., Summer A., Mariani P. Composizione e proteolisi del Parmigiano-Reggiano: rilievi in differenti zone del formaggio stagionato 24 mesi. (1995). *Industria del latte*. Vol.31 (2-3), 17-24.

Pellegrino L., Battelli G., Resmini P. Andamento centripeto della maturazione dei formaggi Grana Padano e Parmigiano-Reggiano. (1997). *Sci. Tecn. Latt.-Cas*. Vol.48, 73-82.

Rajbhandari P., Kindstedt P.S. Compositional factors associated with calcium lactate crystallization in smoked Cheddar cheese. (2005). *Journal of dairy science*. Vol.88 (11), 3737-3744.

Ramlogan M.V., Rouff A.A. An investigation of the thermal behavior of magnesium ammonium phosphate hexahydrate. (2016). *Journal of Thermal Analysis and Calorimetry*. Vol.123 (1), 145-152.

Regolamento (UE) n. 1151/2012 del 21 novembre 2012, sui regimi di qualità dei prodotti agricoli e alimentari.

Resmini P., Volonterio G., Annibaldi S., Ferri G. Studio sulla diffusione del sale nel formaggio Parmigiano-Reggiano mediante l'uso di $Na^{36}Cl$. (1974). *Sci. Tecn. Latt.-Cas*. Vol.25 (4), 149-166.

Rohm H. and Veits V. Comparative texture profiles of different cheese varieties. (1990). *Milchwissenschaft*. Vol.45 (4), 236-239.

Romani S., Sacchetti G., Pittia P., Pinnavaia G. G., Dalla Rosa M. Physical, chemical, textural and sensorial changes of portioned Parmigiano Reggiano cheese packed under different conditions. (2002). *Food science and technology international*. Vol.8 (4), 203-211.

Ruegg M., Moor U. The size distribution and shape of curd granules in traditional Swiss hard and semi-hard cheeses. (1987). *Food Structure*. Vol.6 (1), 6.

Schuetz P., Guggisberg D., Jerjen I., Fröhlich-Wyder M. T., Hofmann J., Wechsler D., & Bachmann H. P. Quantitative comparison of the eye formation in cheese using radiography and computed tomography data. (2013). *International Dairy Journal*. Vol.31 (2), 150-155.

Steffe J.F. Rheological methods in food process engineering. (1996). *Freeman Press, East Lansing*, MI.

Steinegger R. Salt crystals, their chemical composition, development, and prevention. (1901). *Landwirt. Jahrbuch Schweiz*. Vol.15, 132-157.

Swearingen P.A., Adams D.E., Lensmire T.L. Factors affecting calcium lactate and liquid expulsion defects in Cheddar cheese. (2004). *Journal of dairy science*. Vol.87 (3), 574-582.

Szczesniak A.S. Classification of Textural Characteristics. (1963). *Journal of Food Science*. Vol.28 (4), 385-389.

Tansman G.F. (2017). Development and Implementation of Methods to Study Crystallization in Cheese.

Tansman G.F., Kindstedt P.S., Hughes J.M. Crystal fingerprinting: elucidating the crystals of Cheddar, Parmigiano-Reggiano, Gouda, and soft washed-rind cheeses using powder x-ray diffractometry. (2015). *Dairy science & technology*. Vol.95 (5), 651-664.

Tansman G. F. (2014). Exploring the nature of crystals in cheese through X-ray diffraction.

Tosi F., Sandri S., Tedeschi G., Malacarne M., Fossa E. Variazioni di composizione e proprietà fisico-chimiche del Parmigiano-Reggiano durante la maturazione e in differenti zone della forma. (2008). *Scienza e Tecnica Lattiero-Casearia*, Vol.59 (6), 507-528.

Tosi F., Sandri S., Tedeschi G., Fossa E., Franceschi P. Contenuto di umidità, valori di acido lattico, acidi grassi volatili e pH del Parmigiano-Reggiano, in divere zone della pasta, a 72 ore dalla produzione. (2007). *Sci. Tecn. Latt.-Cas*. Vol.58, 291-301.

Tuckey S.L. and Ruehe H.A. An x-ray diffraction analysis of Cheddar cheese. (1938). *Journal of Dairy Science.* Vol.21 (12), 777-789.

Tunick M.H. Activation energy measurements in rheological analysis of cheese. (2010). *International dairy journal*. Vol.20 (10), 680-685.

Tunick M. H. Rheology of dairy foods that gel, stretch, and fracture. (2000). *Journal of Dairy Science*. Vol.83 (8), 1892-1898.

Vanevenhoven D.W. A Characterization of the Rheology of Raw Milk Gouda Cheese. (2012). *Technology*. Vol.35, 207-214.

Walstra P. Rheology of curd and cheese. (1983). *Netherlands Milk and Dairy Journal*. Vol.37 (1-2), 93-94.

Zannoni M., Nanni M., Mora R. Influenza di diverse modalità di affioramento sulle caratteristiche casearie del latte e sul formaggio Parmigiano-Reggiano ottenuto. (1984). *Scienza e Tecnica Lattiero-Casearia*. Vol.35, 541-556.

Zannoni L., Corradini C., Bottazzi V., Scolari G.L., Emaldi G.C., Toppini P.M., Francani R. Indagine sui fattori che possono influenzare l'evolversi del processo di maturazione del formaggio Grana. (1979). *Scienza e tecnica lattiero casearia*.

Zapparoli G.A., Neviani E. Corretta acidificazione del formaggio grana. (2005). *Latte*. Vol.9, 68-72.

Zapparoli G.A., Duroni F. Quadro analitico di acidi grassi volatili, pH ed umidità in formaggio grana “scelto” da 1 a 20 mesi di stagionatura. (1997). *Sci. Tecn. Latt.-Cas*. Vol.48, 297-304.

SITOGRAPHY

ISTAT, URL https://www.istat.it

https://www.parmigiano-reggiano.it

https://www.cheesescience.org/crystal_types/